Universitat Autònoma de Barcelona

Telomere Deprotection and the Maintenance of Genome Integrity: Discrepancy Between Telomere Shortening and Shelterin Dysfunction

Aina Bernal Martínez

Universitat Autònoma de Barcelona

Departament de Biologia Cel·lular, Fisiologia i Immunologia

Doctoral Thesis

Telomere Deprotection and the Maintenance of Genome Integrity: Discrepancy Between Telomere Shortening and Shelterin Dysfunction

Aina Bernal Martínez

Universitat Autònoma de Barcelona
Novembre 2018

Universitat Autònoma de Barcelona

Departament de Biologia Cel·lular, Fisiologia i Immunologia

Telomere Deprotection and the Maintenance of Genome Integrity: Discrepancy Between Telomere Shortening and Shelterin Dysfunction

Aina Bernal Martínez

Report submitted to qualify for the *Doctor Philosaphiœ* Degree in Cell Biology with International Mention at the *Universitat Autònoma de Barcelona*

Memòria presentada per optar al Grau de Doctora en Biologia Cel·lular amb Menció Internacional per la Universitat Autònoma de Barcelona

Memoria presentada para optar al Grado de Doctora en Biología Celular con Mención Internacional por la *Universitat Autònoma de Barcelona*

Director / Directora

Dr. Laura Tusell Padrós

Universitat Autònoma de Barcelona
Novembre 2018

Universitat Autònoma de Barcelona

Departament de Biologia Cel·lular, Fisiologia i Immunologia

Unitat de Biologia Cel·lular

La Dra. Laura Tusell Padrós, professora agregada del Departament de Biologia Cel·lular, Fisiologia i Immunologia de la Universitat Autònoma de Barcelona

CERTIFICA:

Que Aina Bernal Martínez ha realitzat sota la meva dirección el treball d'investigació que s'exposa a la memoria titulada "Telomere Deprotection and the Maintenance of Genome Integrity: Discrepancy between Telomere Shortening and Shelterin Dysfunction" per optar al Grau de Doctora en Biologia Cel·lular amb Menció Internacional per la UAB.

Que aquest treball s'ha realitzat a la Unitat de Biologia Cel·lular del Departament de Biologia Cel·lular, Fisiologia i Immunologia de la Universitat Autònoma de Barcelona.

I per a que consti, firma el present certificat.

Bellaterra, 13 de Novembre de 2018

Directora	Doctoranda
Dr. Laura Tusell Padrós	Aina Bernal Martínez

Als meus pares, a la meva família i als meus amics,
Per donar-me forces,
per creure en mi,
per fer-me ser valenta i millor persona.

This thesis was funded by:

Ministerio de Economía y competitividad (Spain) (SAF2013-43801-P)

Generalitat de Catalunya (Spain) (2014 SGR-524)

The author was supported by a Universitat Autònoma de Barcelona fellowship (456-01-1/2012) and a grant for a short stay abroad (ESTPIF2016-06). The author is a member of a consolidated research group (2017 SGR-503) recognized by the Generalitat de Catalunya (Spain).

This thesis could not be possible without the great contribution of:

Dr. Matthew J. Smalley, Dr. Giusy Tornillo and Dr. Glorianne Lazaro (Cardiff University, UK) for placing their confidence in me.

Clínica Planas for the polite manners with patients and for obtaining mammary samples.

Dr. Carme Nogués Sanmiquel (Universitat Autònoma de Barcelona, Spain) for the MCF-10A cell line.

Dr. Lenhard Rudolph and Dr. André Lechel (Leibniz Institute on ageing-Fritz Lipmann Institute, USA) for the inducible construct and technical assistance.

Dr. Ian Fraser (Laboratory of Systems Biology, USA) for the rtTA3 plasmid.

Dr. Joan Aurich-Costa (Cellay, Inc, USA) for oligoFISH probes.

Dr. Jordi Surrallés and his research team (Universitat Autònoma de Barcelona, Spain) for technical assistance.

Dr. Neus Agell Jané and her research team (Universitat Barcelona, Spain) for technical assistance.

Dr. Joanquin Arribas and his research team (VHIO, Spain) for the animal experiments and technical support.

Scientific Facilities at Universitat Autònoma de Barcelona (Spain), with an special mention to Servei de Cultius cel·lulars, Producció d'Anticossos i Citometria (SCAC), Laboratori de Luminiscència de Espectroscòpia de Biomolècules (LLEB), Servei de Microscòpia (SM) and Unitat Tècnica de Protecció Radiològica (UTPR-UAB).

Scientific Facilities at Universitat de Barcelona (Spain), with an special mention to Servei de Citometria.

At first, I was afraid, I was petrified. Kept thinking, I could never live without you by my side.
But then I spent so many nights thinking, how you did me wrong. And I grew strong and I learned how to get along.

Gloria Gaynor, I will survive

If you now you are on the right track.
If you have this inner knowledge.
Then nobody can turn you off… no matter what they say.

Barbara McClintock

Aquesta tesi ha estat finançada per:

Ministerio de Economía y competitividad (Espanya) (SAF2013-43801-P)

Generalitat de Catalunya (Espanya) (2014 SGR-524)

L'autora ha rebut una beca predoctoral (456-01-1/2012) procedent de la Universitat Autònoma de Barcelona i una beca per tal de realitzar una estada a un centre estranger (ESTPIF2016-06), també procedent de la Universitat Autònoma de Barcelona. L'autora és membre d'un grup d'investigació consolidat i reconegut (2017 SGR-503) per la Generalitat de Catalunya (Espanya).

Aquesta tesi no hagués estat possible sense la gran contribució de:

El Dr. Matthew J. Smalley, la Dra. Giusy Tornillo i la Dra. Glorianne Lazaro (Cardiff University, UK) per la seva confiança i suport.

A la Clínica Planas pel tracte amb els pacients i la obtenció de mostres.

La Dra. Carme Nogués Sanmiquel (Universitat Autònoma de Barcelona, Espanya) per la cessió de la línia cel·lular MCF-10A.

El Dr. Lenhard Rudolph i el Dr. André Lechel (Leibniz Institute on ageing-Fritz Lipmann Institute, USA) pel casset induïble i la seva assistència tècnica.

El Dr. Ian Fraser (Laboratory of Systems Biology, USA) per la cessió del plàsmid rtTA3.

El Dr. Joan Aurich Costa (Cellay, Inc, USA) per la cessió de sondes oligoFISH.

El Dr. Jordi Surrallés i el seu grup de recerca (Universitat Autònoma de Barcelona, Espanya) per l'assistència tècnica.

La Dra. Neus Agell Jané i el seu grup de recerca (Universitat Barcelona, Espanya) per l'assistència tècnica.

Dr. Joaquin Arribas i el seu grup de recerca (VHIO, Espanya) pels experiments amb els ratolins i per l'assistència técnica.

Els Serveis Científico-técnics de la Universitat Autònoma de Barcelona (Espanya), amb una especial menció al Servei de Cultius cel·lulars, Producció d'Anticossos i Citometria (SCAC), el Laboratori de Luminiscència de Espectroscòpia de Biomolècules (LLEB), el Servei de Microscòpia (SM) i la Unitat Tècnica de Protecció Radiològica (UTPR-UAB).

Els Serveis Científico-Técnics de la Universitat de Barcelona (Espanya), amb una especial menció al Servei de Citometria.

Cada hora fer, sa darrera mata

Llegenda del rellotge de sol situat a la casa Vila, Palma

CONTENTS

Abreviations

53BP1	Q12888[1]	TP53-binding protein 1
ALT		Alternative lengthening of telomeres
alt-NHEJ		Alternative NHEJ
APB		ALT-associated promyelocytic leukaemia body
ATM	Q13315	Serine-protein kinase ATM
ATR	Q13535	Serine/Threonine-protein kinase ATR
B		TRF2 Basic domain
BFB		Breakage-fusion-bridge
BLM	P54132	Bloom syndrome protein
BRCA1	P38398	Breast cancer type 1 susceptibility protein
BUB1	O43683	Mitotic checkpoint serine/threonine-protein kinase BUB1
BUB3	O43684	Mitotic checkpoint protein BUB3
BUBR1	O60566	Mitotic checkpoint serine/threonine-protein kinase BUB1 beta
c-NHEJ		Classical NHEJ
CDKN2A	P42771	Cyclin-dependent kinase inhibitor 2A gene
CDT1	Q9H211	DNA replication factor Cdt1
CHK1	O14757	Serine/threonine-protein kinase Chk1
CHK2	O96017	Serine/threonine-protein kinase Chk2
CIN		Chromosome instability
CRISPR		Clustered regularly interspaced short palindromic repeats
CST		CTC1-STN1-TEN
CTC1	Q2NKJ3	CST complex subunit CTC1
CtIP	Q99708	DNA endonuclease RBBP8
d-loop		Displacement loop
DCIS		Ductal carcinoma *in situ*
DDR		DNA damage response
DKC1	O60832	H/ACA ribonucleoprotein complex subunit DKC1
DNA-PK		DNA-dependent protein kinase
DNA-PKcs	P78527	DNA-dependent protein kinase catalytic subunit
DOX		Doxycycline
ds-DNA		Double stranded-DNA
DSB		Double strand breaks
E2F		Transcription factor E2F family
E6	P03126	Protein E6
E7	P03129	Protein E7
EXO1	Q9UQ84	Exonuclease 1
FBS		Foetal bovine serum

[1] Swissprot number of the human variant

G4		Guanine quadruplexes
GAR1	Q9NY12	H/ACA ribonucleoprotein complex subunit 1
H		TRF1/2 Hinge domain
H2AX	P16104	Histone H2AX
HJ		Holiday junction
HMEC		Human mammary epithelial cell
hnRNPA1	P09651	Heterogeneous nuclear ribonucleoprotein A1
HPV-16		Human papillomavirus type 16
HR		Homologous recombination
HRP		Horseradish peroxidase
iDDR		Inhibitor of DDR region
Ku70	P12956	X-ray repair cross-complementing protein 6
Ku80	P13010	X-ray repair cross complementing protein 5
LATS2	Q9NRM7	Serine/Threonine-protein kinase LATS2
M		TRF1/2 Myb domain
Mad1	Q9Y6D9	Mitotic spindle assembly checkpoint protein MAD1
Mad2	Q13257	Mitotic spindle assembly checkpoint protein MAD2A
MRE11	P49959	Double-strand break repair protein MRE11
MRN		MRE11/RAD50/NBS1
MTS		Multitelomeric signals
MYC	P01106	Myc proto-oncogen protein
NBS1	O60934	Nibrin
NHEJ		Non-homologous end joining
NHP2	Q9NX24	H/ACA ribonucleoprotein complex subunit 2
NOP10	Q9NPE3	H/AC ribonucleoprotein complex subunit 3
NOP10-NHP2-GAR		Nucleolar protein family A member 1
p107	P28749	Retinoblastoma-like protein 1
p130	Q08999	Retinoblastoma-like protein 2
$p16^{INK4a}$	P42771	Cyclin-dependent kinase inhibitor 2A protein
p53	P04637	Cellular tumour antigen p53
p57	P49918	Cyclin-dependent kinase inhibitor 1C
PARP1	P09874	Poly [ADP-ribose] polymerase 1
PD		Population doubling
PINX1	Q96BK5	PIN2/TERF1-interacting telomerase inhibitor 1
POL		DNA Polymerase
POT1	Q9NUX5	Protection of telomeres protein 1
pRb	P06400	Retinoblastoma-associated protein
PVDF		Polyvinylidene fluoride
RAD50	Q92878	DNA repair protein RAD50
RAD51D	O75771	DNA repair protein RAD51 homolog 4
RAP		Repeat-addition processivity
RAP1	Q9NYB0	Telomeric repeat-binding factor 2-interacting protein 1

RIF1	Q5UIP0	Telomere-associated protein 1
RNF168	Q8IYW5	E3 ubiquitin-protein ligase RNF168
RPA		Replication protein A (RPA1-RPA2-RPA3)
RPA1	P27694	Replication protein A 70kDa-binding subunit
RPA2	P15927	Replication protein A 32 kDa subunit
RPA3	P35244	Replication protein A 14kDa subunit
RTEL1	Q9NZ71	Regulator of telomere elongation helicase 1
SAC		Spindle assembly checkpoint
SH-TO		Modified MCF-10A cell line; constitutively expresses shp53 and conditionally expresses TRF2$^{\Delta B\Delta M}$
shp53		short hairpin specific for p53
SLX4	Q8IY92	Structure-specific endonuclease subunit SLX4
ss-DNA		Single stranded-DNA
SSB		Single strand breaks
STN1	Q9H668	CST complex subunit STN1
SV-TO		Modified MCF-10A cell line; constitutively expresses SV40LT and conditionally expresses TRF2$^{\Delta B\Delta M}$
SV40LT		Simian vacuolating virus 40 Large T antigen
t-circle		Telomeric circle
t-loop		Telomeric loop
T-SCE		Telomere sister chromatid exchange
TACC2	Q95359	Transforming acidic coiled-coil-containing protein 2
TCAB1	Q9BUR4	Telomerase Cajal body protein 1
TEN	Q86WV5	CST complex subunit TEN1
TERC		Telomerase RNA component
TERRA		Telomeric repeat-containing RNA
TERT	O14746	Telomerase reverse transcriptase
TGF-β	P01137	Transforming growth factor beta-1 proprotein
Thr		Threonine
TIF		Telomere dysfunction-induced *foci*
TIN2	Q9BSI4	TERF1-interacting nuclear factor
TO		Modified MCF-10A cell line; conditionally expresses TRF2$^{\Delta B\Delta M}$ that expresses inducible cassette TRF2$^{\Delta B\Delta M}$
TPP1	Q96AP0	Adrenocortical dysplasia protein homolog
TREX1	Q9NSU2	Three-prime repair exonuclease 1
TRF		Telomeric restriction fragments
TRF1	P54274	Telomeric repeat-binding factor 1
TRF2	Q15554	Telomeric repeat-binding factor 2
TRFH		TRF1/2 Homodimerisation domain
vHMEC		variant HMEC
vHMEC-shp53		Modified vHMEC cell line; constitutively expresses a shp53
WRN	Q14191	Werner syndrome ATP-dependent helicase
WWTR1	Q9GZV5	WW domain-containing transcription regulator protein 1
XLF	Q9H9Q4	Non-homologous end-joining factor 1
XRCC1	P18887	X-ray repair cross-complementing protein 1

XRCC4	Q13426	X-ray repair cross-complementing protein 4
YAP1	P46937	Transcriptional coactivator YAP

Abstract

Telomeres are nucleoprotein structures that cap the end of chromosomes and protect them from illegitimate recombination through a lariat conformation or t-loop that is mainly promoted by TRF2 protein. Dysfunctional telomeres have been proved to be a mechanism capable of originating chromosome instability (CIN) in mouse and human cells, and promote tumorigenesis in mouse models.

This dissertation thesis aims to generate immortalised but unstable cells due to telomere deprotection through progressive telomere shortening and by TRF2 depletion, and to evaluate their tumorigenic potential. In **Work I**, $p16^{INK4a}$-deficient human mammary epithelial cells (vHMECs) lacking or not for p53 function through specific short-hairpin RNA inactivation, were karyotyped at different population doublings to evaluate chromosomal abnormalities and their evolution. In the absence of telomerase, vHMECs progressively shortened their telomeres and subsequent end-to-end fusions initiated breakage-fusion-bridge (BFB) cycles and promoted CIN. However, these unstable cells finally succumbed to cell cycle arrest, independently of their p53 checkpoint status. In contrast, hTERT overexpression in p53-proficient vHMECs resulted in cells able to proliferate indefinitely with a nearly stable karyotype, while immortalised p53-deficient cells showed signs of CIN that could be permissive with an evolving karyotype.

In **Work II** and **Work III**, acute telomere deprotection was induced by t-loop disassembly through transient expression of the dominant negative form of TRF2 ($TRF2^{\Delta B\Delta M}$) in the mammary cell line MCF-10A and in immortalised HMEC derived from cosmetic reductions of four healthy donors, respectively. In **Work II**, acute telomere deprotection phenotype was reflected by the presence of TIFs and by an increase of end-to-end fusions and anaphase bridges after $TRF2^{\Delta B\Delta M}$ induction. Anaphase bridges are considered the prelude to breakage-fusion-bridge cycles and subsequent karyotype reorganisations. However, no scars of BFB cycles or highly reorganised cells have been observed after transient expression of $TRF2^{\Delta B\Delta M}$, independently of the status of p53 and pRb proteins. Instead, diploid cells were enriched after successive cycles of telomere deprotection induction, thus suggesting that excessive telomere deprotection could be detrimental for the origin of cells with highly reorganised karyotypes. According with these results, in **Work III**, immortalised HMEC through hTERT and SV40LT overexpression transiently expressing $TRF2^{\Delta B\Delta M}$ (HMEC-TO) exhibited an increase of anaphase bridges. But after a minimum of five cycles of telomere protection and deprotection, $TRF2^{\Delta B\Delta M}$ expressing cells did not display scars of telomere deprotection and ongoing BFB cycles. In contrast to MCF-10A derived cell lines, the HMEC-TO cell lines exhibited a progressive increase of polyploid cells as a consequence of SV40LT immortalisation process. Independently of the cause of polyploidy increase, cells exposed to $TRF2^{\Delta B\Delta M}$ expression cycles did not exhibit a telomere dysfunction phenotype or either a tumorigenic potential, thus suggesting that $TRF2^{\Delta B\Delta M}$ expression provoked a deleterious effect over $TRF2^{\Delta B\Delta M}$ expressing cells and prevented CIN emergence.

In conclusion, the present dissertation provides evidence that telomere dysfunction acts as a double sword mechanism for genome integrity. On the one hand, telomere shortening induces a mild and progressive DNA damage that firstly is compatible with cell viability, until damage is high enough to induce cell death. On the contrary, shelterin dysfunction affects widely to all chromosomes inducing an

exacerbated cell response that is deleterious for cell viability and karyotype reorganisation. This Thesis illustrate that acute telomere deprotection through shelterin dysfunction could be a useful tool to impinge an exacerbated DNA damage and maintain genome integrity in human mammary cells.

Els telòmers són estructures nucleoprotèiques que segellen l'extrem cromosòmic i el protegeixen de la reparació il·legítima mitjançant la formació d'un llaç telomèric anomenat t-loop que està modulat per la proteïna TRF2. En les últimes dècades, s'ha demostrat que la disfunció telomèrica és un mecanisme capaç d'originar inestabilitat cromosòmica (CIN) en cèl·lules humanes i de ratolí i promoure la tumorigènesis en models murins.

L'objectiu d'aquesta tesi és immortalitzar cèl·lules telomèricament inestables i avaluar el seu potencial tumorigènic mitjançant la desprotecció telomèrica a través de l'escurçament telomèric o de la disfunció de la proteïna TRF2. En el **Treball I**, cèl·lules epitelials mamàries humanes deficients per $p16^{INK4a}$ (vHMECs) i deficients o no per p53 ($p53^{+/+}$) foren cariotipades a diferents temps de doblatge per avaluar la presència d'anomalies cromosòmiques i l'evolució del cariotip. En l'absència de la telomerasa, els telòmers s'escurçaren de forma progressiva fins esdevenir desprotegits, i la subseqüent reparació il·legítma dels extrems afavorí l'entrada en cicles de ruptura-fusió-pont (BFB) i disparà la CIN. Tanmateix, les cèl·lules inestables finalment moren independentment de la funcionalitat de p53. Per contra, la sobreexpressió d'hTERT en les cèl·lules vHMEC-$p53^{+/+}$ afavoreix la proliferació indefinida amb un cariotip gairebé estable, mentre que la immortalització de les cèl·lules vHMEC-shp53 amb signes de CIN és permissiva amb la proliferació cel·lular i l'evolució del cariotip.

Al **Treball II** i al **Treball III**, la desprotecció telomèrica aguda va ser induïda mitjançant l'expressió transitòria d'un dominant negatiu de TRF2 ($TRF2^{\Delta B\Delta M}$). El dany telomèric agut fou avaluat en la línia cel·lular epitelial mamària MCF-10A (**Treball II**) i en cèl·lules epitelials mamàries (HMECs) immortalitzades derivades de pacients sanes (**Treball III**). Al **Treball II**, la desprotecció telomèrica mitjançant $TRF2^{\Delta B\Delta M}$ generà un increment de TIFs, fusions telomèriques i ponts anafàsics. Els ponts anafàsics es consideren els inductors dels cicles (BFB) i de la posterior reorganització cariotípica. No obstant, no s'observaren reorganitzacions cromosòmiques derivades dels cicles BFB després de l'expressió transitòria del $TRF2^{\Delta B\Delta M}$, independentment de la funcionalitat de les proteïnes p53 i pRb. Després de successius cicles de desprotecció telomèrica, s'observà un increment en el nombre de cèl·lules diploides, tot suggerint que l'excessiu dany telomèric evitaria la proliferació d'aquelles cèl·lules que podrien esdevenir altament reorganitzades. Al **Treball III** s'expressà $TRF2^{\Delta B\Delta M}$ en HMECs immortalitzades mitjançant hTERT i l'antigen SV40LT (HMEC-TO). L'expressió transitòria del $TRF2^{\Delta B\Delta M}$ induí l'increment de ponts anafàsics, però les cèl·lules tampoc presentaren reorganitzacions pròpies dels cicles BFB en marxa. A diferència del **Treball II**, les cèl·lules poliploides incrementaren arrel del procés d'immortalització. Independentment de la causa d'aquest increment en les cèl·lules poliploides, les cèl·lules exposades als cicles d'expressió de $TRF2^{\Delta B\Delta M}$ no presentaven un fenotip associat a la disfunció telomèrica, ni tampoc un potencial tumorigènic, tot suggerint que l'expressió del mutant $TRF2^{\Delta B\Delta M}$ provoca un efecte deleteri sobre la viabilitat cel·lular i l'inici de la CIN.

En resum, la present tesi evidencia que el grau de dany telomèric és una eina de doble fil en el manteniment de la integritat genòmica. Per una banda, l'escurçament telomèric indueix un dany cel·lular progressiu i lleu, compatible amb la viabilitat cel·lular. Quan el dany telomèric assoleix un cert llindar, la cèl·lula activa mecanismes dependents i independents de p53 que indueixen la seva mort. Pel contrari, la

disfunció de TRF2 afecta a un nombre molt elevat de telòmers i indueix una exagerada resposta cel·lular que la fa incompatible amb la viabilitat cel·lular i la reorganització del cariotip. Aquesta tesi demostra que la desprotecció simultània d'un nombre elevat de telòmers pot ser una eina útil per generar un dany al DNA molt elevat i mantenir la integritat genòmica.

Introduction

1. Brief history of telomeres

Pioneer studies by Dr. Müller in *Drosophila melanogaster* showed that after X-ray irradiation, chromosomes broke, fused and rearranged with each other (Muller, 1938). However, these chromosomal rearrangements barely involved the chromosome termini, thus suggesting an inability of chromosome ends to fuse with the broken chromosomes. These studies led Dr. Müller to describe telomeres (from the Greek *telos*, "end", and *meros*, "part") as structures that seal the end of linear chromosomes and are functionally different from the rest of the chromosome (Muller, 1938). Simultaneously, Dr. McClintock's studies in *Zea mays* illustrated that after a mechanical chromatid breakage during meiotic anaphase I, single broken chromatids from each homologue chromosome fused at the position of the breakage. This fusion led to the formation of a dicentric chromatid. Subsequently, in the following anaphase (anaphase II), this dicentric chromatid could not freely segregate, as the two centromeres were pulled to the opposite poles of the cell. Then, due to the generated tension, the resulting chromatid bridge finally broke. The new broken ends were predisposed to fuse to each other in the daughter cells, forming a new dicentric chromatid, which would again start a new breakage-fusion-bridge (BFB) cycle (McClintock, 1941). Like Dr. Müller, she noticed that these fusions barely involved the end of unbroken chromosomes (McClintock, 1941; Muller, 1938). Therefore, both studies strongly suggested that telomeres protect chromosome ends from illegitimate rejoining and are essential for chromosome stability.

It was late in the 1970s that Dr. Blackburn and Dr. Gall elucidated the specific features of the *Tetrahymena termophila* telomeric sequence (Blackburn & Gall, 1978). This ciliate contains extrachromosomal linear molecules that encode for ribosomal RNA. These linear DNA material are flanked by 3'-$(TTGGGG)_n$-5' repeats, where n is between 20 and 70 repeats, and finishes in an undescribed stable structure (Blackburn & Gall, 1978). These features give the telomeric repeats the ability to function as a stable DNA end. Years later, Dr. Szostak and Dr. Blackburn generated a linear plasmid flanked with telomeric repeats from *Tetrahymena termophila* and they inserted it into *Saccharomyces cerevisiae* (Szostak & Blackburn, 1982). The *Tetrhaymena* plasmids remained stable inside the yeast cells (Szostak & Blackburn, 1982), thus, suggesting that the structural features of telomeres are highly conserved through evolution (Szostak & Blackburn, 1982). Indeed, telomeres are conserved G-rich sequences that end in a G-rich overhang (Wright *et al*, 1997), but they can vary between organisms in sequence, length, and number of repeats (Telomerase Database, 2013). These differences are notable in the case of invertebrates, plants, protozoa and fungi (Telomerase Database, 2013). In contrast telomere sequence in vertebrates is highly conserved being $(TTAGGG)_n$, regardless of telomere length and repeats (Meyne *et al*, 1989; Moyzis *et al*, 1988).

Dr. Szostak and Dr. Blackburn also reported that telomeres from *Tetrahymena* became longer and heterogeneous inside *Saccharomyces* (Szostak & Blackburn, 1982). Dr. Shampay *et al* went into detail about this oddity and found that the telomeres from *Tetrahymena* inserted in *Saccharomyces* contained the sequence of yeast telomeres, $C_{1\text{-}3}A$ instead of $(TTGGGG)_n$, in an apparently non-template-manner (Shampay *et al*, 1984). This report suggested that some yeast enzymes played a fundamental role in telomere replication. Following this line of evidence, in 1985, Dr. Greider and Dr. Blackburn found that *Tetrahymena* cell free extracts added TTGGGG repeats onto synthetic telomere primers, and this strand

elongation was the template for the synthesis of the complementary C-rich strand (Greider & Blackburn, 1985). The enzyme responsible for the addition of new telomeric restriction fragments (TRF) and telomere elongation *in vivo* was telomerase. Telomerase is a ribonucleic protein and has two different properties: first it hybridises with the 3' overhang (G-rich strand) through its RNA component (TERC), and secondly it elongates the telomeres through its catalytic domain (TERT) (Greider & Blackburn, 1987). In 1997, Dr. Cech *et al* described human telomerase, showing that its activity is related to the expression of hTERT catalytic domain (Lingner *et al*, 1997; Nakamura *et al*, 1997).

The connection between DNA loss due to inability to fully replicate DNA, as a cause of cell death was first associated by Dr. Olovnikov in 1973. He proposed the Theory of Marginotomy (Olovnikov, 1973) in which the limited division potential of human fibroblast (replicative senescence) observed by Dr. Hayflick and Dr. Moorhead (Hayflick & Moorhead, 1961) was related to the shortening of telomeres in every mitosis, due to the inability of conventional DNA polymerases to fully replicate telomeres. This theory was corroborated in the 1990s, when Dr. Harley *et al* described that the telomere length from human fibroblasts was inversely correlated with cell age *in vitro* and *in vivo* (Harley *et al*, 1990; Allsopp *et al*, 1992). This telomere shortening was influenced by three factors: the absence of telomerase expression in somatic human cells (Allsopp *et al*, 1992), the impossibility to fully replicate chromosome ends (Watson, 1972) and lastly the active degradation of the 5' chain to generate a single stranded-DNA, essential for t-loop formation and telomere-end protection (Makarov *et al*, 1997; Wright *et al*, 1997). The loss of telomeric sequences results in a progressive telomere shortening until a critical length is reached. At this point, the Hayflick limit, the cells enter into replicative senescence, i.e. the cells are arrested at G1 with an stable karyotype, although they are metabolically active (Hayflick & Moorhead, 1961; Campisi & d'Adda di Fagagna, 2007). Moreover, when telomerase was expressed in normal human somatic cells, they exceeded their normal lifespan by at least 20 population doublings (PDs) with a normal karyotype (Bodnar *et al*, 1998). Thus, establishing a causal relationship between telomere shortening and *in vitro* cellular senescence (Bodnar *et al*, 1998).

Mouse mTERC$^{-/-}$ models demonstrated the deleterious effect of telomere shortening on embryonic development, age-related diseases and lifespan (Blasco *et al*, 1997; Lee *et al*, 1998; Rudolph *et al*, 1999). However, the deletion or malfunction of critical genome-keeper proteins, such as p53, could spin the deleterious effect of telomere dysfunction. Instead, p53 deficiencies together with telomere shortening enhanced chromosome instability and promoted the generation of carcinoma tumours (Chin *et al*, 1999; Artandi *et al*, 2000).

2. Telomere Structure: DNA and Proteins

2.1. DNA

Mammalian telomeres are formed by TTAGGG tandem DNA repeats (Moyzis *et al*, 1988) that end in a single-stranded 3'-guanosine rich overhang (G-rich overhang or 3' overhang) (FIGURE 1A) (Wright *et al*, 1997; Makarov *et al*, 1997). Although the telomere structure is highly conserved among mammals, there is inter- and intra-species telomere length variability. For example, human telomeres length is between 9

and 15 kb (Allsopp *et al*, 1992), whereas telomere length in mice ranges from 10-80 kb (Zijlmans *et al*, 1997). Similarly, length variability between species also occurs in the G-rich overhang (Klobutcher *et al*, 1981; Wright *et al*, 1997; Makarov *et al*, 1997). In the case of human cells, the overhang measures between 150-200 nucleotides (Wright *et al*, 1997; Makarov *et al*, 1997), but in ciliated protozoans it is only 12-16 bases in length (Klobutcher *et al*, 1981). Importantly, this conserved DNA structure at the chromosome end plays an essential role in the formation of the telomeric-loop (t-loop), the lariat structure that caps linear chromosomes (FIGURE 1B-B') (Griffith *et al*, 1999). T-loops have been visualised in several organisms in the Eukarya domain, including ciliates, protists, plants, invertebrates and vertebrates (Griffith *et al*, 1999; Doksani *et al*, 2013; Raices *et al*, 2008; Cesare *et al*, 2003; Muñoz-Jordán *et al*, 2001; Murti & Prescott, 1999). In short, the t-loop originates through the invasion and pairing of the G-rich single-stranded (ss) overhang into the preceding C-strand of the ds-telomeric DNA tract, while the G-strand of the ds-telomeric DNA is displaced (Griffith *et al*, 1999). This G-rich overhang invasion process generates, a displacement-loop or d-loop in addition to the t-loop (FIGURE 1B).

T-loop formation and maintenance are promoted by specific proteins that interact with telomeric DNA throughout the cell cycle. Indeed, telomeric DNA is intimately associated with six proteins called shelterins that induces topology changes in the telomeric DNA chain to facilitate t-loop formation. Moreover, these proteins unwind telomeric DNA to assist telomere replication, modulate telomere protection and DDR (DNA Damage Response) activation and are also involved in the regulation of telomere elongation (Griffith *et al*, 1999; Sfeir & de Lange, 2012; Wu *et al*, 2012; Abreu *et al*, 2010). The lack of any shelterin protein, except RAP1 (Sfeir *et al*, 2010), results in telomere dysfunction, DDR activation, cell growth arrest and early embryonic lethality in mice (Karlseder *et al*, 2003; Chiang *et al*, 2004; Celli & de Lange, 2005; Hockemeyer *et al*, 2006; Wu *et al*, 2006; Kibe *et al*, 2010). In humans, mutations in some of these proteins are related with telomere disorders or telomeropathies (TIN2 in dyskeratosis congenita autosomal dominant 3 and 5, MIM numbers 613990 and 268130; TPP1 in dyskeratosis congenita autosomal recessive 7 and autosomal dominant 6, MIM number 616553), or enhance tumorigenesis (POT1 in glioma and melanoma, MIM number 616568 and 615848) (OMIM. Human genetics knowledge for the world, 2018).

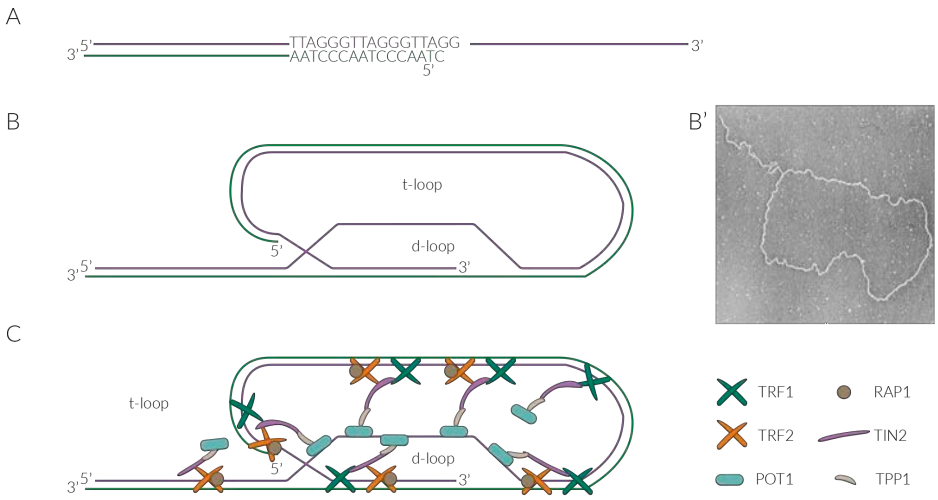

FIGURE 1. Telomere structure. **A.** Human telomeric DNA includes TTAGGG repeats that extends around 15 kb and ends in single stranded-DNA chain, the G-rich overhang. **B.** Telomeric DNA folds up and invades the previous double stranded-telomeric track to finally conform the t-loop structure. **B'.** Micrograph of t-loop from HeLa cells, obtained by Griffith *et al* 1999. **C.** The telomeric DNA is not a naked structure. The shelterin proteins bind to and associate specifically with telomeric DNA. These proteins induce conformational changes and regulate telomere elongation and protection.

2.2. Proteins: Shelterins

Shelterin proteins are a group of six proteins that specifically coat the telomeric DNA and regulate telomeric processes throughout the cell cycle (FIGURE 1C). These shelterin proteins are: telomeric repeat-binding factor 1 and 2 (TRF1 and TRF2), protection of telomeres protein 1 (POT1), TERF1-interacting nuclear factor (TIN2), Adrenocortical dysplasia protein homolog (ACD, also called TPP1), and Ras-related protein 1 (RAP1) (FIGURE 2). Shelterin proteins can be found as a single complex composed by the six proteins or different subcomplexes of interaction consisting mainly in TRF1-TIN2-TPP1-POT1 or RAP1-TRF2-TIN2-TPP1-POT1. Only three of them interact directly with the telomeric DNA. TRF1 and TRF2 interact with ds-DNA (Zhong *et al*, 1992; Chong *et al*, 1995; Broccoli *et al*, 1997) while POT1 interacts with single stranded-DNA (ss-DNA) (Baumann & Cech, 2001; Baumann *et al*, 2002). The other three shelterins modulate the telomere structure and function through protein-protein interactions (FIGURE 2). TIN2 directly links TRF1 and TRF2 (Ye *et al*, 2004a; Liu *et al*, 2004a) and indirectly POT1 through TPP1 binding (Liu *et al*, 2004b; Takai *et al*, 2011). Finally, RAP1 interacts specifically with TRF2 (Bae & Baumann, 2007; Sarthy *et al*, 2009; Arat & Griffith, 2012). Besides their interconnection, shelterin proteins act as a hub for other protein-protein interactions to regulate telomere protection and elongation (Palm & de Lange, 2008; Nandakumar *et al*, 2012; Zhong *et al*, 2012; Abreu *et al*, 2010; Frank *et al*, 2015).

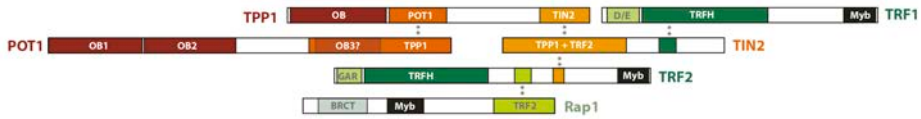

FIGURE 2. Shelterin proteins. The six shelterin proteins are integrated in a single complex through TIN2. This complex is anchored to telomeric repeats through Myb domains of TRF1 and TRF2 and OB folds of POT1. Protein protein interactions are indicated with asterisks. Adapted from (Palm & de Lange, 2008).

TRF2

TRF2 was first described by Dr. Broccoli *et al* as a highly conserved homodimer protein localised in all human telomeres that specifically binds to duplex TTAGGG repeats (Broccoli *et al*, 1997). TRF2 architecture consists of a basic (B) domain at its N-terminus, an homodimerisation (TRFH) domain, a flexible hinge (H) domain and a Myb (M) domain (FIGURE 3) (Broccoli *et al*, 1997). The B domain is essential for t-loop formation and prevention of Holliday-junction resolution (Wang *et al*, 2004; Fouché *et al*, 2006a). The TRFH and the H domains are involved in protein-protein interactions (Broccoli *et al*, 1997; Kim *et al*, 2009; Chen *et al*, 2008; Li *et al*, 2000; Okamoto *et al*, 2013). Specifically, TRFH contains the homodimerisation domain and also interacts with several proteins to regulate overhang processing and telomere protection to early DDR activation (Kim *et al*, 2009; Chen *et al*, 2008; Okamoto *et al*, 2013). Likewise, the H domain also contains a motif related to DDR that can sever the DNA signalling cascade at an advanced step (iDDR motif). Besides that, the hinge domain is essential for TRF2 direct association with TIN2 and RAP1 (FIGURE 2). These interactions are important for the shelterin complex formation and the efficient regulation of non-homologous end joining (NHEJ) activity (Kim *et al*, 2009; Chen *et al*, 2008; Li *et al*, 2000). Finally, the M domain directly binds with ds-DNA telomeric repeats (Broccoli *et al*, 1997).

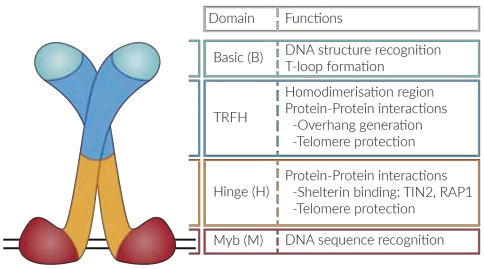

FIGURE 3. TRF2 structure and functions. TRF2 is a homodimer protein that directly interacts with telomeric DNA and multiple proteins. TRF2 is a key protein for t-loop conformation and is essential for telomere protection. Figure adapted from (Arnoult & Karlseder, 2015).

First TRF2 functions were evidenced by studies with a dominant negative form of TRF2, devoid of the B and the M domain ($TRF2^{\Delta B \Delta M}$), which demonstrated its implication in the formation of t-loops (Steensel *et al*, 1998). The modified protein was able to dimerise with endogenous TRF2. However, TRF2-$TRF2^{\Delta B \Delta M}$ complexes lacked the DNA binding capacity and consequently endogenous TRF2 was displaced from telomeres. At the chromosome level, the absence of TRF2 at telomeres resulted in unprotected chromosomes and the formation of end-to-end chromosome fusions (Steensel *et al*, 1998; Karlseder *et*

al, 1999). This is in agreement with studies showing the requirement of TRF2 for t-loop formation (Griffith *et al*, 1999; Doksani *et al*, 2013). However, the specific mechanism by which TRF2 promotes the lariat structure is still unknown. To enlighten how t-loops are formed, some studies suggest that the ability of TRF2 to modify the DNA topology is correlated with its 3' overhang invasion capabilities. Indeed, TRF2 generates positive supercoils and promotes DNA condensation. At the same time the untwisting of the DNA regions flaking the TRF2 binding sites, due to its condensation activity, favours telomeric DNA invasion (FIGURE 4) (Amiard *et al*, 2007). In these sense, strand invasion depends firstly on the interaction of TRF2 with the DNA, both in a structure specific dependent-manner (B domain) and through sequence recognition (M domain), and secondly on the ability of TRF2 to condensate the telomeric DNA (B and TRFH domain) (Amiard *et al*, 2007; Poulet *et al*, 2012). Moreover, other TRF2 interactors, such as TRF1-TERRA (Telomeric repeat-containing RNA) and RAP1, could modulate DNA condensation and, together with HR proteins, could regulate the overhang invasion (Poulet *et al*, 2012; Janoušková *et al*, 2015; Nečasová *et al*, 2017; Verdun & Karlseder, 2006; Lee *et al*, 2018).

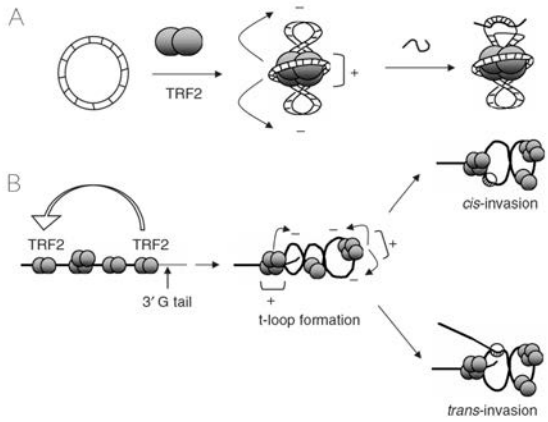

FIGURE 4. Proposed model for TRF2 mediation in DNA topology and DNA invasion. **A.** Model for TRF2 action in a telomeric plasmid. TRF2 would promote DNA condensation, and the formation of supercoils, but at the same time, would untwist other regions near the TRF2-DNA junctions. These relaxed regions could be new sites for DNA invasion. **B.** Model for TRF2 action in telomeric DNA. The condensation mediated by TRF2 would put 3' overhang closer to the ds-DNA, and then facilitate its invasion. The invasion could involve the overhang from the same DNA molecule (cis-invasion) or could involve the overhang of another telomere (trans-invasion). Figure from (Amiard *et al*, 2007).

In addition to the role of TRF2 in t-loop formation, it also protects the DNA ends from a complete **activation of the DNA damage response and repair activities** when the t-loop structure disorganises. Whereas long telomeres accommodate enough TRF2 to generate the t-loop and block DDR signalling (Cesare & Karlseder, 2013), insufficient TRF2 molecules drives t-loop to collapse. At this point, deprotected telomeres can coexist in two different states. In one state, the deprotected telomeres activate the DDR through ATM phosphorylation but retain enough TRF2 dimers to prevent repair activities. Early steps of DDR activation are demonstrated at unfolded ends by the presence of what are known as telomere-induced *foci* (TIFs), an accumulation of DDR proteins at chromosome termini (Takai *et al*, 2003). Besides that, another level of deprotection is observed when telomeres do not have enough

TRF2 dimers to prevent the full DDR cascade. At this point, NHEJ repair activities induce end-to-end fusions (Steensel *et al*, 1998; Smogorzewska *et al*, 2002; Celli & de Lange, 2005; Okamoto *et al*, 2013; Cesare & Karlseder, 2013). These different levels of deprotection pinpoint TRF2 as a master protein in DDR activation at telomeres. Indeed, TRF2 controls DDR activation through two independent steps (Okamoto *et al*, 2013). Firstly through a direct association with ATM, in which TRF2 prevents ATM dissociation and phosphorylation (Karlseder *et al*, 1999, 2004; Okamoto *et al*, 2013), and secondly, through its iDDR motif that prevents DDR propagation at the level of E3 ubiquitin ligase RNF168, which is essential for NHEJ activation (Okamoto *et al*, 2013). This dual modulation of the DDR by TRF2 is essential during S-phase, as allows t-loop disorganisation for telomeric replication while preventing NHEJ activation.

Another function of TRF2 during replication depends on **relieving topological constrains** that would hinder replication fork progression, such as the telomeric loop itself or the presence of G-quadruplexes (G4), a secondary DNA structure formed by G-rich DNA sequences. TRF2 helps the replication machinery to unwind the t-loops and G4 regions through the regulator of telomere elongation helicase 1 (RTEL1), Werner's syndrome protein (WRN) helicase and the exonuclease Apollo (Vannier *et al*, 2012; Sarek *et al*, 2015; Opresko, 2008; Ye *et al*, 2010). Despite the assistance of these proteins, the telomeric replication fork easily stalls due to the telomeric nature and configuration (Fouché *et al*, 2006b). In this circumstance, the replication machinery regresses and originates intermediate structures based on four DNA-stranded junctions called chickenfoot structures (FIGURE 5). In extratelomeric regions, the chickenfoot structures are disentangled *via* p53, which increases the rate of Holliday junction (HJ) cleavage by resolvase enzymes (Fouché *et al*, 2006b). In telomeric regions, these chickenfoot structures are recognised by TRF2, due to the ability of its B domain to recognise ds/ss-DNA transitions (Stansel *et al*, 2001; Fouché *et al*, 2006a). At that point, TRF2 recruits factors to unwind DNA and restart replication, such as the RecQ helicases WRN and Bloom syndrome helicase (BLM) (Fouché *et al*, 2006a). Strikingly, while TRF2 promotes HJs to form the t-loop it simultaneously prevents the completion of HJs, which would be catastrophic for the telomere structure by inhibiting resolvases (Poulet *et al*, 2009).

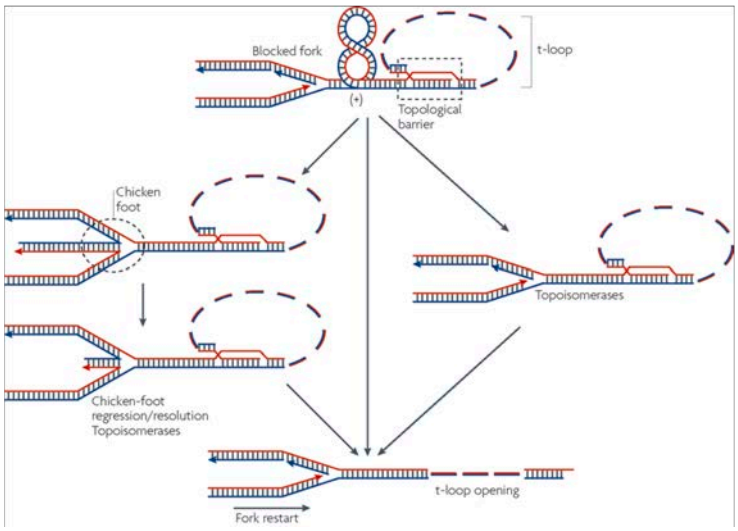

FIGURE 5. During telomere replication, replication forks easily stall, giving rise to intermediate structures that are signalled as DNA damage by ATM and ATR. This event gathers DNA damage factors and repair factors to restart replication, process 3' overhang ends and to conform and stabilise d-loop and hence the t-loop structure. Figure from (Gilson & Géli, 2007).

Another essential TRF2 function consists of the **formation of the G-rich overhang**, although other shelterin proteins such as POT1 and TPP1 are also needed to do so. After DNA replication, two types of ends are generated. While the leading ends conclude as a blunt extremity, the lagging end finishes with a short 3' overhang due to the end-replication problem (Watson, 1972). At this point, leading and lagging ends are processed differentially to generate an appropriate 3' overhang (FIGURE 6). The blunt end is initially resected by Apollo, which is recruited by TRF2 (van Overbeek & de Lange, 2006). Then the emergence of ss-DNA induces TPP1-POT1 recruitment to the overhang and subsequent POT1[1] loading blocks further Apollo processing (Wu *et al*, 2012). This does not occurs at the lagging strand, as POT1B binds to the short ss-DNA 3' overhang resulting from the incomplete DNA replication and blocks Apollo action (van Overbeek & de Lange, 2006; Wu *et al*, 2010). Then, when both ends have an small 3' overhang (Cannavo *et al*, 2013), the 5'-C rich-strand is degraded by exonuclease 1 (EXO1), thus overelongating the overhang during S/G2-phase (Wu *et al*, 2012). Then EXO1 is indirectly blocked by TPP1-POT1 through RIF1 (Kibe *et al*, 2016), and TPP1 recruits the CTC1-STN1-TEN (CST) complex, which subsequently recruits the polymerase α (POL-α), essential to fill in ss-DNA and restore the overhang length (Wu *et al*, 2012). During overhang resection, the presence of TPP1-POT1 at ss-DNA prevents the engagement of the NHEJ pathway leading to activation to DDR activation (Lam *et al*, 2010).

[1] These experiments have been conducted in mouse cells. Unlike human cells, mice cells have two POT1 proteins, POT1A and POT1B (Hockemeyer *et al*, 2006). POT1A is associated with ATR activation and elicits DDR at telomeres. POT1B is implicated in 3' overhang generation. Currently, the implication of human POT1 in the generation of 3' overhang needs to be determined.

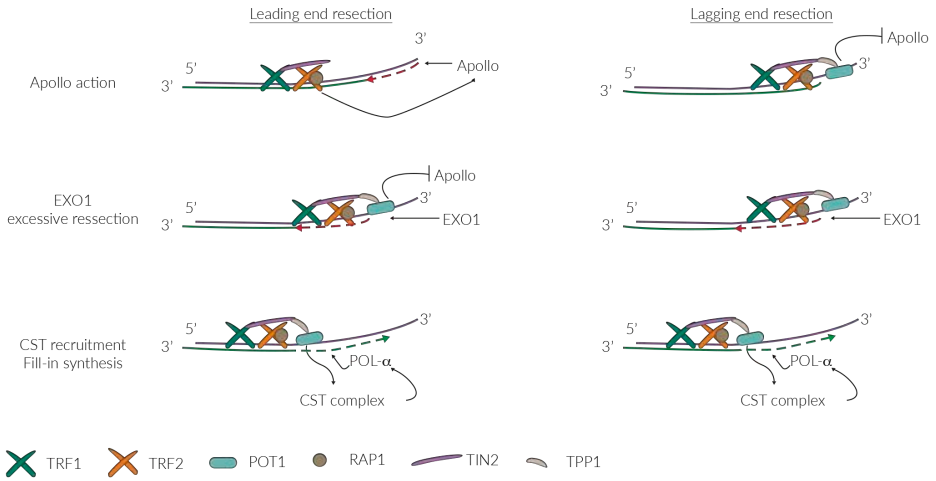

FIGURE 6. Shelterin implication in the G-rich overhang generation at leading and lagging ends.

Finally, as stated before, TRF2 promotes different types of **homologous recombination (HR) reactions**. But strikingly, at the same time, TRF2 blocks the termination of recombination events (Fouché *et al*, 2006a; Poulet *et al*, 2009; Nora *et al*, 2010). Specifically, during t-loop formation and just after telomeric invasion, TRF2 preferentially locates at or near ds/ss-DNA junctions (Stansel *et al*, 2001), and stabilises the strand invasion by binding to the resulting HJ (Fouché *et al*, 2006a; Poulet *et al*, 2009; Nora *et al*, 2010). At that point TRF2, together with RAP1, stabilises the HJ at the telomeric loop, thus blocking the activity of the HJ resolvases that would ultimately lead to t-loop excision (Rai *et al*, 2016). Similarly, TRF2 also prevents other HR events that can be produced at the chromosome terminus such as telomere sister exchanges (T-SCE) (Opresko, 2008; Vannier *et al*, 2012) or the alternative lengthening of telomeres (ALT) pathway (Pickett & Reddel, 2015).

TRF1

TRF1 is a homodimer protein structurally similar to TRF2 as both genes are considered paralogs (FIGURE 2) (Broccoli *et al*, 1997). In addition, although both proteins bind to ds-telomeric DNA, their functions of both proteins are significantly different. In contrast to TRF2, TRF1 has in its N-terminus an acidic domain, which inhibits DNA condensation and subsequent DNA invasion (Poulet *et al*, 2012). Finally, TRF1 interacts with TIN2 through the TRFH domain (Chen *et al*, 2008; Ye *et al*, 2004a), which allows the formation of a cohesive shelterin complex and a synergistic regulation of telomere protection and telomerase recruitment through TPP1-POT1 (Ye *et al*, 2004a; Zimmermann *et al*, 2014; Loayza & de Lange, 2003; Okamoto *et al*, 2008).

Classically, TRF1 has been documented to control telomere length by **regulating telomerase access** to the telomere. The overexpression of TRF1 in the HT1080 telomerase-positive tumour-cell line results in a gradual and progressive telomere shortening (Van Steensel & de Lange, 1997). In contrast, the expression of a dominant negative form of TRF1 ($TRF1^{66-385}$) that lacks the acidic and the Myb domain displaces TRF1 from telomeres and telomeres become longer (Van Steensel & de Lange, 1997;

Smogorzewska *et al*, 2000). This effect of TRF1 on telomere length is enforced by its interaction with PINX1, a protein that connects TRF1 to telomerase and regulates telomerase in a negative manner (Soohoo *et al*, 2011).

Besides the TRF1 function in telomere length homeostasis, it also plays an essential role in **controlling topological barriers during telomere replication**. As stated earlier, telomeres are G-rich and highly repetitive structures prone to form G-quadruplexes (G4) that prevent the normal replication fork progression (Hänsel-Hertsch *et al*, 2017). TRF1 binds to telomeric sequences and assists replication machinery by promoting DNA unwinding through the action of BLM and RTEL1 helicases (Bosco & de Lange, 2012). TRF1 also associates with topoisomerase IIα and Timeless, and their cooperation facilitates the telomeric DNA replication and resolution of telomeric intermediates (Leman *et al*, 2012; D'Alcontres *et al*, 2014). Moreover, during telomeric replication, it is suggested that TRF1 modulates TIN2-TPP1-POT1 to prevent replication-dependent loading of replication protein A (RPA) and activation of ataxia telangiectasia and Rad3 related (ATR) (Zimmermann *et al*, 2014). Overall, TRF1 protects chromosome ends against topological barriers that could unleash stalling replication forks and telomere fragility. In the absence of TRF1, the telomeres at metaphase appear broken or decondensed, showing multitelomeric signals (MTS) and an increase in chromosomal fusions (Okamoto *et al*, 2008; Martínez *et al*, 2009; Sfeir *et al*, 2009). This telomere fragility that resembles conventional aphidicolin-induced fragile sites is due to replication stress, as only occurs in cells that have passed through S-phase without TRF1 (Martínez *et al*, 2009; Sfeir *et al*, 2009). Fragile sites have been identified as heritable specific loci on human chromosomes that exhibit non-random gaps, constrictions or breaks after specific cell culture conditions (Lukusa & Fryns, 2008). In the case of TRF1 depletion, telomeric replication could be incomplete and could result in ss-telomeric regions or gaps. These ss-gaps are prone to load RPA protein and subsequent activation of ATR after replication fork progression (FIGURE 7) (Zimmermann *et al*, 2014). Therefore, ATR is activated as consequence of replication problems associated with TRF1 absence. This activation is mechanistically different from POT1 displacement from overhang that leads to single-stranded G rich overhang deprotection.

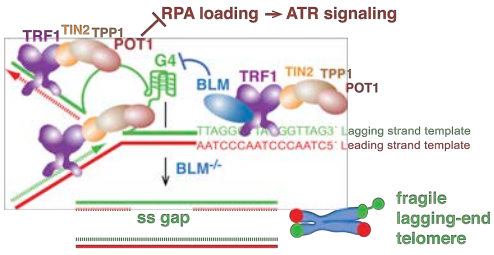

FIGURE 7. Model of replicative protection mediated by TRF1. TRF1 facilitate replication fork progression, while POT1 binds to the G-rich strand. TRF1 modulates TIN2-TPP1-POT1 and prevents RPA loading at ss-DNA and ATR activation. In the absence of TRF1 or BLM, replication problems are frequently observed and are biased towards lagging strands DNA synthesis. Figure from (Zimmermann *et al*, 2014).

Another suggested function for TRF1 is to control **chromatid cohesion during mitosis** (Ohishi *et al*, 2014; D'Alcontres *et al*, 2014) as in addition to telomeres, TRF1 also associates with mitotic spindle and

kinetochores (Nakamura *et al*, 2001). TRF1 overexpression induces mitotic failure with spindle aberrations (Muñoz *et al*, 2009). Moreover, some authors suggest that TRF1 directly associates with the spindle assembly checkpoint (SAC) proteins Mad1, Mad2 and BUBR1 (Muñoz *et al*, 2009; D'Alcontres *et al*, 2014), as well as with Aurora A kinase (Ohishi *et al*, 2010). Given that TRF1, together with Aurora A, has an essential role in the recruitment of Aurora B kinase at centromeres, TRF1 depletion results in loss of sister cohesion and merotelic attachments, which ultimately results in lagging chromosomes and micronuclei formation (Ohishi *et al*, 2014).

Finally, it has been suggested that TRF1 would **assist t-loop formation** and prevent the formation of R-loops, a three-stranded structure composed by DNA and RNA that will cause telomere loss (Lee *et al*, 2018). As mentioned earlier, TRF2 can stimulate DNA invasion to ds-telomeric DNA (Amiard *et al*, 2007; Poulet *et al*, 2012). Moreover, TRF2 could also promote the invasion of TERRA, with the subsequent formation of R-loops (Lee *et al*, 2018). The authors suggest that TRF1 would play a direct role in inhibiting the invasion of TERRA to ds-telomeric DNA, without affecting the DNA invasion (Lee *et al*, 2018). This inhibition would be achieved by blocking TERRA-TRF2 association (Lee *et al*, 2018).

POT1 and TPP1

POT1 is the third shelterin protein that directly interacts with ss-telomeric DNA through its two OB (oligonucleotide/oligosaccharide binding) folds, a DNA or RNA binding motif (Baumann & Cech, 2001; Baumann *et al*, 2002; Mitton-Fry *et al*, 2002). POT1 has specificity for ss-telomeric repeats, and can bind to the 3' overhang, the displaced chain when the t-loop is formed and/or other telomeric ss-DNA arising as a consequence of secondary DNA structures, such as G4 (Loayza *et al*, 2004). However, TPP1-TIN2 is needed for POT1 recruitment to telomeres, and stable association of POT1 with the shelterin complex (Liu *et al*, 2004b; Ye *et al*, 2004b; Hockemeyer *et al*, 2007). In line with this, POT1 is intimately associated with TPP1 and to TIN2 to form a complete shelterin complex (FIGURE 2) (Ye *et al*, 2004b; Liu *et al*, 2004b).

POT1 and TPP1 cooperate and together regulate overhang generation, the telomere protection, the telomerase recruitment of telomerase to telomeres and telomerase dependent-elongation (Wang *et al*, 2007; Hockemeyer *et al*, 2007; Wu *et al*, 2012). TPP1-POT1 act as a **telomerase recruitment and telomerase processivity factor** (Wang *et al*, 2007). In fact, TPP1 physically interacts with telomerase and recruits it after overhang generation (Zaug *et al*, 2010; Nandakumar *et al*, 2012), although, some authors suggest that this TPP1-telomerase interaction could also be mediated by TIN2 (Frank *et al*, 2015; Abreu *et al*, 2010). Besides that, it has been suggested that POT1 could be implicated in telomerase engagement to the 3' overhang (Hockemeyer & Collins, 2015). POT1 can slide on the ss-DNA by diffusing through the 3' overhang until the 3' end. And in view of the interaction of POT1 with TPP1 and TPP1 with telomerase, the diffusion of POT1 to the 3' end could bring telomerase closer to the overhang (FIGURE 8) (Hwang *et al*, 2012). However, at the same time, POT1 competes with telomerase for overhang association, and in fact POT1 deficiency results in overelongated telomeres (Ye *et al*, 2004b). Moreover, TPP1-POT1 prevents telomerase dissociation and stimulates the addition of multiple telomeric repeats after telomerase is assembled, a process called telomerase processivity (Wang *et al*, 2007), though other

shelterins could also act as processivity factors (Lim *et al*, 2017). In human cells, in a single binding and extension event, telomerase can add around 60 nucleotides (Zhao *et al*, 2009, 2011). It has been suggested that telomerase action is inhibited by the length of the overhang, and/or by the CST complex, which is recruited by TPP1 (Armstrong & Tomita, 2017; Chen *et al*, 2012; Feng *et al*, 2017). As TPP1 could recruit both telomerase and CST complex, CST complex might compete with telomerase for the 3' overhang.

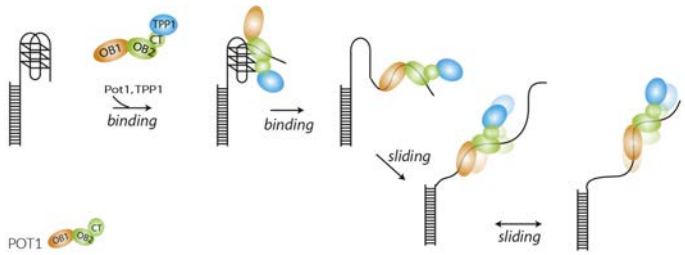

FIGURE 8. Sliding feature of POT1-TPP1. OB1, OB2 are the oligonucleotide/oligosaccharide binding folds from POT1 and CT represents the POT1 C-terminal. Figure from (Hwang *et al*, 2012).

The **telomere protection** function of POT1 depends on its capacity to bind the ss-telomeric DNA (Gong & de Lange, 2010). The protein RPA identifies single stranded breaks, binds ss-DNA, induces ATR activation and promotes DNA breakage repair. At telomeres, during replication, POT1 displaces RPA through the regulation of TERRA and the heterogeneous nuclear ribonucleoprotein A1 (hnRNP A1) (FIGURE 9) (Flynn *et al*, 2011). However, POT1 is less abundant than RPA and both proteins have similar affinities for telomeric DNA (Takai *et al*, 2011). It has been suggested that POT1 needs to be associated with TPP1 and TIN2 for an efficient RPA displacement (Takai *et al*, 2011), Therefore, the TPP1-POT1 complex, together with TIN2, are essential for telomere protection as they prevent the activation of ATR activation (Denchi & de Lange, 2007; Takai *et al*, 2011). The deficiency of any of these proteins results in overelongated overhangs (Hockemeyer *et al*, 2006; Kibe *et al*, 2016; Takai *et al*, 2011), which could induce HR and the generation of T-SCEs (Wu *et al*, 2006; Takai *et al*, 2011), an homologous recombination process between sister chromatids, and telomere circles (Wu *et al*, 2006). They also exhibit an strong DDR activation, reflected in ATR (Denchi & de Lange, 2007; Kibe *et al*, 2016; Takai *et al*, 2011; Frescas & de Lange, 2014) and ATM (Wu *et al*, 2006; Guo *et al*, 2007; Takai *et al*, 2011; Frescas & de Lange, 2014) activation, TIFs positive cells (Wu *et al*, 2006; Guo *et al*, 2007; Kibe *et al*, 2016; Frescas & de Lange, 2014; Denchi & de Lange, 2007; Xin *et al*, 2007; Takai *et al*, 2011) and a mild fusion phenotype (Hockemeyer *et al*, 2006; Guo *et al*, 2007; Frescas & de Lange, 2014; Denchi & de Lange, 2007; Takai *et al*, 2011).

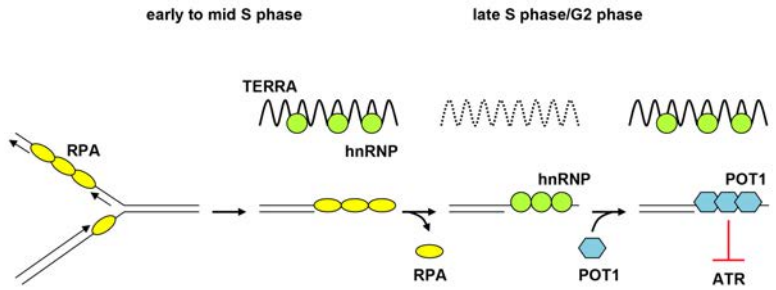

FIGURE 9. Model for RPA displacement and POT1 protection during telomeric replication. When DNA is replicated, RPA binds to ss-DNA in a structure-specific manner. At early S-phase, TERRA prevents RPA displacement by sequestering hnRNPs. At middle S-phase, TERRA levels decrease, and hnRNP is released. As a consequence, RPA is displaced from ss-DNA. At late S-phase TERRA levels increased and again recruits hnRNP. However, at this point, it is POT1 that binds irreversibly to ss-DNA in the presence of hnRNP instead of RPA. Finally, the presence of POT1 at ss-DNA prevents ATR activation. Figure from (Flynn *et al*, 2011).

TIN2

TIN2 is the central component of the shelterin complex as it is connected to POT1, TRF2 and TRF1 and its associated partners (FIGURE 2) and thus has the **essential structural task of maintaining and coordinating the shelterin proteins** (Ye *et al*, 2004a, 2004b; Liu *et al*, 2004b; Frescas & de Lange, 2014). TIN2 stabilises TRF2 at telomeres (Ye *et al*, 2004a), and is essential, through TPP1, for the recruitment of POT1 to the shelterin complex and ss-telomeric DNA (Liu *et al*, 2004b; Ye *et al*, 2004b). Moreover, as mentioned before, TIN2 interacts with TRF1 (Chen *et al*, 2008). Therefore, TIN2 depletion affects in the interaction between shelterin proteins. Accordingly, in cells that lack TIN2 the POT1-TPP1 complex is absent from telomeres and results in a phenotype equivalent to POT1 deficiency (Ye *et al*, 2004a; Takai *et al*, 2011; Frescas & de Lange, 2014) (SEE POT1 SECTION). Moreover, TIN2 stabilises TRF2 at telomeres and protects TRF1 from the action of tankyrases (Ye & de Lange, 2004; Ye *et al*, 2004a). TIN2 is reported to modulate the repression of ATM exerted by TRF2, without influencing subsequent NHEJ repair (Takai *et al*, 2011). It has been suggested that TIN2 depletion partially affects the presence of TRF2 and TRF1 at telomeres. While TIN2 depletion is equal to POT1-TPP1 removal, TIN2 abrogation is not associated with telomere fragility, thus suggesting that a small fraction of TRF1 is enough for proper telomeric replication (Takai *et al*, 2011; Frescas & de Lange, 2014).

Finally, it has been suggested that TIN2 plays a role in **telomerase recruitment**. Firstly, TIN2 protects TRF1 from poly(ADP-ribosyl)ation (PARP) by tankyrase 1. This TRF1 modification would displace TRF1 from telomeres allowing the accommodation of telomerase and subsequent telomere elongation (Ye & de Lange, 2004). Secondly and as mentioned earlier, TIN2 together with TPP1 could play a direct role in recruiting telomerase to telomeres (Frank *et al*, 2015; Abreu *et al*, 2010).

RAP1

The last shelterin protein is RAP1, a highly conserved protein from yeast to humans in both structural and protein functions (Hardy *et al*, 1992). Human RAP1 comprises 4 domains; from the N- to C-terminus

there is a BRCA1 C-terminal (BRCT), a Myb, a coiled-coil, and the RAP1-specific protein-interaction domain (RCT) (Kabir *et al*, 2010). The latter is essential for RAP1-TRF2 interaction, thus allowing recruitment of RAP1 to telomeres (FIGURE 2) (Li *et al*, 2000).

RAP1 **modifies the ability of TRF2 to bind and recognise telomeric DNA** (Arat & Griffith, 2012; Janoušková *et al*, 2015; Nečasová *et al*, 2017). It is suggested that RAP1 associated with TRF2 prevents unspecific TRF2-DNA interactions that are mediated by the B domain of TRF2 in a non-dependent sequence manner (FIGURE 10) (Janoušková *et al*, 2015). Therefore, RAP1 is proposed to partially release TRF2 molecules, thus enhancing the selectivity of TRF2 for DNA (Janoušková *et al*, 2015). This release might not affect TRF2 molecules placed near ss-DNA/ds-DNA junctions (Janoušková *et al*, 2015). In addition, the presence of RAP1 could be implicated in relieving DNA condensation, which is promoted by TRF2 (SEE TRF2 SECTION). Indeed, RAP1 stimulates the action of helicases, therefore promoting DNA unwinding (Nečasová *et al*, 2017). It is suggested that this balance between DNA winding and unwinding DNA is implicated in d-loop formation and stabilisation (Nečasová *et al*, 2017).

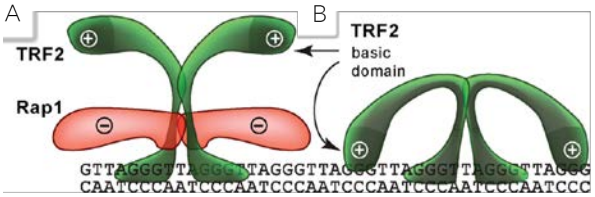

FIGURE 10. Model for improved selectivity of TRF2 for telomeric DNA mediated by RAP1. **A.** Specific TRF2-DNA interaction as electrostatic interactions between TRF2 and DNA may be blocked by RAP1. **B.** The absence of RAP1 allows non-specific electrostatic interactions between TRF2 and DNA. Figure from (Janoušková *et al*, 2015).

RAP1 also **cooperates with TRF2 to block NHEJ and HR** (Bae & Baumann, 2007; Sarthy *et al*, 2009; Sfeir *et al*, 2010; Rai *et al*, 2016). Given that TRF2 prevents the activation of ATM and DDR at telomeres, it has been proposed that the recruitment of human RAP1 at telomeres could also block NHEJ activation (Bae & Baumann, 2007; Sarthy *et al*, 2009), though some controversies exist (Sfeir *et al*, 2010; Chen *et al*, 2011). A prevalent role for RAP1 in HR has been assigned too, as in response to stress, human RAP1 co-immunoprecipitates with proteins related to HR and chromatin structure such as the Ku heterodimer, MRE11, RAD50, and PARP1 (O'Connor *et al*, 2004). In fact, an increase in T-SCEs has been detected when TRF2 and Ku70 are absent in mice fibroblast or when a TRF2 mutant, which lacks the RAP1 interacting domain, is expressed (Sfeir *et al*, 2010; Chen *et al*, 2011). This suggests that RAP1 is essential to repress HR at telomeres. Finally, it has been reported that RAP1 would prevent the location of PARP1 at telomeres, which would be responsible for the Holliday junction resolvase SLX4 activation and subsequent homologous recombination at telomeres (Sfeir *et al*, 2010; Rai *et al*, 2016).

3. Telomere length homeostasis

3.1. Telomere elongation: *de novo* addition and the ALT pathway

In most eukaryotes, telomere length is maintained by telomerase, which is a specialised reverse transcriptase that adds telomeric repeats to the 3' ends of chromosomes (Greider & Blackburn, 1985, 1987). Telomerase is composed of an RNA template (TERC), a catalytic domain (TERT) and the dyskerin complex, which stabilises telomerase and includes DKC1-NOP10-NHP2-GAR1 and TCAB1 (Nakamura *et al*, 1997; Lingner *et al*, 1997; Egan & Collins, 2010; Venteicher *et al*, 2009).

Telomerase expression, location, and action is tightly regulated. It is during S-phase that telomerase is transported to telomeres from Cajal bodies and/or the nucleoplasm (Tomlinson *et al*, 2006; Schmidt & Cech, 2015; Lewis & Tollefsbol, 2016; Hockemeyer & Collins, 2015). Once DNA replication is completed and the overhang has been processed, telomerase may assemble to telomeres and elongate them (Dionne & Wellinger, 1996). However, telomerase does not extend every telomere in every cell cycle. Indeed, telomerase elongation occurs preferentially at short telomeres (Teixeira *et al*, 2004; Bianchi & Shore, 2007). Even though initial hypothesis suggested an inverse correlation between the number of shelterin proteins and the telomerase recruitment, a much more complex process than a mere steric block of telomerase access to telomeres is envisaged due to the multiple proteins involved in telomerase recruitment. For example, TPP1 physically interacts and recruits telomerase, whereas TRF1 and POT1 prevent telomerase access to the overhang. In this sense, since shelterin stoichiometry studies reveal that TRF1 is much more abundant than TPP1 (Takai *et al*, 2010), this supports the notion that telomerase should be preferentially blocked at long telomeres. Indeed, TRF1 blocks telomerase through PINX1, a direct telomerase inhibitor (Soohoo *et al*, 2011), so longer telomeres would recruit more PINX1 and exert a higher telomerase inhibitor than shorter ones (Soohoo *et al*, 2011).

Recent studies suggest that TPP1-TIN2 and shelterin modifications could be implicated in telomerase recruitment. TPP1, through a TEL-patch motif, physically interacts and recruits telomerase (Zaug *et al*, 2010; Nandakumar *et al*, 2012). Some studies suggest that this recruitment requires TPP1-TIN2 association (Abreu *et al*, 2010; Frank *et al*, 2015). In fact, TIN2 is needed for TPP1 recruitment to telomere *in vivo*. Moreover, TIN2-TPP1 complex needs to be associated to DNA through TRF1, TRF2 or POT1, to efficiently act as a telomerase processivity factor (FIGURE 11) (Lim *et al*, 2017). Alternatively, TIN2 prevents TRF1 parylation, the addition of poly-ADP-riboses by tankyrases (Ye & de Lange, 2004). Parylated-TRF1 is partially and temporally released from telomeres (Smith & de Lange, 2000). This modification, together with the lower amount of TRF1 at telomeres, might be needed for telomerase access. Overall, TIN2 seems to be an upstream factor in telomerase recruitment and telomerase block.

Once telomerase is recruited at short telomeres, the 3' overhang needs to be captured by the active site of telomerase. This telomerase engagement seems to be orchestrated by TPP1-POT1, as it is suggested that the sliding motion of POT1 localises TPP1-telomerase at the overhang end (FIGURE 8) (Hwang *et al*, 2012). Nevertheless, it is suggested that POT1 competes with telomerase for overhang engagement, as POT1 deficiency results in overelongated telomeres (Ye *et al*, 2004b; Kelleher *et al*, 2005). For that

reason, it remains unknown how exactly telomerase is engaged to the 3' overhang. Once telomerase is engaged, telomeric DNA aligns with TERC (Feng *et al*, 1995), and new telomeric repeats are added to the 3' end (Greider & Blackburn, 1987; Nakamura *et al*, 1997; Lingner *et al*, 1997). Telomere elongation occurs without telomerase dissociation from telomeres (Zhao *et al*, 2011), which is called repeat-addition processivity (RAP) (Greider, 1991). Two models have been proposed to explain how telomerase repositions at the 3' end. And they differ in terms of which component, the telomeric DNA or the RNA template, is displaced. In the first one, the RNA template shifts, while telomeric DNA remains at or near the telomerase active site (Wu *et al*, 2017). Alternatively, the second model suggests that the newly synthesised DNA loops out due to structural flexibility of telomerase. Then the RNA template relocates at the end of DNA strand allowing further telomeric elongation (Yang & Lee, 2015). Despite the model used by telomerase, telomere elongation stops when telomerase dissociates from telomeres. This dissociation might be expedited through structural conformations adopted by long G-tails (Armstrong & Tomita, 2017). In addition, the CST complex, which interacts with TPP1-POT1, also competes and displaces telomerase from the 3' overhang (Chen *et al*, 2012). In actual fact, as mentioned before (SEE TRF2 SECTION), CST complex promotes the fill-in of the C-strand by recruiting polymerase-α (POL-α) (Chen *et al*, 2012).

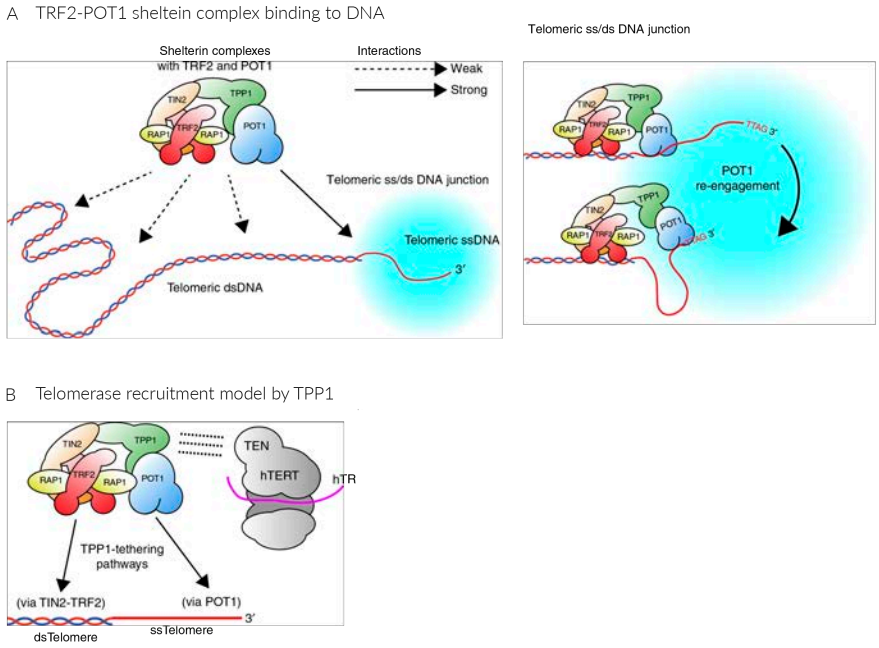

FIGURE 11. Model for shelterin binding to DNA and telomerase recruitment. **A.** TRF2-TIN2-TPP1-POT1 preferentially binds to ds/ss-DNA junctions due to the preferentially binding of TRF2 for ds-DNA and POT1 for ss-DNA. POT1 could slide for ss-DNA until the 3' end is reached. **B.** Telomerase is recruited through TPP1 and brings closer telomeres and telomerase due to its connection with TRF2-TIN2 and POT1-TIN2. Figure from (Lim *et al*, 2017).

Although telomerase is the main mechanism of telomere elongation, some cells can maintain telomere length independently of telomerase expression (Bryan *et al*, 1995; Bryan & Reddel, 1997). Alternative-lengthening of telomeres (ALT) is a mechanism that elongates telomeres based on recombination

(Dunham *et al*, 2000). In yeast, this recombinant mechanism is used as a backup to maintain telomere length and overcome senescence (Lundblad & Szostak, 1989; Lundblad & Blackburn, 1993). In telomerase-negative human cells, ALT can rapidly increase or decrease the length of the telomeres, resulting in chromosomes with high telomere length heterogeneity (Murnane *et al*, 1994; Bryan *et al*, 1995).

Two non-exclusive mechanisms based on recombination have been proposed to explain telomere elongation in ALT cells (Cesare & Reddel, 2010). The first of these, the unequal T-SCE model, proposes that after T-SCE one sister telomere will grow longer at the expense of the other. Therefore, one daughter cell would inherit shorter telomeres, and the other would inherit larger telomeres (FIGURE 12A). This unequal telomere lengthening might determine their proliferative capacity, as the cell with the shortest telomeres would achieve earlier senescence than the one with the longest telomeres (Cesare & Reddel, 2010).

The second model proposes a homologous recombination dependent-synthesis (FIGURE 12B). Specifically, a telomeric sequence is used as a template for the new synthesis of telomeric repeats. This template could be a telomeric sequence from another chromosome or a telomeric-circle (t-circle), i.e. circular telomeric ss- or ds-DNA, that could act as a rolling template. T-circles are frequently located in ALT-associated promyelocytic leukaemia bodies (APBs), ring-shaped nuclear bodies which are frequently observed in ALT cells. In addition to t-circles, APBs could contain linear telomeric DNA, PLM protein, telomeric proteins such as TRF1, TRF2 and HR related proteins (Yeager *et al*, 1999; Henson *et al*, 2002). The abundance of T-circles and APBs supports a roll-and-spread mechanism (Cesare & Griffith, 2004; Wang *et al*, 2004). And, unlike the unequal T-SCE model, this model results in a net gain of telomeric length as new telomeric repeats are synthesised *de novo* from a template (FIGURE 12B) (Cesare & Reddel, 2010).

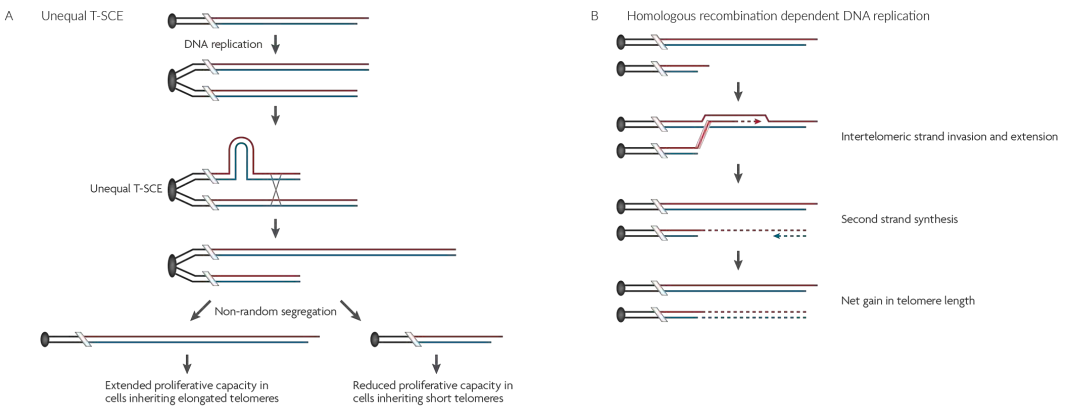

FIGURE 12. Proposed models for lengthening mechanisms in ALT cells. **A.** Unequal T-SCE model in which two daughter cells might inherit different telomere lengths as a result of T-SCE previous to cell division. **B.** Homologous recombination dependent DNA replication model. This model uses a template for a net telomere elongation. Figure from (Cesare & Reddel, 2010).

3.2. Telomere shortening: Trimming and end replication problem

Apart from elongation mechanisms, two other mechanisms are involved in telomere shortening. The trimming process results in a sudden massive deletion of telomeric sequences (Pickett *et al*, 2009). While the end replication problem is a progressive shortening of the telomeric DNA track inherent to replication of linear chromosomes (Watson, 1972; Olovnikov, 1973).

Trimming occurs when over-lengthened telomeres originate as a consequence of hTERT overexpression (Pickett *et al*, 2009), thus suggesting that to maintain telomere stability and integrity, telomere length must be balanced, not too short but not too long. Indeed, over-lengthened telomeres could induce replication stress due to G-rich and repetitive sequences nature of telomeres (Rivera *et al*, 2017). In HeLa cells when telomerase was overexpressed, telomere length of chromosomes increased until it reached a plateau. (Pickett *et al*, 2009). The stabilisation of the telomere length was accompanied by an increase in t-circles, extrachromosomal telomeric repeats, t-complex DNA [a highly branched telomeric DNAs with large numbers of internal single strand portions (Nabetani & Ishikawa, 2009)], and C-rich telomeric overhangs (Pickett *et al*, 2009, 2011), a phenotype often observed in ALT cells. The presence in HeLa cells of ALT features, although infrequent after trimming (Pickett *et al*, 2009; Rivera *et al*, 2017), were surprising as the Hela cell line is considered a telomerase-positive cell line.

Trimming was documented to occur in male germline in humans, especially in those individuals with larger telomeres, and in normal lymphocytes after telomerase upregulation (Pickett *et al*, 2011). In addition, telomere trimming has been described in two mice laboratory strains with larger telomeres (Pickett *et al*, 2011). This process occurs during G2/M, after the DNA synthesis and before chromatid separation (Pickett *et al*, 2009). Although the exact mechanisms behind the trimming process are still unknown, the absence of TIFs suggests that the trimming process does not result in telomere uncapping or telomere deprotection (Pickett *et al*, 2009). Moreover, it has been suggested that HR proteins are implicated. Indeed, HR-related proteins such as NBS1 or XRCC3 could promotes t-circles formation and C-overhang generation (Rivera *et al*, 2017). Finally, the simultaneous knockdown of NBS1 and XRCC3 results in telomere lengthening (Rivera *et al*, 2017).

In humans, not all cell types express telomerase abundantly. Indeed, telomerase is only expressed in germline tissues, most adult stem cells compartments and embryonic stem cells, since it is needed for cell self-renewal and proliferation. Therefore, telomerase expression is negligible in most somatic cells, thus bringing to light the end replication problem (Watson, 1972; Olovnikov, 1973). The limitations of the two main DNA polymerases (POL-δ or -ε) and the generation of the 3' overhang impede the complete replication of linear DNA. In eukaryotes, DNA replication initiates at multiple sites in the chromosome and then moves progressively along the parental DNA [replication process reviewed by (O'Donnell *et al*, 2013)]. This active region, known as replication fork, contains among others the DNA polymerases needed to synthesise the new daughter strands. Notoriously, these POL cannot start DNA synthesis by themselves, though they are able to elongate an existent RNA or DNA fragment. For that reason, to initiate replication, a small RNA primer is synthesised by the DNA POL-α-primase complex, which is

subsequently elongated by the POL-δ or -ε. Moreover, given the antiparallel nature of the duplex DNA and that polymerisation by POL only occurs in the 5' to 3' direction, the replication fork has an asymmetric structure. One of the daughter strands is synthesised continuously in the 5'-3' direction and is known as the leading strand. Whereas the lagging strand grows in a discontinuous manner by synthesising short DNA molecules called Okazaki fragments that are afterwards connected by ligase 1 (Okazaki *et al*, 1968; Sugimoto *et al*, 1968). This DNA synthesis mechanism encounters a problem when the replication fork reaches the chromosome end. In particular, a major concern is how the lagging ends are completely replicated at telomeres, as once each end RNA primer is removed, no POL (POL-δ or -ε) can load and synthesise the last chromosome nucleotides (FIGURE 13). Moreover, and in addition to the reduction in length due to replication intrinsic limitations, the resection of C-rich strand to overhang generation contributes substantially to the telomeric shortening (FIGURE 13), thus determining the cellular replicative potential (Hayflick & Moorhead, 1961; Olovnikov, 1973; Harley *et al*, 1990; Wu *et al*, 2012).

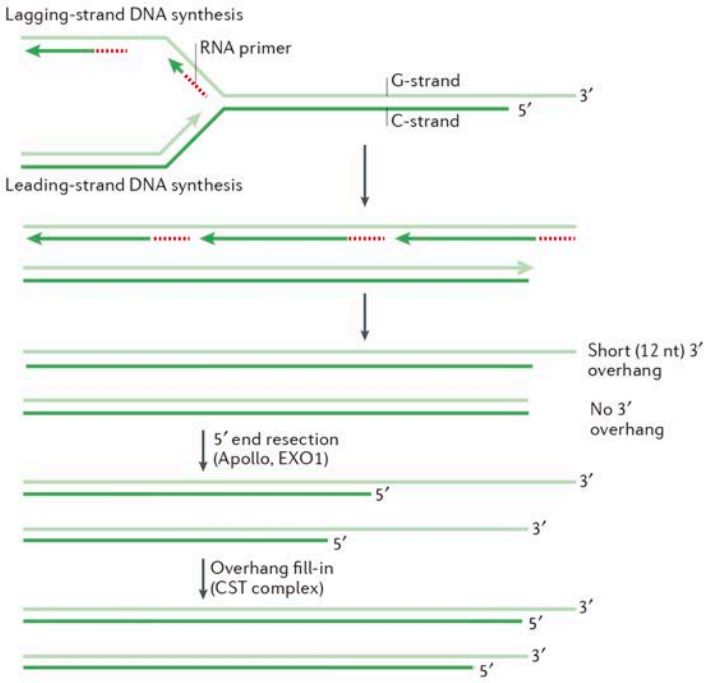

FIGURE 13. End replication problem model. Linear chromosomes cannot be fully replicated as the last RNA primer is lost in each cell division. Moreover, the resection of C-rich strand by Apollo and EXO1 contributes substantially to telomere shortening. This telomere loss can be offset with telomerase activity, as this enzyme has a telomeric template to assist the addition of new repeats at the 3' end. Figure adapted from (Maciejowski & de Lange, 2017).

4. Telomere deprotection: when the T-loop is compromised

As mentioned, primary human cells exhibited a replicative potential limit or cellular senescence (Hayflick & Moorhead, 1961) that has been associated to the progressive telomere shortening due to the end replication problem and the absence of telomerase activity (Harley *et al*, 1990). In the same way that

hTERT overexpression entails immortalisation and avoids senescence (Bodnar *et al*, 1998), the overexpression of TRF2 also delays the entrance in senescence by protecting extremely short telomere although it does not immortalise the cells (Karlseder *et al*, 2002). Therefore, senescence is a side effect of the telomere protection loss owing to telomere shortening or shelterin dysfunction.

4.1. Dysfunctional telomeres are recognised as DSB/SSB

Telomere deprotection entails p53 activation and, depending on cell type, the entrance into senescence or apoptosis (Shay *et al*, 1991; Hara *et al*, 1991; Karlseder *et al*, 1999) as a critical and potent tumour suppression pathway. The analysis of senescent human fibroblast revealed that many DDR markers are localised at extremely short telomeres, thus suggesting that DDR factors contribute to the cell growth arrest (di Fagagna *et al*, 2003). The inhibition of ATM and ATR proteins, main sensors of DSBs and SSBs, or CHK1 and CHK2, S- and G2-checkpoint proteins, allows senescent cells to exit senescence and reinitiate proliferation (di Fagagna *et al*, 2003).

The importance of ATM signalling for detection of unprotected telomeres comes also by the prevention of 53BP1 accumulation at telomeres by PI3K inhibitors (Takai *et al*, 2003). 53BP1 protein is responsible for inducing DNA repair activities through NHEJ (Dimitrova *et al*, 2008). When TRF2 is abrogated by short-hairpin RNA against TRF2 or displaced by $TRF2^{\Delta B \Delta M}$ from telomeres, 53BP1 protein localises at chromosome ends (Takai *et al*, 2003). Consequently, ATM deficient cells fail to detect dysfunctional telomeres when TRF2 is inhibited (Takai *et al*, 2003). Overall, dysfunctional telomeres are detected mainly by ATM which activates and recruits other DDR factors, such as H2AX and 53BP1, and are visualised as telomere dysfunction induced foci (TIFs) (Takai *et al*, 2003). This ATM activation arises when telomeres are structurally linearised by altered TRF2 (Van Ly *et al*, 2018) or excessively short telomeres. ATM is suppressed at chromosome ends when telomeres are in a t-loop conformation (Van Ly *et al*, 2018). TRF2 binds ATM and prevents its activation at telomeres by inhibiting ATM autophosphorylation and ATM oligomers dissociation (Karlseder *et al*, 2004).

In addition to eliciting a DDR mediated by activation of ATM, when telomere protection is compromised through POT1 deficiency or excessively short telomeres, ATR and DNA-PKCs signalling are promoted as a consequence of overhang deprotection and chromosome end exposure, respectively (Takai *et al*, 2003; Guo *et al*, 2007; Denchi & de Lange, 2007). Indeed, POT1 competes with RPA protein for telomeric ss-DNA, and indirectly prevents ATR activation (Flynn *et al*, 2011). But, in case of overhang deprotection or TPP1-POT1 abrogation, RPA binds to ss-DNA and activates ATR, which phosphorylates CHK1 (Guo *et al*, 2007; Denchi & de Lange, 2007). The activation of ATR could indirectly drive to ATM activation through dicentric formation and BFB cycles resolution (Wu *et al*, 2006; Guo *et al*, 2007). Moreover, ATR activation can also promote repair processes, considering that the simultaneous abrogation of ATM, TRF2 and POT1 in cells but not ATR results in TIFs formation and telomeric fusions (Denchi & de Lange, 2007).

Overall, the abundance of shelterin proteins depends on the length of telomeres and determines the protection status. TRF2 and POT1 proteins sense telomere length and regulate DDR activation.

Therefore, when a critical length is reached, deprotected telomeres lead to both ATM and ATR activation through TRF2 and POT1 mediation respectively.

4.2. Telomeres coexist in 3 protection states

The occurrence of spontaneous telomere deprotection in immortalized cancer cells during replicative aging, as well as the presence of dysfunctional telomeres resistant to repair processes suggested a model of telomere protection. This model relies on a telomere length and the abundance of shelterin proteins, mainly TRF2, and proposes three different states of protection (Cesare *et al*, 2009).

In the first state of protection, the capped structure, or **closed-state,** occurs when telomeres are long enough to conform t-loop structure and accommodate enough TRF2 proteins along telomeric chromatin (FIGURE 14A). This state confers plenty protection against DDR activation, as chromosome ends are masked by the t-loop, and TRF2 prevents ATM activation (Cesare *et al*, 2009).

Telomere shortening and subsequent reduction of TRF2 proteins lead to an **intermediate state** of protection. This state of protection displays dysfunctional telomeres (TIFs) resistant to chromosome fusions. In other words, telomeres are not long enough to conform t-loop, activating ATM and H2AX, but retain enough TRF2 protein levels to prevent chromosome end fusions (FIGURE 14B) (Cesare *et al*, 2009). Besides that, intermediate telomeres can also be originated when t-loop assembly fails after DNA replication, or when TRF2 levels diminish or POT1 inhibition takes place (FIGURE 14B). Although intermediate telomeres are detected as DSB and activate DDR signalling, they functionally differ from internal DSB (Cesare *et al*, 2013). Intermediate telomeres do not engage CHK2 activation, a downstream target of ATM. This effect is due to TRF2-CHK2 interaction, in which CHK2 phosphorylation site (Thr68) is masked (Buscemi *et al*, 2009). After internal DSBs, CHK2 phosphorylation contributes to G2/M checkpoint. In case of intermediate telomeres, the absence of CHK2 phosphorylation avoids the checkpoint activation (Cesare *et al*, 2013). As consequence, intermediate telomeres are passed through mitosis and accumulate in the daughter cells (Cesare *et al*, 2013; Kaul *et al*, 2012). This intermediate state telomeres are fusion resistant, as TRF2 exerts a major inhibition through NHEJ activation than DSB signalling. NHEJ is inhibited upstream of 53BP1, as TRF2, through the iDDR motif, indirectly inhibits RFN168, which is essential for its recruitment (Okamoto *et al*, 2013). Therefore, intermediate telomeres could be considered as a fusion resistant DDR-positive telomeres that protect cells from illegitimate rejoining. In fact, in human fibroblasts, once a threshold of 4-5 fusion-resistant TIFs is reached, G1 cells enter into p53-dependent replicative senescence, assuring an stable karyotype (Kaul *et al*, 2012).

Although human fibroblasts stop dividing when a DNA damage threshold is achieved, the abrogation of p53 and pRb allows continued proliferation with the subsequent telomere erosion (Shay *et al*, 1991). The **uncapped telomeres** are those telomeres that cannot prevent NHEJ repair. This state is mainly achieved when telomeres are too short and do not retain enough TRF2 protein levels, or otherwise uncapped telomeres could originate after a complete loss of TRF2 protein (FIGURE 14C) (Cesare *et al*, 2009). Uncapped telomeres are first signalled by ATM and γ-H2AX and are subsequently repaired, giving rise to

end-to-end fusions, which could fire chromosome instability (CIN) because of their entrance into BFB cycles (Hoffelder *et al*, 2004; Soler *et al*, 2005).

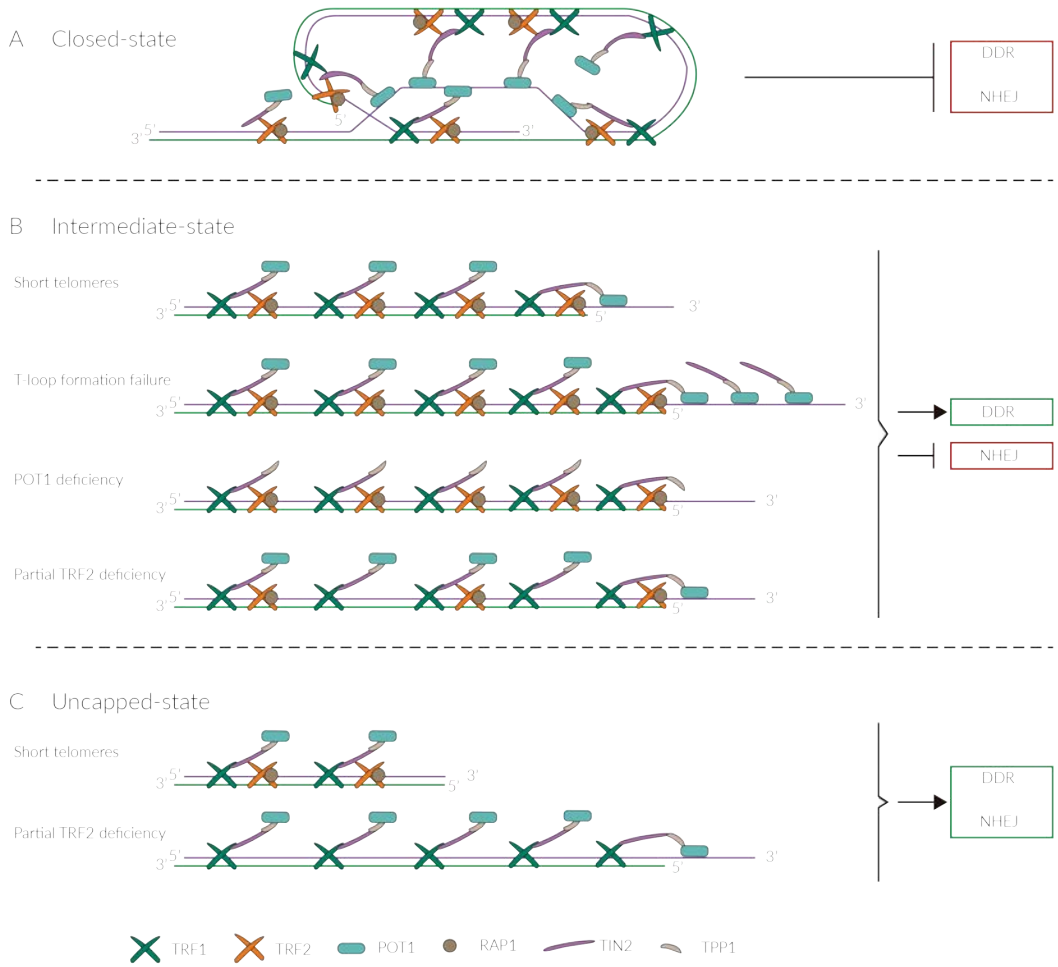

FIGURE 14. The three states of a telomere protection model. **A.** The closed-state confers a full protection *status* as prevents DDR activation and repair processes. This protection state is achieved when telomeres are long enough to conform t-loop structure, and there are enough shelterin proteins to support it. **B.** The intermediate state confers a partial protection *status* as dysfunctional telomeres are detected as DSBs. However, the presence of enough TRF2 proteins prevents the activation of NHEJ. This state of deprotection could originate as consequence of telomere shortening, a failure in t-loop conformation or shelterin deficiency. **C.** In case of uncapped-state, telomeres are too short and do not contain enough shelterin proteins to prevent DSB signalling. Therefore, DDR is activated and leads to NHEJ activation that ends-up in end-to-end fusions.

4.3. DSB repair activities at dysfunctional telomeres: NHEJ and HR

As mentioned before, telomeres confer chromosomal protection against illegitimate recombination and degradation. Classically, this protection was attributed to the telomeric length. The longer telomeres are, the longer they would be protected. However, as mentioned before, the telomeric protection does not depend completely on the telomeric length, as a balance between telomere length and shelterin protein is needed (Karlseder *et al*, 2002; Cesare *et al*, 2009; Cesare & Karlseder, 2013). In this case, deprotected telomeres, regardless whether it is due to telomere shortening or TRF2 abrogation (Bailey *et al*, 2001;

Karlseder *et al*, 2002; Smogorzewska & de Lange, 2002), are preferentially repaired through NHEJ, as 53BP1 and ligase 4 are involved in telomeric fusions (Smogorzewska *et al*, 2002). Nevertheless, telomeric protection is much more complex and redundant. Indeed, besides NHEJ, shelterin proteins and t-loop conformation prevents HR, alternative-NHEJ (alt-NHEJ) and the 5' end resection (FIGURE 15) (Wang *et al*, 2004; Sfeir & de Lange, 2012).

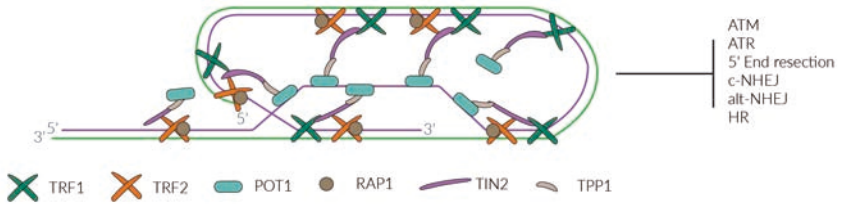

FIGURE 15. Telomeres confer chromosome end-protection. The closed structure of t-loop together with the shelterin proteins prevent the end resection, ATM and ATR activation as well the repair pathways classical NHEJ, alternative NHEJ and homologous recombination.

Classical (or canonical) NHEJ (c-NHEJ) pathway is activated after a DSB is detected, and requires the 53BP1 recruitment and ligase 4 (FIGURE 16) (Smogorzewska *et al*, 2002). TRF2 modulates c-NHEJ at several steps. First of all, and as mentioned, TRF2 through iDDR motif at the H domain blocks the recruitment of RNF168, which is essential for 53BP1 recruitment at DSBs (Okamoto *et al*, 2013). Moreover, unlike Ku in genomic DNA, TRF2 interacts with Ku70 and prevents tetramerization of the Ku70/80 heterodimers located at DNA ends (Ribes-Zamora *et al*, 2013; Doksani *et al*, 2013). Ku70/80 is a ring shape heterodimer that localises at the DSBs and is essential for the progression of c-NHEJ. In case of telomere deprotection, Ku70/80 dimer is formed, associates with DNA and tetramerise with another Ku70/80 dimer. Then, the Ku tetramer (Ku70/80-Ku70/80) interacts with kinase catalytic subunit (DNA-PKcs) to conform DNA-dependent protein kinase (DNA-PK) (Gottlieb & Jackson, 1993). Finally, DNA-PK promotes the ligation of DSB or dysfunctional telomeres through the recruitment of XRCC4-XLF-ligase 4 complex (Calsou *et al*, 2003; Smogorzewska *et al*, 2002; Lieber, 2010).

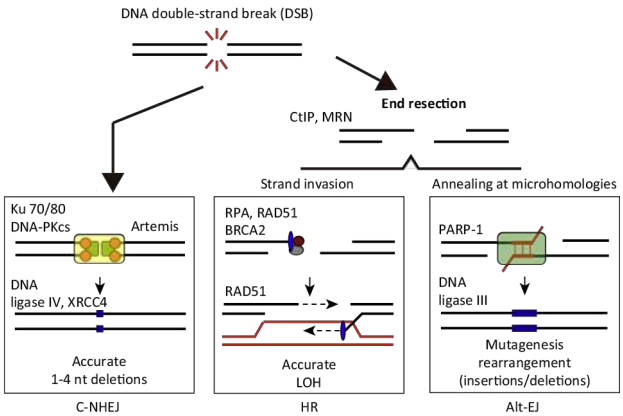

FIGURE 16. DNA repair pathways. DSBs at NHEJ are mainly repaired by NHEJ. Shelterin proteins also block end-resection that are the prelude of HR and alternative-NHEJ. Figure adapted from (Ceccaldi *et al*, 2016).

Homologous recombination (HR) (FIGURE 16) machinery is implicated in the formation and conformation of the telomeric protective structure just after telomeric DNA replication (Verdun *et al*, 2005; Verdun & Karlseder, 2006). More specifically, during telomeric replication, TRF2 is reported to cooperate with RTEL1 to properly unfold t-loop structure, probably by displacing 3' end of the telomere to allow t-loop unwinding (Vannier *et al*, 2012). Unfolded t-loop is proposed to create an stalled replication fork-like structure that could be detected by MRE11 and RPA, activating ATR/ATM-dependent response (Verdun & Karlseder, 2006). This signalling activation would be necessary to finish telomere replication and promote 3' overhang generation (Verdun & Karlseder, 2006). Finally, 3' overhangs invade the ds-telomeric sequences in a HR-dependent reaction, thus conforming t-loop protective structure (Verdun & Karlseder, 2006). Deficiency in HR proteins (Jaco *et al*, 2003; Tarsounas *et al*, 2004), shelterin proteins (Wang *et al*, 2004; Rai *et al*, 2016) or t-loop associated proteins such as RTLE1 (Vannier *et al*, 2012) would lead to t-loop resection and telomere shortening, mediated by the Holliday junction resolvase XRCC3 and NBS1 (Wang *et al*, 2004). Alternatively, T-SCEs or ALT are products of HR activity. The inhibition of TRF2, RAP1 or POT1 in context of Ku70/80 deficiency stimulates exchange of sequences telomeres on sister chromatids (Sfeir & de Lange, 2012; Celli *et al*, 2006; Palm *et al*, 2009). However, how Ku and shelterin proteins prevent HR is not well understood (Lazzerini-Denchi & Sfeir, 2016). About ALT, the inhibition of several proteins implicated in repair, such as MRN, BLM, WRN, RPA, XRCC3, RAD51D or others results in loss of ALT features and/or telomere shortening (Gocha *et al*, 2013).

Alternative-NHEJ (alt-NHEJ) is a backup mechanism in case of c-NHEJ or HR failure as it is repressed by TRF1, TRF2, POT1 and Ku proteins (Sfeir & de Lange, 2012). The simultaneous abrogation of POT1 or TPP1 in TRF2-ATM deficient mice results in telomere fusions due to 3'overhang deprotection and ATR activation (Denchi & de Lange, 2007). In contrast to c-NHEJ, alt-NHEJ can depend on CtIP and MRN as upstream factors that will promote the 5' end resection (FIGURE 16) (Rass *et al*, 2009; Rai *et al*, 2010; Lee-Theilen *et al*, 2011; Zhang & Jasin, 2011). It has been suggested that 53BP1 blocks alt-NHEJ as prevents the initial 5' resection through RIF1 (Zimmermann *et al*, 2013; Rai *et al*, 2010; Rybanska-Spaeder *et al*, 2014). Moreover, this repair pathway used PARP1, XRCC1, ligase 3 and POL θ to repair DNA damage (Audebert *et al*, 2004; Wang *et al*, 2005, 2006; Robert *et al*, 2009; Cheng *et al*, 2011; Simsek *et al*, 2011). POL θ is an error prone and terminal transferase-like activity polymerase that randomly inserts nucleotides at the junction of telomeres fused (Mateos-Gomez *et al*, 2015; Wood & Doublié, 2016). This polymerase could contribute to the high frequency of deletions and insertions (Nussenzweig & Nussenzweig, 2007). These factors together with regions of microhomology and translocations constitute the hallmarks of alt-NHEJ (Nussenzweig & Nussenzweig, 2007).

Finally, chromosome ends are protected from **nucleolytic processing at 5' end**. This protection occurs even when TRF1 and TRF2 have been depleted from cells, or when this depletion occurs simultaneously to Ku deficiency (Sfeir & de Lange, 2012). In addition, the simultaneous abrogation of TRF1-53BP1 or TRF2-53BP1 prevents end resection. However, the TRF1-TRF2 double-knockout and the 53BP1 results in an increase of 3'overhang signal, promoted by CtIP, BLM and EXO1, and telomere fusions (Sfeir & de Lange, 2012). More specifically, 53BP1 prevents the end resection through RIF1 in an ATM and ATR dependent manner (Zimmermann *et al*, 2013; Kibe *et al*, 2016). Moreover, this resection inhibition

prevents BRCA1 accumulation at DSBs (Zimmermann *et al*, 2013). BRCA1 is one of the main mediators of HR. Therefore by blocking 5' resection, HR is indirectly prevented, and c-NHEJ could be promoted (Bunting *et al*, 2010; Zimmermann *et al*, 2013).

5. Telomere dysfunction and CIN

Cellular senescence or apoptosis are not the only fates that could originate from telomere dysfunction. In fact, some cell types can bypass this growth barrier due to cell-cycle checkpoint deficiencies and continue proliferating. For example, human mammary epithelial cells (HMECs), can bypass an stress linked frost growth barrier (stasis) due to hypermethylation of CDK2AN promoter (FIGURE 17) (Brenner *et al*, 1998). Once occurred, cells can continue dividing up to a second growth barrier, which is determined by an exhaustion of telomere length and very reorganised karyotypes (agonescence or crisis) (FIGURE 17) (Garbe *et al*, 2009).

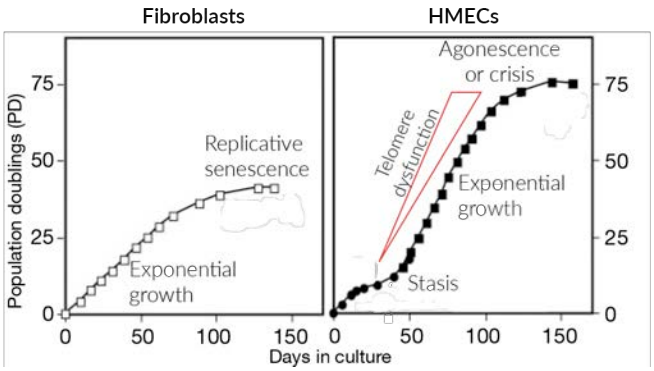

FIGURE 17. Differences in cell culture growth between human fibroblast cell lines and human mammary epithelial cell lines (HMECs). After stasis, chromosome instability is fired due to telomere dysfunction. Very reorganised HMECs will die by p53 dependent mechanisms (agonescence) or by p53-independent mechanisms (crisis). Figure adapted from (Romanov *et al*, 2001).

The study of HMECs during this second proliferative window has revealed that eroded telomeres can be repaired with each other and fire BFB cycles, which would massively scramble the cell karyortype [reviewed by (Genescà et al, 2011)] (FIGURE 18). Telomere dysfunction originates structural reorganisations when a chromatin bridge is formed and breaks during cell division (FIGURE 18). Specifically, dicentric chromosomes can be pulled to opposite spindle poles and bridge in the cell equator during anaphase (FIGURE 18) (McClintock, 1941). Usually, those bridges break due to the strong tension exerted by the mitotic spindle, or suffer chromothripsis, a hazardous process of breakage and repair of DNA (Stephens *et al*, 2011; Maciejowski & de Lange, 2017) that is usually associated with an hypermutation process called kataegis (Nik-Zainal *et al*, 2012; Roberts *et al*, 2013; Maciejowski *et al*, 2015) (FIGURE 19). Then, the resulting chromosome fragments can be included in the main nucleus or form micronucleus, in which case chromosome fragment could be degraded. Therefore, daughter cells would inherit highly fusogenic and unbalanced genomic material. Finally, the broken ends can easily re-join with another deprotected telomeres or other genomic DSBs (Latre *et al*, 2003; Tusell *et al*, 2008) and engender new dicentric chromosomes that would be susceptible to re-start a new BFB cycle (FIGURE

18). Altogether, BFB cycles are the main mechanism for the generation of structural imbalances such as deletions, amplifications, and non-reciprocal translocations (Hoffelder *et al*, 2004; Soler *et al*, 2005; Tusell *et al*, 2008).

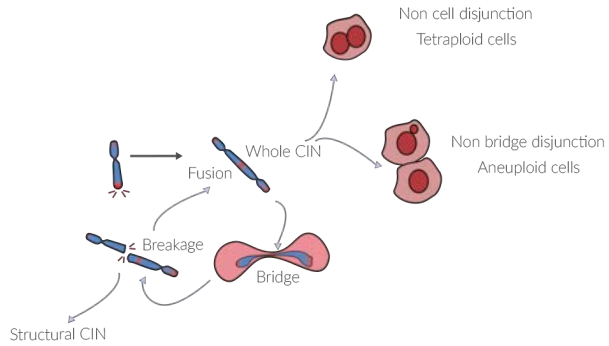

FIGURE 18. Telomere dysfunction, BFB cycles and CIN

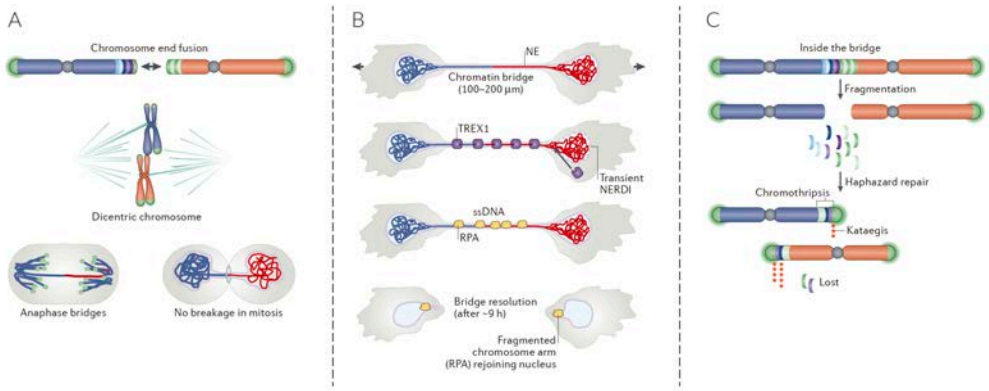

FIGURE 19. Chromothripsis and kataegis. **A.** Dicentric chromosomes can be formed when telomeres become uncapped. Both can be pulled on opposite poles and form an anaphase bridge. **B.** If chromatin bridge persists, nuclear membrane is partially disrupted to allow the entrance of TREX1 exonuclease. As a result of TREX1 action, ss-DNA is formed and detected by RPA. RPA signalling persists once the bridge has been resolved until the following cell cycle, when illegitimate re-joining and kataegis are presumed to take place. **C.** The chromatin bridge is fragmented in multiple fragments that are randomly repaired. During this process kataegis occurs and introduces hypermutated clusters. Figure from (Maciejowski & de Lange, 2017).

Sometimes, anaphase bridge do not break, thus leading to numerical imbalances. It has been reported that dicentric chromosomes erroneously segregate during cell division (Pampalona *et al*, 2010). These segregation errors could originate aneuploid daughter cells through non-disjunction in which the main nucleus of one cell will inherit the whole dicentric chromatid and the other one will lose it; otherwise the dicentric chromatids could lag during ana-telophase and be included into a micronucleus in the next interphase (FIGURE 18) (Pampalona *et al*, 2010). The cause of dicentric chromatids lagging during anaphase is probably because of the opposite tensional forces exerted by k-fibers (Pampalona *et al*, 2016). More specifically, it has been described that k-fibers bound to bridged kinetochores might be in an hyperstable attachment as slightly shorten and possibly elongate during anaphase (Pampalona *et al*,

2016). The balance between the shortening and the lengthening of the opposite k-fibers will determine the dicentric segregation to the same pole (Pampalona *et al*, 2016).

Moreover, telomere dysfunction can engender tetraploid cells through distinct mechanisms. Specifically, vHMECs fail to complete cytokinesis when persistent anaphase bridges in the cell equator induce furrow regression (FIGURE 18), even in p53 proficient cells (Pampalona *et al*, 2012). Besides, tetraploidization occurs through endoreduplication process when persistent telomere damage due to POT1A/B depletion induces an extended G2 phase that result in mitosis bypass (Davoli *et al*, 2010; Davoli & de Lange, 2012). More specifically, the sustained G2 arrest disturbs the fluctuation between CDT1 and geminin. Normally, CDT1 licences replication origins and is expressed during G1 and in early S phase; on the other hand, geminin is an inhibitor of CDT1 and prevents relicensing of the replication origins and its expression starts at S phase and decreases at the end of mitosis. POT1A/B double knockout cells exhibit a prolonged geminin S/G2 phase that is followed by a geminin loss without mitosis and a G1-like state (Davoli *et al*, 2010; Davoli & de Lange, 2012). Eventually, cells could enter in a subsequent S phase and followed by mitosis, thus originating two tetraploid cells. Tetraploid cells are usually arrested through p53 protein and the Hippo tumour suppressor pathway, as this pathway senses the presence of extra centrosomes (Ganem *et al*, 2014). But in case of p53 deficiencies, tetraploid cells can proliferate further thus originating highly reorganised daughter cells due to the presence of multi- o pseudobipolar divisions and the illicit microtubule-kinetochore attachments (Vitale *et al*, 2011).

6. Telomere dysfunction: learning from mouse models

In contrast to humans, the majority of cells in the mouse express telomerase (Prowse & Greider, 1995). Additionally, mice telomeres are longer than human telomeres. This suggests that telomeres are not a limiting factor in mice lifespan. To understand the role of telomeres, telomere dysfunction and telomerase in the ageing process and in cancer development, several mouse models lacking mTERC or the shelterin proteins have been developed.

6.1. Progressive telomere deprotection: telomere shortening

The abrogation of telomerase from mice has developed to reproduce telomere shortening in mice and analyse the systemic effect of telomerase absence. *Terc*-deficient mouse model (*mTerc*$^{-/-}$) results in viable and fertile mice as long as their telomeres are long enough (Blasco *et al*, 1997; Lee *et al*, 1998). It has been reported that telomeric length regresses over a ratio of 4.8 ± 2.4 kb per generation, when the *mTerc*$^{-/-}$ progeny is intercrossed to each other (Blasco *et al*, 1997). At the 4th generation, telomeres lacked detectable telomere repeats, and leaded to chromosome abnormalities, end-to-end fusions and aneuploidy (Blasco *et al*, 1997). It was at the 6th generation when mice became infertile due to defects in reproductive system of both males and female mice (Blasco *et al*, 1997; Lee *et al*, 1998). In addition to infertility, telomere shortening results in early embryonic lethality, whose penetrance increased over *mTerc*$^{-/-}$ generations (Herrera *et al*, 1999a). More specifically, the absence of telomerase and the

progressive telomere shortening is fatal for proper central nervous system, as *mTerc*$^{-/-}$ embryos fail to close the neural tube (Herrera *et al*, 1999a).

In adult mice, the effects of telomere shortening affects systemically, with more emphasis to the most proliferative cells and high renewal organs such as skin, reproductive organs and haematopoietic system as well as to the lymphocyte mitogenic response (Lee *et al*, 1998; Rudolph *et al*, 1999). In fact, the wound reepithelization at late generation mice (Rudolph *et al*, 1999) or the extensive clonal expansion of B and T cells against a mitogen stimulus (Herrera *et al*, 1999b, 2000) are seriously compromised due to the low proliferative capacity. Not only that, but telomerase deficiency and progressive telomere shortening result in a reduction of life expectancy and aged related diseases (Rudolph *et al*, 1999; Herrera *et al*, 1999b). An excessive telomere shortening correlates with thinner fat cell layer between the dermis and the skeletal muscle of mice, thus contributing to a decreased body weight at the end of mice life (Rudolph *et al*, 1999). In addition, angiogenic potential, which is suggested to result in vascularisation defects, is impaired (Franco *et al*, 2002). Indeed, it might be related to wound healing, tissue repair, or other vascular and heart diseases, as the frequency of these diseases increases with human age. Finally, telomerase-deficient mice models exhibit a progressive cardiac myocyte hypertrophy and heart abnormalities over generations (Leri *et al*, 2003). These defects are exacerbated in the 5th generation mice, in which telomere length become critical (Leri *et al*, 2003). More specifically, cardiac myocyte proliferation is attenuated concomitantly with a *p53* and apoptosis activation, thus leading to cardiac myocyte hypertrophy (Leri *et al*, 2003).

The impair effect over cell growth suggests that telomere shortening and telomerase abrogation could lead to cancer resistance. In fact, telomere shortening exerts its anti-proliferative effect when telomeres are critically short in late generation of a cancer-prone mice strain, which is *mTerc*$^{-/-}$-*Cdkn2a*$^{-/-}$ (Greenberg *et al*, 1999). In the same line, telomere shortening confers cancer resistance after chemically induced carcinogenesis (González-Suárez *et al*, 2000). While 1st generation *mTerc*$^{-/-}$ has a similar incidence of tumour development than *mTerc*$^{+/+}$, cancer development is greatly reduced in the 5th generation mice (González-Suárez *et al*, 2000), reinforcing that telomeres have an antitumoral effect. As mentioned earlier, shorter telomeres are recognised as DSB and activate p53 signalling pathway, suggesting that short telomeres could be implicated in the apoptotic response, cell cycle arrest and mice death within the 6th generation (González-Suárez *et al*, 2000).

In contrast, *p53* abrogation increases the potential viability and fertility of *mTerc*$^{-/-}$ mice and, while, *mTerc*$^{-/-}$-*p53*$^{+/+}$ could inbreed six generations, *mTerc*$^{-/-}$-*p53*$^{+/-}$ mice inbreed eight generations (Chin *et al*, 1999). Indeed, *p53* abrogation represents an advantage at late generations, as rescues cell proliferation, cellularity and prevents cell death (Blasco *et al*, 1997; Chin *et al*, 1999). However, this proliferative extension comes with a price: *mTerc*$^{-/-}$-*p53*$^{-/-}$ cells are prone for karyotype reorganisation and aneuploidy (Chin *et al*, 1999; Artandi *et al*, 2000). Indeed, deprotected telomeres tend to fuse, subsequently entering in BFB cycles, which fire chromosome instability and aneuploidy (Chin *et al*, 1999; Artandi *et al*, 2000). Therefore, telomere shortening in p53 deficiency context is suggested to promote cellular transformation and neoplastic process (Chin *et al*, 1999; Artandi *et al*, 2000).

However, telomeric function restoration by telomerase or ALT is suggested to be essential for a full malignant transformation, as the majority of cancer cells have telomerase activity (Kim *et al*, 1994; Shay & Bacchetti, 1997). In line with this hypothesis, two different telomerase deficient mice models exhibited tumour formation and prostate metastases or lymphoma infiltration after telomerase reactivation (Ding *et al*, 2012; Hu *et al*, 2012). These data suggest that telomerase expression after a chromosome instability period is required for the acquisition of new cancer hallmarks. In contrast, telomerase inhibition limited cell proliferation and induced apoptosis. However, as side effect, telomerase inhibition provoked the emergence of ALT mechanisms (Hu *et al*, 2012). This suggests that telomerase and ALT mechanisms alleviate telomeric DNA damage and are necessary for a full malignant phenotype.

6.2. Acute telomere deprotection: shelterin dysfunction

Telomere deprotection through shelterin dysfunction results in early embryonic lethality in *Trf1* (Karlseder *et al*, 2003), *Trf2* (Celli & de Lange, 2005), *Pot1a/b* (Wu *et al*, 2006; Hockemeyer *et al*, 2006), *Tin2* (Chiang *et al*, 2004) or *Tpp1* (Kibe *et al*, 2010) knockout mice. However, the development of conditional knockouts prevents embryonic death and allows the study of the cellular consequences of telomere deprotection due to shelterin dysfunction. In this sense, studies with conditional knockouts for different shelterin proteins, such as *Trf2* (Celli & de Lange, 2005), *Trf1* (Martínez *et al*, 2009) or *Pot1a* (Pinzaru *et al*, 2016) have shown a strong DDR (DNA Damage Response) signalling and the induction of cell senescence through p53/p21 activation (Martínez *et al*, 2009; Pinzaru *et al*, 2016). Consequently, inactivation of p53 increases the survival of shelterin-deficient conditional mice, while increasing the incidence of tumours (Martínez *et al*, 2009; Pinzaru *et al*, 2016; Akbay *et al*, 2013; Else *et al*, 2009). This increase in the tumorigenic potential of shelterin-compromised cells has been associated with the development of CIN and specifically with the presence of telomere-unstable tetraploid cells using a conditional POT1A expression system in mouse fibroblasts (Davoli & de Lange, 2012). Polyploid cells in mice fibroblasts lacking *Pot1a* and showing p53 deficiency, arose through endoreduplication (Hockemeyer *et al*, 2006) when persistent telomere damage arrests cells during S-phase (Davoli *et al*, 2010). Importantly, the dissipation of telomere damage through POT1A restoration allows cell cycle progression of p53-deficient tetraploid cells, which displays supernumerary centrosomes and telomere clustering during interphase (Davoli *et al*, 2010; Davoli & de Lange, 2012), and thus might present an increased plasticity to karyotype rearrangements (Laughney *et al*, 2015).

One of the consequences of cells having twice the number of centrosomes is the formation of multipolar spindles that are rarely compatible with cell survival, due to major genetic imbalances in daughter cells (Brinkley, 2001). However, coalescence of multipolar spindles into bipolarity may favour unresolved merotelic attachments, a phenomenon that has recently been defined as the mechanism underlying the increase in numerical CIN in tetraploid cells (Ganem *et al*, 2009; Silkworth *et al*, 2009). While aneuploidy might hamper proliferation of diploid cells (Thompson & Compton, 2008; Williams *et al*, 2008), it has been determined that doubling the chromosome content efficiently buffers the deleterious effect of steady-state missegregation generated by centrosome clustering (Ganem *et al*, 2007). These long lasting

4N cells would more readily manifest the genetic changes that might lead to transformation. The most direct evidence for the high tumourigenic potential of tetraploid cells comes from the observation that 4N p53-null mammary epithelial mouse cells can initiate tumours in immunocompromised mice, whereas isogenic diploids cannot (Fujiwara *et al*, 2005). Tumourigenesis via this tetraploid intermediate could explain why polyploid cells are observed in early neoplastic stages, and why cancer cells frequently contain supernumerary centrosomes and a high rate of whole chromosome missegregation.

Similar to POT1A conditional deficiency, the inducible expression of TRF2$^{\Delta B\Delta M}$ in a telomerase-proficient mouse model of human hepatocellular carcinoma enhances tumorigenesis in the liver (Begus-Nahrmann *et al*, 2012). The transient expression of TRF2$^{\Delta B\Delta M}$ induced liver tumour cells with high levels of chromosome aberrations, as occurred to 3rd generation *mTerc*$^{-/-}$ mice (Begus-Nahrmann *et al*, 2012). However, some differences were observed between the two models: TRF2$^{\Delta B\Delta M}$ conditional mice exhibited a higher incidence of liver tumours that were bigger and displayed lower levels of DNA damage when compared with those formed in 3rd generation *mTerc*$^{-/-}$ mice (Begus-Nahrmann *et al*, 2012). These differences were associated with the induction of transient acute telomere deprotection periods in a telomerase proficient background, as the telomere reprotection periods alleviated the telomere damage and was permissive with cell viability (Begus-Nahrmann *et al*, 2012).

Overall, mouse studies provide *in vivo* evidence that a period of transient telomere dysfunction, developed through telomeric DNA shortening or shelterin deficiency during early or late stages of tumourigenesis and before telomere stabilisation occurs, promotes chromosomal instability and carcinogenesis in mice models.

7. Telomere dysfunction and human cancer

Most human cancers in the adult population display a myriad of complex chromosomal aberrations that are not always shared by cells of the same tumour or linked to a particular tumour type, which suggest constant genetic reshuffling. This chromosomal diversity among the tumour cell population is thought to be acquired through chromosomal instability (CIN), which can be defined as the continuous formation of new structural and numerical chromosome aberrations, and is one of the most frequent forms of instability in human cancers (Lengauer *et al*, 1998). Several lines of evidence indicate that tumourigenesis in humans is a multistep process in which a succession of genetic changes leads to the progressive conversion of normal human cells into cancer cells. Within a developing tumour, mutations accumulate over time, giving rise to variant cell populations which finally present the ten biological hallmarks that dictate malignant phenotype (Hanahan & Weinberg, 2011). It is becoming clear that CIN is not simply a passenger phenotype, but probably plays a causative role in the onset of a substantial proportion of malignancies (Schvartzman *et al*, 2010). In humans, a large amount of data collected from tumour biopsies suggest that CIN has a founder effect in tumourigenesis, since it is present in all stages of cancer; from precancerous lesions, even before TP53 mutations are acquired (Bartkova *et al*, 2005; Gorgoulis *et al*, 2005), to advanced cancers (Nowell Peter C., 1976; Lengauer *et al*, 1997). In addition, the level of CIN and chromosomal aberrations correlates with tumour grade and prognosis (Carter *et al*, 2006), i.e.

chromosomal aberrations tend to be more numerous in malignant tumours than in benign ones, and both aneuploidy and CIN are associated with poorer prognoses as well as aggressive histopathologic features.

As described in 1.6, studies in different cancer mouse models showing compromised telomeres have highlighted that telomere dysfunction increases tumour initiation by the induction of CIN, but initiated tumours need to reactivate telomerase or recombination based mechanisms (ALT-pathways) for genome stabilisation and full malignant transformation (Hu *et al*, 2012). In addition, the analysis of mice deficient for both telomerase and p53 expanded the view of how telomere dysfunction impacts on the genesis of carcinomas, the main tumour type in human adults (Artandi *et al*, 2000). These studies were critical to establish a relationship between telomere shortening occurring in normal epithelial cells during lifetime and the genesis of epithelial cancers, which are the most common malignancies affecting the human population (Artandi & DePinho, 2010).

Data analysis of different high-throughput sequencing studies to determine cancer relevant genes proposed oncogene-induced DNA replication stress or telomere dysfunction as responsible mechanisms for the presence of genomic instability in many sporadic cancers tumours (Negrini *et al*, 2010). Loss of telomere function seems to be dependent on the impairment of the t-loop structure, and appears from either alteration of telomere-binding proteins or from the progressive telomere shortening that normally occurs under physiological conditions in the majority of replicating cells in tissues. Mutation of shelterin proteins is rare in cancer samples (FIGURE 20) (Sanger Institute, 2018), and this low incidence of mutation could be related to the deleterious effect they have on cell viability (Karlseder *et al*, 2003; Celli & de Lange, 2005; Wu *et al*, 2006; Hockemeyer *et al*, 2006; Chiang *et al*, 2004; Kibe *et al*, 2010). In humans, only mutations in POT1 have been implicated in the onset and progression of familial melanomas, gliomas, angiosarcomas or chronic lymphocytic leukaemia (Shi *et al*, 2014; Robles-Espinoza *et al*, 2014; Bainbridge *et al*, 2015; Calvete *et al*, 2015; Ramsay *et al*, 2013), in which mutations have been specifically correlated with increased telomere fragility and CIN (Ramsay *et al*, 2013; Calvete *et al*, 2015). Other shelterin deficiencies are mainly related to enhanced telomere biogenesis and/or telomerase recruitment, thus supporting a role in later stages of the disease. For instance, TPP1 or RAP1 missense mutations have been implicated in increased susceptibility to melanoma (Aoude *et al*, 2015). TPP1 missense mutations localise near or in the same domain of interaction with POT1, and therefore, could hinder the recruitment of POT1 to the chromosome end (Aoude *et al*, 2015). In addition, mutations in TPP1, adjacent to the telomerase interaction (TEL patch) domain, could favour its interaction with telomerase and its action (Spinella *et al*, 2015). Indeed, cells with mutations that reduce the interaction between TPP1-POT1 exhibit an increased telomere length (Aoude *et al*, 2015).

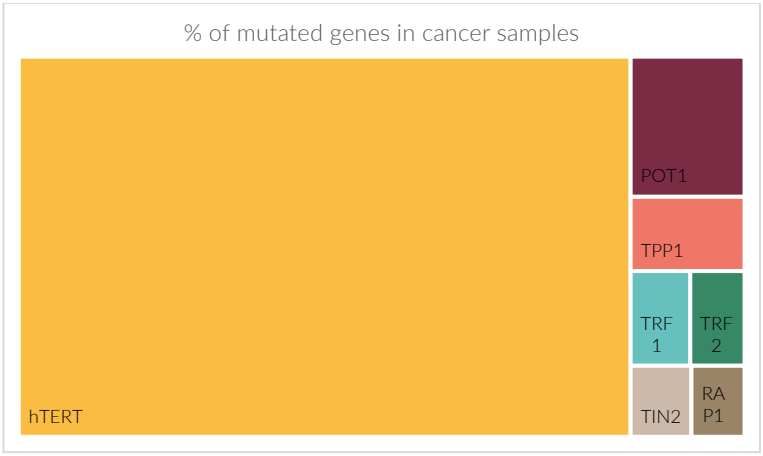

FIGURE 20. Proportion of mutated genes in cancer samples (mutated samples/tumour samples). hTERT: 11,109/84,304; TRF2: 97/32,961; TRF1: 106/32,961; POT1: 310/34,273; TPP1 158/32,961; TIN2 81/32,962; RAP1 70/32,961. (Data from: (Sanger Institute, 2018))

Significantly, telomere length contributes to the regulation of proliferative cell boundaries. The physiological telomere shortening that occurs with natural cell division results in unmasked telomeres that trigger the senescent phenotype, thus limiting the proliferative potential of those cells that are at risk to transformation. Nevertheless, abrogation of checkpoint-response integrity that limits proliferative lifespan might allow cells destined to senesce to further reduce their telomeres and thus initiate the CIN needed for cancer development (Stewart & Weinberg, 2006). Accumulated data support the notion that loss of telomere repeats could also contribute to human carcinogenesis. Excessive telomere shortening is observed in some chronic human diseases associated with high cell turnover, as well as an increased risk of cancer, such as liver cirrhosis (Kitada *et al*, 1995) or pancreatitis (Van Heek *et al*, 2002). In addition, very short telomeres have been reported to be an early alteration in many human cancers (Meeker *et al*, 2004b). Circumstantial support for the importance of transient telomere deficiency in facilitating malignant progression has come, in addition, from comparative analyses of premalignant and malignant lesions in the human breast (Chin *et al*, 2004; Meeker *et al*, 2004a; Raynaud *et al*, 2010). The premalignant lesions did not express significant levels of telomerase and were marked by telomere shortening, anaphase bridges (a hallmark of telomere dysfunction), and nonclonal chromosomal aberrations. In contrast, overt carcinomas exhibited telomerase expression concordantly with the reconstruction of longer telomeres and the fixation, via clonal outgrowth, of the aberrant karyotypes that would seem to have been acquired after telomere failure but before the acquisition of telomerase activity. Of note, it was recently found that early human breast lesions (early DCIS), as well as later invasive ductal carcinoma but not normal breast tissues from healthy volunteers contained telomere fusions (Tanaka *et al*, 2012). Collectively, such observations suggest that human breast precancerous cells go through a period of excessive telomere erosion that may initiate the CIN that, in turn, could promote the tumorigenic process.

Hypothesis and objectives

Evidence in mice models underlines that the development of telomere-dependent chromosome instability endows unstable cells and the onset and progression of neoplasia (Artandi *et al*, 2000). Nonetheless, the evidence demonstration that telomere dysfunction promote human tumourigenesis still remains elusive. Telomere dysfunction has long been held responsible for the initiation of BFB-cycles and their accompanying rearrangements, including non-reciprocal translocations, regional amplifications, segmental deletions, chromothripsis and kataegis (Maciejowski & de Lange, 2017). Moreover, aneuploidy and polyploidy also arise from unmitigated telomere attrition that, when added to this inventory of telomere-related genome instability, provide a framework for the genesis of human tumours carrying heavily rearranged near tetraploid genomes (Maciejowski & de Lange, 2017). Progressive shortening of the telomeric DNA or dysfunction of the shelterin proteins ensue in telomere dysfunction and in the inability to protect the chromosome ends (Cesare & Karlseder, 2013). Whereas accumulated data support the notion that loss of telomere repeats could contribute to human carcinogenesis (Meeker *et al*, 2004a; Tanaka *et al*, 2012), mutations in POT1, TPP1 and RAP1 proteins have been detected in familial cancers, i.e. melanoma (Robles-Espinoza *et al*, 2014; Shi *et al*, 2014; Aoude *et al*, 2015), glioma (Bainbridge *et al*, 2015), angiosarcoma (Calvete *et al*, 2015) or leukaemias (Ramsay *et al*, 2013; Spinella *et al*, 2015). Specifically in breast cancer development, the importance of transient telomere deficiency in facilitating malignant progression has arised from comparative analyses of premalignant and malignant lesions in the human breast (Chin *et al*, 2004; Meeker *et al*, 2004a; Raynaud *et al*, 2010). Of note, it has been recently found that early human breast lesions (early DCIS) as well as later invasive ductal carcinoma contain telomere fusions, but not normal breast tissues from healthy volunteers (Tanaka *et al*, 2012). Collectively, such observations suggest that human breast precancerous cells go through a period of excessive telomere erosion that may initiate the CIN that, in turn, could promote the tumorigenic process. The hypothesis of the present Thesis is that immortalised chromosomally unstable cells arising through distinct telomere dysfunction sources promote human breast carcinomas.

For this purpose, we aimed to:

1. Ascertain whether vHMECs that have flown through a progressive telomere attrition and dysfunctional process might engender unstable cells when immortalised.

2. Evaluate the impact of telomere uncapping through the inducible expression of $TRF2^{\Delta B \Delta M}$, in order to initiate telomere-dependent CIN in immortalised MCF-10A mammary cells.

3. Determine whether cumulative periods of telomere uncapping in immortalised human mammary epithelial cells may eventually provide the advantageous alterations needed for the onset of breast carcinogenesis.

Results

Work I

International Journal of
Molecular Sciences

MDPI

Article

Generation of Immortalised But Unstable Cells after hTERT Introduction in Telomere-Compromised and p53-Deficient vHMECs

Aina Bernal, Elisenda Zafon, Daniel Domínguez, Enric Bertran and Laura Tusell *

Unitat de Biologia Cel·lular, Facultat de Biociències, Universitat Autònoma de Barcelona, 08193 Cerdanyola del Vallès, Spain; aina.bernal@uab.cat (A.B.); elisenda94@gmail.com (E.Z.); irgu00@gmail.com (D.D.); enbegadol@gmail.com (E.B.)
* Correspondence: laura.tusell@uab.cat

Received: 16 May 2018; Accepted: 13 July 2018; Published: 17 July 2018

check for updates

Abstract: Telomeres, the natural ends of chromosomes, hide the linear telomeric DNA from constitutive exposure to the DNA damage response with a lariat structure or t-loop. Progressive telomere shortening associated with DNA replication in the absence of a compensatory mechanism culminates in t-loop collapse and unmasked telomeres. Dysfunctional telomeres can suppress cancer development by engaging replicative senescence or apoptosis, but they can also promote tumour initiation when cell cycle checkpoints are disabled. In this setting, telomere dysfunction promotes increasing chromosome instability (CIN) through breakage-fusion-bridge cycles. Excessive instability may hamper cell proliferation but might allow for the appearance of some rare advantageous mutations that could be selected and ultimately favour neoplastic progression. With the aim of generating pre-malignant immortalised cells, we ectopically expressed telomerase in telomere-compromised variant human mammary epithelial cells (vHMECs), proficient and deficient for p53, and analysed structural and numerical chromosomal aberrations as well as abnormal nuclear morphologies. Importantly, this study provides evidence that while immortalisation of vHMECs at early stages results in an almost stable karyotype, a transient telomere-dependent CIN period—aggravated by p53 deficiency—and followed by hTERT overexpression serves as a mechanism for the generation of immortal unstable cells which, due to their evolving karyotype, could attain additional promoting properties permissive to malignancy.

Keywords: human mammary epithelial cells; telomere dysfunction; chromosome instability; p53; hTERT; cancer

1. Introduction

Telomerase reactivation is a hallmark of carcinogenesis, and the vast majority of human tumours have telomerase activity by upregulating expression of telomerase's catalytic subunit (hTERT) [1]. In addition to replicative immortality, cancer cell hallmarks include sustained proliferative signalling, inhibition of growth suppressors and resistance to cell death [2]. Underlying these hallmarks is the presence of chromosome instability (CIN), a process that fuels genetic heterogeneity among a cell population. It is thought that the presence of an unstable genome expedites the acquisition of traits enabling malignity [2–4], though it has also been proposed that it is a simple by-product of tumour evolution [5].

Multiple mechanisms have been described to enable the development of CIN [6–9]. Among them, telomere damage is believed to trigger CIN when critically short telomeres become dysfunctional and prone to chromosomal fusions in cells lacking proper cell cycle checkpoints. In human tissues,

progressive telomere shortening occurs due to the inability of polymerases to fully replicate the chromosome ends [10,11]. Excessive reduction of the telomere length renders telomeres dysfunctional and the onset of replicative senescence [12,13]. Indeed, human fibroblasts accumulate spontaneous telomere-dysfunction induced foci (TIFs) during cellular lifespan [14]. Cells keep dividing until they reach 4–5 TIFs, and above this threshold, persistent telomere damage enforces cells to become senescent through p53-dependent signalling [14–16]. Notably, cells with abrogated checkpoints may escape the growth arrest and be more tolerant of rampant CIN when fully deprotected telomeres become fusogenic. If left unchecked, this instability will eventually reach lethal levels in the transforming cells, thereby presenting crisis, a second block to the development of cancer [17,18]. It is currently believed that full malignant progression arise from cells in which telomerase or Alternative Lengthening of Telomeres (ALT)-pathway activation and restoration of telomere function appears after a period of telomere instability [18]. At least in murine models, telomerase reactivation in the setting of a pre-existing telomere-induced genome instability is an active driver of carcinogenesis [19].

Previous telomere and cytogenetic studies have documented CIN, reduced telomere length and telomere end fusions in early-stage human breast cancers [20–23], thus supporting telomere dysfunction as a driver of CIN and an inducer of intratumour diversity in this emerging malignancy [24]. These findings, along with the detection of telomerase activity in some breast carcinomas in situ [25–28], suggest that immortalisation of telomere unstable cells through the activation of telomerase could be an early event in the progression of breast carcinogenesis.

Here, with the aim of exploring the impact of hTERT overexpression in breast epithelial cells displaying short dysfunctional telomeres, we have taken advantage of human mammary epithelial cells (HMEC), which have been determined to mimic breast carcinogenesis in vitro [20]. Remarkably, HMECs acquire an extended lifespan in vitro due to the absence of $p16^{INK4a}$ expression [29]. In these proliferating variant HMECs (vHMEC), progressive telomere shortening results in the transit of telomeres from a closed state to an uncapped state and, ultimately, to the gradual appearance of fully unprotected telomeres that are continuously repaired by fusing with each other [30,31]. This reduces the initial damage and allows massive remodelling and scrambling of the genome through endless breakage-fusion-bridge (BFB) cycles on proliferating cells (reviewed in [32]). Nevertheless, these massively reorganised cells ultimately succumb to p53-dependent agonescence, or crisis if p53 function is abrogated [33]. Our studies establish that hTERT overexpression in vHMEC cells before CIN is unleashed enables the immortalisation of cells with a relatively stable karyotype. By contrast, immortalisation of cells after a brief episode of chromosomal instability offered by dysfunctional telomeres avoids the persistent mutator phenotype that hampers cell proliferation. Beyond restoring genome stability and eliminating the DNA-damage signals of unprotected telomeres, the provided data demonstrates the presence of a still-evolving karyotype due to persistent low levels of CIN. At the same time, we show that genomic alterations acquired in immortalised genome-unstable vHMECs are a mixture of random and fixed chromosomal rearrangements that could be potential sources of oncogenic changes and malignant evolution.

2. Results

2.1. Establishment of Immortalised and Non-Immortalised vHMECs with Different Cell Cycle Settings

To study how telomerase and p53 modulate the development and maintenance of CIN in human epithelial cells, $p16^{INK4a}$-deficient HMECs (vHMECs) were genetically modified through lentivirus infection. Genetic modifications consisted of the generation of an immortalised vHMEC cell line by ectopical expression of the catalytic subunit of telomerase (Figure 1). hTERT immortalisation was performed at an early population doubling (PD) before vHMECs developed CIN associated with extensive telomere shortening. On the other hand, young vHMECs were also subjected to constitutive abrogation of p53 through short-hairpin p53 RNA lentiviral particles (Figure 1). After five

PD, immortalisation of p53-deficient vHMECs was conducted through infection with the hTERT lentivirus (Figure 1).

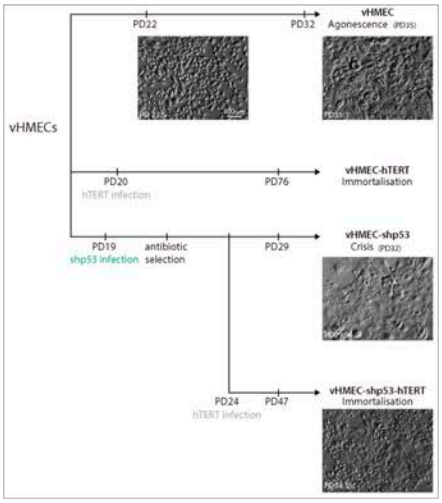

Figure 1. Scheme of the generation and analysis of different vHMEC cell lines. Young vHMECs were immortalised by transduction with hTERT containing lentivirus at PD20 to generate immortalised vHMECs. In addition, young vHMECs at PD19 were also infected with lentiviral particles containing the short hairpin RNA of p53 under the hU6 constitutive promoter to generate p53 compromised finite vHMECs. After a period of selection with puromycin, the cells were expanded and subsequently immortalised with the hTERT lentivirus at PD24. Cytogenetic analysis was performed at PD22 and PD32 for young and aged vHMECs, respectively. Immortalised vHMECs (vHMEC-hTERT) were karyotyped at PD76 and at PD130 (not shown). Finite but p53-deficient vHMECs (vHMEC-shp53) were analysed at PD29 and the immortalised cell line derivative (vHMEC-shp53-hTERT) at PD47. Phase contrast images of the different cell lines at different PD are shown. Scale bar corresponds to 100 μm.

Validation of the genetic modifications was performed by different approaches. Telomerase levels in the different cell lines were tested through hTERT expression by western blotting (Figure 2A), rather than using highly sensitive molecular methodologies such as RT-PCR of hTERT mRNA or RQ-TRAP. Only the cell lines transduced with hTERT showed a clear band for the catalytic subunit of telomerase, thus validating that cell immortalisation took place. In addition, inactivation of the p53 pathway through shRNA was confirmed by the reduced levels of p53 protein and by the fact that increased levels of $p53^{S15}$ were unnoticed after cell exposure of vHMEC-shp53 cells to the DSBs inducer Bleocin™ (Figure 2A).

In addition, the functional status of p53 was determined by assaying the ability of cells to arrest growth after exposure to the microtubule destabilising agent colcemid. Microtubule inhibitors, such as colcemid or nocodazole, physically interfere with microtubule formation and activate the spindle assembly checkpoint (SAC) [34]. This checkpoint monitors kinetochore attachment [35] and delays chromatid separation and exit from mitosis until all kinetochores are saturated with and stably attached to spindle microtubules [36]. As for other checkpoints, an active SAC is not normally capable of blocking exit from mitosis indefinitely. Indeed, cells can evade the mitotic arrest and proceed to the next interphase without chromosome segregation by means of a process termed mitotic slippage or checkpoint adaptation. Under normal conditions, these cells with a tetraploid DNA content

often suffer a long-lasting arrest at G1, most likely due to the induction of cellular senescence [37]. In contrast, polyploid cells that lack functional p53 have an increased ability to re-enter the cell cycle and initiate another round of DNA replication [38–41]. In order to determine if this was the case for our p53-deficient cells, FACS analysis of DNA content was performed after sustained exposure to 50 ng/mL of colcemid during 24 h or 48 h. Following 24 h exposure, there was an increase in cells in the G2/M fraction and a lower number of cells in G1, in both proficient and p53-deficient vHMEC-hTERT cells (Figure 2B), probably reflecting the accumulation of mitotically arrested cells. In contrast, FACS analysis of cells after sustained 48 h colcemid treatment demonstrated the presence of cells with an 8N DNA content compatible with cycling polyploids only in vHMEC-shp53-hTERT cells (Figure 2B).

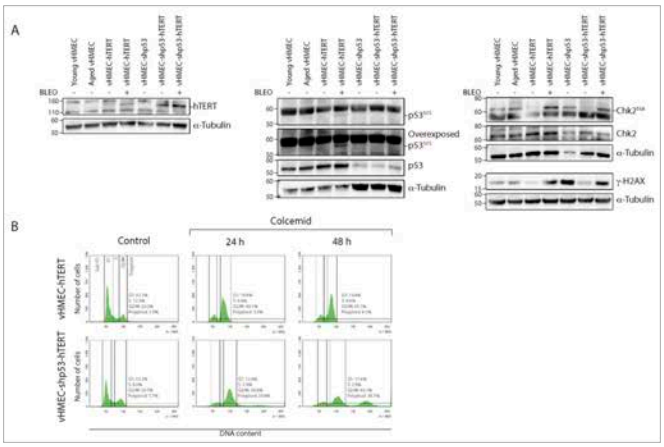

Figure 2. Validation of hTERT immortalisation and p53 downregulation in the different vHMECs. (**A**) Immunoblots of untreated cell lines as well as Bleocin™-treated p53-proficient and deficient immortalised vHMECs. Expression of the catalytic subunit of telomerase (hTERT) was observed at approximately 120 kDa only in the immortalised cell lines. Please note that at 160 kDa there is an unspecific band. A higher expression of hTERT, i.e., stronger band, was observed in the p53-deficient derivatives. α-Tubulin was used as loading control. The same protein extracts were immunoblotted for p53. Diminished levels of p53 were observed in the shp53-vHMEC variants after α-Tubulin normalisation. In addition, the functionality of p53 was validated by checking for the presence of $p53^{S15}$ after DSBs induction by Bleocin™. Only p53-proficient immortalised vHMECs showed enhanced $p53^{S15}$ levels after DNA damage. α-Tubulin was used as loading control. The presence of DNA damage was determined in the different cell lines by blotting γ-H2AX, a marker of DSBs. After α-Tubulin normalisation, the γ-H2AX levels were observed to increase in finite vHMECs concomitant to increasing telomere shortening and specifically when p53 function was abrogated. hTERT immortalisation reduced γ-H2AX levels in both p53-proficient and deficient vHMECs, but in vHMEC-shp53-hTERT DSBs still remained, as the level of γ-H2AX was comparable to that of telomere-compromised vHMECs. Similarly, $Chk2^{T68}$, another marker of DSBs, was noticed in the finite and the Bleocin™-treated immortalised cells; (**B**) Representative cell cycle profiles of vHMEC-hTERT and vHMEC-shp53-hTERT cell lines 24 h and 48 h after colcemid treatment, as well as their respective controls. Cell cycle profiles remained stable throughout the time of the experiment for untreated cells. Colcemid treatment produced an accumulation of cells in the G2/M phase in vHMEC-hTERT. In the p53 compromised cells there was, in addition to the G2/M increase, an accumulation of cycling polyploids, i.e., more than 4N DNA content, specifically at 48 h after treatment. Cell cycle phases are marked and values indicated. A minimum of 10,000 cells were analysed per experiment.

In summary, we have efficiently generated p53-proficient and deficient mortal and immortal vHMEC lines from one individual to investigate the contribution of p53 and telomere status in the karyotypic evolution of epithelial human cells.

2.2. The Negative Impact of Telomere-Erosion on the Karyotype of vHMECs Is Enhanced by Targeted p53 Inactivation

Previous studies on vHMECs have shown that hypermethylation of the CDKN2A promoter allows the proliferation of breast cells carrying extremely short telomeres as well as uncapped chromosomes [29,30]. A direct link between exaggerated telomere shortening and chromosomal aberration formation has been obtained in several different human epithelial cell models [42–45]. To determine whether loss of p53 contributes to the intensification of the telomere-dependent CIN, we first evaluated the karyotype aberrations in unmodified vHMECs at an early culture stage (PD22) just after a period of selection when clones with $p16^{INK4a}$ inactivation acquire proliferation capacity. In addition, a late culture stage (PD32) was analysed to detect abnormalities occurring over time before vHMECs cease proliferation by entering agonescence at approximately PD35 (Figure 1).

Cytogenetic analysis of vHMEC cells was performed using both inverted 4′,6-Diamidino-2-phenylindole dihydrochloride (DAPI) staining and pantelomeric-pancentromeric hybridisation with PNA probes. A total of 26 early passage vHMECs were karyotyped (Table S1). Eleven metaphase cells (42.31%) had an abnormal karyotype (Table 1 and Figure 3A,C). Structural chromosomal aberrations observed were chromosome fusions (fus) or dicentric chromosome (dic) (6 cells), non-reciprocal translocations (nrt) (2 cells), chromatid breaks (ctb) (3 cells) and acentric fragments (ace) (1 cell). The karyotype analysis of in vitro aged vHMECs metaphases after ten PDs (PD32) demonstrated the significant accumulation of aberrant cells with proliferation in the absence of telomerase (Table 1 and Figure 3A,C) (Fisher's exact test, $p < 0.0001$). All aged cells were karyotypically abnormal (100%) (Table S2). The aberration most often observed was the presence of fus or dic (17 cells). Other aberrations were nrt (4 cells), isochromosome (i) (1 cell) and centric fragments (4 cells). Altogether, the accrual of telomere dysfunction in vHMECs results in highly structural rearranged karyotypes with increasing frequency of structural aberrations per cell (Table 2 and Figure 3B) (Kruskal-Wallis test, $p < 0.0001$). Of relevance, end-to-end chromosome fusions, a marker of dysfunctional telomeres, increased with PDs from 0.23 per cell in young vHMECs to 1.1 per cell in the aged vHMECs. None of the fusions observed in our cell lines presented interstitial telomeres at the junction point (Figure S1), and most of the fusion events were located at the chromosome terminus. These results point to telomere attrition, and not to the breakdown of the t-loop due to shelterin problems at the origin of end-to-end fusions.

Besides structural chromosomal aberrations, numerical aberrations were evaluated through oligoFISH labelling of centromere-specific probes in interphase nuclei. This avoids artefactual chromosome loss due to the chromosome spreading technique. The FISH signals distribution of chromosome 6 (CEP6), 12 (CEP12) and 17 (CEP17) was scored in a minimum of 390 cells per condition (Table 3). At early PD, aneuploidy levels among diploid vHMECs were around 6% (Figure 4A) and, in agreement with published reports [46], increased significantly with PDs (Fisher's exact test, $p = 0.0057$). Furthermore, given the already defined tetraploidisation effect of telomere dysfunction in vHMECs and other cell types [47,48], we also evaluated the extent of tetraploid cells in telomere-compromised vHMECs. The oligoFISH scoring of vHMECs demonstrated a significant accumulation of 4N cells with PDs (7.65% vs. 14.73% in vHMECs at PD22 and PD30, respectively; $p = 0.0015$, Fisher's exact test) (Table 3 and Figure 4A). This increase in cell ploidy was also demonstrated by cytometric analysis where a minimum of 10,000 cells were evaluated per condition (10.1% vs. 13.9% in vHMECs at PD25 and PD33, respectively) (Figure 4B). Specifically, telomere dysfunction has been envisaged as a factor capable of interfering with the completion of cytokinesis through chromatin bridges emerging from end-to-end chromosome fusions [48]. For this purpose, mono- and multinucleated cells were also scored in vHMECs. After applying Texas Red-X

Phalloidin to detect the cell cortex and DAPI staining to counterstain DNA, the analyses confirmed a significant increase in the frequency of binucleated cells with the accrual of telomere dysfunction (Fisher's exact test, $p < 0.0001$) (Figure 5A).

Table 1. Cytogenetic analysis in the different vHMEC cell lines.

Cell Line	PD	Analysed Cells n	Abnormal Cells % (n)	Cells with fus/dic % (n)	Cells with nrt % (n)	Cells with Structural AA % (n)	Cells with Clonal Numerical AA % (n)
vHMEC	22	26	42.31 (11)	23.08 (6)	7.69 (2)	42.31 (11)	0.00 (0)
vHMEC	32	20	100.00 (20)	85.00 (17)	20.00 (4)	100.00 (20)	0.00 (0)
vHMEC-shp53	29	23	100.00 (23)	82.61 (19)	21.74 (5)	100.00 (23)	0.00 (0)
vHMEC-hTERT	76	46	91.30 (42)	0.00 (0)	6.52 (3)	17.39 (8)	84.78 (39)
vHMEC-shp53-hTERT	47	54	62.96 (34)	16.67 (9)	50.00 (27)	62.96 (34)	0.00 (0)

PD: population doubling; n: number; AA: aberrations.

Table 2. Distribution of the types of structural chromosome aberrations.

Cell Line	PD	Analysed Cells n	Total AA/Cell Freq. (n)	UNSTABLE AA			STABLE AA		OTHER AA	
				fus/dic n	Ace n	AA/Cell Freq.	nrt/i/mar /del n	AA/Cell Freq.	csb/ctb n	AA/Cell Freq.
vHMEC	22	26	0.46 (12)	6	1	0.27	2	0.08	3	0.12
vHMEC	32	20	1.65 (33)	22	0	1.10	6	0.30	5	0.25
vHMEC-shp53	29	23	3.65 (84)	54	9	2.74	15	0.65	6	0.26
vHMEC-hTERT	76	46	0.17 (8)	0	0	0.00	8	0.17	0	0.00
vHMEC-shp53-hTERT	47	54	1.20 (65)	15	3	0.33	46	0.85	1	0.02

PD: population doubling; n: number; AA: aberrations.

Loss of p53 function may contribute to malignant progression by allowing the proliferation of cells with increased genomic instability. To determine if this was the case in our vHMEC line, a total of 23 vHMEC-shp53 cells were karyotyped at PD29, after shRNA infection (PD19), selection and subsequent cell expansion (Table S3). Similar to late passage p53-proficient vHMECs, no vHMEC-shp53 cell had a normal diploid karyotype (Table 1 and Figure 3A). However, the karyotype complexity was more pronounced in cells lacking p53 function, as the number of structural aberrations per cell increased extensively when p53 function was abrogated (3.65 vs. 1.65 aberrations/cell in vHMEC-shp53 PD29 and vHMEC PD32, respectively; Kruskal-Wallis test, $p < 0.0001$) (Table 2 and Figure 3B,C). Specifically, in p53-deficient vHMECs, there was an increase in marker chromosomes, as the highly reorganised karyotype made more difficult chromosome bands identification. The predominant types of structural changes were fused chromosomes in the form of dic or tricentric, followed by nrt and fragments, either centric or acentric. The analysis of the junction point of fusion events in multicentric chromosomes also demonstrated the absence of telomeric DNA by PNA hybridisation (Figure S1). Of relevance, the dicentric chromosomes in p53-deficient vHMECs were sometimes accompanied by acentric fragments, the consequence of creating chromosome breaks, thus denoting that telomere-shortening was not the only source for dicentric formation in this cell line. In addition, given the major role of p53 in the prevention of tetraploidy by activating apoptosis [49,50], its absence facilitated the generation and survival of tetraploid vHMECs. Although the rise in the polyploid population was not clearly envisaged through FACS analysis, probably by an accumulation of tetraploid cells in G1 (Figure 4B), the oligoFISH analysis demonstrated a significant increase in polyploid cells with the absence of p53 function when comparing both with young or aged vHMECs (Fisher's exact test, $p < 0.0001$ and $p = 0.0047$, respectively) (Table 3 and Figure 4A). This data was also supported by the fourfold increase in multinucleated interphase cells in compromised p53 cells as compared to p53-proficient late passage vHMEC (Fisher's exact test, $p < 0.0001$) (Figure 5A).

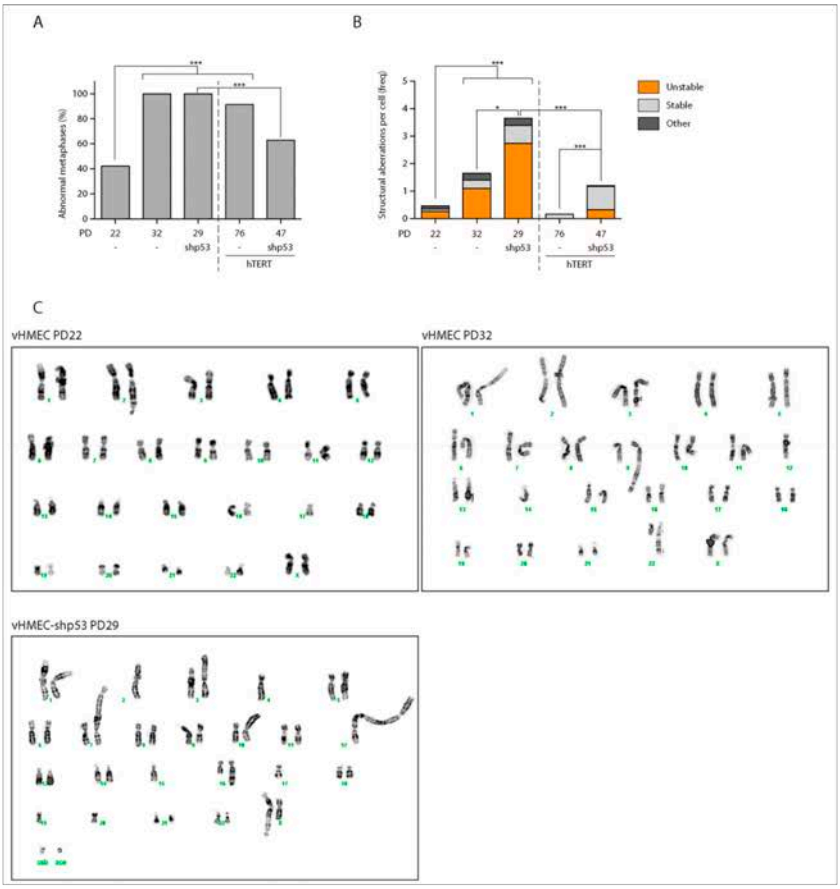

Figure 3. Cytogenetic analysis of the different cell lines. (**A**) Graph displaying the contribution of the telomere status and p53 functionality in the presence of abnormal karyotypes in vHMEC-derived cell lines. Statistical significance after Fisher's exact test comparisons is shown. *** indicates *p*-values lower than 0.001; (**B**) Distribution of the different types of chromosomal structural aberrations: unstable, i.e., fusions or dicentric chromosomes and acentric fragments; stable, i.e., non-reciprocal and reciprocal translocations, isochromosomes, marker chromosomes and deletions; and other, i.e., chromosome and chromatid breaks. Statistical significance after Kruskal-Wallis test and Dunn's multiple comparison post-test is shown. * indicates *p*-values lower than 0.05; *** indicates *p*-values lower than 0.001; (**C**) Example of finite vHMEC karyotypes. At PD22, young vHMECs show 45, XX, fus (2q;17q); at PD32, aged vHMECs show 45, XX, fus (9q;12q), nrt (22q;14q). By contrast, the karyotype of p53 compromised vHMECs demonstrates the complexity of their karyotype. At PD29, vHMEC-shp53 show 40, X, dic (2p;?;12p), nrt (3p;?), dic (4q;7p), dic (10p;?), nrt (16q;?), tetrac (17q;22;X;20p), +ace, +csb.

It should be noted that the Phalloidin-DAPI analysis allowed the identification of an elevated number of incorrectly aligned chromosomes at metaphase and lagging chromatin between segregating complements during anaphase, as well as micronuclei and buds in interphase cells lacking p53 function (Figure 5B,C). These improper chromosome distributions might result in unequal chromatid

segregation among daughter cells, thus constituting a prominent source of aneuploidy. Indeed, centromeric-specific FISH scoring demonstrated an overall significant increase in chromosome number aberrations in shp53-deficient vHMECs (Chi^2 test, $p < 0.0001$) (Figure 4A). In addition, these aneuploid configurations were extremely high among the 4N fraction of vHMEC-shp53 cells (Fisher's exact test, $p < 0.0001$ and $p = 0.0003$, compared to young and aged vHMECs respectively) (Table 3 and Figure 4A). These observations, together with the minor fraction of multipolar divisions observed, suggest that extra centrosomes in p53-deficient tetraploid vHMECs induce transient multipolar spindles that could significantly increase the incidence of merotelic attachments and chromosome mis-segregation rates [51,52].

Table 3. OligoFISH analysis of centromeric specific probes for chromosome 6, 12 and 17.

Cell Line	PD	Cells Analysed n	2N		4N		4N Fraction %
			Cells n	Aneuploidy Freq. (n)	Cells n	Aneuploidy Freq. (n)	
vHMEC	22	392	362	0.06 (23)	30	0.37 (11)	7.65
vHMEC	30	414	353	0.13 (47)	61	0.52 (32)	14.73
vHMEC-shp53	29	430	334	0.14 (47)	96	0.71 (68)	22.33
vHMEC-hTERT	132	846	841	0.05 (44)	5	0.00 (0)	0.59
vHMEC-shp53-hTERT	47	391	352	0.09 (32)	39	0.62 (24)	9.97

PD: population doubling; n: number.

As a whole, progressive telomere dysfunction in vHMECs concomitantly increased the level of chromosomal aberrations, which further expanded in the absence of p53. Of relevance, whereas chromosome aberrations in telomere-compromised vHMECs predominantly affected specific chromosomes (Tables S1 and S2), nearly all the chromosomes participated in structural genome changes when p53 function was abolished (Table S3). Notably, all vHMECs either proficient or deficient for p53 ceased proliferation around PD30 without the emergence of spontaneous immortalised cells, thus indicating that abrogation of p53 function is insufficient to immortalise vHMECs, as has been previously described [33].

2.3. Absence of CIN When hTERT Is Ectopically Expressed in p53-Proficient Young vHMECs

With the aim of generating pre-malignant immortalised cells, we ectopically expressed telomerase in telomere-compromised vHMECs. We assumed that if telomere-dependent BFB-cycles had begun, immortalised cells would maintain some ongoing instability. However, the immortalisation of aged vHMECs was not successful in this cell line as aged vHMECs did not overcome the agonescence limit (PD35) upon hTERT DNA virus delivery. Similarly, it was also not accomplished in late passages of vHMECs derived from other donors (unpublished results). In contrast, ectopic expression of hTERT was successful when infection took place at early passage vHMECs (PD20). Even in the absence of an antibiotic selection procedure, the cells resumed proliferation beyond the agonescence limit. This observation, together with the corroborated hTERT expression by western blotting (Figure 2A), confirmed that immortalisation had taken place.

Examination of the vHMEC hTERT-immortalised cells by cytogenetic analyses at PD76 showed an elevated frequency of aberrant metaphases with an approximately diploid complement of chromosomes (Table 1 and Figures 3A and 6) (Fisher's exact test, p-value < 0.0001). In contrast to telomerase-deficient cells, vHMEC-hTERT cells showed predominantly clonal numerical chromosomal aberrations in the form of trisomy 20 alone (73.9%) or in combination with structural chromosomal aberrations (10.9%) (Table S4). Consistent with vHMEC immortalisation before telomeres became compromised, unstable aberrations such as fus or dic chromosomes were not observed (Figures 3B and 6; Figure S2). The minor structural aberrations detected were nrt and deletions of unspecific chromosomes. In agreement with our observations, chromosome 20 trisomy has been reported to occur after ectopically hTERT expression in pre-stasis [53] and post-stasis HMECs [54,55], as well as

in HMECs where $p16^{INK4a}$ was abrogated through shRNA, BMI-1 [56] or $CDK4^{R24C}$ mutation [57]. Moreover, these studies revealed the association of trisomy 20 with other chromosomal aberrations such as partial or complete trisomy of chromosomes 1q, 5, 7, 8q, 13, 16 and 18 [53–57]. Indeed, further karyotypic analysis of the vHMEC-hTERT at PD130, revealed in addition to trisomy 20, the gain of an extra marker chromosome 20 and an undefined marker chromosome (Figure 6) and/or two nrt, one involving 1q and the other involving 3q.

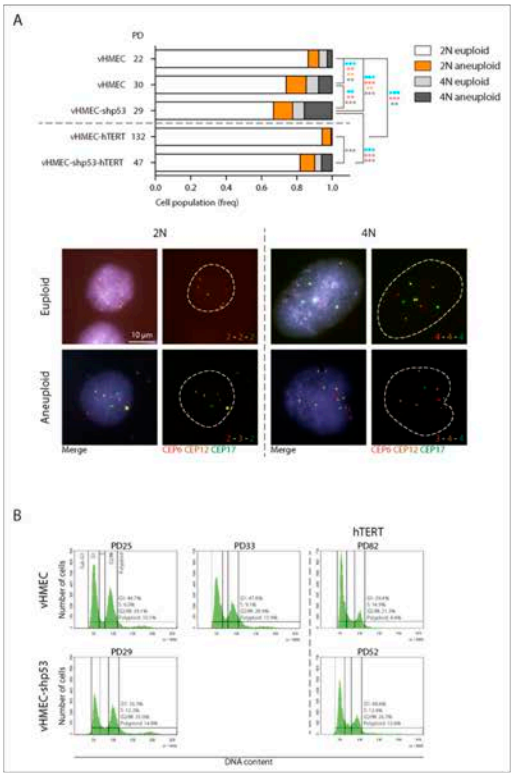

Figure 4. Analysis of chromosome number abnormalities. (**A**) Graph showing the frequency of euploid and aneuploid 2N and 4N among vHMECs after hybridisation with centromeric specific probes for chromosome 6 (CEP6), 12 (CEP12) and 17 (CEP17). Chi^2 test demonstrated a significant increase in cells containing numerical aberrations (blue asterisks). Moreover, tetraploidisation events significantly increased in finite vHMECs with increasing telomere dysfunction and were aggravated when p53 was compromised (Fisher's exact test, red asterisks). Statistical significance after Fisher's exact test comparisons regarding 2N aneuploid and 4N aneuploid cells with asterisks in the same colour code as the legend is shown, and only *p*-values lower than 0.0125 were considered significant. ** indicates *p*-values lower than 0.01; *** indicates *p*-values lower than 0.001. Representative images of diploid and tetraploid cells with euploid and aneuploid configurations of tested centromeric probes are depicted. Scale bar corresponds to 10 μm; (**B**) Representative cell cycle profiles of vHMEC cell lines. FACs analysis also demonstrated the increase of polyploid cells concomitant with PDs in finite vHMECs. Immortalisation of young vHMECs did not engender tetraploids, whereas immortalisation of p53-compromised vHMECs resulted in an average 10% proportion of cycling polyploids. Cell cycle phases are marked and values indicated.

OligoFISH analysis did not reveal abnormal chromosome distribution as a major characteristic of early immortalised vHMECs (Table 3 and Figure 4A), or the presence of polyploid cells (Table 3 and Figure 4). These observances thus corroborate the defined role of telomere dysfunction in the generation of numerical chromosomal aberrations, as the stabilisation of the telomere length abolished the presence of chromatin bridges (Figure 5B,C), the intermediate structures that act for the generation of telomere-dependent CIN, as well as multinucleation events (Figure 5A).

As a whole, ectopic hTERT expression in young vHMECs efficiently immortalised the cells before telomere dysfunction triggered BFB-cycles. Telomerase immortalisation resulted in a relatively stable karyotype, mainly displaying aberrations involving chromosome 20. Moreover, during the 140 PDs the cells were continuously cultured in vitro, they evolved karyotypically, accumulating further chromosome aberrations that could be needed to improve the survival of the immortalised cells.

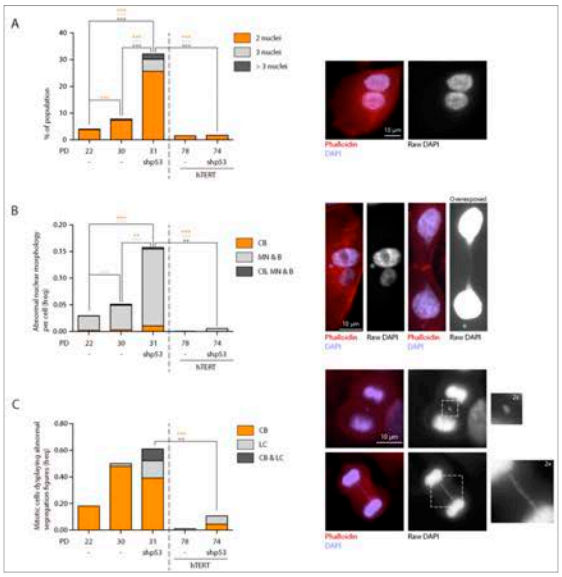

Figure 5. Analysis of abnormal morphologies in vHMEC derivatives. (**A**) Graph showing the percentage of binucleated, trinucleated cells and cells with more than three nuclei in interphase vHMECs. Finite vHMECs showed a significant increase in binucleation with increasing telomere attrition, and this effect was exacerbated when p53 was compromised. Representative images of a binucleated cell are shown. Scale bar corresponds to 10 μm; (**B**) Analysis of abnormal nuclear morphologies, i.e., chromatin bridges (CB), nuclear buds (B) and micronuclei (MN) among the different cell lines. Micronuclei and buds were the most frequent aberrations in vHMECs suffering telomere-dysfunction, followed by chromatin bridges. These aberrations were extremely abundant when p53 was compromised in finite vHMECs. Representative images of interphase cells displaying abnormal nuclear morphologies are shown. Scale bar corresponds to 10 μm; (**C**) Abnormal segregating figures were also observed in mitotic cells. In particular, chromatin bridges (CB) were abundant in those cells showing telomere-dysfunction. Likewise, those cells deficient for p53 were more prone to display lagging chromatin (LC). Representative images of abnormal anatelophases are shown. Scale bar corresponds to 10 μm. In the three graphs, statistical significance after Fisher's exact test comparisons is shown with asterisks in the same colour code as the legend. Only *p*-values lower than 0.0125 after Bonferroni *p*-value correction, were considered significant. ** indicates *p*-values lower than 0.01; *** indicates *p*-values lower than 0.001

2.4. Reduced But Persistent CIN in p53-Deficient vHMECs Immortalised with hTERT

Given that hTERT immortalisation of vHMECs only resulted when lentivirus infection took place in young cells (PD20), we were concerned about the possibility of immortalising p53-deficient vHMECs. If the p53 loss and immortalisation events occur prior to attaining critically short telomeres, it is probable that p53 loss may not necessarily confer genomic instability. Indeed, abrogation of p53 in young vHMEC-hTERT from a different donor did not result in increased cytogenetic aberrations (unpublished results). Likewise, normal vHMECs stably transduced first with hTERT and afterwards with a shRNA against p53, proliferated indefinitely and did not show gross chromosomal alterations [58]. In addition, this also occurred in HCT116 colon tumour-derived immortal human cells [59].

Infection of vHMEC-shp53 with hTERT lentiviral particles at PD24, successfully resulted in immortalised p53-deficient vHMECs. Validation of hTERT expression was assessed by western blotting (Figure 2A) but the confirmation became clear through the active proliferation of vHMEC-shp53-hTERT beyond the crisis barrier and by the absence of a dying morphological appearance (Figure 1). Whereas finite p53-deficient vHMECs stopped proliferation at approximately PD32, the vHMEC-shp53-hTERTs maintained continuous proliferation with no morphological signs of growth defects until at least PD74 (Figure 1). On the whole, although p53 deficiency was not required for immortalisation, inactivation of p53 promoted immortalisation of more aged telomere-compromised vHMECs (PD20 vs. PD24).

The cytogenetic analysis of the vHMEC-shp53-hTERT at PD47 demonstrated that immortalisation significantly reduced the percentage of cells displaying chromosome aberrations when compared to p53-deficient vHMECs (Fisher's exact test, $p = 0.0004$) (Table 1 and Figure 3A), but almost two thirds of cells still displayed an abnormal karyotype. When compared to vHMEC-hTERT, the p53-deficient immortalised cells presented a significantly-increased number of aberrations per cell (Kruskal-Wallis test, $p < 0.0001$) (Figure 3B). In addition, stabilisation of telomere ends in a p53-deficient settling statistically increased the frequency of stable chromosome aberrations when compared to non-immortalised cell lines (Fisher's exact test, $p = 0.0007$; $p < 0.0001$ and $p < 0.0001$, when compared to young, aged and shp53-deficent vHMECs respectively) (Table 2). These aberrations were mainly non-reciprocal translocations, some of which were fixed on the karyotype and were shared by different cells (Table S5). In addition, although unstable aberrations significantly decreased with immortalisation (Fisher's exact test, $p = 0.0008$) (Figure 3B), fused chromosomes (16.67% of metaphases) and centric or acentric chromosome fragments, signs of ongoing BFB-cycles, were still detected in immortalised p53-deficient vHMECs (Figure 6 and Figure S3). Accordingly, western blot analysis of phosphorylated H2AX at S139 (γ-H2AX), a hallmark of DSBs [60], confirmed a remaining fraction of DSBs in vHMEC-shp53-hTERT after α-Tubulin normalisation (Figure 2A). Whereas γ-H2AX levels increased in finite vHMECs concomitant to PDs and to p53-deficiencies, a reduction of DSBs was observed when p53-proficient vHMECs were immortalised with hTERT (Figure 2A). Of relevance, the level of γ-H2AX signalling in vHMEC-shp53-hTERT was comparable to that of telomere-compromised vHMECs, thus validating the cytogenetic results. The presence of DSBs was further evaluated by the presence of the activated form of the serine/threonine kinase Chk2, a key component of the DNA damage response. $Chk2^{T68}$ was detected in all cell lines except the immortalised ones, thus demonstrating a reduction in DNA damage with cell immortalisation (Figure 2A).

Persistent chromosomal aberrations were not only of a structural type, as numerical aberrations were also scored in the vHMEC-shp53-hTERT cells. Immortalisation of p53 deficient vHMECs significantly reduced the overall frequency of numerical aberrations, as well as the frequency of polyploids (Chi^2 and Fisher's exact test, $p < 0.0001$) (Figure 4). Even so, the survival of unstable tetraploids was promoted as there was a significant fraction of polyploid cells with aneuploid configurations in comparison with vHMEC-hTERT (Table 3 and Figure 4A).

In sum, hTERT expression in p53-compromised vHMECs after BFB cycles are initiated results in the generation of an immortalised cell line that exhibits low CIN levels. This remaining CIN results in

the heterogeneous presence of structural, numerical and ploidy aberrations and is visualised by the exhibition of anaphase bridges as well as lagging chromatin during cell division.

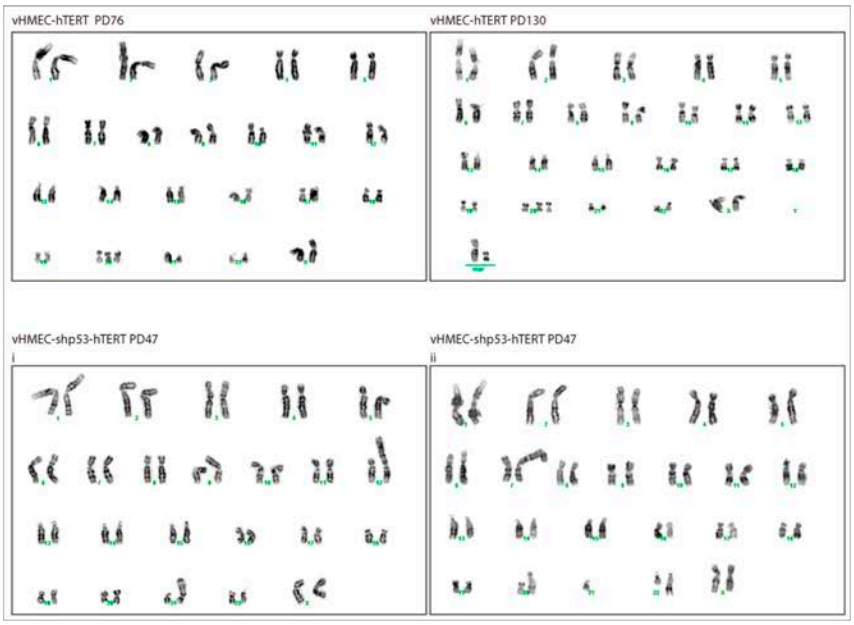

Figure 6. Karyotypes of immortalised p53-proficient and deficient vHMECs. Immortalisation of young vHMECs resulted in few chromosomal aberrations; the karyotype shown at PD76 is 47, XX, del (10p), +20. When the immortalised vHMECs were again karyotyped after 54 PDs (PD130), in addition to trisomy 20, two clonal marker chromosomes were observed. By contrast, immortalisation of p53-compromised vHMECs resulted in the accumulation of stable and unstable structural chromosome aberrations. Two karyotypes are shown: (**i**) 46, XX, nrt (9p;?), nrt (12p;?), dic (21p;?) and (**ii**) 45, XX, idic (7p;7p), +7, dic (20p;?), tric (22q;?;?), −21.

3. Discussion

In vivo studies in the mouse have revealed the constraining or promoting role of telomeres in cancer development. This dual capacity depends on the genetic context where dysfunctional telomeres occur, as highlighted by their enhanced tumorigenic potential when p53 is co-deleted [17,18,61]. Besides that, telomerase reactivation in the setting of a pre-existing telomere-induced genome instability period is required to actively drive carcinogenesis [19]. In humans, the finding of highly recurrent activating mutations in the hTERT gene promoter [1], together with widespread p53 mutations in cancer [62], provide support for the idea that circumvention of a telomere-p53 checkpoint is also essential for carcinogenesis in humans.

In the breast, short telomeres and widespread genomic instability can first be observed in premalignant lesions such as ductal carcinoma in situ (DCIS) [20,22], a stage where the p53 and Rb pathways are usually inactivated [63–65], suggesting that these lesions develop from cells expressing insufficient telomerase for telomere length maintenance. Cultured human mammary epithelial cells (HMECs) derived from cosmetic reductions are used to provide a better understanding of the molecular mechanisms and interactions involved in breast cancer development. Seminal studies by Stampfer laboratory defined a model for senescence barriers in cultured HMECs that evidenced the unique

features of breast human cells. HMECs obtained from tissue explants proliferate for a few PDs before entering a growth plateau. Nevertheless, and in contrast to most epithelial cells, HMECs possess the ability to overcome this barrier owing to $p16^{INK4a}$ promoter inactivation [29]. Subsequently, vHMECs resume proliferation for additional PDs until progressive telomere dysfunction concomitantly generates an increasing level of chromosomal aberrations that ultimately becomes lethal to the cell [30]. Specifically, studies in vHMECs derived from different donors have illustrated how the formation of dicentric chromosomes set in motion BFB-cycles, a mechanism capable of producing rapid and widespread changes in gene dosage as well as complex structural rearrangements [31,46,48,66,67]. In this study, and coincident with these observations, an enhanced complexity of the karyotype occurred in the finite and p53-competent vHMECs as PDs increased, presumably because of concomitant telomere attrition. Although the telomere length was not monitored and could be a limitation of the study, PNA telomeric FISH analysis in the finite vHMECs demonstrated a gradual increase of chromosomes with shorter telomeres, most likely compromised, throughout the cell culture. Moreover, the abrogation of p53 function in these cells resulted, as already reported [68], in a higher accumulation of aberrations per cell and, in a growth defect at earlier times than p53-proficient vHMECs. Moreover, the abrogation of p53 function in these cells resulted, as already reported, in a higher accumulation of aberrations per cell [68] and in a growth defect at earlier times than p53-proficient vHMECs. Collectively, the autocatalytic nature of BFB-cycles during rampant telomere attrition massively scrambles the genome yielding a wide range of lesions. Notably, the abrogation of p53 likely exacerbated short-telomere driven instability by increasing the fraction of structural and numerical chromosomal aberrations per cell, but specifically promoting the incidence of tetraploids. Strikingly, unstable tetraploid cells are believed to contribute to oncogenesis [69,70]. The enhanced tumorigenic capacity of tetraploid cells [69–75] could be expedited by their increased tolerance to chromosome mis-segregation events [76]. In this scenario, it is envisaged that telomere dysfunction may trigger genomic instability by fuelling rearranged karyotypes where structural, numerical and ploidy aberrations coexist. Eventually, the cumulative effect of centrosome-clustering on the preceding unstable polyploids could lead to further cellular genome remodelling that might contribute to epithelial carcinogenesis. Rare immortalisation events, probably arising due to the generation of additional errors during the genetic instability period, have occasionally been documented [77–79]. Nevertheless, the extensive reorganization and ongoing CIN, in the telomere-compromised vHMEC lines studied ultimately threatened cell viability as both p53-proficient and deficient vHMECs finally enter a growth plateau without the emergence of immortal outgrowths. This is in accordance with the described evidence that the extent of mutations cannot increase endlessly without adversely affecting cell fitness [80–82], and implies the existence of a threshold of genomic instability that the cell could tolerate [83].

It is speculated that a brief, or at least transient, episode of genomic instability offered by dysfunctional telomeres would avoid the persistent mutator phenotype that hampers cell proliferation, but might allow for the appearance of some rare advantageous mutations that would be selected and eventually favour neoplastic progression. Among them, telomerase reactivation in those highly reorganised cells would somehow reduce genome instability to a level compatible with the rescue of the cellular fitness, thus providing a route for transformation. With the aim of generating pre-malignant immortalised vHMECs, we ectopically expressed telomerase catalytic subunit in p53-proficient and deficient cells. Human telomerase is minimally composed of two components, the telomerase reverse transcriptase (hTERT) protein and the telomerase RNA template component (hTR). In addition, given that hTR is ubiquitously expressed, hTERT is considered the rate-limiting component that determines telomerase activity. The attempt to immortalise telomere-compromised aged vHMECs was unsuccessful, but hTERT expression in young vHMECs before BFB-cycles were set in motion resulted in immortalised cells with a stable karyotype that mainly displayed aberrations involving chromosome 20. These aberrations have been observed in a variety of immortalised epithelial cells such as oesophageal, nasopharyngeal, bronchial, ovarian surface, uroepithelial or Meibomian gland among others [84–88].

Since immortalisation, in those studies, was induced not only through hTERT expression but through HPVE6E7 or SV40 virus [84–88], the non-random occurrence of chromosome 20q gains strongly suggests that this genetic aberration contributes to the cellular immortalisation process. By contrast, hTERT expression in telomere-compromised and already reorganised p53-deficient vHMECs was sufficient to sustain cell viability beyond the agonescent/crisis limit, but at the cost of reducing their intrinsic chromosome instability. Nevertheless, more than half of the hTERT immortalised vHMEC-shp53 cells still showed an abnormal karyotype, displaying both structural, numerical and ploidy aberrations. Notably, even though hTERT overexpression promoted a shift of chromosome aberrations towards stable-type, stabilisation of telomere ends did not, in any case, completely abolish the presence of unstable aberrations. Specifically, dicentric and tricentric chromosomes, as well as acentric fragments and deleted chromosomes, were evidenced in the metaphase plates of vHMEC-shp53-hTERT cells. Furthermore, the presence of lagging chromatin as well as chromatin bridges during cell division denoted actively ongoing BFB cycles and the more likely evolution of the karyotype.

As a whole, our results demonstrate that hTERT overexpression provides a route out of telomere crisis, as stabilisation of telomere ends rescued cellular fitness. However, only the immortalisation of cells that have progressed through a period of telomere-dependent CIN resulted in evolving karyotypes containing both fixed and random chromosomal aberrations. This persistent but reduced CIN would allow for further genome complexity and would thus facilitate the acquisition of the mutations needed to ultimately transform cells to malignity. Consistent with this, the generation of potentially neoplastic cells will occur when telomerase reactivation takes place after CIN has been triggered and before it reaches an intolerable level that leads to cell extinction. If this happens, telomere-dependent induced CIN can play a significant role in the generation of the karyotypic aberrations and the genomic instability observed in human breast carcinomas.

4. Materials and Methods

4.1. Cell Lines

Post-stasis variant human mammary epithelial cells (vHMECs) were obtained from Cell Applications Inc. (San Diego, CA, USA). vHMECs were cultured with serum-free MEpiCM medium supplemented with MEpiCGS and penicillin/streptomycin (all from ScienCell Research Laboratories, Carlsbad, CA, USA), or with M87AX [89]. Growth conditions were 5% CO_2 and 37 °C. Culture population doublings (PDs) were calculated using the formula: $PD = PD_{initial} + \log_2 (N_{final}/N_{initial})$, where $N_{initial}$ is the number of viable cells plated, and N_{final} is the number of viable cells harvested.

4.2. Lentiviral Vectors, Lentivirus Production and Transduction

The lentiviral construct for p53 short hairpin RNA (shp53 pLKO.1 puro) was from Dr Bob Weinberg (Addgene plasmid #19119) and the hTERT lentivirus was supplied by the Viral Vector Facility, CNIC, Madrid, Spain. To generate lentiviral particles, the psPAX2 and pMD2.G plasmids together with the plasmid containing the gene of interest, were introduced in HEK 293T packaging cells using Calphos Mammalian Transfection kit (Clontech, Mountain View, CA, USA). Supernatants were collected at 48 and 72 h post-transfection and concentrated using Amicon 100,000 centrifugal filter units (Merck-Millipore, Burlington, MA, USA).

4.3. Western Blotting

Proteins were extracted with 2% SDS, 67 mM Tris HCl (pH 6.8) containing protease and phosphatase inhibitors. Protein extracts were sonicated twice at 25% amplitude for 15 s, boiled at 95 °C for 15 min and centrifuged at 20,000 *g* for 10 min. Proteins were quantified using the BCA method and absorbance was read at 540 nm with a Victor3 spectrophotometer (PerkinElmer,

Waltham, MA, USA). The proteins (30 µg) were separated using 10% acrylamide or 10% Bis-Tris gels (Life Technologies, Carlsbad, CA, USA, ThermoFisher Scientific, Waltham, MA, USA) at 35 mAmp and transferred onto nitrocellulose membranes at 30 V. Membranes were blocked with 5% non-fat milk or BSA. Primary antibodies used were: rabbit anti-hTERT (Rockland, 600-401-252S), rabbit anti-$p53^{S15}$ (ThermoFisher Scientific, 14H61L24), mouse anti-p53 (ThermoFisher Scientific, DO-1), rabbit anti-$Chk2^{T68}$ (Cell Signalling, 2661, Danvers, MA, USA), mouse anti-Chk2 (Millipore, 05-649) and mouse anti-γH2AX (Upstate; 07-164). The specificity of the hTERT antibody was validated in primary human mammary epithelial cells derived from reduction mammoplasty tissue at passage 2 (data not shown). Furthermore, mouse anti-α-Tubulin (Sigma, B-5-1-2, St. Louis, MO, USA) was used as loading control. Primary antibodies were incubated overnight at 4 °C. Secondary anti-mouse or anti-rabbit horseradish peroxidase (HRP) conjugated antibodies were used and incubated for 1 h at room temperature. Chemiluminescent detection was performed using HRP solution and luminol (Millipore), and images were acquired using Chemidoc, processed with Quantity One software and analysed with ImageLab™ 6.0.0 (BioRad, Hercules, CA, USA).

4.4. Drug Treatments

DSBs were generated in vHMECs and derivatives through exposure to the radiomimetic drug Bleocin™ (Calbiochem, Merck-Chemicals, Darmstadt, Germany), a bleomycin compound, at a final concentration of 2.5 µg/mL. The drug was washed out after 1 h exposure and the cells were left to recover for 60 min before protein extraction.

Colcemid (GIBCO) at a final concentration of 50 ng/mL was added to asynchronously proliferating p53-proficient and deficient vHMEC-hTERT cells. After 24 h of colcemid exposure, the cells were collected and fixed in 70% ethanol and kept frozen until FACS processing. Additional experiments consisted of 48 h colcemid treatment before fixation.

4.5. Obtaining Metaphase Cells and End-to-End Fusion Scoring Criteria

Exponentially-growing vHMEC cell lines were exposed to colcemid (0.5 µg/mL) for 2 h. Cells were trypsinised, swollen in 0.075 M KCl and fixed in methanol:acetic acid (3:1). Cell suspensions were dropped onto clean slides and stored at −20 °C until use. For end-fusion scoring purposes, slides were first stained with DAPI. Then the metaphase plates were captured, and the karyotype was performed by reverse DAPI staining, which results in a reproducible G band-like pattern that allows for accurate individual chromosome identification before the chromosomes become swollen by the denaturation step. Afterwards, the slides were hybridised with the PNA probes and the metaphases were relocated to analyse the telomere and centromere status of each chromosome. A fusion event was considered when the connection between chromatids (1 or 2) was verified on the initial DAPI stained image. This procedure reduces the possibility of end-fusion events being confused with mere alignment of chromosomes.

4.6. In Situ Fluorescence Hybridisation

Telomere and centromere PNA-FISH: Metaphase spreads were hybridised with pantelomeric (Rho-$(CCCTAA)_3$, PE Biosystems, Foster City, CA, USA) and pancentromeric (FITC-AAACACTC TTTTTGTAGA, Panagene, Daejeon, South Korea) PNA probes. Denaturation took place at 80 °C for 3 min and hybridisation was performed at 37 °C for 2 h in a humid chamber. Afterwards, slides were washed twice with 70% formamide for 15 min, followed by three TNT (Trizma Base 50 mM, NaCl 150 mM and Tween-20 0.25%) washes for 5 min. Dehydrated slides were counterstained with DAPI.

OligoFISH: Interphase nuclei spreads were treated with pepsin-HCl at 37 °C for 10 min, post-fixed with formaldehyde-$MgCl_2$ and denatured with 70% formamide at 74 °C. Specific centromeric probes for chromosomes 6 (Gold DY539), 12 (Red DY590) and 17 (Green DY490) (Cellay, Inc., Cambridge, MA,

USA) were hybridised for 2 h in a humid chamber followed by one 5 min wash with 0.2 × SSC − 0.1% SDS at 50 °C and a 2 × SSC wash. Cells were dehydrated and counterstained with DAPI.

4.7. DAPI and Texas Red-X Phalloidin Staining

For the analysis of abnormal nuclear morphologies in interphase or mitosis, cells were cultured on coverslips and fixed with 4% paraformaldehyde for 10 min at 37 °C and rinsed twice in phosphate buffer solution (PBS). Then, cells were permeabilised with 1% Triton X-100 at room temperature during 10 min, rinsed briefly and stained for 5 min in 1 µL solution of Texas Red-X-Phalloidin [200 IU/mL] (Molecular probes) in 1 mL 1 × PBS − 0.1% Tween20-0.5% foetal calf serum. After two or more washes with PBS, coverslips were allowed to dry and counterstained with DAPI.

4.8. Fluorescent Microscopy and Fluorescent Images

Fluorescent staining was visualised under an Olympus BX60 microscope equipped with epifluorescent optics and a camera (Applied Imaging, Inc., Grand Rapids, MI, USA). The fluorochromes were visualised through simple filters and images were captured and analysed using Cytovision software (Applied Imaging, Inc.).

4.9. Flow Cytometry

For cell cycle analysis, the cells were harvested and fixed in 70% ethanol and kept at −20 °C until processing.

The fixed cells were permeabilised with 1 × PBS − 1%Triton X-100 solution and stained with propidium iodide solution (PBS − 1% Triton X-100, propidium iodide 45 µg/mL, and RNase 0.2 mg/mL) before cytometric processing. Analysis was performed under a FACSCalibur (Beckton Dickinson, Franklin Lakes, NJ, USA). Sample excitation was done with a 488 nm laser and a minimum of 10,000 events were collected per sample. Single cells were gated first by forward scatter (FSC) and side scatter (SSC), and DNA content of single cells was measured on FL3 (670 nm long pass filter) and plotted vs. number of cells. The data were analysed with BD FACSDiva software v7.0.

4.10. Statistical Analysis

Data analysis was carried out with GraphPad Prism version 5 software (GraphPad Software Inc., La Jolla, CA, USA). Normality distribution was tested by Saphiro-Wilk normality test. Data sets were compared using Chi^2 test, Fisher's exact test, and Kruskal-Wallis test followed by Dunn's multiple comparison post-test. *p*-values less than 0.05 were considered significant. When multiple comparisons were made, the Bonferroni p-value correction was applied and only *p*-values lower than 0.0125 were considered significant.

Supplementary Materials: Supplementary materials can be found at http://www.mdpi.com/1422-0067/19/7/2078/s1.

Author Contributions: A.B. participated in the study design, contributed to the experimental work, analysed the data and co-drafted the manuscript. E.Z. contributed to the experimental work and to data interpretation. D.D. performed part of the experimental work. E.B. contributed to the Phalloidin-DAPI experiments and to data interpretation. L.T. conceived and designed the study, performed part of the experimental work, interpreted the data and co-drafted the manuscript. All the authors critically reviewed the manuscript and approved the final version.

Funding: This research was funded by MINECO (SAF2013-43801-P). A.B. is supported by a *Universitat Autònoma de Barcelona* fellowship (456-01-1/2012). A.B. and L.T. are members of the 2017 SGR-503 (*Generalitat de Catalunya*).

Acknowledgments: We are grateful to Joan Aurich-Costa (Cellay, Inc; Cambridge, MA, USA) for providing us with oligoFISH probes and the services from the *Universitat Autònoma de Barcelona* (*SCAC_Unitat de Cultius i de Citometria*). The lentiviral construct for p53 short hairpin RNA (shp53 pLKO.1 puro) was from Bob Weinberg (Addgene plasmid #19119).

Conflicts of Interest: The authors declare no conflicts of interest and the founding sponsors played no part in the study design, data collection, analysis or interpretation, writing of the manuscript, and the decision to publish the results.

References

1. Barthel, F.P.; Wei, W.; Tang, M.; Martinez-Ledesma, E.; Hu, X.; Amin, S.B.; Akdemir, K.C.; Seth, S.; Song, X.; Wang, Q.; et al. Systematic analysis of telomere length and somatic alterations in 31 cancer types. *Nat. Genet.* **2017**, *49*, 349–357. [CrossRef] [PubMed]
2. Hanahan, D.; Weinberg, R.A. Hallmarks of cancer: The next generation. *Cell* **2011**, *144*, 646–674. [CrossRef] [PubMed]
3. Michor, F.; Iwasa, Y.; Vogelstein, B.; Lengauer, C.; Nowak, M.A. Can chromosomal instability initiate tumorigenesis? *Semin. Cancer Biol.* **2005**, *15*, 43–49. [CrossRef] [PubMed]
4. Chen, J.; Fu, L.; Zhang, L.Y.; Kwong, D.L.; Yan, L.; Guan, X.Y. Tumor suppressor genes on frequently deleted chromosome 3p in nasopharyngeal carcinoma. *Chin. J. Cancer* **2012**, *31*, 215–222. [CrossRef] [PubMed]
5. Kops, G.J.; Weaver, B.A.; Cleveland, D.W. On the road to cancer: Aneuploidy and the mitotic checkpoint. *Nat. Rev. Cancer* **2005**, *5*, 773–785. [CrossRef] [PubMed]
6. Loeb, L.A. Human cancers express mutator phenotypes: Origin, consequences and targeting. *Nat. Rev. Cancer* **2011**, *11*, 450–457. [CrossRef] [PubMed]
7. Negrini, S.; Gorgoulis, V.G.; Halazonetis, T.D. Genomic instability—An evolving hallmark of cancer. *Nat. Rev. Mol. Cell Biol.* **2010**, *11*, 220–228. [CrossRef] [PubMed]
8. Kolodner, R.D.; Cleveland, D.W.; Putnam, C.D. Aneuploidy drives a mutator phenotype in cancer. *Science* **2011**, *333*, 942–943. [CrossRef] [PubMed]
9. Thompson, S.L.; Bakhoum, S.F.; Compton, D.A. Mechanisms of chromosomal instability. *Curr. Biol.* **2010**, *20*, R285–R295. [CrossRef] [PubMed]
10. Olovnikov, A.M. A theory of marginotomy: The incomplete copying of template margin in enzymic synthesis of polynucleotides and biological significance of the phenomenon. *J. Theor. Biol.* **1973**, *41*, 181–190. [CrossRef]
11. Daniali, L.; Benetos, A.; Susser, E.; Kark, J.D.; Labat, C.; Kimura, M.; Desai, K.; Granick, M.; Aviv, A. Telomeres shorten at equivalent rates in somatic tissues of adults. *Nat. Commun.* **2013**, *4*, 1597. [CrossRef] [PubMed]
12. Harley, C.B.; Futcher, A.B.; Greider, C.W. Telomeres shorten during ageing of human fibroblasts. *Nature* **1990**, *345*, 458–460. [CrossRef] [PubMed]
13. Takai, H.; Smogorzewska, A.; De Lange, T. DNA damage foci at dysfunctional telomeres. *Curr. Biol.* **2003**, *13*, 1549–1556. [CrossRef]
14. Kaul, Z.; Cesare, A.J.; Huschtscha, L.I.; Neumann, A.A.; Reddel, R.R. Five dysfunctional telomeres predict onset of senescence in human cells. *EMBO Rep.* **2011**, *13*, 52–59. [CrossRef] [PubMed]
15. D'Adda di Fagagna, F.; Reaper, P.M.; Clay-Farrace, L.; Fiegler, H.; Carr, P.; von Zglinicki, T.; Saretzki, G.; Carter, N.P.; Jackson, S.P. A DNA damage checkpoint response in telomere-initiated senescence. *Nature* **2003**, *426*, 194–198. [CrossRef] [PubMed]
16. Cesare, A.J.; Hayashi, M.T.; Crabbe, L.; Karlseder, J. The telomere deprotection response is functionally distinct from the genomic DNA damage response. *Mol. Cell* **2013**, *51*, 141–155. [CrossRef] [PubMed]
17. Chin, L.; Artandi, S.E.; Shen, Q.; Tam, A.; Lee, S.L.; Gottlieb, G.J.; Greider, C.W.; Depinho, R.A. p53 deficiency rescues the adverse effects of telomere loss and cooperates with telomere dysfunction to accelerate carcinogenesis. *Cell* **1999**, *97*, 527–538. [CrossRef]
18. Artandi, S.E.; Chang, S.; Lee, S.L.; Alson, S.; Gottlieb, G.J.; Chin, L.; DePinho, R.A. Telomere dysfunction promotes non-reciprocal translocations and epithelial cancers in mice. *Nature* **2000**, *406*, 641–645. [CrossRef] [PubMed]
19. Ding, Z.; Wu, C.J.; Jaskelioff, M.; Ivanova, E.; Kost-Alimova, M.; Protopopov, A.; Chu, G.C.; Wang, G.; Lu, X.; Labrot, E.S.; et al. Telomerase reactivation following telomere dysfunction yields murine prostate tumors with bone metastases. *Cell* **2012**, *148*, 896–907. [CrossRef] [PubMed]
20. Chin, K.; de Solorzano, C.O.; Knowles, D.; Jones, A.; Chou, W.; Rodriguez, E.G.; Kuo, W.-L.L.; Ljung, B.-M.M.; Chew, K.; Myambo, K.; et al. In situ analyses of genome instability in breast cancer. *Nat. Genet.* **2004**, *36*, 984–988. [CrossRef] [PubMed]

21. Meeker, A.K.; Hicks, J.L.; Gabrielson, E.; Strauss, W.M.; De Marzo, A.M.; Argani, P. Telomere shortening occurs in subsets of normal breast epithelium as well as in situ and invasive carcinoma. *Am. J. Pathol.* **2004**, *164*, 925–935. [CrossRef]
22. Meeker, A.K.; Argani, P. Telomere shortening occurs early during breast tumorigenesis: A cause of chromosome destabilization underlying malignant transformation? *J. Mammary Gland Biol. Neoplasia* **2004**, *9*, 285–296. [CrossRef] [PubMed]
23. Tanaka, H.; Abe, S.; Huda, N.; Tu, L.; Beam, M.J.; Grimes, B.; Gilley, D. Telomere fusions in early human breast carcinoma. *Proc. Natl. Acad. Sci. USA* **2012**, *109*, 14098–14103. [CrossRef] [PubMed]
24. Ellsworth, R.E.; Blackburn, H.L.; Shriver, C.D.; Soon-Shiong, P.; Ellsworth, D.L. Molecular heterogeneity in breast cancer: State of the science and implications for patient care. *Semin. Cell Dev. Biol.* **2017**, *64*, 65–72. [CrossRef] [PubMed]
25. Sugino, T.; Yoshida, K.; Bolodeoku, J.; Tahara, H.; Buley, I.; Manek, S.; Wells, C.; Goodison, S.; Ide, T.; Suzuki, T.; et al. Telomerase activity in human breast cancer and benign breast lesions: Diagnostic applications in clinical specimens, including fine needle aspirates. *Int. J. Cancer* **1996**, *69*, 301–306. [CrossRef]
26. Bednarek, A.K.; Sahin, A.; Brenner, A.J.; Johnston, D.A.; Aldaz, C.M. Analysis of telomerase activity levels in breast cancer: Positive detection at the in situ breast carcinoma stage. *Clin. Cancer Res.* **1997**, *3*, 11–16. [PubMed]
27. Poremba, C.; Shroyer, K.R.; Frost, M.; Diallo, R.; Fogt, F.; Schäfer, K.L.; Bürger, H.; Shroyer, A.L.; Dockhorn-Dworniczak, B.; Boecker, W. Telomerase is a highly sensitive and specific molecular marker in fine-needle aspirates of breast lesions. *J. Clin. Oncol.* **1999**, *17*, 2020–2026. [CrossRef] [PubMed]
28. Shpitz, B.; Zimlichman, S.; Zemer, R.; Bomstein, Y.; Zehavi, T.; Liverant, S.; Bernehim, J.; Kaufman, Z.; Klein, E.; Shapira, Y.; et al. Telomerase activity in ductal carcinoma in situ of the breast. *Breast Cancer Res. Treat.* **1999**, *58*, 65–69. [CrossRef] [PubMed]
29. Brenner, A.J.; Stampfer, M.R.; Aldaz, C.M. Increased p16 expression with first senescence arrest in human mammary epithelial cells and extended growth capacity with p16 inactivation. *Oncogene* **1998**, *17*, 199–205. [CrossRef] [PubMed]
30. Romanov, S.R.; Kozakiewicz, B.K.; Holst, C.R.; Stampfer, M.R.; Haupt, L.M.; Tlsty, T.D. Normal human mammary epithelial cells spontaneously escape senescence and acquire genomic changes. *Nature* **2001**, *409*, 633–637. [CrossRef] [PubMed]
31. Soler, D.; Genescà, A.; Arnedo, G.; Egozcue, J.; Tusell, L. Telomere dysfunction drives chromosomal instability in human mammary epithelial cells. *Genes Chromosom. Cancer* **2005**, *44*, 339–350. [CrossRef] [PubMed]
32. Genescà, A.; Pampalona, J.; Frías, C.; Domínguez, D.; Tusell, L. Role of telomere dysfunction in genetic intratumor diversity. *Adv. Cancer Res.* **2011**, *112*, 11–41. [PubMed]
33. Garbe, J.C.; Holst, C.R.; Bassett, E.; Tlsty, T.D.; Stampfer, M.R. Inactivation of p53 function in cultured human mammary epithelial cells turns the telomere-length dependent senescence barrier from agonescence into crisis. *Cell Cycle* **2007**, *6*, 1927–1936. [CrossRef] [PubMed]
34. Musacchio, A.; Salmon, E.D. The spindle-assembly checkpoint in space and time. *Nat. Rev. Mol. Cell Biol.* **2007**, *8*, 379–393. [CrossRef] [PubMed]
35. Rieder, C.L.; Schultz, A.; Cole, R.; Sluder, G. Anaphase onset in vertebrate somatic cells is controlled by a checkpoint that monitors sister kinetochore attachment to the spindle. *J. Cell Biol.* **1994**, *127*, 1301–1310. [CrossRef] [PubMed]
36. Rieder, C.L.; Cole, R.W.; Khodjakov, A.; Sluder, G. The checkpoint delaying anaphase in response to chromosome monoorientation is mediated by an inhibitory signal produced by unattached kinetochores. *J. Cell Biol.* **1995**, *130*, 941–948. [CrossRef] [PubMed]
37. Andreassen, P.R.; Lohez, O.D.; Lacroix, F.B.; Margolis, R.L. Tetraploid state induces p53-dependent arrest of nontransformed mammalian cells in G1. *Mol. Biol. Cell* **2001**, *12*, 1315–1328. [CrossRef] [PubMed]
38. Borel, F.; Lohez, O.D.; Lacroix, F.B.; Margolis, R.L. Multiple centrosomes arise from tetraploidy checkpoint failure and mitotic centrosome clusters in p53 and RB pocket protein-compromised cells. *Proc. Natl. Acad. Sci. USA* **2002**, *99*, 9819–9824. [CrossRef] [PubMed]
39. Casenghi, M.; Mangiacasale, R.; Tuynder, M.; Caillet-Fauquet, P.; Elhajouji, A.; Lavia, P.; Mousset, S.; Kirsch-Volders, M.; Cundari, E. p53-independent apoptosis and p53-dependent block of DNA rereplication following mitotic spindle inhibition in human cells. *Exp. Cell Res.* **1999**, *250*, 339–350. [CrossRef] [PubMed]

40. Cross, S.M.; Sanchez, C.A.; Morgan, C.A.; Schimke, M.K.; Ramel, S.; Idzerda, R.L.; Raskind, W.H.; Reid, B.J. A p53-dependent mouse spindle checkpoint. *Science* **1995**, *267*, 1353–1356. [CrossRef] [PubMed]
41. Vogel, C.; Kienitz, A.; Hofmann, I.; Müller, R.; Bastians, H. Crosstalk of the mitotic spindle assembly checkpoint with p53 to prevent polyploidy. *Oncogene* **2004**, *23*, 6845–6853. [CrossRef] [PubMed]
42. Deng, W.; Tsao, S.W.; Guan, X.Y.; Lucas, J.N.; Cheung, A.L.M. Role of short telomeres in inducing preferential chromosomal aberrations in human ovarian surface epithelial cells: A combined telomere quantitative fluorescence in situ hybridization and whole-chromosome painting study. *Genes Chromosom. Cancer* **2003**, *37*, 92–97. [CrossRef] [PubMed]
43. Deng, W.; Tsao, S.W.; Guan, X.Y.; Lucas, J.N.; Si, H.X.; Leung, C.S.; Mak, P.; Wang, L.D.; Cheung, A.L.M. Distinct profiles of critically short telomeres are a key determinant of different chromosome aberrations in immortalized human cells: Whole-genome evidence from multiple cell lines. *Oncogene* **2004**, *23*, 9090–9101. [CrossRef] [PubMed]
44. Der-Sarkissian, H.; Bacchetti, S.; Cazes, L.; Londoño-Vallejo, J.A. The shortest telomeres drive karyotype evolution in transformed cells. *Oncogene* **2004**, *23*, 1221–1228. [CrossRef] [PubMed]
45. Plug-DeMaggio, A.W.; Sundsvold, T.; Wurscher, M.A.; Koop, J.I.; Klingelhutz, A.J.; McDougall, J.K. Telomere erosion and chromosomal instability in cells expressing the HPV oncogene 16E6. *Oncogene* **2004**, *23*, 3561–3571. [CrossRef] [PubMed]
46. Pampalona, J.; Soler, D.; Genescà, A.; Tusell, L. Whole chromosome loss is promoted by telomere dysfunction in primary cells. *Genes Chromosom. Cancer* **2010**, *49*, 368–378. [CrossRef] [PubMed]
47. Davoli, T.; Denchi, E.L.; de Lange, T. Persistent telomere damage induces bypass of mitosis and tetraploidy. *Cell* **2010**, *141*, 81–93. [CrossRef] [PubMed]
48. Pampalona, J.; Frías, C.; Genescà, A.; Tusell, L. Progressive telomere dysfunction causes cytokinesis failure and leads to the accumulation of polyploid cells. *PLoS Genet.* **2012**, *8*, e1002679. [CrossRef] [PubMed]
49. Castedo, M.; Coquelle, A.; Vivet, S.; Vitale, I.; Kauffmann, A.; Dessen, P.; Pequignot, M.O.; Casares, N.; Valent, A.; Mouhamad, S.; et al. Apoptosis regulation in tetraploid cancer cells. *EMBO J.* **2006**, *25*, 2584–2595. [CrossRef] [PubMed]
50. Senovilla, L.; Vitale, I.; Galluzzi, L.; Vivet, S.; Joza, N.; Younes, A.B.; Rello-Varona, S.; Castedo, M.; Kroemer, G. p53 represses the polyploidization of primary mammary epithelial cells by activating apoptosis. *Cell Cycle* **2009**, *8*, 1380–1385. [CrossRef] [PubMed]
51. Ganem, N.J.; Godinho, S.A.; Pellman, D. A mechanism linking extra centrosomes to chromosomal instability. *Nature* **2009**, *460*, 278–282. [CrossRef] [PubMed]
52. Silkworth, W.T.; Nardi, I.K.; Scholl, L.M.; Cimini, D. Multipolar Spindle Pole Coalescence is a Major Source of Kinetochore Mis-Attachment and Chromosome Mis-Segregation in Cancer Cells. *PLoS ONE* **2009**, *4*, e6564. [CrossRef] [PubMed]
53. Garbe, J.C.; Vrba, L.; Sputova, K.; Fuchs, L.; Novak, P.; Brothman, A.R.; Jackson, M.; Chin, K.; LaBarge, M.A.; Watts, G.; et al. Immortalization of normal human mammary epithelial cells in two steps by direct targeting of senescence barriers does not require gross genomic alterations. *Cell Cycle* **2014**, *13*, 3423–3435. [CrossRef] [PubMed]
54. Toouli, C.; Huschtscha, L.; Neumann, A. Comparison of human mammary epithelial cells immortalized by simian virus 40 T-Antigen or by the telomerase catalytic subunit. *Oncogene* **2002**, *21*, 128–139. [CrossRef] [PubMed]
55. Rao, K.; Bryant, E.; O'Hara Larivee, S.; McDougall, J.K. Production of spindle cell carcinoma by transduction of H-Ras 61L into immortalized human mammary epithelial cells. *Cancer Lett.* **2003**, *201*, 79–88. [CrossRef]
56. Haga, K.; Ohno, S.; Yugawa, T.; Narisawa-Saito, M.; Fujita, M.; Sakamoto, M.; Galloway, D.A.; Kiyono, T. Efficient immortalization of primary human cells by $p16^{INK4a}$-specific short hairpin RNA or Bmi-1, combined with introduction of hTERT. *Cancer Sci.* **2007**, *98*, 147–154. [CrossRef] [PubMed]
57. Joshi, P.S.; Modur, V.; Cheng, J.; Robinson, K.; Rao, K. Characterization of immortalized human mammary epithelial cell line HMEC 2.6. *Tumour Biol.* **2017**, *39*. [CrossRef] [PubMed]
58. Ulbricht, U.; Sommer, A.; Beckmann, G.; Lutzenberger, M.; Seidel, H.; Kreft, B.; Toschi, L. Isogenic human mammary epithelial cell lines: Novel tools for target identification and validation. Comprehensive characterization of an isogenic human mammary epithelial cell model provides evidence for epithelial-mesenchymal transition. *Breast Cancer Res. Treat.* **2013**, *138*, 437–456. [CrossRef] [PubMed]

59. Bunz, F.; Fauth, C.; Speicher, M.R.; Dutriaux, A.; Sedivy, J.M.; Kinzler, K.W.; Vogelstein, B.; Lengauer, C. Targeted inactivation of p53 in human cells does not result in aneuploidy. *Cancer Res.* **2002**, *62*, 1129–1133. [PubMed]
60. Rogakou, E.P.; Pilch, D.R.; Orr, A.H.; Ivanova, V.S.; Bonner, W.M. DNA double-stranded breaks induce histone H2AX phosphorylation on serine 139. *J. Biol. Chem.* **1998**, *273*, 5858–5868. [CrossRef] [PubMed]
61. Roake, C.M.; Artandi, S.E. Control of Cellular Aging, Tissue Function, and Cancer by p53 Downstream of Telomeres. *Cold Spring Harb. Perspect. Med.* **2017**, *7*, a026088. [CrossRef] [PubMed]
62. Olivier, M.; Hollstein, M.; Hainaut, P. TP53 Mutations in Human Cancers: Origins, Consequences, and Clinical Use. *Cold Spring Harb. Perspect. Biol.* **2010**, *2*, a001008. [CrossRef] [PubMed]
63. Holst, C.R.; Nuovo, G.J.; Esteller, M.; Chew, K.; Baylin, S.B.; Herman, J.G.; Tlsty, T.D. Methylation of $p16^{INK4a}$ promoters occurs in vivo in histologically normal human mammary epithelia. *Cancer Res.* **2003**, *63*, 1596–1601. [PubMed]
64. Shackney, S.E.; Silverman, J.F. Molecular evolutionary patterns in breast cancer. *Adv. Anat. Pathol.* **2003**, *10*, 278–290. [CrossRef] [PubMed]
65. Hui, R.; Macmillan, R.D.; Kenny, F.S.; Musgrove, E.A.; Blamey, R.W.; Nicholson, R.I.; Robertson, J.F.; Sutherland, R.L. *INK4a* gene expression and methylation in primary breast cancer: Overexpression of $p16^{INK4a}$ messenger RNA is a marker of poor prognosis. *Clin. Cancer Res.* **2000**, *6*, 2777–2787. [PubMed]
66. Tusell, L.; Soler, D.; Agostini, M.; Pampalona, J.; Genescà, A. The number of dysfunctional telomeres in a cell: One amplifies; more than one translocate. *Cytogenet. Genome Res.* **2008**, *122*, 315–325. [CrossRef] [PubMed]
67. Pampalona, J.; Roscioli, E.; Silkworth, W.T.; Bowden, B.; Genescà, A.; Tusell, L.; Cimini, D. Chromosome Bridges Maintain Kinetochore-Microtubule Attachment throughout Mitosis and Rarely Break during Anaphase. *PLoS ONE* **2016**, *11*, 1–17. [CrossRef] [PubMed]
68. Seewaldt, V.L.; Mrózek, K.; Sigle, R.; Dietze, E.C.; Heine, K.; Hockenbery, D.M.; Hobbs, K.B.; Caldwell, L.E. Suppression of p53 function in normal human mammary epithelial cells increases sensitivity to extracellular matrix-induced apoptosis. *J. Cell Biol.* **2001**, *155*, 471–486. [CrossRef] [PubMed]
69. Fujiwara, T.; Bandi, M.; Nitta, M.; Ivanova, E.V.; Bronson, R.T.; Pellman, D. Cytokinesis failure generating tetraploids promotes tumorigenesis in p53-null cells. *Nature* **2005**, *437*, 1043–1047. [CrossRef] [PubMed]
70. Davoli, T.; de Lange, T. Telomere-driven tetraploidization occurs in human cells undergoing crisis and promotes transformation of mouse cells. *Cancer Cell* **2012**, *21*, 765–776. [CrossRef] [PubMed]
71. Duelli, D.M.; Padilla-Nash, H.M.; Berman, D.; Murphy, K.M.; Ried, T.; Lazebnik, Y. A virus causes cancer by inducing massive chromosomal instability through cell fusion. *Curr. Biol.* **2007**, *17*, 431–437. [CrossRef] [PubMed]
72. Nguyen, H.G.; Makitalo, M.; Yang, D.; Chinnappan, D.; Hilaire, C.S.; Ravid, K.; St Hilaire, C.; Ravid, K. Deregulated Aurora-B induced tetraploidy promotes tumorigenesis. *FASEB J.* **2009**, *23*, 2741–2748. [CrossRef] [PubMed]
73. Olaharski, A.J.; Sotelo, R.; Solorza-Luna, G.; Gonsebatt, M.E.; Guzman, P.; Mohar, A.; Eastmond, D.A. Tetraploidy and chromosomal instability are early events during cervical carcinogenesis. *Carcinogenesis* **2006**, *27*, 337–343. [CrossRef] [PubMed]
74. Galipeau, P.C.; Cowan, D.S.; Sanchez, C.A.; Barrett, M.T.; Emond, M.J.; Levine, D.S.; Rabinovitch, P.S.; Reid, B.J. 17p (p53) allelic losses, 4N (G2/tetraploid) populations, and progression to aneuploidy in Barrett's esophagus. *Proc. Natl. Acad. Sci. USA* **1996**, *93*, 7081–7084. [CrossRef] [PubMed]
75. Davoli, T.; de Lange, T. The causes and consequences of polyploidy in normal development and cancer. *Annu. Rev. Cell Dev. Biol.* **2011**, *27*, 585–610. [CrossRef] [PubMed]
76. Dewhurst, S.M.; McGranahan, N.; Burrell, R.A.; Rowan, A.J.; Gronroos, E.; Endesfelder, D.; Joshi, T.; Mouradov, D.; Gibbs, P.; Ward, R.L.; et al. Tolerance of Whole-Genome Doubling Propagates Chromosomal Instability and Accelerates Cancer Genome Evolution. *Cancer Discov.* **2014**, *4*, 175–185. [CrossRef] [PubMed]
77. Gao, Q.; Hauser, S.H.; Liu, X.L.; Wazer, D.E.; Madoc-Jones, H.; Band, V. Mutant p53-induced immortalization of primary human mammary epithelial cells. *Cancer Res.* **1996**, *56*, 3129–3133. [PubMed]
78. Gollahon, L.S.; Shay, J.W. Immortalization of human mammary epithelial cells transfected with mutant p53 (273his). *Oncogene* **1996**, *12*, 715–725. [PubMed]
79. Stampfer, M.R.; Garbe, J.; Nijjar, T.; Wigington, D.; Swisshelm, K.; Yaswen, P. Loss of p53 function accelerates acquisition of telomerase activity in indefinite lifespan human mammary epithelial cell lines. *Oncogene* **2003**, *22*, 5238–5251. [CrossRef] [PubMed]

80. Herr, A.J.; Ogawa, M.; Lawrence, N.A.; Williams, L.N.; Eggington, J.M.; Singh, M.; Smith, R.A.; Preston, B.D. Mutator suppression and escape from replication error-induced extinction in yeast. *PLoS Genet.* **2011**, *7*, e1002282. [CrossRef]
81. Sniegowski, P.D.; Gerrish, P.J.; Johnson, T.; Shaver, A. The evolution of mutation rates: Separating causes from consequences. *Bioessays* **2000**, *22*, 1057–1066. [CrossRef]
82. Nowak, M.; Schuster, P. Error thresholds of replication in finite populations mutation frequencies and the onset of Muller's ratchet. *J. Theor. Biol.* **1989**, *137*, 375–395. [CrossRef]
83. Andor, N.; Maley, C.C.; Ji, H.P. Genomic Instability in Cancer: Teetering on the Limit of Tolerance. *Cancer Res.* **2017**, *77*, 2179–2185. [CrossRef] [PubMed]
84. Zhang, H.; Jin, Y.; Chen, X.; Jin, C.; Law, S.; Tsao, S.W.; Kwong, Y.L. Cytogenetic aberrations in immortalization of esophageal epithelial cells. *Cancer Genet. Cytogenet.* **2006**, *165*, 25–35. [CrossRef] [PubMed]
85. Jin, Y.; Zhang, H.; Tsao, S.W.; Jin, C.; Lv, M.; Strömbeck, B.; Wiegant, J.; Wan, T.S.; Yuen, P.W.; Kwong, Y.L. Cytogenetic and molecular genetic characterization of immortalized human ovarian surface epithelial cell lines: Consistent loss of chromosome 13 and amplification of chromosome 20. *Gynecol. Oncol.* **2004**, *92*, 183–191. [CrossRef] [PubMed]
86. Coursen, J.D.; Bennett, W.P.; Gollahon, L.; Shay, J.W.; Harris, C.C. Genomic instability and telomerase activity in human bronchial epithelial cells during immortalization by human papillomavirus-16 E6 and E7 genes. *Exp. Cell Res.* **1997**, *235*, 245–253. [CrossRef] [PubMed]
87. Savelieva, E.; Belair, C.D.; Newton, M.A.; DeVries, S.; Gray, J.W.; Waldman, F.; Reznikoff, C.A. 20q gain associates with immortalization: 20q13.2 amplification correlates with genome instability in human papillomavirus 16 E7 transformed human uroepithelial cells. *Oncogene* **1997**, *14*, 551–560. [CrossRef] [PubMed]
88. Liu, S.; Hatton, M.P.; Khandelwal, P.; Sullivan, D.A. Culture, immortalization, and characterization of human meibomian gland epithelial cells. *Investig. Ophthalmol. Vis. Sci.* **2010**, *51*, 3993–4005. [CrossRef] [PubMed]
89. Garbe, J.C.; Bhattacharya, S.; Merchant, B.; Bassett, E.; Swisshelm, K.; Feiler, H.S.; Wyrobek, A.J.; Stampfer, M.R. Molecular distinctions between stasis and telomere attrition senescence barriers shown by long-term culture of normal human mammary epithelial cells. *Cancer Res.* **2009**, *69*, 7557–7568. [CrossRef] [PubMed]

Supplementary Materials

Table S1. Chromosome analysis of young vHMECs at PD22.

Karyotype	number
46, XX	15
46, XX, ctb(13q)	1
45, XX, fus(11p;22q)	1
43, XX, ctb(6q), -3, -16, -22	1
46, XX, ctb(10q)	1
46, XX, fus(21p;19q)	1
46, XX, nrt(14p)	1
46, XX, +ace	1
45, XX, fus(2q;17q)	1
46, XX, nrt(4p), fus(19q;22q)	1
92, XXXX, fus(3p;3q)	1
94,XXXX, +2, +12, fus(19q;20p), -20, +22	1
TOTAL	**26**

Table S2. Chromosome analysis of aged vHMECs at PD32.

Karyotype	number
43, X, nrt(5q), fus(9q;22q), fus(19p;22q)	1
45, XX, fus(Dq;22q), +csb	1
45, XX, fus(12q;13q)	1
45, X, nrt(1q), fus(14q;22p), csb(Xp)	1
43, XX, fus(12q;14q), fus(14q;22p), -20	1
43, XX, dic(9q;?;14q), -18, -22	1
45, XX, fus(9q;12q), nrt(22q,14q)	1
45, XX, fus(12q;?;14q)	1
46, XX, +csb, +csb	1
44, XX, +csb	1
45, XX, fus(14p;22q)	1
43, XX, fus(2q;14q)	1
42, XX, fus(20q;22q), several losses	1
44, X, fus(12q;?;22q), -X	1
45, XX, fus(12q;16), -21, +mar	1
44, XX, i(14q), +14	1
43, XX, fus(9q;14q), nrt(22q;14q), fus(18p;21p)	1
?, XX, fus(2q;14q)	1
92,XXXX, fus(9q;21q), fus(9q;21q)	1
92,XXXX, fus(9q;21q), fus(14p;14p)	1
TOTAL	**20**

Table S3. Chromosome analysis of vHMEC-shp53 at PD29.

Karyotype	number
23, mar(Xq), dic(2q;?;2q), dic(2q;?;3q), dic(12q;18q), +11	1
35, XX, dic(2q;17q), dic(3q;5q), dic(8q;20q), ntr(9q;?), +12, +12, ntr(12q;?), dic(14q;21q+), +ace, +ace, +ace	1
Pseudotriploid, dic(7p;18q), +ace	1
43, XX, ntr(3q;?), -1, -7, -17	1
76, XXXX, dic(3q;21q), del(5p), dic(18q;21p)	1
40, XX, dic(12q;22q), csb(12p), +ace, +ace	1
40, XX, dic(9q;11p)	1
29, X, dic(2q;16q), dic(3q;17q), dic(12p;?), csb(?)	1
45, XX, t(4q;9q), nrt(11p;?), -14	1
37, XX, +mar	1
42, XX, tric(7p;?;15q), dic(21q;19q), -16	1
41, X, tric(12q;21;?;10p), dic(19q;20p), +mar	1
33, XX, dic(3q;12q), tric(19q;?;14q), +ace, +mar	1
31, XX, +csb	1
44, XX, dic(14q;20p), dic(15p;17q)	1
42, XX, dic(11p;?), tric(21q;19;22q), +ace	1
40, XX, dic(2p;17p), dic(12p;16q), -5, -9, -14, -16	1
80, del(2p), nrt(2q;?), tric(3q;17;?;22q), dic(7q;?;15p), del(14p), dic(17q;?;22q), dic(20p;21p)	1
39, XX, dic(19p;21q)	1
40, X, dic(2p;?;12p), nrt(3p;?), dic(4q;7p), dic(10p;?), nrt(16q;?), tetrac(17q;22;X;20p), +ace, +csb	1
Pseudotriploid, r(3), r(3), tric(12q;?;20q), tric(12q;?;20q), dic(21q;19), dic(22q;?)	1
43, XX, tric(2q;17;12q), -16	1
38, XX, dic(12q;12q), dic(21q;?;19p), dic(16q;?)	1
TOTAL	**23**

Table S4. Chromosome analysis of vHMEC-hTERT at PD76.

Karyotype	number
46, XX	4
47, XX, +20	34
47, XX, nrt(15q;?), +20	1
47, XX, nrt(5q;?), +20	1
47, XX, del(17p), +20	1
47, XX, del(10p), +20	2
46, XX, del(18p)	1
46, XX, nrt(16q;?)	1
46, XX, -16, +mar	1
TOTAL	**46**

Table S5. Chromosome analysis of vHMEC-shp53-hTERT at PD47.

Karyotype	number
46, XX	16
45, XX, -14	1
45, XX, -22	1
46, XX, -11, +mar	1
46, XX, -20, +mar	1
41, X, -7, -12, -17, -18	1
45, XX, tric(9p;?;15p), nrt(12p:?), -19, nrt(20p;?)	1
46, XX, nrt(21q;?)	3
46, XX, dic(20q;?;17p)	1
46, XX, nrt(12p:?), dic(18p;19p), nrt (21q;?)	1
46, XX, dic(9p;?;21p), nrt(12p:?)	1
45, XX, nrt(12p:?), -19	1
46, XX, nrt(12p:?)	1
46, XX, nrt(9p;?), nrt(12p:?), dic(21p;?)	1
46, XX, nrt(9p;?), nrt(12p;?), nrt(20p;?)	1
46, XX, nrt(9p;?), nrt(12p;?), nrt(21p;?)	1
48, XX, nrt(12p;?), nrt(21q;?), +del, +ace, +ace	1
45, XX, del(9p), nrt(12p;?), -16, +ace	1
45, XX, idic(7p;7p), +7, dic(20p;?), tric(22q, ?; ?), -21	1
45, XX, nrt(12p:?), -21	6
46, XX, dic(6p;14p), dic(9p;?), nrt(12p;?), dic(13p;14p), nrt(21q;?)	1
46, XX, nrt(3q;?), del(Xq)	1
46, XX, nrt(3q;?)	2
47, XX, nrt(9p;?), nrt(21p;?), +21	1
45, XX, del(3p), -21	1
46, XX, dic(20q;?)	1
46, XX, del(1q), nrt(17q;?)	1
46, XX, nrt(9p;?), nrt(12p;?), nrt(21p;?)	1
46, XX, del(3p), dic(20q;?)	1
92, XXXX	1
87, XXXX, -12, nrt(12p:?), nrt(12p:?), -21, -22	1
TOTAL	**54**

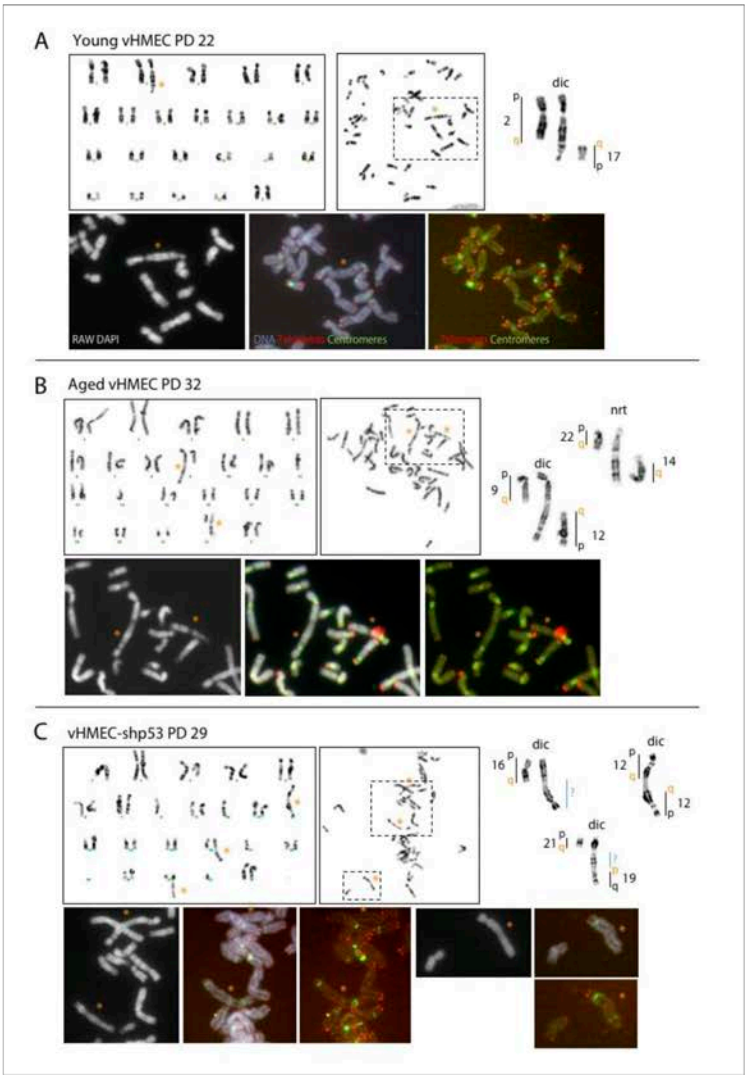

Figure S1. Procedures of the cytogenetic analysis of the finite cell lines. The karyotype, the metaphase spread and the reorganised chromosomes are shown. The rearranged chromosomes are indicated with an asterisk. Moreover, partial images from the metaphase after in situ hybridisation with pancentromeric and pantelomeric PNA probes, which corresponds to the discontinuous line box, are shown. From left to right, the raw image of DAPI; the merged image of DNA (blue) and PNA centromeric (green) and telomeric (red) probes; and the combination of PNA probes only. (A) Karyotype of a young vHMEC at PD22 showing an end-to-end fusion between 2q and 17q. (B) Karyotype of an aged vHMEC at PD32 showing an end-to-end fusion between 9q and 12q as well as a non-reciprocal translocation (nrt) between 22q and 14q. (C) Karyotype of a vHMEC-shp53 at PD29 showing an end-to-end fusion between 12q and 12q as well as two dicentric chromosomes not completely defined. Note the absence of telomere FISH signals at the fusion point of all the dicentric chromosomes displayed.

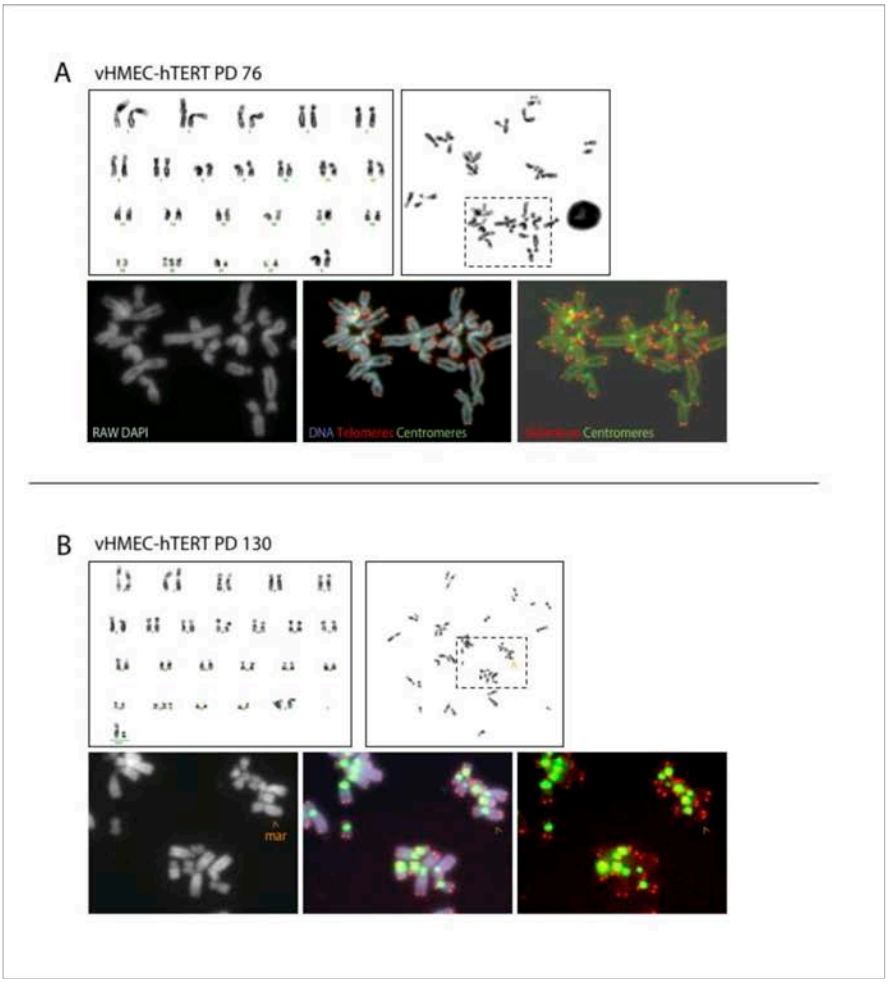

Figure S2. Procedures of the cytogenetic analysis of the vHMEC-hTERT cell line. The karyotype and the metaphase spread are shown. Moreover, partial images from the metaphase after *in situ* hybridisation with pancentromeric and pantelomeric PNA probes, which corresponds to the discontinuous line box, are shown. From left to right, the raw image of DAPI; the merged image of DNA (blue) and PNA centromeric (green) and telomeric (red) probes; and the combination of PNA probes only. **(A)** Karyotype of vHMEC-hTERT at PD76 showing trisomy 20. **(B)** Karyotype of vHMEC-hTERT at PD130 showing two marker (mar) chromosomes in addition to trisomy 20. Open arrows indicate one of the marker chromosomes.

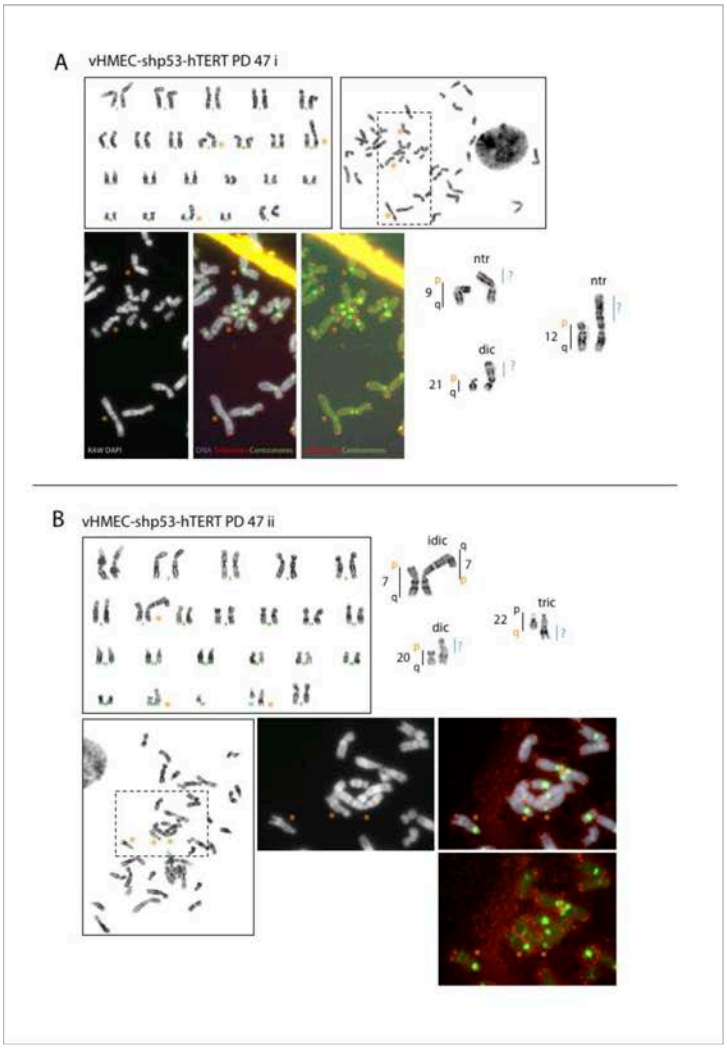

Figure S3. Procedures of the cytogenetic analysis of the vHMEc-shp53-hTERT cell line. The karyotype, the metaphase spread and the reorganised chromosomes are shown. The rearranged chromosomes are indicated with an asterisk. Moreover, partial images from the metaphase after *in situ* hybridisation with pancentromeric and pantelomeric PNA probes, which corresponds to the discontinuous line box, are shown. From left to right, the raw image of DAPI; the merged image of DNA (blue) and PNA centromeric (green) and telomeric (red) probes; and the combination of PNA probes only. **(A)** Karyotype of a vHMEC-shp53-hTERT at PD47 showing two ntr, as well as one dicentric chromosomes not completely defined. **(B)** A second karyotype of a vHMEC-shp53-hTERT at PD47 showing an end-to-end fusion between 7p arms of two distinct chromosomes, as well as one dicentric and one tricentric chromosomes not completely defined. Note the absence of telomere FISH signals at the fusion point of all the dicentric chromosomes displayed.

Work II

www.oncotarget.com Oncotarget, 2018, Vol. 9, (No. 43), pp: 27151-27170

Research Paper

Acute telomere deprotection prevents ongoing BFB cycles and rampant instability in p16^{INK4a}-deficient epithelial cells

Aina Bernal[1], Marc Moltó-Abad[1,2], Daniel Domínguez[1] and Laura Tusell[1]

[1]Unitat de Biologia Cel·lular, Facultat de Biociències, Universitat Autònoma de Barcelona, 08193 Cerdanyola del Vallès, Spain

[2]Current address: Unitat de Malalties Minoritàries, Hospital Universitari de la Vall d'Hebron, 08035 Barcelona, Spain

Correspondence to: *Laura Tusell,* ***email:*** *laura.tusell@uab.cat*

Keywords: *MCF-10A; breast epithelial cells; chromosome instability; telomere-dysfunction; TRF2$^{\Delta B\Delta M}$*

Received: *June 28, 2017* ***Accepted:*** *May 13, 2018* ***Published:*** *June 05, 2018*

ABSTRACT

Telomere dysfunction drives chromosome instability through endless breakage-fusion-bridge (BFB) cycles that promote the formation of highly rearranged genomes. However, reactivation of telomerase or ALT-pathway is required for genome stabilisation and full malignant transformation. To allow the unrestricted proliferation of cells at risk of transformation, we have established a conditional system of telomere deprotection in p16^{INK4a}-deficient MCF-10A cells with modified checkpoints. After sustained expression of a dominant negative form of the shelterin protein TRF2 (TRF2$^{\Delta B\Delta M}$), cells with telomere fusion did progress to anaphase but no signs of ongoing BFB cycles were observed, thus anticipating proliferation defects. Indeed, 96 h TRF2$^{\Delta B\Delta M}$ expression resulted in noticeable growth proliferation defects in the absence of cell cycle disturbances. Further transient periods of 96 h telomere uncapping did not result in cell cycle disturbances either. And reduction of the telomere damage to short acute deprotection periods did not in any case engender cells with a reorganised karyotype. Strikingly, the growth arrest imposed in cells showing dysfunctional telomeres was not accompanied by an activation of the DNA damage response at cellular level, or by the presence of visible markers of senescence or apoptosis. We propose that the deprotection of many telomeres simultaneously, even for a short time, results in a local activation of the cellular stress response which consequently triggers gradual cell withdrawal from cell cycle, restraining the onset of genomic instability.

INTRODUCTION

Telomeres are nucleoprotein complexes that cap the ends of chromosomes, thus preventing illegitimate recombination processes. By adopting a t-loop structure, telomeres ensure genomic stability by providing chromosome end protection [1, 2, and reviewed by 3]. The most deleterious outcome of telomere deprotection is the formation of chromosome end-to-end fusions, which may fire breakage-fusion-bridge (BFB) cycles and rampant chromosome instability (CIN) [4–6, and reviewed by 7]. In certain types of epithelial cancers, telomere dysfunction is considered to be a key trigger for CIN and a promoter of tumourigenesis [8, 9]. Specifically in the breast, studies support the view that telomere dysfunction can precede disease progression and is not simply a biomarker of advanced disease [10–13]. Indeed, qFISH studies have indicated modest telomere shortening occurring in hyperplasia, a more significant reduction becoming prevalent as early as ductal carcinoma *in situ* (DCIS) [14, 15], and the presence of significantly short telomeres in malignant breast cells compared to normal surrounding breast tissue [16]. The impact of telomeres in breast carcinogenesis is further supported by the detection of telomere-to-telomere fusion, a hallmark of telomere dysfunction, in early stage breast tumours, including DCIS [17].

Telomeres that can no longer exert end-protective functions because of excessive telomere attrition or alterations in the components of the shelterin complex itself, are recognised as sites of DNA damage and recruit the same repair factors that are associated with double strand breaks (DSBs) at other sites of the genome [18, 19]. Unprotected chromosome ends impinge on signalling kinases ATM and ATR to activate a DNA damage response (DDR) that via p53-p21$^{Waf1/Cip1}$ or pRb-p16^{INK4a} axis leads to checkpoint-mediated cell cycle arrest and senescence or apoptosis [20, 21]. Among the shelterin proteins, TRF2 (telomere repeat binding factor 2) is at the heart of the molecular events that maintain telomere integrity in mammals [22–24, and reviewed by 25]. TRF2 binding to DNA *in vitro* stimulates strand invasion, adopting structures that resemble t-loops [2]. Furthermore, the frequency of t-loops *in vivo* is significantly reduced in cells lacking TRF2, implicating this sheltering subunit in its formation and/or stabilisation [26]. It has been previously reported that expression of the truncated form of TRF2 (TRF2$^{\Delta B\Delta M}$), which lacks the Basic and Myb domains, interferes with the accumulation of the endogenous TRF2 protein at telomeres [22]. Depletion of TRF2 in normal cells using RNAi, dominant-negative alleles or Cre-mediated deletion typically results in a non-reversible telomere dysfunction phenotype that induces strong DNA damage signalling and stalls cell cycle progression [19, 22, 23, 27]. Therefore, telomere dysfunction acts as a tumour suppressive mechanism in cells with a functional DDR by limiting the expansion of unstable cell populations harbouring precancerous mutations. In sharp contrast, dysfunctional telomeres in cells with a limited DDR might allow the proliferation of damaged cells at risk of transformation if telomere length is stabilised through telomerase activation or ALT-pathways.

With the aim of generating heavily rearranged but telomerase stabilised epithelial human cells, we generated a versatile experimental system of telomere deprotection where TRF2$^{\Delta B\Delta M}$ expression is controlled by a doxycycline inducible promoter in the non-tumorigenic epithelial mammary cell line MCF-10A. We reasoned that limiting the telomere insult to brief periods might allow for a bypass of the acute cellular responses to dysfunctional telomeres. Besides that, given that telomere dysfunction can either prevent or promote tumourigenesis depending on the intactness of the DDR system, we used different approaches to experimentally inhibit the p53/pRb pathways. Our results demonstrate that, after 96 h of sustained TRF2$^{\Delta B\Delta M}$ expression, the telomere dysfunction phenotype increased with checkpoint protein inactivation, with the greatest impact seen in SV40LT transduced MCF-10A cells. However, evidence of chromosome specific structural aberrations or extensive aneuploid configurations compatible with ongoing BFB cycles were unnoticed in cells lacking p16^{INK4a} only or along with p53 inactivation, thus supporting the incapacity of p16^{INK4a}-deficient cells to cope with acute telomere damage. Even periods of short acute telomere deprotection did not dramatically alter the cell cycle profile of p16^{INK4a}-deficient cells or give rise to an intensification of the telomere-dependent CIN over time. Collectively, this indicates that cells experiencing transient acute telomere damage cannot overcome the severe proliferation defect imposed by uncapped telomeres and are destined to die.

RESULTS

The MCF-10A cell line is a spontaneously immortalised, but non-transformed human mammary epithelial cell line derived from breast tissue [28]. This cell line maintains telomere length through telomerase, but its expression is low [29, 30], making it hard to see a clear band of hTERT by western blotting (Supplementary Figure 1). Furthermore, despite being commonly recognised as normal cells, the karyotype is cytogenetically abnormal (Supplementary Figure 2A) and harbours genetic abnormalities commonly associated with cultured mammary epithelial cells such as deletion of the locus containing p16^{INK4a} and p14^{ARF}, as well as MYC amplification [31, 32].

Establishment of conditional TRF2$^{\Delta B\Delta M}$ MCF-10A cell lines with different cell cycle settings

Different MCF-10A cell lines were generated to display telomere dysfunction in a regulated manner through doxycycline (DOX)-induced expression of TRF2$^{\Delta B\Delta M}$ (Figure 1A). The MCF-10A T/O TRF2$^{\Delta B\Delta M}$ (TO) cell line was generated after serially transducing MCF-10A cells with lentiviral particles containing the inducible TRF2$^{\Delta B\Delta M}$ cassette and the rtTA3 transactivator (Figure 1B). Because abrogation of the p53 and pRb pathways is needed in human cells to bypass senescence and to initiate rampant telomere-dependent CIN, we established a second MCF-10A T/O TRF2$^{\Delta B\Delta M}$ inducible cell line where p53 expression was constitutively abolished using short-hairpin p53 RNA lentiviral particles (SH-TO) (Figure 1B). After antibiotic selection, diminished levels of p53 were verified through western blotting (Figure 1C and Supplementary Figure 3A). Besides that, inactivation of the p53 pathway was confirmed by the fact that increased levels of p53^{S15} and p21$^{Waf1/Cip1}$ were practically unnoticed after cell exposure to the DSBs inducer Bleocin™ (Figure 1C and Supplementary Figure 3A) and by the increased ability of tetraploid cells to re-enter the cell cycle and initiate another round of DNA replication after 24 h colcemid exposure and release (Supplementary Figure 4). Moreover, as an independent way of inactivating the pRb and p53 pathways, we generated a third TRF2$^{\Delta B\Delta M}$ conditional MCF-10A model (SV-TO) by transducing TO cells with a lentivirus that constitutively expresses the Large T antigen gene from SV40 and mCherry

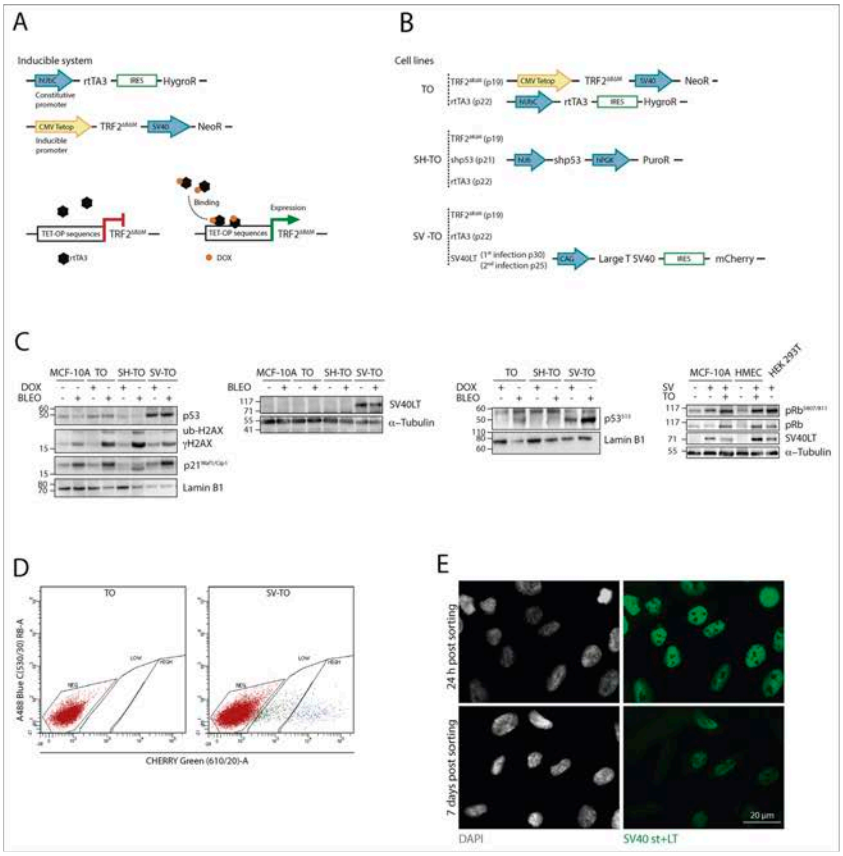

Figure 1: Generation of different MCF-10A cell lines with inducible TRF2$^{\Delta B\Delta M}$ expression. (A) Scheme of the conditional TET-ON expression system for TRF2$^{\Delta B\Delta M}$. The doxycycline-inducible system consisted in the constitutive expression of the rtTA3 protein through the hUbC (Ubiquitin C) promoter and the TRF2$^{\Delta B\Delta M}$ protein under the inducible CMV (Citomegalovirus)-Tetop promoter. In the absence of the tetracycline-derivative doxycycline (DOX), the rtTA3 protein is unable to bind to the TET-OP sequences located at the promoter; consequently, gene expression is repressed. In contrast, when DOX is added to the cell culture, it binds to rtTA3, which subsequently undergoes a conformational change that allows it to bind to the inducible promoter, starting TRF2$^{\Delta B\Delta M}$ transcription. **(B)** All cell lines (TO; SH-TO and SV-TO) contained the doxycycline-expression system. In addition to these modifications, SH-TO cell lines were transduced with the short hairpin RNA of p53 under the hU6 constitutive promoter. And the SV-TO cell line expressed the SV40 Large T antigen and mCherry under the CAG (CMV enhancer-chicken beta actin) constitutive promoter. All constructs contained a selectable marker or a resistence gene for selection purposes, under the same or a different promoter. The inducible MCF-10A cell lines (TO; SH-TO; SV-TO) were generated through serial transduction with TRF2$^{\Delta B\Delta M}$ (passage 19), rtTA3 (passage 22), shp53 (passage 21) or SVLT40-mCherry (passage 25 and 30) lentivirus. **(C)** Immunoblots of untreated and DOX- or Bleocin™-treated MCF-10A and TO, SH-TO and SV-TO cell lines. Diminished levels of p53 were observed in the SH-TO cell line as well as reduced levels of p53^{S15} and p21$^{Waf1/Cip1}$ after DSBs induction by Bleocin™, thus validating short hairpin RNA p53 inactivation. In SV-TO cells, western blots confirmed the presence of SV40 Large T antigen. In this cell line, higher p53 and p53^{S15} levels are observed due to p53 stabilisation by LT antigen. After DSBs induction by Bleocin™ exposure, both TO and SV-TO cells showed enhanced p53^{S15} and p21$^{Waf1/Cip1}$ levels. The loss of the G1 growth suppressor function of pRb was determined by the ratio between pRb$^{S807-811}$/total pRb. Cell lines containing the SV40LT antigen showed higher pRb$^{S807/811}$ levels than uninfected cell lines, thus supporting inactivation of pRb protein. **(D)** SV-TO cells were selected by FACS of cells expressing mCherry. SV40LT-mCherry uninfected TO cells were used as control to discard cell autofluorescence. The FACS profile of SV-TO MCF-10A cell line shows weakly and strongly mCherry expressing populations. For the following experiments, SV-TO cells with strong mCherry expression were used. **(E)** SV40 T-antigens (st+LT) immunofluorescence in SV-TO cells 24 h and one week after FACS sorting. Immunofluorescent images, captured under the same exposure conditions, denote the partial loss of T-antigen expression over time. Scale bar corresponds to 20 µm.

(Figure 1B). The translation product of SV40LT functions as a viral oncoprotein, which upon binding to p53 and pRb proteins inhibits their functions [33]. Selection of SV40LT containing cells was done by fluorescence activated cell sorting (FACS) of mCherry positive cells (Figure 1D) and afterwards SV40LT expression was validated by western blot, immunofluorescence and flow cytometry. As expected, the Large T antigen was present in SV-TO whole cell extracts and detected in the nucleus of transduced cells by immunofluorescence (Figure 1C and 1E). However, we found that SV40LT expressing cells were gradually lost from the culture (Figure 1E). Additional experiments with the $p16^{INK4a}$-deficient MCF-10A cells demonstrated again the loss of SV40LT positive cells with time (Supplementary Figure 5A and 5B). This leaking effect was previously reported to occur in $p16^{INK4a}$-deficient human mammary epithelial cells (vHMECs) transduced with SV40 early region (st and LT antigens) [34, 35]. To validate this, HMECs derived from cosmetic breast reductions were transduced with the same SV40LT antigen-mCherry vector. In this case, HMECs-hTERT were infected at an early population doubling (PD 6.92) before $p16^{INK4a}$ inactivation takes place and we did not pick clones or select for mCherry cells by FACS. In those HMECs-hTERT-SV40LT, the leaking effect was not observed. But most importantly, the analysis of SV40LT antigen levels by western blotting and flow cytometry at PD>92.31, demonstrated that cells were still positive for the Large T antigen (Supplementary Figure 5B and 5C). As a whole, and confirming previous studies, breast epithelial cells $p16^{INK4a}$-deficient are refractory to SV40 transformation. The reason why this occurs is unknown and further experiments would be needed to ascertain it.

Even though the generation of a stable SV-TO cell line over time was unsuccessful, at the time of the analysis, immunoblots revealed the presence of the SV40LT antigen (Figure 1C). The infection of cells with Large T antigen presumably renders the cells oblivious to the DNA damage checkpoint by inactivating both pRb and p53. SV40LT antigen triggers $p53^{S15}$ and stabilises p53 protein, but it is suggested that the direct interaction between SV40LT and p53 inhibits its function as a transcription factor [36]. In SV-TO cells, immunoblots demonstrated stabilisation of p53 by a higher expression of both $p53^{S15}$ and p53 in comparison with the other cell lines (Figure 1C and Supplementary Figure 3A). However, after Bleocin™ treatment the cells were capable of upregulating $p53^{S15}$ and $p21^{Waf1/Cip1}$ (Figure 1C and Supplementary Figure 3A). Given that it was not clear whether upregulation was due to the improper p53 pathway inactivation or to the presence of SV-TO cells lacking the SV40LT antigen, the response of SV-TO cells to acute colcemid treatment was also evaluated. Coincident with SH-TO cells, a significant polyploid population was observed in SV-TO cells 48 h after colcemid treatment (Supplementary Figure 4) thus supporting that at least the p53 pathway was abrogated in some cells. To determine the functional inactivation of the pRb pathway we tested the expression of the retinoblastoma pocket protein pRb (p105) and its phosphorylated form $pRb^{S807/811}$ (Figure 1C), as Large T antigen binds and inactivates pRb pocket proteins [37]. The ratio of $pRb^{S807/811}$/pRb was low in those cells not containing the SV40LT antigen (Supplementary Figure 3B). In cells expressing the LT antigen, pRb was in a more hyper-phosphorylated state and higher $pRb^{S807/811}$/pRb ratios were detected, thus suggesting alleviation of the pRB-mediated repression checkpoint.

Finally, the specific genetic changes present in the parental MCF-10A cell line were evaluated (Supplementary Figure 2A). The modal karyotype at p15 was defined as 47, XX, i(1q), del(1q), +1, der(3)t(3;9), der(8)t(8;8), der(9)t(9;3;5). In addition to these clonal aberrations, previously described in the literature [38–40], some signs of CIN were found. A total of 10.81% of non-modified MCF-10A metaphases showed non-clonal chromosome aberrations including chromosome fragments, chromatid breaks and one dicentric chromosome that showed telomeric FISH signals at the fusion point (Supplementary Table 1). Karyotyping by reverse DAPI banding was also performed in the uninduced TO, SH-TO and SV-TO cell lines to determine the cytogenetic impact of the genetic modifications (Supplementary Figure 2 and Supplementary Table 1). Collectively, these data suggested that the establishment of the TET-ON inducible system did not have a deleterious effect on the karyotype of MCF-10A epithelial cells. By contrast, and as previously reported [41], diminished levels of p53 resulted in an increase of cells containing chromosome aberrations with regard to the parental MCF-10A (Supplementary Figure 2). This adverse effect was markedly opposed if disruption was achieved through short hairpin RNA interference or SV40LT infection. Whereas shp53 resulted in an increase in non-clonal unstable aberrations that included rejoined broken chromosomes, acentric fragments and chromosome breaks, SV40LT transduction resulted in clonal stable chromosome aberrations (Supplementary Figure 2). This divergent result could be explained by the time elapsed between infection and the cytogenetic analysis. Due to the loss of SV40LT expression, SV-TO cells were analysed shortly after transduction and sorting, while much time passed between infection, selection and chromosome analysis in the SH-TO cell line. Given that the chromosome damage induced by SV40LT is an active process that gradually increases with serial cell passage [42] (Supplementary Figure 5D), the prompt analysis of the SV-TO cell line after transduction avoided the adverse evolution of the karyotype.

Variable intensity of telomere dysfunction upon 96 h sustained $TRF2^{\Delta B \Delta M}$ expression in the modified MCF-10A cell lines

To validate the efficacy of the inducible system, we exposed the parental MCF-10A and the three modified

cell lines to doxycycline for 96 h. The expression of the truncated TRF2$^{\Delta B\Delta M}$ protein upon DOX addition was demonstrated by immunoblotting protein extracts from untreated and DOX-treated cells with full length TRF2 antibodies (Figure 2A and Supplementary Figure 3C).

Then, the telomere dysfunction phenotype was evaluated through a deep cytogenetic analysis of metaphase spreads from 96 h DOX-treated and uninduced matched cells. Overall, the frequency of aberrant metaphases significantly increased in the TO cell line expressing TRF2$^{\Delta B\Delta M}$ (8.57% vs. 45.45%; p= 0.0002), but strikingly this was not the case for SH-TO (55.56% vs. 67.39%; p= 0.3594) nor for SV-TO (71.05% vs. 82.86%; p= 0.2767) (Figure 2B and Supplementary Table 1). This observation was probably due to the high frequency of abnormal karyotypes induced by p53 or p53/pRb inactivation. Indeed, clear evidence of the telomere dysfunction phenotype was observed when only metaphase spreads showing chromosome fusions were considered (Figure 2C). TRF2$^{\Delta B\Delta M}$ expression for 4 days induced a significant increase in metaphase cells showing end-to-end fusions (TO p= 0.0002; SH-TO p= 0.0072 and SV-TO p< 0.0001) (Supplementary Table 1). On average, there were 0.65 fusion events per cell in TO, 1.67 in SH-TO and 2.14 in SV-TO after expression of the dominant negative form of TRF2, which is statistically higher than the rates observed in matched uninduced cell lines (Mann-Whitney U-test; TO p= 0.0003; SH-TO p= 0.0035 and SV-TO p< 0.0001) (Figure 2D and Supplementary Table 1). Chromosome-type fusions, i.e. dicentric chromosomes formed during G1 were more frequently observed than chromatid-type fusions, which typically originate in the G2 phase of the cell cycle (Supplementary Figure 6). Usually both types of fusions involved two chromosomes, though multiple concatenated chromosomes were occasionally observed in the SH-TO and SV-TO cell lines (Figure 2E). At that point, in order to unambiguously demonstrate that telomere fusions were due to chromosome ends lacking sufficient TRF2 protection, we performed PNA-FISH experiments with pancentromeric and pantelomeric PNA-probes. In uninduced cells, most fusion events did not display TTAGGG FISH signals at the junction point, probably indicating DSB-DSB rejoining as origin. By contrast, after TRF2$^{\Delta B\Delta M}$ expression, the vast majority of fusion events displayed telomeric FISH signals at the fusion point (94.29% telomere positive fusions in TO, 84.72% in SH-TO and 91.55% in SV-TO) (Figure 3A and 3B, and Supplementary Table 2), thus demonstrating the presence of telomeric DNA and validating the efficacy of our telomere dysfunction inducible system.

Additionally, the telomere dysfunction phenotype was assessed by analysing the presence of anaphase bridges. A minimum of 215 anaphases were examined in uninduced and doxycycline-treated modified cell lines (Supplementary Table 3). The presence of cells with chromatin bridges during anaphase was low in TO and SV-TO cells not expressing the truncated TRF2 protein (3.72% and 4.21%, respectively). By contrast, the percentage of cells displaying anaphase bridges in uninduced SH-TO increased to 18.93%, which is statistically higher than the others (p< 0.0001) (Figure 3C and 3D, and Supplementary Table 3). This agrees with the high frequency of chromosome fusion events displayed by SH-TO cells when TRF2$^{\Delta B\Delta M}$ was not induced (Supplementary Table 1). After 96 h of acute telomere dysfunction, there was a significant increase in cells containing anaphase bridges in all the cell lines expressing TRF2$^{\Delta B\Delta M}$ when compared with matched uninduced cell lines (p< 0.0001) (Figure 3C and 3D, and Supplementary Table 3).

Overall, the expression of TRF2$^{\Delta B\Delta M}$ during 96 h leads to a telomere-dysfunction phenotype whose level of intensity depends on the functionality of cell cycle checkpoints. TO cells, which are p16^{INK4a}-deficient but present wild-type p53, showed the lowest percentage of cells with end-to-end fusions, as well as the smallest frequency of fusions per cell. In sharp contrast, the telomere-dysfunction phenotype was exacerbated in the SV40 LT antigen transduced cells, thus confirming that disabled cell-cycle checkpoints allow the accumulation and survival of cells containing telomere damage.

Acute telomere deprotection fires BFB cycles but prevents the development of CIN

Cells undergoing telomere dysfunction set in motion BFB cycles that, following chromatin bridge resolution, give rise to chromosome structural aberrations, gains and losses of chromosomes (aneuploidy) and regional amplification (reviewed by [7, 43]). Most recently, chromothripsis and kataegis have also been documented to occur after chromatin bridge fragmentation [44]. Besides that, several studies in human cells and in the mouse have clearly shown that deprotection of chromosome ends leads to polyploidisation events [45, 46].

To evaluate the presence of telomere-dependent CIN we analysed for BFB cycles scars in the form of structural chromosome aberrations other than end-to-end fusions. Structural reorganisations such as non-clonal non-reciprocal translocations (NRT) were few and did not increase after TRF2$^{\Delta B\Delta M}$ expression. This result was quite unexpected, given the significant increase of cells with chromatin bridges after telomere damage.

Besides that, FISH analysis with three different centromeric specific probes was also conducted to ascertain whether TRF2$^{\Delta B\Delta M}$ expression engendered numerical chromosome changes. Chromosomes #6, #12 and #17 were selected for their uninvolvement in numerical aberrations in the parental MCF-10A and uninduced cell lines (Supplementary Figure 2). The specificity of the centromeric probes was determined on metaphase chromosomes (Figure 4A) and aneuploid configurations were evaluated in a minimum of

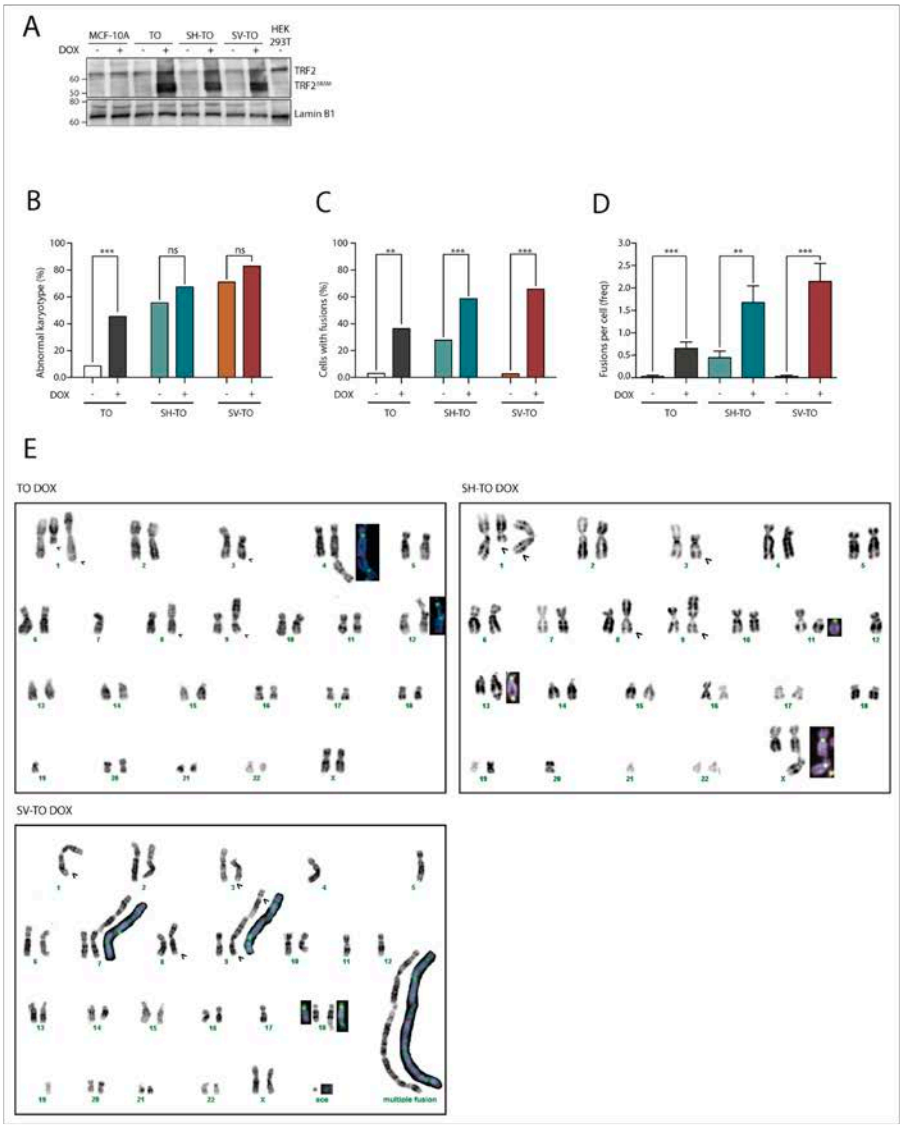

Figure 2: TRF2$^{\Delta B\Delta M}$ expression induces chromosome end-to-end fusions in all inducible cell lines. (A) Immunoblots of MCF-10A, TO, SH-TO and SV-TO cell lines with and without DOX and HEK 293T. After 96 h of DOX treatment, the inducible cell lines expressed the truncated TRF2$^{\Delta B\Delta M}$ protein (50 kDa); in contrast, uninduced cell lines, MCF-10A parental cell line and HEK 293T cells displayed only the endogen TRF2 protein (66 kDa). Lamin B1 was used as loading control. **(B)** After sustained expression of TRF2$^{\Delta B\Delta M}$ for 96 h there was a significant increase in aberrant metaphases only in TO cells when compared to uninduced matched cells. **(C)** Nevertheless, the efficacy of the inducible system was validated by the statistical increase of cells with end-to-end fusions in all inducible cell lines. **(D)** Moreover, a high incidence of fusions per cell was found in all modified cell lines after sustained TRF2 depletion. Data was presented as mean + SEM. **(E)** Example of TO, SH-TO and SV-TO karyotypes after 96 h of TRF2$^{\Delta B\Delta M}$ expression. Open arrows indicate clonal aberrations in the parental MCF-10A cell line. Insets in the karyotype show rearranged chromosomes stained with centromeric (green) and telomeric (red) PNA probes. Note the presence of telomere FISH signals at the fusion point of chromatid- or chromosome-type end-to-end fusions.

284 interphase nuclei of treated and untreated cells (Supplementary Table 4). The percentage of 2N aneuploid cells ranged from 4.66% to 14.10% and, upon doxycycline addition, this fraction did not increase in any of the modified cell lines (p= 0.0743, p= 0.9162 and p= 0.2567, for TO and SH-TO and SV-TO, respectively) (Figure 4B and 4C). Tetraploid events in uninduced TO cells were few (Figure 4C and 4D), but according to the role of p53 in limiting the proliferation of polyploids, the fraction of tetraploid cells in untreated SH-TO and SV-TO cells was significantly higher than in TO (p< 0.0001 and p= 0.0094, respectively). Nevertheless, tetraploidisation events in SV-TO cells were significantly fewer than those in SH-TO cells, which was unexpected considering that SV40LT also inhibits p53 function. Strikingly, upon TRF2$^{\Delta B\Delta M}$ expression the fraction of tetraploid cells was exacerbated only in SH-TO cells (p= 0.0099). This result was quite surprising as given the elevated level of end-to-end fusions in SV-TO metaphases, we rather expected similar results for the SV-TO cell line. However, such was not the case, and indeed we found that the fraction of 4N cells in induced SV-TO was similar to that observed in treated TO cells (p= 0.3349). Moreover, the fraction of tetraploid cells displaying aneuploid configurations increased upon TRF2$^{\Delta B\Delta M}$ expression when p53 was attenuated (2.78% vs. 7.04% in SH-TO and 0.86% vs. 1.91% in SV-TO), however statistical significance was only denoted for SH-TO cells (p= 0.0059) (Figure 4C).

As a whole, chromosome banding of metaphase spreads and centromeric-specific FISH analysis in interphase nuclei demonstrated the failure of long-term telomere deprotection to induce extensive structural and

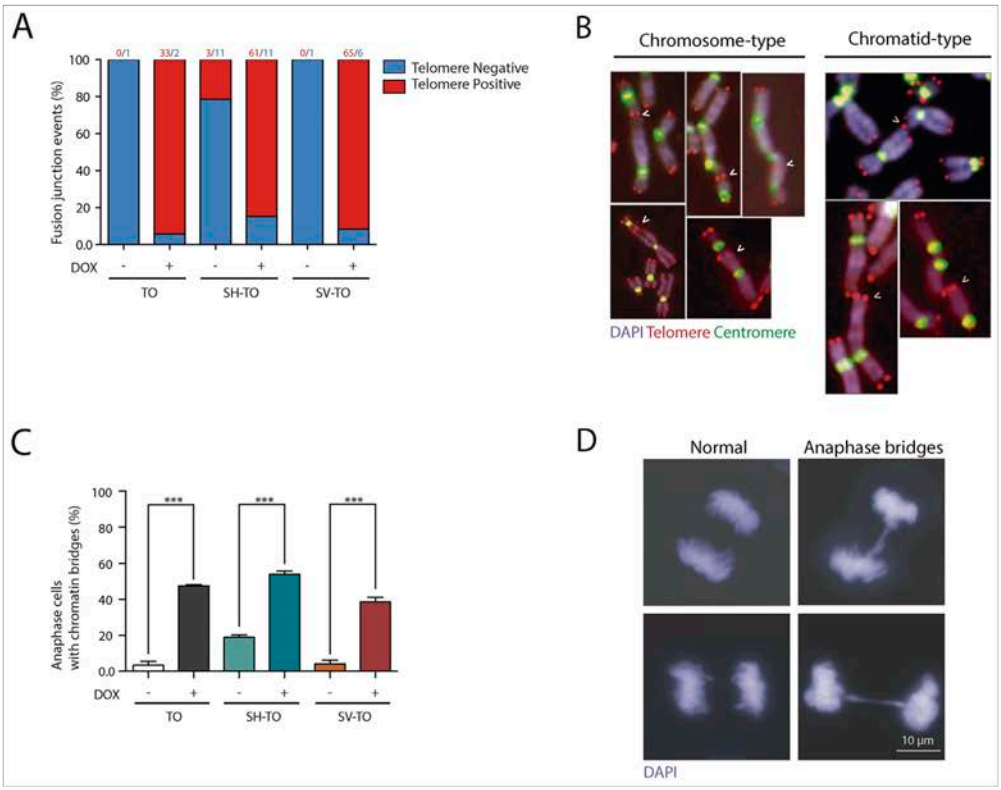

Figure 3: TTAGGG-positive fusions and anaphase bridges after sustained TRF2$^{\Delta B\Delta M}$ expression. (A) TRF2$^{\Delta B\Delta M}$ expression significantly increased the percentage of fusion events displaying TTAGGG repeats at the fusion point, thus confirming that fusions occurred because of the unfolded t-loop structure and not telomere DNA shortening. The number of events of each category is shown above the bars. **(B)** TRF2 stripped telomeres mostly fused at the G1 cell cycle phase, giving rise to chromosome-type fusions. Chromatid-type fusions that formed in G2 were also observed, although to a lower extent. **(C)** The expression of TRF2$^{\Delta B\Delta M}$ also increased the proportion of anaphase cells with chromatin bridges, another marker of telomere dysfunction. Data are presented as mean + SEM from three independent experiments. **(D)** Representative images of anaphase cells without (left) and with (right) chromatin bridges. Scale bar corresponds to 10 µm.

numerical changes compatible with ongoing BFB cycles. Therefore, these data suggest that sustained 96 h of acute telomere deprotection prevents active proliferation of cells suffering telomere damage.

Transient cycles of 96 h acute telomere damage results in proliferation defects in the absence of cell cycle alterations, DDR activation and visible senescent and apoptotic markers

Whereas persistent disruption of TRF2 activates a DDR that signals cell cycle arrest or apoptosis [23, 24], the fate of cells experiencing transient periods of acute telomere deprotection remains unclear. To this end, cell cycle progression studies were conducted in the modified MCF-10A cell lines after switching on/off TRF2$^{\Delta B\Delta M}$ expression. First, we analysed DOX-mediated cell cycle profile changes in unmodified MCF-10A cells to assess potential detrimental effects of DOX on cell proliferation [47]. After 24 h or 96 h exposure, we did not find evidence that 1 μg/ml DOX affected the cell cycle profile of unmodified MCF-10A cells (Mann-Whitney U-test; p> 0.05) (Supplementary Figure 7).

Then, asynchronous untreated cultures, subjected to doxycycline for 96 h, as well as those recovered after one or two cycles of 96 h DOX exposure and washout, were monitored by FACS analyses of DNA content. No significant alterations were observed in the cell cycle

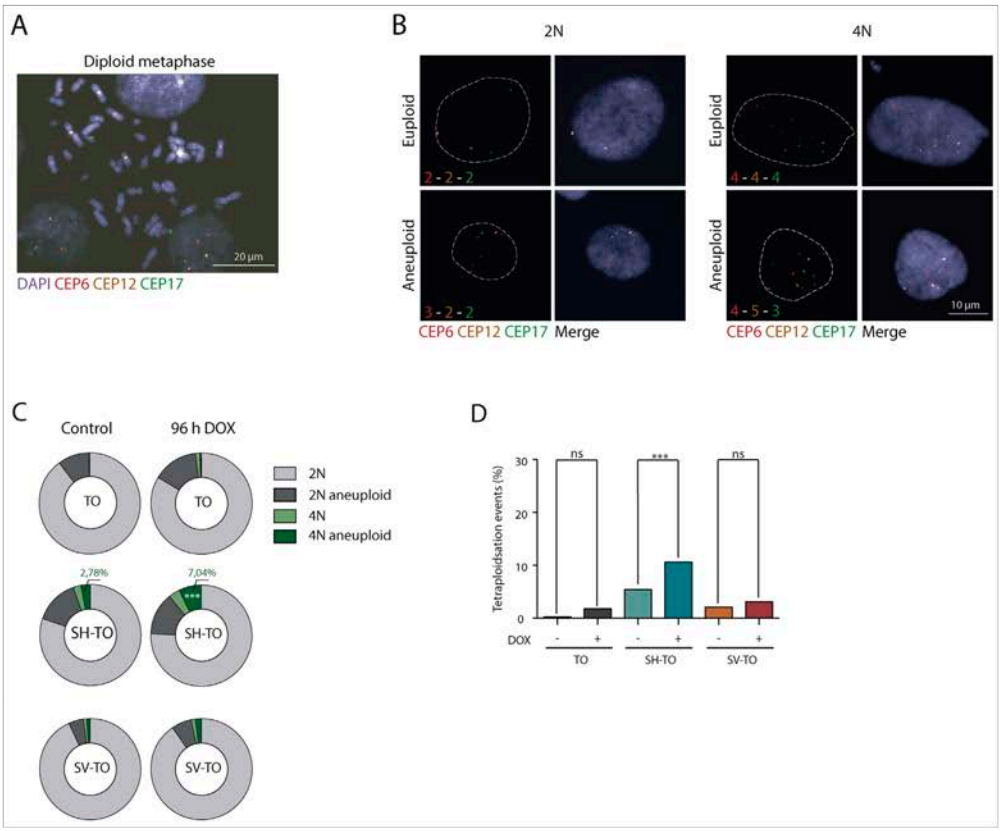

Figure 4: Tetraploidisation is not the usual fate of cells experiencing sustained TRF2$^{\Delta B\Delta M}$ expression. (A) Representative image of a diploid metaphase, showing the specificity of the centromeric probes tested: chromosomes 6 (red), 12 (yellow) and 17 (green). Scale bar corresponds to 20 μm. **(B)** Representative images of diploid and tetraploid cells with euploid and aneuploid configurations of tested centromeric probes. Scale bar corresponds to 10 μm. **(C)** Aneuploid configurations after TRF2 depletion only increased in the 4N fraction of SH-TO cells. **(D)** Percentage of tetraploid cells before and after TRF2$^{\Delta B\Delta M}$ expression. Tetraploid cells significantly increased in the SH-TO cell line after DOX treatment. In contrast, this was not the case for TO or SV-TO cell lines (p= 0.0375 and p= 0.3122, respectively; Bonferroni p-value correction= 0.0167).

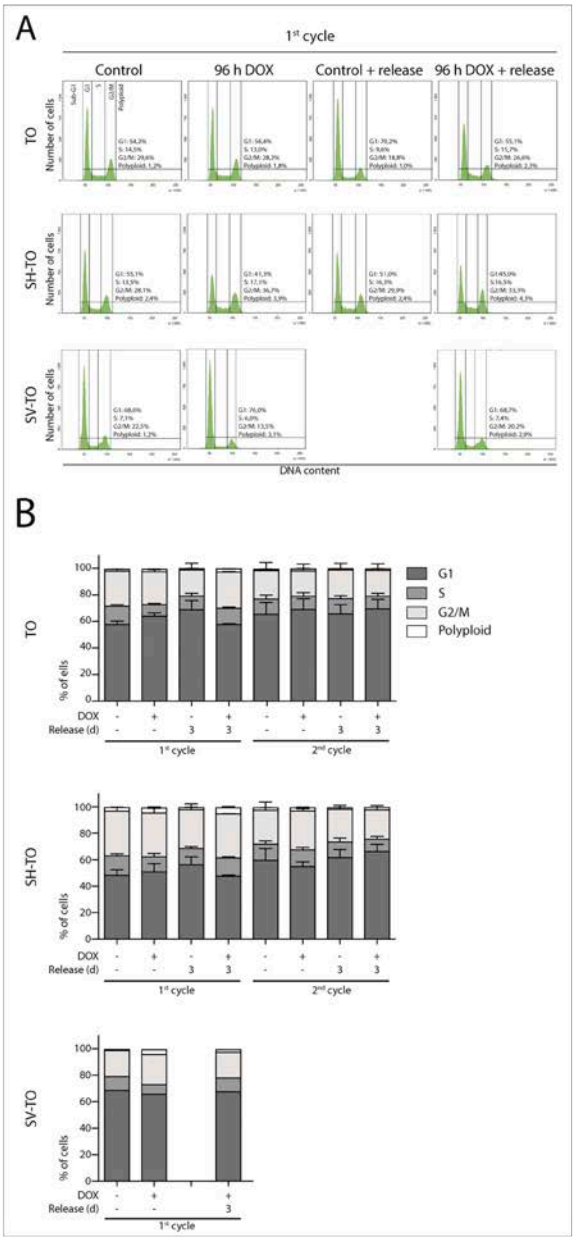

Figure 5: Absence of cell cycle profile disturbances after long TRF2$^{\Delta B \Delta M}$ expression periods. **(A)** Representative cell cycle profiles of TO, SH-TO and SV-TO cell lines during the first cycle of 96 h DOX treatment and their respective controls. Cell cycle profiles remained stable throughout the time of the experiment. Cell cycle phases are marked and values indicated. **(B)** Cell cycle phases distribution among TO, SH-TO cell lines (first and second cycle) and SV-TO cell line (first cycle) after 96 h DOX experiments. No statistical differences were observed between control and treated samples (Mann-Whitney test). A minimum of 10,000 cells were analysed per experiment. Data are presented as mean + SEM from three independent experiments, except for SV-TO cell line, in which only one experiment is shown.

profile of the modified cell lines after 96 h of sustained TRF2$^{\Delta B\Delta M}$ expression or after three days release (first DOX cycle) (Mann-Whitney U-test; p> 0.05) (Figure 5A and 5B). Moreover, exposure of TO and SH-TO cells to a second cycle of TRF2$^{\Delta B\Delta M}$ expression did not perturb the cell cycle profile either (Mann-Whitney U-test; p> 0.05). These observations agreed with the absence of changes in the S-phase index after 96 h telomere damage analysed through incorporation of BrdU (data not shown, only one experiment). Although the cell cycle arrest was not detected, TRF2$^{\Delta B\Delta M}$ sustained expression during four days resulted in a significant reduction of cell proliferation in both TO and SH-TO cells (Mann-Whitney U-test; TO p= 0.0087; SH-TO p= 0.0032) (Figure 6A). Despite the fact that end-to-end telomere fusions can slow progression through mitosis thus misleading cell proliferation changes, the absence of genomic instability compatible with ongoing BFB cycles also supports the notion that cells stop proliferation and ultimately senesce or die. However, no obvious senescent morphology was observed in the modified MCF-10A cells undergoing TRF2 depletion (Figure 6A). Furthermore, TRF2$^{\Delta B\Delta M}$ expressing cells were indistinguishable from control cultures by SA-β-galactosidase activity staining (Kruskal Wallis and Dunn's multiple comparison test; p> 0.05) (Figure 6B), which agrees with studies reporting abrogation of senescence in p16^{INK4a}-deficient cells [48]. These results together with the observation that apoptosis is triggered in p16^{INK4a}-deficient mammary adenocarcinoma MCF7 cell line upon TRF2$^{\Delta B\Delta M}$ expression [23], evoked that the reduced proliferation in the modified MCF-10A cells was most likely due to cell death resulting from telomere damage. Nonetheless, a marked appearance of a Sub-G1 fraction of cells by FACS analysis compatible with apoptosis was not observed after 96 h TRF2$^{\Delta B\Delta M}$ expression (Figure 5A).

What is more, the response of several proteins involved in the DDR was considerably reduced in cells constitutively expressing TRF2$^{\Delta B\Delta M}$ during 96 h when compared to cells treated with the DSB-inducer Bleocin™ (Figure 1C and Supplementary Figure 3A). Monoubiquitination of H2AX (ub-H2AX), which functions as a proximal regulator in the DDR by initiating the DNA damage signalling through efficient γ-H2AX formation [49] was prominent in TO, SH-TO and SV-TO cells exposed to Bleocin™. By contrast, in DOX treated TO and SH-TO cells there was a reduced level of ub-H2AX. Only SV-TO cells showed a marked higher level of ub-H2AX, which could be related to the focal accumulation of γ-H2AX associated with SV40LT antigen infection [50]. Furthermore, expression of p53, p53^{S15} and p21$^{Waf1/Cip1}$ followed the same trend, with a higher induction in Bleocin™ treated cells. In the face of telomere dysfunction induced by TRF2$^{\Delta B\Delta M}$ expression, neither p53 nor p53 phosphorylation and p21$^{Waf1/Cip1}$ upregulation could be detected in TO and SH-TO cells. As a whole, no evidence that 96 h of telomere dysfunction precipitates a DDR in the p16^{INK4a}-deficient MCF-10A cells was found. This low level of DNA damage elicited after TRF2 depletion could be the reason for the ambiguous fate of cells carrying telomere damage.

Even transient cycles of 24 h acute telomere dysfunction do not result in massive CIN

Given that acute telomere dysfunction for 96 h impacted on the development of CIN and the growth rate of cells with telomere damage, we investigated whether shorter periods of telomere deprotection would allow the generation of endless BFB cycles and massive CIN.

Both TO and SH-TO cells were exposed to successive 24 h periods of DOX treatment and washout. Cells retrieved after one or further 24 h DOX periods showed also an unaltered cell cycle profile (Mann-Whitney U-test; p> 0.05) (Figure 7A and 7B). Moreover, cells that received five cycles of 24 h DOX and recovery retained the parental MCF-10A karyotype. Chromosome aberrations in the form of end-to-end fusions were observed, but no signs of ongoing BFB cycles were present in metaphase cells of TO or SH-TO after five 24 h DOX cycles. In addition, oligoFISH analysis revealed a significant reduction in aberrant cells after the fifth 24 h DOX cycle compared to uninduced matched cells (p= 0.0244 and p= 0.0006 for TO and SH-TO, respectively) (Figure 8A). In view of these results, expression of TRF2$^{\Delta B\Delta M}$ was evaluated in those cells subjected to the fifth doxycycline cycle to determine whether the unperturbed cell cycle profile and the decreased frequency of aneuploid configurations, at that time, were due to an increase outgrowth of cells with diminished TRF2$^{\Delta B\Delta M}$ expression. However, this was not the case, as western blot analysis demonstrated that cells retained TRF2$^{\Delta B\Delta M}$ expression during the fifth cycle of 24 h DOX in much the same way that cells express TRF2$^{\Delta B\Delta M}$ after 96 h of doxycycline (Figure 8B and Supplementary Figure 3C). Then, we verified that 24 h of DOX exposure were sufficient to induce TRF2$^{\Delta B\Delta M}$ expression and that, after DOX washout, TRF2$^{\Delta B\Delta M}$ levels were reduced (Figure 8C and Supplementary Figure 3C). Finally, the efficacy of 24 h of DOX exposure in promoting uncapped telomeres was revealed by the presence of primary end-to-end fusions and telomere dysfunction induced *foci* (TIFs) in mitotic cells (Figure 8D).

Together, these results somehow support the notion that p16^{INK4a}-deficient MCF-10A cells, even in an impaired p53 background, cannot withstand short periods of acute telomere damage and are designated to stop proliferation and die.

DISCUSSION

In human primary cells replication-dependent telomere attrition leads to the accumulation of dysfunctional telomeres, which have been recognised

to play a relevant role in controlling the proliferative boundaries and fate of human cells. It is known that cells containing fewer than five dysfunctional telomeres can proliferate without halting the cell cycle [51], but above this threshold, cells enter senescence. Hence, the natural ends of chromosomes function as tumour suppressors by limiting the outgrowth of incipient tumour cells. At this point, full deprotection of telomeres is not occurring, as

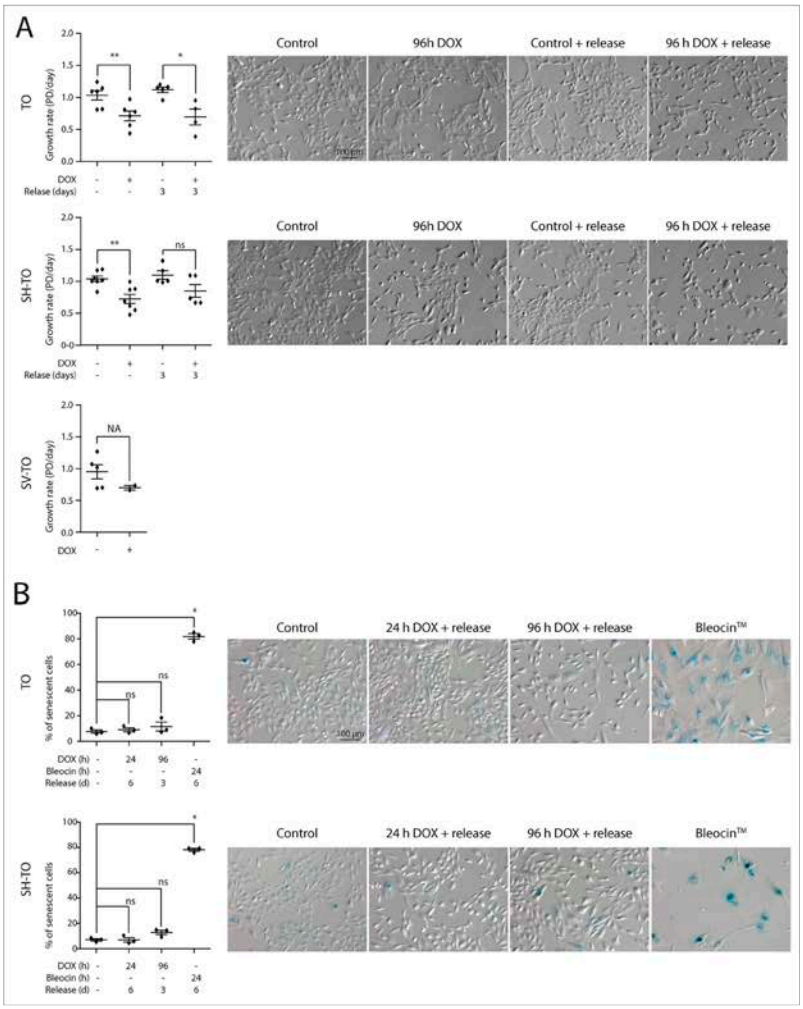

Figure 6: Reduced growth of cells displaying acute telomere dysfunction in the absence of a senescent phenotype. (A) Growth rate experiments in the modified cell lines after 96 h DOX exposure or after three days release from exposure demonstrate a reduced proliferation of cells displaying uncapped telomeres (TO cell line: 96 h DOX p= 0.0087, 96 h DOX and release p= 0.0159; SH-TO cell line: 96 h DOX p= 0.0032, 96 h DOX and release p= 0.2222). Analysis was performed from at least three independent experiments and analysed by Mann-Whitney test. Statistical analysis of SV-TO cells was not assessable (NA) due to the reduced number of replicates. At the right side, representative contrast field images of control and treated cells. Scale bar corresponds to 100 μm. **(B)** SA-β-galactosidase activity staining was analysed only in TO and SH-TO cell lines. The cells were exposed to 24 h or 96 h DOX and analysed after six or three day release, respectively. As positive control, the cells were treated with the DSBs-inducer Bleocin™ during 24 h and processed 6 days later. Analysis was performed on three replicates and Kuskal-Wallis test and Dunn's multiple comparison post-test. At the right side, representative bright field images of control and treated cells. Scale bar corresponds to 100 μm.

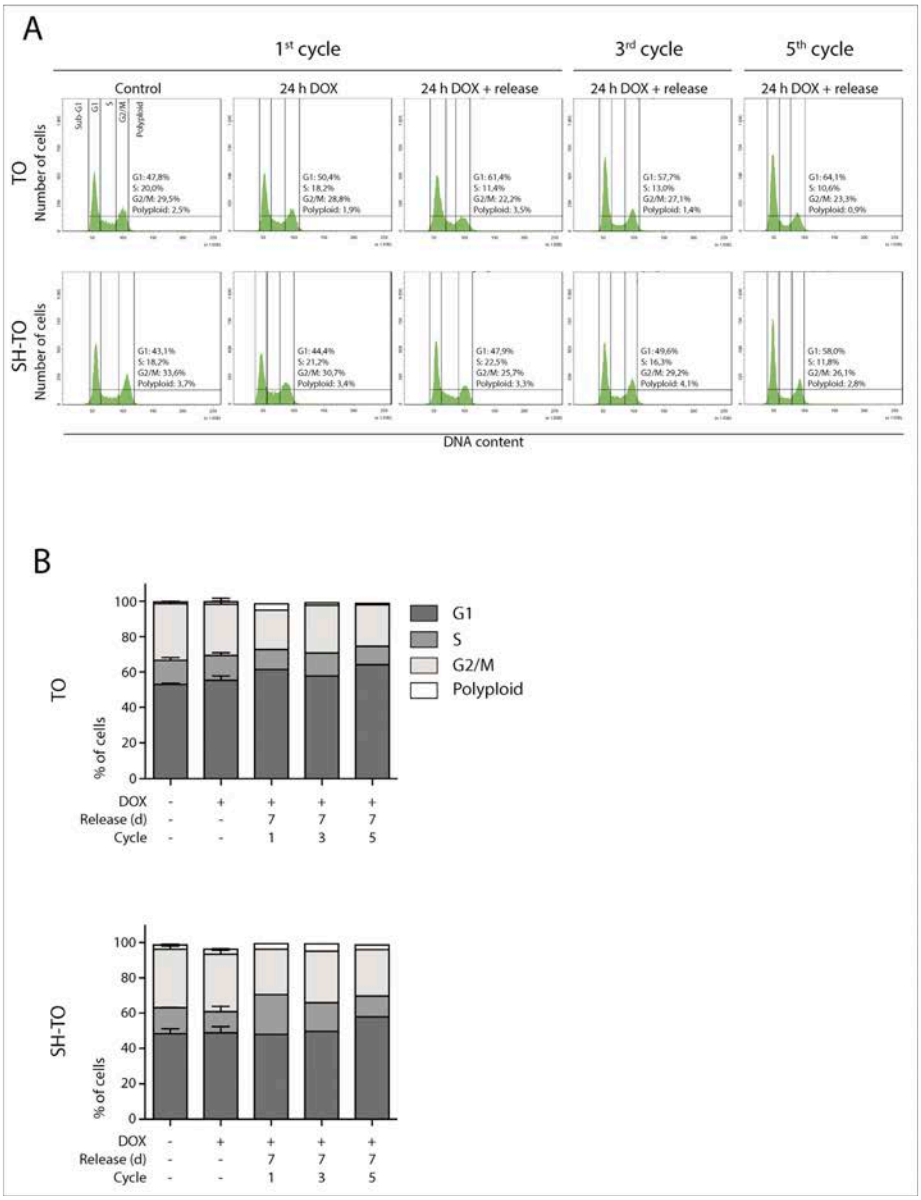

Figure 7: Short TRF2$^{\Delta B\Delta M}$ expression periods did not alter the cell cycle profile. (A) Representative cell cycle profiles of TO and SH-TO cell lines after periods of short TRF2$^{\Delta B\Delta M}$ expression. The first column shows the control cells. Subsequent columns show 24 h of sustained DOX treatment, 24 h of DOX treatment and 7 days of release, from the first, third and fifth DOX cycle, respectively. Cell cycle profiles remain stable during 24 h of DOX treatment, as well after their release during five cycles of TRF2$^{\Delta B\Delta M}$ expression. Cell cycle phases are marked and values indicated. **(B)** Cell cycle phases distribution among TO and SH-TO cell lines after 24 h DOX exposure experiments. No statistical differences were observed between control and DOX samples treated during 24 h (Mann-Whitney test). Data are presented as mean + SEM from three independent experiments, except for 24 h of DOX treatment and release of the first, the third and the fifth cycles, in which only one experiment is shown. A minimum of 10,000 cells were analysed per experiment.

end-to-end chromosome fusions are not observed [51]. Circumvention of this growth arrest, in most human cells, needs combined inactivation of p53 and pRb pathways. Strikingly, primary HMECs cultured *in vitro* can avoid the M1 growth arrest by spontaneous silencing of the *CDKN2A* gene through promoter hypermethylation [52, 53]. In the absence of $p16^{INK4a}$ expression, HMECs acquire an extended lifespan, where further telomere shortening results in the progressive transit of telomeres from a closed state to an uncapped state. As human telomeres are heterogeneously sized, physiological telomere erosion in vHMECs leads to the gradual appearance of unprotected telomeres that are continuously repaired by fusing with each other [5]. This reduces the initial damage and allows massive remodelling and scrambling of the genome through endless BFB cycles on proliferating cells (reviewed in [43]). Nevertheless, these proliferating unstable cells finally succumb to p53-dependent growth arrest, called agonescence, or crisis if p53 function is abrogated [54]. It is thought that stabilisation of telomere length in these genome unstable cells would alleviate DNA damage and rescue cellular fitness at a cost of driving to malignancy.

With the aim of generating immortal mammary cells that have passed through a period of telomere instability, we have set up a reversible system of acute telomere deprotection by controlling the expression of $TRF2^{\Delta B\Delta M}$ in the $p16^{INK4a}$-deficient MCF-10A breast epithelial cell line. We hypothesised that transient periods of telomere dysfunction through shelterin modification in telomerase

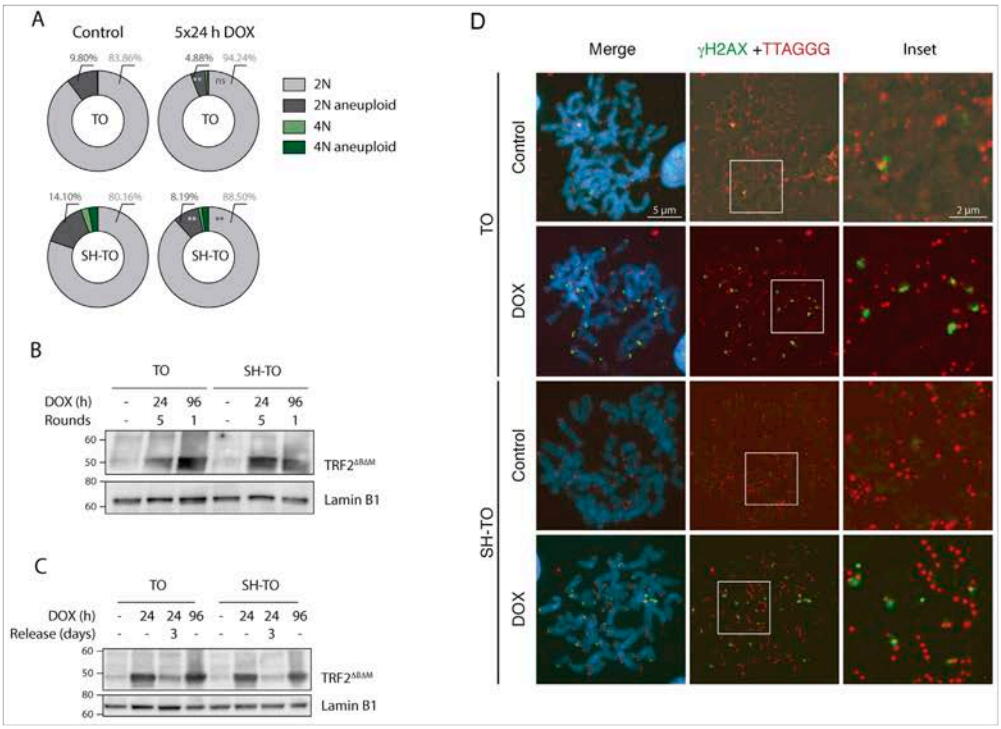

Figure 8: Short cycles of $TRF2^{\Delta B\Delta M}$ expression do not generate unstable cells. (A) Reduction in 2N-aneuploid cells in TO and SH-TO cell lines when repeated $TRF2^{\Delta B\Delta M}$ expression periods were induced (p= 0.0064 and p= 0.0036, respectively). **(B)** Immunoblot of $TRF2^{\Delta B\Delta M}$ expression in TO and SH-TO cells denotes that the expression of $TRF2^{\Delta B\Delta M}$ was not diluted over time. Protein levels during the fifth 24 h DOX treatment were similar to those observed after 96 h of sustained acute telomere deprotection. Lamin B1 was used as loading control. **(C)** Immunoblot of $TRF2^{\Delta B\Delta M}$ expression after 24 h or 96 h of sustained DOX treatment and after 3 days of recovery from 24 h DOX in TO and SH-TO cell lines. Note that 24 h of DOX treatment was enough to induce the expression of $TRF2^{\Delta B\Delta M}$ and protein levels were similar between 24 h and 96 h of sustained $TRF2^{\Delta B\Delta M}$ expression. Three days after DOX removal, $TRF2^{\Delta B\Delta M}$ was still present but to a lesser extent. Lamin B1 was used as loading control. **(D)** Representative images of γH2AX *foci* (green) and telomere (red) PNA hybridisation in metaphase TO and SH-TO cells. TIFs were observed in both cell lines after 24 h of sustained DOX treatment. Insets indicate colocalisation of γH2AX *foci* and telomere DNA. Scale bar corresponds to 5 μm in the images and to 2 μm in the insets.

proficient cells would drive BFB cycles and produce some degree of ongoing instability at a level compatible with cell viability. Our study demonstrates that controlled TRF2 depletion efficiently produced a telomere dysfunction phenotype in the modified MCF-10A cell lines. Nevertheless, we did not find clear evidence of ongoing BFB cycles, such as secondary chromosome aberrations with interstitial telomeric DNA sequences, increased aneuploid configurations in interphase nuclei or the accumulation of cells with 8C DNA content compatible with cycling polyploids. Despite the fact that the increased fraction of anaphase cells with chromatin bridges could reflect cell cycle progression, the lack of telomere-dependent CIN somehow denotes the absence of long term proliferation of cells with telomere damage. Indeed, reduced cell growth was discernible in the modified cell lines exposed to TRF2$^{\Delta B\Delta M}$. But the proliferation defects were not accompanied by cell cycle disturbances or visible markers of senescence or apoptosis. What is more, 96 h of telomere dysfunction did not precipitate a DDR comparable to the one elicited by the DSBs-inducer Bleocin™. The low level of DNA damage inflicted after TRF2 depletion could be the reason for the ambiguous disappearance of cells carrying telomere damage. Thus, it seems likely that TRF2$^{\Delta B\Delta M}$ expression induces proliferation defects in p16^{INK4a}-deficient MCF-10A breast epithelial cells that conclude in their clearance from the cell culture, presumably because of a telomere capping defect rather than cell death associated with telomere-dependent extensive genome instability.

In contrast to progressive telomere shortening, the expression of TRF2$^{\Delta B\Delta M}$ suddenly evokes the direct transition of several telomeres from a closed to a deprotected state [27, 55]. In primary fibroblasts, the cellular response to TRF2$^{\Delta B\Delta M}$ expression somehow recapitulates telomere-dependent replicative senescence, but cells stop division, displaying telomere-to-telomere fusions, chromatin bridges at anaphase, and nearly tetraploid karyotypes [20, 22, 23]. The growth arrest imposed by TRF2 deletion in primary fibroblasts is overridden by combined inactivation of p53 and pRb pathways through SV40LT [20] or HPV16 E6E7 [56] infection. Also, when p16^{INK4a} inhibition is combined with p53 inactivation, a nearly complete bypass of telomere-induced senescence is achieved [48]. Even though, the telomere damage inflicted results, in all instances, in lethal genome instability [20, 48, 56]. Unlike fibroblasts, the proliferation restraint elicited by sustained TRF2$^{\Delta B\Delta M}$ expression in p16^{INK4a}-deficient MCF-10A cells was not circumvented by short hairpin p53 inactivation, thus revealing a distinct cellular response of the mammary epithelial lineage to TRF2 depleted telomeres. Such cell lineage discrepancy was probably not related to the intensity of the telomere damage inflicted, as the rate of cells containing end-to-end fusions and the frequency of end fusions per cell were similar between the Jacobs and de Lange study and the results presented herein [48]. The most likely interpretation is that epithelial cells showing p16^{INK4a} deficiencies are highly sensitive to acute DNA damage derived from sustained TRF2$^{\Delta B\Delta M}$ expression and are committed to stop proliferating and probably die. This assumption is also reinforced by the presence of meta-TIFs after 24 h TRF2$^{\Delta B\Delta M}$ expression and by the karyotype analysis of cells retrieved after transient periods of short TRF2$^{\Delta B\Delta M}$ expression. The reduction in the telomere insult to shorter periods again demonstrated a lack of hallmarks compatible with ongoing BFB cycles. Altogether, these data suggest that even brief TRF2 depletion periods in p16^{INK4a}-deficient MCF-10A cells leads to a level of telomere damage that is incompatible with cell proliferation, and supports the view that the telomere insult itself, and not the genomic instability associated with BFB cycles, is responsible for the deleterious effects on cell proliferation [57].

In summary, the severity of the cellular responses to progressive or acute telomere dysfunction are not analogous among mammary epithelial cells and seems to be dependent on the severity of the telomere damage impinged. p16^{INK4a}-deficient breast epithelial cells react to the minor damage of progressive telomere uncapping by stimulating repair and cell survival at a cost of unleashing genome instability through the onset of BFB cycles [43]. Conversely, TRF2-depleted telomeres in p16^{INK4a}-deficient mammary MCF-10A cells results in a proliferative block that prevents the generation of genome unstable cells. This halt in cell cycle progression is not due to the sustained telomere damage, as even transient cycles of short TRF2 deprotection were unable to drive chromosome instability. We propose that the deprotection of many telomeres simultaneously, above a certain DNA damage threshold, probably results in a local activation of the cellular stress response that consequently triggers cell withdrawal from cell cycle to maintain genomic integrity.

MATERIALS AND METHODS

Cell lines

Non-transformed human mammary epithelial MCF-10A cells, provided by Dr Carme Nogués, and derived cell lines were cultured in DMEM:F12 (GIBCO, ThermoFisher Scientific) supplemented with 2% tetracycline-free horse serum (GIBCO), cholera toxin (100 ng/ml) (Sigma-Aldrich), hEGF (20 ng/ml) (Sigma-Aldrich), hydrocortisone (0.5 µg/ml) (Sigma-Aldrich), insulin (10 µg/ml) (Sigma-Aldrich) and 1% penicillin/streptomycin (GIBCO). Post-stasis variant human mammary epithelial cells (vHMECs) were obtained from Cell Applications Inc. (San Diego, CA, USA). Pre-stasis HMECs were established from reduction mammoplasty tissue in accordance with previously reported methods [58]. The patient signed a written consent form allowing

their tissue to be used for biological research; this consent was obtained by the medical staff at the hospital prior to surgery. All work with human derived material was reviewed and approved by the Human Subjects Protection Committee of the Universitat Autònoma de Barcelona. vHMECs and HMECs were cultured with serum-free MEpiCM medium supplemented with MEpiCGS and penicillin/streptomycin (all from ScienCell Research Laboratories, Carlsbad, CA, USA), or with M87AX [59]. HEK 293T cells were cultured in DMEM (GIBCO) supplemented with 10% of foetal bovine serum (GIBCO) and 1% of penicillin/streptomycin.

Growth conditions were 5% CO_2 and 37ºC. Culture population doublings (PDs) were calculated using the formula: $PD = PD_{initial} + \log_2 (N_{final}/N_{initial})$, where $N_{initial}$ is the number of viable cells plated, and N_{final} is the number of viable cells harvested.

Lentiviral vectors

A lentiviral tetracycline-inducible TRF2$^{\Delta B\Delta M}$ construct was generated by cloning the inducible TRF2$^{\Delta B\Delta M}$ cassette from a pBluescript.KS vector (courtesy of Dr Lenhard Rudolph) into a neomycin resistant promoter-less lentivector (Amsbio) using X-baI restriction sites. The Tet-regulated transcriptional transactivator protein rtTA3 containing hygromycin resistance was a kind gift from Dr Iain Fraser. The lentiviral construct for p53 short hairpin RNA (shp53 pLKO.1 puro) was from Dr Bob Weinberg (Addgene plasmid #19119), and the lentiviral plasmid for SV40LT (pRRLsin-SV40 T antigen-IRES-mCherry) was from Dr Snorri Thorgeirsson (Addgene plasmid #58993). The hTERT lentivirus was supplied by Viral Vector Facility, CNIC, Spain.

Lentivirus production and transduction

To generate lentiviral particles, the psPAX2 and pMD2.G plasmids together with the plasmid containing the gene of interest were introduced in HEK 293T packaging cells using Calphos Mammalian Transfection kit (Clontech). Supernatants were collected at 48 and 72 h post-transfection and concentrated using Amicon 100,000 centrifugal filter units (Merck-Millipore).

The MCF-10A T/O TRF2$^{\Delta B\Delta M}$ (TO) cell line was generated by lentiviral transduction of MCF-10A cells with the TRF2$^{\Delta B\Delta M}$ inducible cassette and the rtTA3 transactivator, with polybrene (4 μg/ml) (Sigma-Aldrich). Transduced cells were selected first with G418 (300 μg/ml) (Sigma-Aldrich) and afterwards with hygromycin (300 μg/ml) (Sigma-Aldrich). The MCF-10A T/O TRF2$^{\Delta B\Delta M}$-SHP53 (SH-TO) was generated by lentiviral transduction of shp53 and selection with puromycin (0.75 μg/ml). The MCF-10A T/O TRF2$^{\Delta B\Delta M}$-SV40LT (SV-TO) cell line was generated by transduction of MCF-10A T/O TRF2$^{\Delta B\Delta M}$ with SV40LT-mCherry lentiviral particles. Selection of the different transduced cells was performed through one week culture with the appropriate antibiotic or, in the case of SV-TO cells, through FACS sorting of mCherry positive cells.

vHMECs expressing hTERT (vHMEC-hTERT) were generated by lentiviral transduction of vHMECs with the hTERT lentivirus at PD 21. HMECs-hTERT expressing SV40LT were generated by lentiviral transduction of SV40LT-mCherry lentiviral particles at passage 2 (PD 6.92).

Expression of TRF2$^{\Delta B\Delta M}$

Induction of telomere dysfunction in the different conditional cell lines was performed by culturing the cells with regular MCF-10A medium containing 1 μg/ml doxycycline (DOX) (Sigma-Aldrich). Long-term telomere dysfunction experiments consisted of the persistent exposure of cells to DOX for 96 h. In all experiments, fresh DOX was added to the cell culture each 48 h. Moreover, conditional studies were conducted where telomere dysfunction was switched on and switched off by the addition/removal of DOX from the culture medium. Long-term exposure cycles consisted of 96 h of sustained TRF2$^{\Delta B\Delta M}$ expression and 3 days without DOX, whereas in short-term cycles, cells where treated with DOX for 24 h and then were exposed to DOX-free medium for 7 days.

Western blotting

Proteins were extracted with 2% SDS, 67 mM Tris HCl (pH 6.8) or RIPA lysis buffer, containing protease and phosphatase inhibitors. Protein extracts were sonicated twice at 25% amplitude for 15 s, boiled at 95ºC for 15 min and centrifuged at 20,000 g for 10 min. Proteins were quantified using the BCA method and absorbance was read at 540 nm with a Victor3 spectrophotometer (PerkinElmer). The proteins (30 μg) were separated using 3-8% Tris-acetate or 10% Bis-Tris gels (Life Technologies, ThermoFisher Scientific) at 35 mAmp and transferred onto nitrocellulose or PVDF membranes at 30 V. Membranes were blocked with 5% non-fat milk or BSA. Primary antibodies used were: mouse anti-SV40 st+LT Ag (Santa Cruz; sc-148), rabbit anti-pRb$^{S807/811}$ (Cell Signaling; D20B12), mouse anti-pRB (Cell Signaling; 4H1), rabbit anti-p53^{S15} (ThermoFisher Scientific, 14H61L24), mouse anti-p53 (ThermoFisher Scientific, DO-1), mouse anti-γH2AX (Upstate; 07-164), rabbit anti-p21$^{Waf1/Cip1}$ (Cell Signaling; 12D1) and mouse anti-TRF2 (Novus Biologicals; 4A794.15). Furthermore, mouse anti-α-Tubulin (Sigma, B-5-1-2) and rabbit anti-lamin B1 (Abcam; ab16048) were used as loading controls. Primary antibodies were incubated overnight at 4ºC. Secondary anti-mouse or anti-rabbit horseradish peroxidase (HRP) conjugated antibodies were used and incubated for 1 h at room temperature. Chemiluminescent detection was performed using HRP

solution and luminol (Life Technologies), and images were acquired using Chemidoc, processed with Quantity One software and analysed with ImageLab™ 6.0.0 (BioRad).

Drug treatments

DSBs were generated in MCF-10A and derivatives through exposure to the radiomimetic drug Bleocin™ (Calbiochem, Merck-Chemicals; Germany), a bleomycin compound, at a final concentration of 2.5 μg/ml. The drug was washed out after 1 h exposure and the cells were left to recover for 60 min before protein extraction.

Colcemid (GIBCO) at a final concentration of 50 ng/ml was added to asynchronously proliferating TO, SH-TO and SV-TO cells. After 24h of colcemid exposure, the cells were collected and fixed in 70% ethanol and kept frozen until FACS processing. Additional experiments consisted of 24 h colcemid treatment, washout and 24 h or 48 h release before fixation.

Obtaining metaphase cells and end-to-end fusion scoring criteria

Exponentially growing MCF-10A and, untreated and doxycycline-treated MCF-10A modified cell lines were exposed to colcemid (0.5 μg/ml) for 2 h. Cells were trypsinised, swollen in 0.075 M KCl and fixed in methanol:acetic acid (3:1). Cell suspensions were dropped onto clean slides and stored at -20ºC until use. For end-fusion scoring purposes, slides were first stained with DAPI. Then, the metaphase plates were captured and the karyotype was performed by reverse DAPI staining, which results in a reproducible G band-like pattern that allows for accurate individual chromosome identification before the chromosomes became swollen by the denaturation step. Afterwards, the slides were hybridised with the PNA probes and the metaphases were relocated to analyse the telomere and centromere status of each chromosome. A fusion event was considered when the connection between chromatids (1 or 2) was verified on the initial DAPI stained image. This procedure reduces the possibility of end-fusions events being confused with mere alignment of chromosomes.

In situ fluorescence hybridisation

Telomere and centromere PNA-FISH

Metaphase spreads were hybridised with pantelomeric (Rho-$(CCCTAA)_3$, PE Biosystems) and pancentromeric (FITC-AAACACTCTTTTTGTAGA, Panagene) PNA probes. Denaturation took place at 80ºC for 3 min and hybridisation was performed at 37ºC for 2 h in a humid chamber. Afterwards, slides were washed twice with 70% formamide for 15 min, followed by three TNT (Trizma Base 50 mM, NaCl 150 mM and Tween20 0.25%) washes for 5 min. Dehydrated slides were counterstained with DAPI.

OligoFISH

Interphase nuclei spreads were treated with pepsin-HCl at 37ºC for 10 min, post-fixed with formaldehyde-$MgCl_2$ and denatured with 70% formamide at 74ºC. Specific centromeric probes for chromosomes 6 (Gold DY539), 12 (Red DY590) and 17 (Green DY490) (Cellay, Inc.) were hybridised for 2 h in a humid chamber followed by one 5 min wash with 0.2xSSC-0.1%SDS at 50ºC and a 2xSSC wash. Cells were dehydrated and counterstained with DAPI.

DAPI staining, immunofluorescence and TIFs (telomere dysfunction induced *foci*)

For anaphase bridge scoring, cells cultured on coverslips were fixed with 4% paraformaldehyde (PFA) at 37ºC, rinsed twice in PBS, allowed to dry and counterstained with DAPI.

For immunofluorescence, cells were fixed in 4% PFA for 10 min at 37ºC, permeabilised with 1% Triton X-100 at room temperature and blocked with 5% FBS-0.1% Triton X-100- KCM buffer. Then SV40 st+LT Ag (1:200) primary mouse antibody was incubated overnight at 4ºC. Conjugated chicken Alexa Fluor 488-antimouse antibody (1:500, ThermoFisher Scientific) was incubated for 1 h. Cells were counterstained with DAPI.

For the TIF assay, cells were treated with DOX for 24 h. The following day, chromosome spreads were obtained as described by [60]. Briefly, after 25 min of colcemid (20 ng/ml), the cells were trypsinised and resuspended to a final concentration of $5x10^4$ cells/ml in hypotonic solution (0.2% Trisodium Citrate-0.2% KCl). Thereafter, the cells were cytocentrifuged 10 min at 1,000 rpm and the slides were air dried. Afterwards, the slides were treated with pre-extraction buffer for 5 min, 1% Triton X-100- KCM buffer for 10 min and fixed with 4% PFA for 10 min. Permeabilisation was also performed with chilled absolute methanol during 20 min. Cells were blocked with 2% FBS-0.1% Triton X-100- 100 μg/ml RNAse- TrisNaCl for 30 min at 37ºC, and mouse anti-γH2AX (1:500, clone JBW301 Millipore) antibody was incubated at 4ºC. Conjugated chicken Alexa Fluor 488-antimouse was incubated for 1 h. Slides were fixed again in 2% PFA for 10 min and dehydrated through an ethanol series. Samples and pantelomeric probe (Rho-$(CCCTAA)_3$, PE Biosystems) were co-denatured at 80ºC for 4 min, and hybridised overnight at 37ºC in a humid chamber. Slides were washed once with 70% formamide-Tris and twice with PBST. To ensure γH2AX staining, conjugated Alexa Fluor 488-antimouse was re-incubated for 30 min. Cells were dehydrated and counterstained with DAPI.

Fluorescent microscopy and fluorescent images

Most fluorescent staining was visualised under an Olympus BX60 microscope equipped with epifluorescent

optics and a camera (Applied Imaging, Inc.). In the case of TIFs analysis, an Olympus BX61 epifluorescence microscope with motorized x-y stage (BX-UCB, Olympus) was used to acquire images as a Z-stack (total of 7 planes of 2.11 μm each). The fluorochromes were visualised through simple filters and images were captured and analysed using Cytovision software (Applied Imaging, Inc.).

Flow cytometry and live cell sorting

For tracking S phase cells, a pulse of 10 μM BrdU was carried out for 30 minutes. Afterwards, the cells were rinsed, trypsinised, centrifuged and fixed with 70% ethanol. For cell cycle analysis or SV40 st+LT detection, the cells were harvested and fixed in 70% ethanol and kept at -20ºC until processing.

For SV40 st+LT and BrdU analysis, the fixed cells were permeabilised with 1xPBS-1%Triton X-100 solution. In the case of BrdU detection, DNA was denatured with HCl 2N-0.1% Triton X-100. After 30 min, denaturation was blocked by adding tetraborate solution (0.1 M). Before antibody detection, every sample was divided into two tubes, one for mouse anti-SV40 st+LT Ag (Santa Cruz; sc-148) or mouse anti-BrdU (Santa Cruz, sc32323) and subsequent Alexa Fluor 488-antimouse secondary antibody. The second tube was used as a negative control of the secondary antibody.

All cells were stained with propidium iodide solution (PBS-1% Triton X-100, propidium iodide 45 μg/ml, and RNase 0.2 mg/ml) before cytometric processing. Analysis was performed under a FACSCalibur (Beckton Dickinson). Sample excitation was done with a 488 nm laser and a minimum of 10,000 events were collected per sample. Single cells were gated first by forward scatter (FSC) and side scatter (SSC), and DNA content of single cells was measured on FL3 (670 nm long pass filter) and plotted vs. number of cells. Alternatively, A488 fluorescence was detected on FL1 (530/30 nm band pass filter) and was plotted vs. propidium iodide. The data were analysed with BD FACSDiva software v7.0.

For live cell experiments, cells were trypsinised and resuspended in PBS. Sorting of mCherry positive cells was carried out using a FACSAria I SORP sorter (Beckton Dickinson). Excitation of the sample was done using a 488 nm laser for FSC and green fluorescence parameters, and a 561 nm laser was used for the excitation of mCherry and SSC signals. Cells were gated according to their FSC vs. SSC parameters. Red emission from mCherry (610/20 nm) excited with the yellow laser (561 nm) was plotted vs. green emission (530/30 nm) from the 488 nm laser on a dot plot in order to discriminate mCherry positive cells.

Senescence associated beta-galactosidase staining

TO and SH-TO cells treated with DOX (1 μg/ml) for 24 h and 96 h and left to recover until the seventh day were seeded at a concentration of 7,500 cells/well. A positive control consisted of cells treated with Bleocin™ (2.5 μg/ml) for 24 h and left to recover until the seventh day. In Bleocin™ experiments 50,000 cells/well were seeded. The Senescence β-Galactosidase Cell Staining Kit (Cell Signaling) was used according to the manufacturer's instructions. The cells were examined under a light microscope (Olympus IX71) and those cells with blue staining were considered positive for β-galactosidase activity. We estimated the percentage of β-galactosidase staining by analysing 5 individual fields per well from three replicates.

Statistical analysis

Data analysis was carried out with GraphPad Prism version 5 software (GraphPad Software Inc.). Normality distribution was tested by Saphiro-Wilk normality test. Data sets were compared using Fisher's exact test, Mann-Whitney test, Kruskal-Wallis test and Dunn's multiple comparison post-test. P-values less than 0.05 were considered significant. When multiple comparisons were done, the Bonferroni p-value correction was applied and indicated.

Abbreviations

ALT-pathway – Alternative Lengthening of Telomeres pathway
BFB – Breakage Fusion Bridge
BrdU – 5-bromo-2'deoxyUridine
CDKN2A – Cycling Dependent Kinase Inhibitor 2A
CIN – Chromosome INstability
DAPI – 4′,6-diamidino-2-phenylindole
DCIS – Ductal Carcinoma *In Situ*
DDR – DNA Damage Response
DOX – Doxycycline
DSB – Double Strand Break
hEGF – human Epidermal Growth Factor
HMEC – Human Mammary Epithelial Cell
NRT – Non Reciprocal Translocation
PD – Population Doubling
Rho – Rhodamine
TIF – Telomere-dysfunction Induced *Foci*
TRF2 – Telomere Repeat binding Factor 2
vHMEC – variant Human Mammary Epithelial Cell

Author contributions

AB participated in study design, performed most of the experimental work, analysed the data, drafted the manuscript and critically reviewed it. MMA contributed to the experimental work and to data interpretation. DD contributed to study design, performed part of the experimental work, interpreted the data, and critically revised the manuscript. LT conceived and designed the study, performed part of the experimental work,

interpreted the data, co-drafted and critically reviewed the manuscript. All authors read and approved the final manuscript.

ACKNOWLEDGMENTS

We gratefully acknowledge Lenhard Rudolph and André Lechel (Leibniz Institute on Ageing-Fritz Lipmann Institute, Jena, Germany) for the inducible construct and their invaluable help; Iain Fraser (Laboratory of Systems Biology, NIAID, Bethesda, USA) for the rttA3 plasmid; Joan Aurich-Costa (Cellay, Inc; Cambridge, USA) for providing us with oligoFISH probes; Carme Nogués (*Universitat Autònoma de Barcelona*) for the MCF-10A cell line; Jordi Surrallés's Laboratory (*Universitat Autònoma de Barcelona*) for technical assistance; and the services from the *Universitat Autònoma de Barcelona* (SCAC_*Unitat de Cultius i de Citometria*) and the *Universitat de Barcelona (CCiT_Servei de Citometria*).

CONFLICTS OF INTEREST

The authors declare that they have no conflicts of interest.

FUNDING

This work was funded by *MINECO* (SAF2013-43801-P). The Cell Biology Unit is supported by *Generalitat de Catalunya* (2014SGR-524). AB and DD were supported by a *Universitat Autònoma de Barcelona* fellowship (456-01-1/2012) and *Generalitat de Catalunya* fellowship (2013FI_B200188), respectively.

REFERENCES

1. Griffith JD, Comeau L, Rosenfield S, Stansel RM, Bianchi A, Moss H, De Lange T. Mammalian telomeres end in a large duplex loop. Cell. 1999; 97:503–14. https://doi.org/10.1016/S0092-8674(00)80760-6.
2. Stansel RM, De Lange T, Griffith JD. T-loop assembly *in vitro* involves binding of TRF2 near the 3′ telomeric overhang. EMBO J. 2001; 20:5532–40. https://doi.org/10.1093/emboj/20.19.5532.
3. Lazzerini-Denchi E, Sfeir A. Stop pulling my strings — what telomeres taught us about the DNA damage response. Nat Rev Mol Cell Biol. 2016; 17:364–78. https://doi.org/10.1038/nrm.2016.43.
4. Counter CM, Avilion AA, Lefeuvrel CE, Stewart NG, Greider CW, Harley CB, Bacchettil S. Telomere shortening associated with chromosome instability is arrested in immortal cells which express telomerase activity. EMBO J. 1992; 11:1921–29.
5. Soler D, Genescà A, Arnedo G, Egozcue J, Tusell L. Telomere dysfunction drives chromosomal instability in human mammary epithelial cells. Genes Chromosomes Cancer. 2005; 44:339–50. https://doi.org/10.1002/gcc.20244.
6. Pampalona J, Soler D, Genescà A, Tusell L. Whole chromosome loss is promoted by telomere dysfunction in primary cells. Genes Chromosomes Cancer. 2010; 49:368–78. https://doi.org/10.1002/gcc.
7. Maciejowski J, de Lange T. Telomeres in cancer: tumour suppression and genome instability. Nat Rev Mol Cell Biol. 2017; 18:175–86. https://doi.org/10.1038/nrm.2016.171.
8. Meeker AK, Hicks JL, Platz EA, March GE, Bennett CJ, Delannoy MJ, De Marzo AM. Telomere shortening is an early somatic DNA alteration in human prostate tumorigenesis. Cancer Res. 2002; 62:6405–9.
9. Meeker AK, Hicks JL, Iacobuzio-Donahue CA, Montgomery EA, Westra WH, Chan TY, Ronnett BM, De Marzo AM. Telomere length abnormalities occur early in the initiation of epithelial carcinogenesis. Clin Cancer Res. 2004; 10:3317–26. https://doi.org/10.1158/1078-0432.CCR-0984-03.
10. Meeker AK, Hicks JL, Gabrielson E, Strauss WM, De Marzo AM, Argani P. Telomere shortening occurs in subsets of normal breast epithelium as well as in situ and invasive carcinoma. Am J Pathol. 2004; 164:925–35. https://doi.org/10.1016/S0002-9440(10)63180-X.
11. Poonepalli A, Banerjee B, Ramnarayanan K, Palanisamy N, Putti TC, Hande MP. Telomere-mediated genomic instability and the clinico-pathological parameters in breast cancer. Genes Chromosomes Cancer. 2008; 47:1098–109. https://doi.org/10.1002/gcc.20608.
12. Simpson K, Jones RE, Grimstead JW, Hills R, Pepper C, Baird DM. Telomere fusion threshold identifies a poor prognostic subset of breast cancer patients. Mol Oncol. 2015; 9:1186–93. https://doi.org/10.1016/j.molonc.2015.02.003.
13. Ennour-Idrissi K, Maunsell E, Diorio C. Telomere Length and Breast Cancer Prognosis: a systematic review. Cancer Epidemiol Biomarkers Prev. 2017; 26:3–10. https://doi.org/10.1158/1055-9965.EPI-16-0343.
14. Chin K, de Solorzano CO, Knowles D, Jones A, Chou W, Rodriguez EG, Kuo WL, Ljung BM, Chew K, Myambo K, Miranda M, Krig S, Garbe J, et al. In situ analyses of genome instability in breast cancer. Nat Genet. 2004; 36:984–8. https://doi.org/10.1038/ng1409.
15. Meeker AK, Argani P. Telomere shortening occurs early during breast tumorigenesis: a cause of chromosome destabilization underlying malignant transformation? J Mammary Gland Biol Neoplasia. 2004; 9:285–96. https://doi.org/10.1023/B:JOMG.0000048775.04140.92.
16. Odagiri E, Kanda N, Jibiki K, Demura R, Aikawa E, Demura H. Reduction of telomeric length and c-erbB-2 gene amplification in human breast cancer, fibroadenoma, and gynecomastia. Relationship to histologic grade and clinical parameters. Cancer. 1994; 73:2978–84. https://doi.org/10.1002/1097-0142(19940615)73:12<2978::AID-CNCR2820731215>3.0.CO;2-5.

17. Tanaka H, Abe S, Huda N, Tu L, Beam MJ, Grimes B, Gilley D. Telomere fusions in early human breast carcinoma. Proc Natl Acad Sci U S A. 2012; 109:14098–103. https://doi.org/10.1073/pnas.1120062109.

18. d'Adda di Fagagna F, Reaper PM, Clay-Farrace L, Fiegler H, Carr P, von Zglinicki T, Saretzki G, Carter NP, Jackson SP. A DNA damage checkpoint response in telomere-initiated senescence. Nature. 2003; 426:194–8. https://doi.org/10.1038/nature02118.

19. Takai H, Smogorzewska A, de Lange T. DNA damage foci at dysfunctional telomeres. Curr Biol. 2003; 13:1549–56. https://doi.org/10.1016/S0960-9822(03)00542-6.

20. Smogorzewska A, de Lange T. Different telomere damage signaling pathways in human and mouse cells. EMBO J. 2002; 21:4338–48. https://doi.org/10.1093/emboj/cdf433.

21. Fujita K, Horikawa I, Mondal AM, Jenkins LMM, Appella E, Vojtesek B, Bourdon JC, Lane DP, Harris CC. Positive feedback between p53 and TRF2 during telomere-damage signalling and cellular senescence. Nat Cell Biol. 2010; 12:1205–12. https://doi.org/10.1038/ncb2123.

22. van Steensel B, Smogorzewska A, de Lange T. TRF2 protects human telomeres from end-to-end fusions. Cell. 1998; 92:401–13. https://doi.org/10.1016/S0092-8674(00)80932-0.

23. Karlseder J, Broccoli D, Dai Y, Hardy S, de Lange T. p53- and ATM-dependent apoptosis induced by telomeres lacking TRF2. Science. 1999; 283:1321–5. https://doi.org/10.1126/science.283.5406.1321.

24. Karlseder J, Smogorzewska A, de Lange T. Senescence induced by altered telomere state, not telomere loss. Science. 2002; 295:2446–9. https://doi.org/10.1126/science.1069523.

25. Feuerhahn S, Chen LY, Luke B, Porro A. No DDRama at chromosome ends: TRF2 takes centre stage. Trends Biochem Sci. 2015; 40:275–85. https://doi.org/10.1016/j.tibs.2015.03.003.

26. Doksani Y, Wu JY, de Lange T, Zhuang X. Super-resolution fluorescence imaging of telomeres reveals TRF2-dependent T-loop formation. Cell. 2013; 155:345–56. https://doi.org/10.1016/j.cell.2013.09.048.

27. Denchi EL, de Lange T. Protection of telomeres through independent control of ATM and ATR by TRF2 and POT1. Nature. 2007; 448:1068–71. https://doi.org/10.1038/nature06065.

28. Soule HD, Maloney TM, Wolman SR, Peterson WD, Brenz R, Mcgrath CM, Russo J, Pauley RJ, Jones RF, Brooks SC. Isolation and characterization of a spontaneously immortalized isolation and characterization of a spontaneously immortalized human breast. Cancer Res. 1990; 50:6075–86.

29. Rubis B, Holysz H, Gladych M, Toton E, Paszel A, Lisiak N, Kaczmarek M, Hofmann J, Rybczynska M. Telomerase downregulation induces proapoptotic genes expression and initializes breast cancer cells apoptosis followed by DNA fragmentation in a cell type dependent manner. Mol Biol Rep. 2013; 40:4995–5004. https://doi.org/10.1007/s11033-013-2600-9.

30. Listerman I, Sun J, Gazzaniga FS, Lukas JL, Blackburn EH. The major reverse transcriptase-incompetent splice variant of the human telomerase protein inhibits telomerase activity but protects from apoptosis. Cancer Res. 2013; 73:2817–28. https://doi.org/10.1158/0008-5472.CAN-12-3082.

31. Stampfer MR, Yaswen P. Culture models of human mammary epithelial cell transformation. J Mammary Gland Biol Neoplasia. 2000; 5:365–78. https://doi.org/10.1023/A:1009525827514.

32. Elenbaas B, Spirio L, Koerner F, Fleming MD, Zimonjic DB, Donaher JL, Popescu NC, Hahn WC, Weinberg RA. Human breast cancer cells generated by oncogenic transformation of primary mammary epithelial cells. Genes Dev. 2001; 15:50–65. https://doi.org/10.1101/gad.828901.monly.

33. Lane DP, Simanis V, Bartsch R, Yewdell J, Gannon J, Mole S. Cellular targets for SV40 Large T-antigen. Proc R Soc London Ser B, Biol Sci. 1985; 226:25–42. https://doi.org/10.1098/rspb.1985.0077.

34. Huschtscha LI, Neumann AA, Noble JR, Reddel RR. Effects of Simian virus 40 T-antigens on normal human mammary epithelial cells reveal evidence for spontaneous alterations in addition to loss of p16INK4a expression. Exp Cell Res. 2001; 265:125–34. https://doi.org/10.1006/excr.2001.5178.

35. Toouli CD, Huschtscha LI, Neumann AA, Noble JR, Colgin LM, Hukku B, Reddel RR. Comparison of human mammary epithelial cells immortalized by simian virus 40 T-Antigen or by the telomerase catalytic subunit. Oncogene. 2002; 21:128–39. https://doi.org/10.1038/sj/onc/1205014.

36. Farmer G, Bargonetti J, Zhu H, Friedman P, Prywes R, Prives C. Wild-type p53 activates transcription *in vitro*. Nature. 1992; 358:83–86. https://doi.org/10.1038/358083a0.

37. An P, Sáenz Robles MT, Pipas JM. Large T antigens of polyomaviruses: amazing molecular machines. Annu Rev Microbiol. 2012; 66:213–36. https://doi.org/10.1146/annurev-micro-092611-150154.

38. Worsham MJ, Pals G, Schouten JP, Miller F, Tiwari N, Van Spaendonk R, Wolman SR. High-resolution mapping of molecular events associated with immortalization, transformation, and progression to breast cancer in the MCF10 model. Breast Cancer Res Treat. 2006; 96:177–86. https://doi.org/10.1007/s10549-005-9077-8.

39. Marella NV, Malyavantham KS, Wang J, Matsui S, Liang P, Berezney R. Cytogenetic and cDNA microarray expression analysis of MCF10 human breast cancer progression cell lines. Cancer Res. 2009; 69:5946–53. https://doi.org/10.1158/0008-5472.CAN-09-0420.

40. Wade MA, Sunter NJ, Fordham SE, Long A, Masic D, Russell LJ, Harrison CJ, Rand V, Elstob C, Bown N, Rowe D, Lowe C, Cuthbert G, et al. C-MYC is a radiosensitive locus in human breast cells. Oncogene. 2015; 34:4985–94. https://doi.org/10.1038/onc.2014.427.

41. Weiss MB, Vitolo MI, Mohseni M, Rosen DM, Denmeade SR, Park BH, Weber DJ, Bachman KE. Deletion of p53 in human mammary epithelial cells causes chromosomal instability and altered therapeutic response. Oncogene. 2010; 29:4715–24. https://doi.org/10.1038/onc.2010.220.

42. Ray FA, Meyne J, Kraemer PM. SV40 T antigen induced chromosomal changes reflect a process that is both clastogenic and aneuploidogenic and is ongoing throughout neoplastic progression of human fibroblasts. Mutat Res. 1992; 284:265–73. https://doi.org/10.1016/0027-5107(92)90011-P.

43. Genescà A, Pampalona J, Frías C, Domínguez D, Tusell L. Role of telomere dysfunction in genetic intratumor diversity. Adv Cancer Res. 2011; 112:11–41. https://doi.org/10.1016/B978-0-12-387688-1.00002-8.

44. Maciejowski J, Li Y, Bosco N, Campbell PJ, De Lange T. Chromothripsis and kataegis induced by telomere crisis. Cell. 2015; 163:1641–54. https://doi.org/10.1016/j.cell.2015.11.054.

45. Davoli T, Denchi EL, de Lange T. Persistent telomere damage induces bypass of mitosis and tetraploidy. Cell. 2010; 141:81–93. https://doi.org/10.1016/j.cell.2010.01.031.

46. Pampalona J, Frías C, Genescà A, Tusell L. Progressive telomere dysfunction causes cytokinesis failure and leads to the accumulation of polyploid cells. PLoS Genet. 2012; 8:e1002679. https://doi.org/10.1371/journal.pgen.1002679.

47. Ahler E, Sullivan WJ, Cass A, Braas D, York AG, Bensinger SJ, Graeber TG, Christofk HR. Doxycycline Alters Metabolism and Proliferation of Human Cell Lines. PLoS One. 2013; 8:e64561. https://doi.org/10.1371/journal.pone.0064561.

48. Jacobs JJ, de Lange T. Significant role for p16INK4a in p53-independent telomere-directed senescence. Curr Biol. 2004; 14:2302–8. https://doi.org/10.1016/j.cub.2004.12.025.

49. Pan MR, Peng G, Hungs WC, Lin SY. Monoubiquitination of H2AX protein regulates DNA damage response signaling. J Biol Chem. 2011; 286:28599–607. https://doi.org/10.1074/jbc.M111.256297.

50. Boichuk S, Hu L, Hein J, Gjoerup OV. Multiple DNA damage signaling and repair pathways deregulated by Simian Virus 40 Large T antigen. J Virol. 2010; 84:8007–20. https://doi.org/10.1128/JVI.00334-10.

51. Kaul Z, Cesare AJ, Huschtscha LI, Neumann AA, Reddel RR. Five dysfunctional telomeres predict onset of senescence in human cells. EMBO Rep. 2011; 13:52–59. https://doi.org/10.1038/embor.2011.227.

52. Brenner AJ, Stampfer MR, Aldaz CM. Increased p16 expression with first senescence arrest in human mammary epithelial cells and extended growth capacity with p16 inactivation. Oncogene. 1998; 17:199–205. https://doi.org/10.1038/sj.onc.1201919.

53. Romanov SR, Kozakiewicz BK, Holst CR, Stampfer MR, Haupt LM, Tlsty TD. Normal human mammary epithelial cells spontaneously escape senescence and acquire genomic changes. Nature. 2001; 409:633–7. https://doi.org/10.1038/35054579.

54. Garbe JC, Holst CR, Bassett E, Tlsty T, Stampfer MR. Inactivation of p53 function in cultured human mammary epithelial cells turns the telomere-length dependent senescence barrier from agonescence into crisis. Cell Cycle. 2007; 6:1927–36. https://doi.org/10.4161/cc.6.15.4519.

55. Celli GB, de Lange T. DNA processing is not required for ATM-mediated telomere damage response after TRF2 deletion. Nat Cell Biol. 2005; 7:712–8. https://doi.org/10.1038/ncb1275.

56. Cesare AJ, Hayashi MT, Crabbe L, Karlseder J. The telomere deprotection response is functionally distinct from the genomic DNA damage response. Mol Cell. 2013; 51:141–55. https://doi.org/10.1016/j.molcel.2013.06.006.

57. Hayashi MT, Cesare AJ, Rivera T, Karlseder J. Cell death during crisis is mediated by mitotic telomere deprotection. Nature. 2015; 522:492–6. https://doi.org/10.1038/nature14513.

58. LaBarge MA, Garbe JC, Stampfer MR. Processing of human reduction mammoplasty and mastectomy tissues for cell culture. J Vis Exp. 2013; 71:e50011. https://doi.org/10.3791/50011.

59. Garbe JC, Bhattacharya S, Merchant B, Bassett E, Swisshelm K, Feiler HS, Wyrobek AJ, Stampfer MR. Molecular distinctions between stasis and telomere attrition senescence barriers shown by long-term culture of normal human mammary epithelial cells. Cancer Res. 2009; 69:7557–68. https://doi.org/10.1158/0008-5472.CAN-09-0270.

60. Cesare AJ, Heaphy CM, O'Sullivan RJ. Visualization of telomere integrity and function *in vitro* and *in vivo* using immunofluorescence techniques. Curr Protoc Cytom. 2015; 73:12.40.1–31. https://doi.org/10.1002/0471142956.cy1240s73.

www.oncotarget.com Oncotarget, Supplementary Materials

Acute telomere deprotection prevents ongoing BFB cycles and rampant instability in p16^{INK4a}-deficient epithelial cells

SUPPLEMENTARY MATERIALS

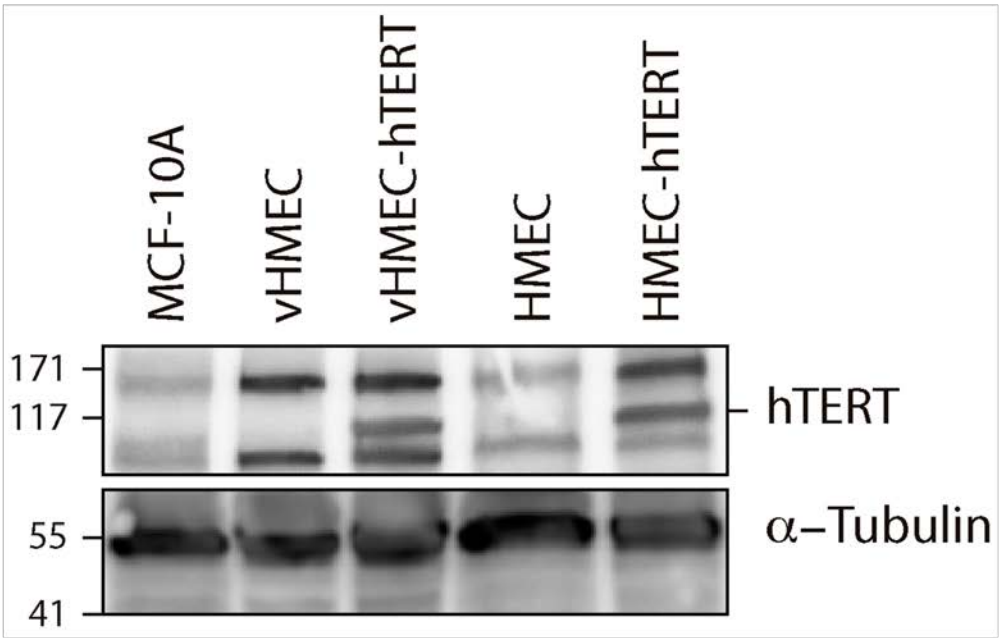

Supplementary Figure 1: hTERT protein levels in MCF-10A cells, as well as vHMECs and HMECs transduced/not transduced with hTERT. Telomerase activity was assessed through expression of the hTERT catalytic subunit. As positive controls vHMECs and HMECs non-transduced and transduced with hTERT lentiviral particles were used. A clear band at approximately 120 kDa was detected in cells transduced with the hTERT lentivirus. MCF-10A protein extracts did not demonstrate a discernible hTERT band.

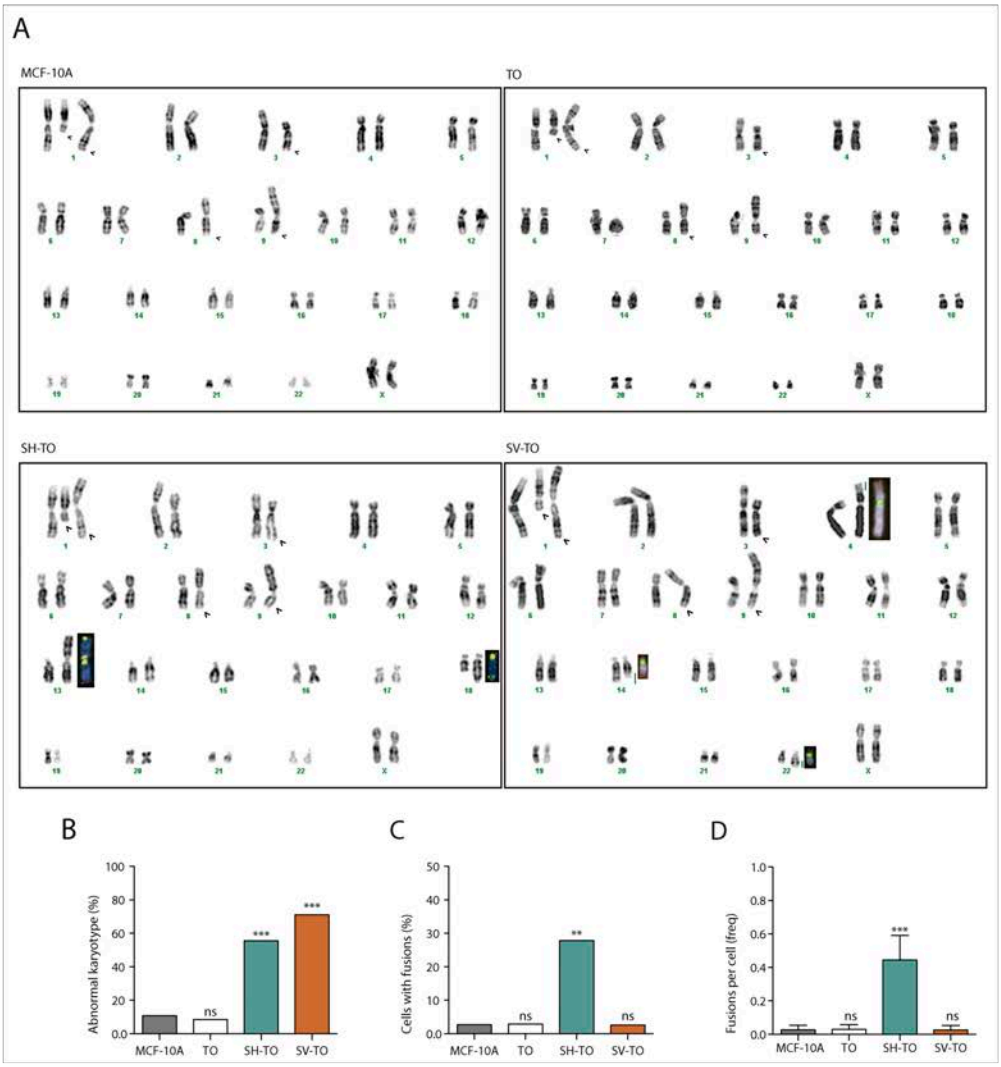

Supplementary Figure 2: Cytogenetic characterisation of MCF-10A and uninduced derivatives. (A) MCF-10A; TO; SH-TO and SV-TO representative karyotypes. Open arrows indicate clonal aberrations in the parental MCF-10A cell line. Uninduced TO cells presented the same karyotype as the parental cell line. However, SH-TO and SV-TO cell lines showed additional aberrations. In SH-TO, these consisted mainly of dicentric chromosomes, while non-reciprocal translocations were observed in the SV-TO cell line. Insets in the karyotype show rearranged chromosomes stained with centromeric (green) and telomeric (red) PNA probes. Green lines denote gains or losses. **(B)** Proportion of abnormal karyotypes in each cell line relative to the basal MCF-10A karyotype. No karyotype differences were observed when comparisons were made with uninduced TO cells. In contrast, abrogation of p53 (SH-TO) and p53/Rb pathways (SV-TO) significantly increased the incidence of abnormal karyotypes. No significant differences were observed between SH-TO and SV-TO cells. **(C)** In uninduced cells, the percentage of metaphases containing chromosome fusions was low except in the SH-TO cell line. This reflects that the rearranged karyotype observed in SV-TO cells results from chromosome aberrations other than dicentrics. **(D)** Accordingly, only uninduced SH-TO cells showed a significant increase in the frequency of fusion events per cell. Importantly, most of these fusion events (78.57%, Supplementary Table 2) did not show telomeric FISH signals at the fusion point, thus supporting rejoining of broken DNA ends as origin. Data are presented as mean + SEM.

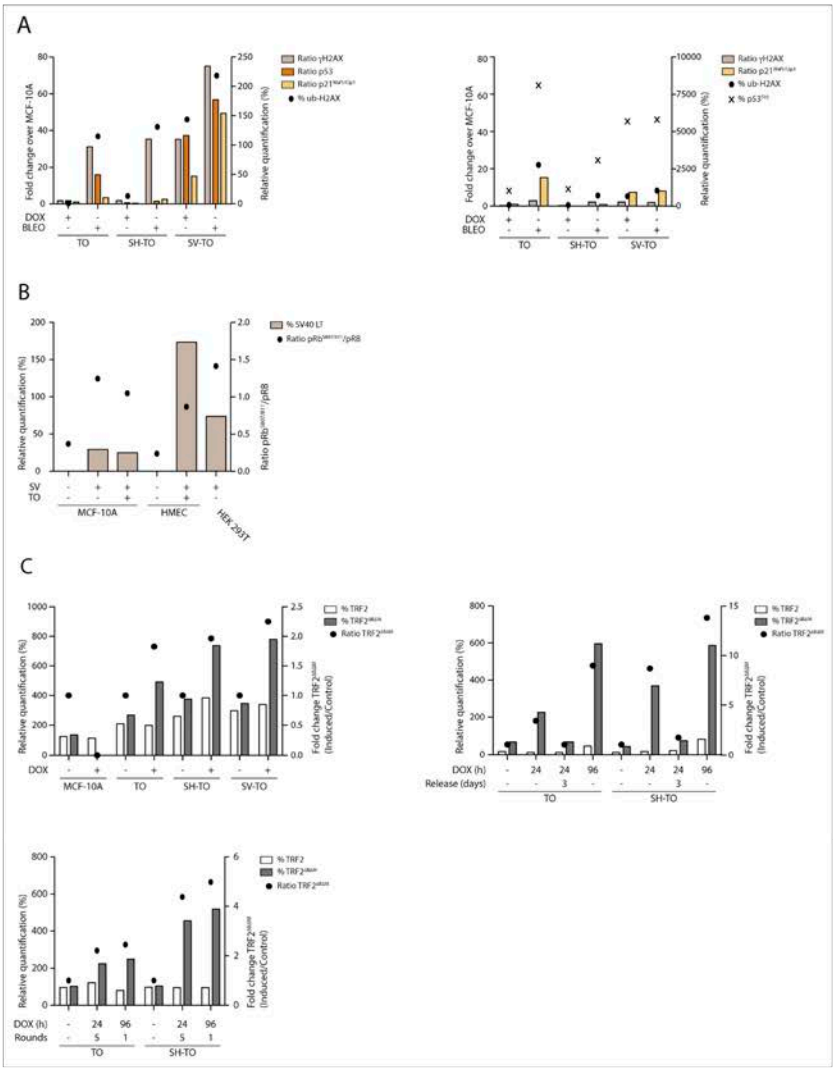

Supplementary Figure 3: Western blot protein quantification. Optical density units of each protein were obtained by ImageLab software. These data were normalised for the loading control Lamin B1 or α-Tubulin. Moreover, additional normalisation was performed by considering protein loading efficiencies. **(A)** The quantification values of ub-H2AX and $p53^{S15}$ were plotted as dots and crosses at the right axis, respectively. The relative abundance of p53, γH2AX and $p21^{Waf1/Cip1}$ in each cell line was compared to the protein levels of untreated MCF-10A cells (not shown), and were plotted as solid bars at the left axis. **(B)** The ratio of $pRb^{S807/811}$ quantification values in relation to the pRb ones were plotted as dots at the right axis. The quantification values of SV40LT was plotted as solid bars at the left axis. **(C)** The quantification values of TRF2 and $TRF2^{\Delta B\Delta M}$ in each cell line were plotted as solid bars at the left axis. The ratio of $TRF2^{\Delta B\Delta M}$ quantification values in the DOX-treated cell lines in relation to the $TRF2^{\Delta B\Delta M}$ of the respective untreated control cells, were plotted as dots at the right axis.

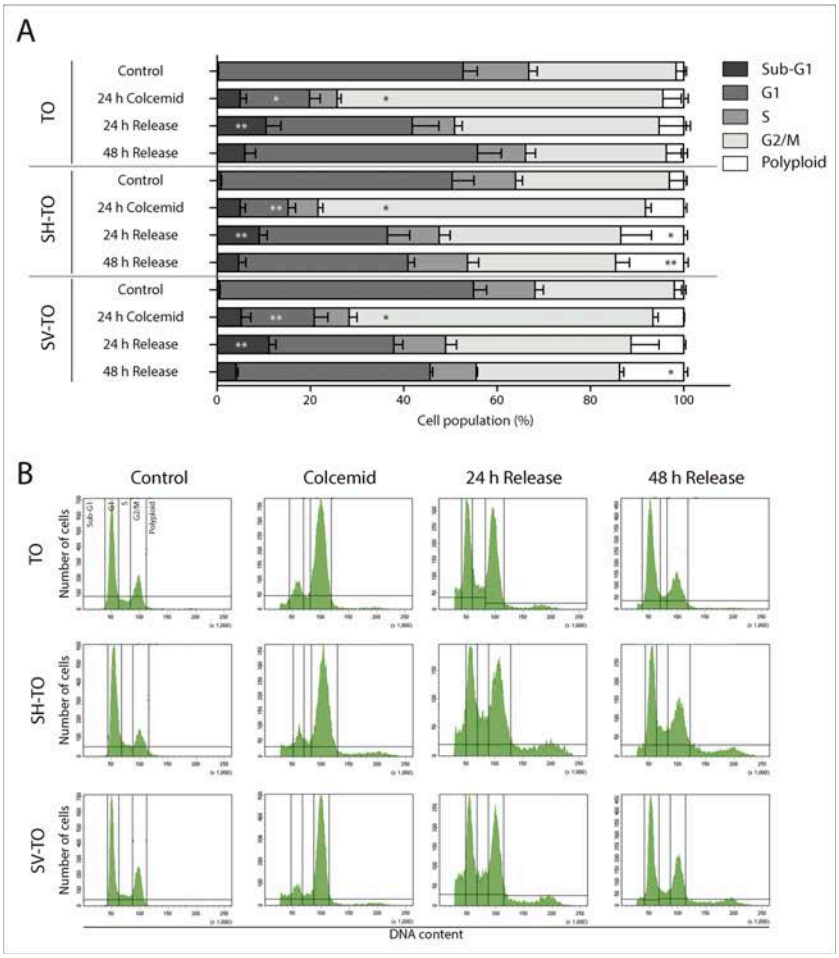

Supplementary Figure 4: Tetraploid checkpoint functional analysis. (A) Distribution of cell cycle phases among TO, SH-TO and SV-TO cell lines, in control conditions, treated with colcemid (50 ng/ml) for 24 h, and after a release of 24 h and 48 h. Acute colcemid treatment produced a significant accumulation of cells in G2/M phase that was accompanied by a reduced G1 fraction of cells (Kruskal Wallis and Dunn's comparison test; $p< 0.05$). Cell death was significantly denoted in the following 24 h after colcemid treatment and washout (Kruskal Wallis and Dunn's comparison test; $p< 0.05$). Only in SH-TO and SV-TO cell lines, there was an increased tetraploid population 48 h after colcemid treatment. These data indicate that only SH-TO and SV-TO cell lines allowed the proliferation of tetraploid cells. Data are presented as mean + SEM from three independent experiments. **(B)** Representative plots of cell cycle profiles from each cell line and condition. Cell cycle phases are marked.

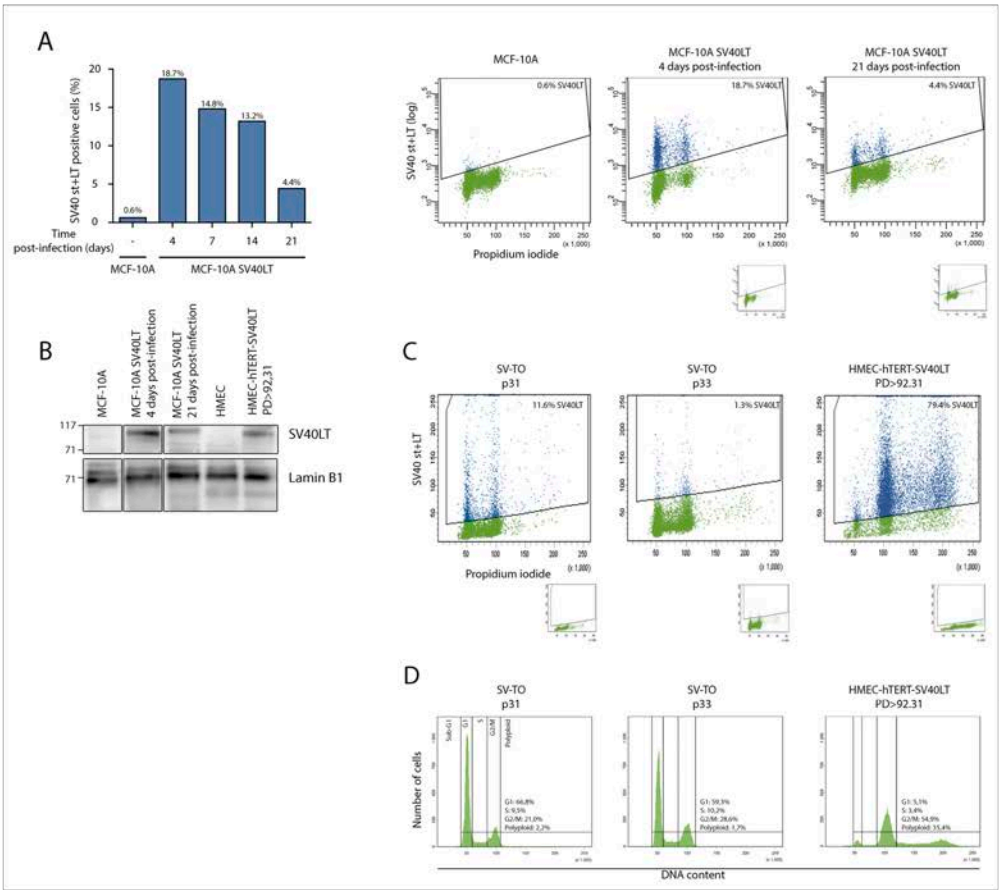

Supplementary Figure 5: Leaking of SV40LT antigens with PDs in MCF-10A. (A) MCF-10A cells were infected with SV40LT-mCherry vector and the percentage of SV40LT positive cells was evaluated by flow cytometry using antibodies against SV40 st+LT during three weeks. Four days after infection, 18.7% of cells were positive for SV40 st+LT. This percentage steadily decreased with days in culture. Three weeks after infection, only 4.4% of cells expressed SV40 st+LT antigens. Representative cytometric plots of MCF-10A and SV40LT infected MCF-10A are shown. The absolute percentage of SV40LT cells, where positive cells of the A488 control have been subtracted, is shown. The respective control A488 plots are the smaller ones depicted. **(B)** Immunoblot of control MCF-10A, MCF-10A infected with SV40LT four days and three weeks after infection and not infected HMEC (around PD 3) and HMEC-hTERT infected with SV40LT. Only cells infected with the SV40LT-mCherry vector expressed the SV40LT antigen. **(C)** Cytometric plots of SV40 st+LT expression in SV-TO cells at p31 and p33 also demonstrated the leaking effect. In contrast, 79.4% of HMEC-hTERT infected with the SV40LT-mCherry vector at PD 6.92 and analysed by flow cytometry at PD >92.31 expressed the SV40 st+LT. The absolute percentage of SV40LT cells, where positive cells of the A488 control have been subtracted, is shown. The respective control A488 plots are the smaller ones depicted. **(D)** Representative cell cycle plots of SV-TO cells at p31 and p33 and HMEC-hTERT-SV40LT at PD >92.31. An abnormal cell cycle profile was only observed in the HMEC-hTERT-SV40LT cells where a 35.4% of cells were >4N.

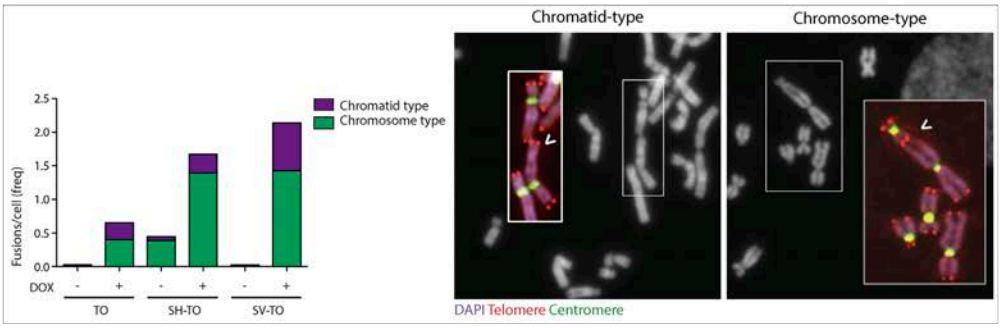

Supplementary Figure 6: TRF2$^{\Delta B \Delta M}$ expression induces chromosome and chromatid end-to-end fusions in all inducible cell lines. (A) Distribution of chromosome-type and chromatid-type fusion per cell in uninduced and induced cell lines. Most fusions were produced at G1, i.e. were of the chromosome-type, although chromatid-type fusions were also observed. **(B)** Partial images showing a chromosome-type fusion and a chromatid-type fusion. In the raw image of DAPI, the physical connexion between chromosome arms, through only one or both chromatids, is observed. The insets show the telomere and centromere status of the fusion events, confirming that each fusion event is labelled with the telomeric PNA probe.

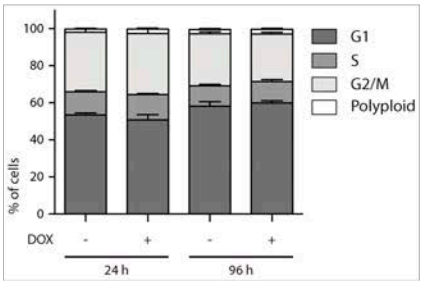

Supplementary Figure 7: Doxycycline does not alter the cell cycle profile of parental MCF-10A cells. Propidium iodide-based cell cycle analysis was performed after exposure of MCF-10A cells to 1 µg/ml DOX during 24 h or 96 h. Assay was performed in triplicate, with error bars representing + SEM. Data were analysed by Mann-Whitney U-test, comparing control *vs.* treated group, and p-values were higher than 0.05.

Supplementary Table 1: Abnormal karyotypes and chromosome end fusions in MCF-10A and inducible variants expressing TRF2$^{\Delta B \Delta M}$

Cell line	DOX treatment	Cells analysed n	% of abnormal karyotype (n)*	% of cells with fusions (n)	Fusions per cell (n)
MCF10A	-	37	10.81 (4)	2.70 (1)	0.03 (1)
TO	-	35	8.57 (3)	2.86 (1)	0.03 (1)
TO	96 h	55	45.45 (25)	36.36 (20)	0.65 (36)
SH-TO	-	36	55.56 (20)	27.78 (10)	0.44 (16)
SH-TO	96 h	46	67.39 (31)	58.70 (27)	1.67 (77)
SV-TO	-	38	71.05 (27)	2.63 (1)	0.03 (1)
SV-TO	96 h	35	82.86 (29)	65.71 (23)	2.14 (75)

* Relative to the basal karyotype (includes cells with fusions).

Supplementary Table 2: Telomere status of fusion's junction point in untreated or DOX-treated cell lines

Cell line	DOX treatment	Cells analysed n	Total fusions n	% of telomere negative fusions (n)	% of telomere positive fusions (n)
TO	-	35	1	100.00 (1)	0 (0.0) (0)
TO	96 h	55	35	5.71 (2)	94.29 (33)
SH-TO	-	36	14	78.57 (11)	21.43 (3)
SH-TO	96 h	46	72	15.28 (11)	84.72 (61)
SV-TO	-	38	1	100.00 (1)	0.00 (0)
SV-TO	96 h	35	71	8.45 (6)	91.55 (65)

* The number of fusion events where the telomere status of the junction point was resolved is less than the total number of fusions due to hybridization technique pitfalls.

Supplementary Table 3: Anaphase cells containing chromatin bridges after TRF2$^{\Delta B\Delta M}$ expression

Cell line	DOX treatment	Cells examined (n)	% of cells with anaphase bridges (n)
TO	-	215	3.72 (8)
TO	96 h	318	45.60 (145)
SH-TO	-	243	18.93 (46)
SH-TO	96 h	490	53.06 (260)
SV-TO	-	736	4.21 (31)
SV-TO	96 h	608	38.16 (232)

Supplementary Table 4: Numerical chromosome changes after persistent or transient telomere deprotection

Cell line	DOX treatment	Cells examined (n)	2N		4N	
			% of euploid (n)	% of aneuploid (n)	% of euploid (n)	% of aneuploid (n)
TO	-	439	89.98 (395)	9.79 (43)	0.23 (1)	0.00 (0)
TO	96 h	285	83.86 (239)	14.39 (41)	1.40 (4)	0.35 (1)
TO	5x24 h	451	94.24 (425)	4.88 (22)	0.67 (3)	0.22 (1)
SH-TO	-	539	80.52 (434)	14.10 (76)	2.60 (14)	2.78 (15)
SH-TO	96 h	284	75.70 (215)	13.73 (39)	3.52 (10)	7.04 (20)
SH-TO	5x24 h	452	88.50 (400)	8.19 (37)	1.33 (6)	1.99 (9)
SV-TO	-	580	93.28 (541)	4.66 (27)	1.21 (7)	0.86 (5)
SV-TO	96 h	419	90.45 (379)	6.44 (27)	1.19 (5)	1.91 (8)

Supplementary Materials

Table S1. Chromosome analysis of young vHMECs at PD22.

Karyotype	number
46, XX	15
46, XX, ctb(13q)	1
45, XX, fus(11p;22q)	1
43, XX, ctb(6q), -3, -16, -22	1
46, XX, ctb(10q)	1
46, XX, fus(21p;19q)	1
46, XX, nrt(14p)	1
46, XX, +ace	1
45, XX, fus(2q;17q)	1
46, XX, nrt(4p), fus(19q;22q)	1
92, XXXX, fus(3p;3q)	1
94,XXXX, +2, +12, fus(19q;20p), -20, +22	1
TOTAL	**26**

Work III

In preparation

Absence of cellular transformation and tumorigenic potential of SV40LT-hTERT immortalised HMECs after telomere uncapping

Introduction

In adult humans, cancers are predominantly of epithelial origin, a tissue where there is continuous cell renewal. These cycles of proliferation and replacement are especially prominent in the breast where, in each menstrual cycle, a regulated-hormonally proliferation of the epithelial cells is followed by the regression of the epithelium. It could be therefore assumed that given their high rate of cell division mammary epithelial cells are susceptible to increased telomeric erosion. In fact, evidence of telomere shortening has been observed in premalignant mammary lesions (Meeker *et al*, 2004). And the implication of telomere dysfunction in the origin of breast cancer was supported by experimental studies comparing premalignant and malignant lesions (Chin *et al*, 2004; Raynaud *et al*, 2010). While the premalignant lesions were characterised by the presence of excessively short telomeres and non-clonal chromosomal aberrations, the carcinomas contained chromosomes with longer telomeres, exhibited telomerase activity and the presence of clonal chromosomal anomalies presumably fixed in the karyotype after suffering a period of telomere dysfunction. Finally, convincing proof of the presence of telomere dysfunction in mammary carcinogenesis is the observation of telomere-telomere fusions by means of TAR (telomere-associated repeat) fusion PCR in premalignant breast cancer lesions (DCIS) and not in normal breast tissue (Tanaka *et al*, 2012). Thus, all these observations would give relevance to telomere-dependent chromosomal instability (CIN) as one of the key factors in the onset of mammary carcinogenesis.

Our studies in human primary epithelial cells derived from the mammary gland (vHMECs) have allowed us to establish a direct connection between physiological telomere dysfunction and the generation of massive chromosome instability (Soler *et al*, 2005; Tusell *et al*, 2008; Pampalona *et al*, 2010a, 2010b; Tusell *et al*, 2010; Pampalona *et al*, 2012), which would be at the base of the tumour process (Genescà *et al*, 2011). In these primary cells, spontaneous hypermethylation of the CDKN2A promoter makes it possible to evade senescence and enter a second phase of cell proliferation, where excessive telomeric shortening results in an exorbitant CIN that ends in agonescence or cell crisis. It is believed that only those genetically unstable cells that are capable of activating mechanisms to stabilise the telomere length will be able to avoid cell death associated with genetic chaos and possibly acquire a malignant phenotype. However, when telomerase is artificially reactivated in vHMECs that present CIN derived from telomere dysfunction, the instability of immortalised cells is drastically reduced [(**Work I**) which is (Bernal *et al*, 2018b)].

Another way to obtain immortal unstable cells that have been passed through a telomere dysfunction period is by the modification of shelterin proteins. Among them, TRF2 is essential for t-loop conformation and DNA damage response (DDR) modulation (Buscemi *et al*, 2009; Okamoto *et al*, 2013; Cesare *et al*, 2013). Indeed, the absence of this protein leads to end-to-end fusions, growth arrest and senescence or cell death (Steensel *et al*, 1998; Karlseder *et al*, 1999; Celli & de Lange, 2005; Denchi & de Lange, 2007).

This also occurs when a mutant form of TRF2 lacking the Basic and the Myb domains ($TRF2^{\Delta B\Delta M}$) is expressed, as it displaces endogenous TRF2 from telomeric DNA (Steensel *et al*, 1998; Smogorzewska & de Lange, 2002). Whereas the persistent/constitutive expression of $TRF2^{\Delta B\Delta M}$ leads to the death of the cells (Smogorzewska & de Lange, 2002), the inducible/conditional expression of $TRF2^{\Delta B\Delta M}$ in a telomerase active background would allow the cells to acquire a moderate and tolerated CIN, which would lead to unstable cells potentially susceptible to malignant transformation. In fact, conditional expression of $TRF2^{\Delta B\Delta M}$ in mice enhances CIN inception and hepatocarcinoma development (Begus-Nahrmann *et al*, 2012). Moreover, transient dysfunction of POT1A in mice induces the formation of unstable-tetraploid cells and promotes cell transformation and tumour development (Davoli & de Lange, 2012). With the aim of developing a novel preclinical model to determine whether telomere-driven unstable cells were capable of initiating mammary carcinogenesis, we have established an inducible TET-ON system for $TRF2^{\Delta B\Delta M}$ in mammary epithelial cells derived from aesthetic reduction.

Results and discussion

Isolation and immortalisation of human mammary epithelial cells.

This study is based on the processing and immortalisation of human mammary epithelial cells (HMECs) from healthy donors. Mammary tissue from four different patients was processed to obtain of human mammary epithelial cells. Patients read and provided written informed consent for the collection and use of tissue samples for research purposes, according to protocols approved by Human Subjects Protection Committee of Universitat Autònoma de Barcelona. Coded mammary tissue was minced through mechanical and enzymatic digestion and isolated organoids were cultured for HMECs proliferation (FIGURE 21A).

In order to prevent telomere shortening and p53 and pRb activation, cells were transduced by the catalytic subunit of telomerase (hTERT) and the Large T antigen from the Simian virus 40 (SV40LT). The hTERT transduction was performed immediately after HMECs isolation from organoid cultured (passage 1, except for CP5 which was transduced at PD 5.15). The coding hTERT lentivirus did not express a selection marker. To allow hTERT expression, the following week cells were transduced with lentiviral particles containing SV40LT and mCherry under the same promoter (CP3 PD 6.92; CP4 PD 6.72; CP5 PD 5.61; 14p PD 4.00). Validation of successful HMECs transduction was performed by western blot at early PD after virus infection (CP3 PD 17.98; CP4 PD 18.64; CP5 PD 15.60; 14p PD 13.42) (FIGURE 21B). Moreover, SV40LT expression was also validated at 60 PDs after transduction through flow cytometry, as it has been reported that SV40LT is diluted over cell passages in deficient $p16^{INK4a}$ mammary cell lines (Huschtscha *et al*, 2001; Toouli *et al*, 2002) [(Work II) which is (Bernal *et al*, 2018a)]. At that time, the four immortalised and modified cell lines (HMEC-TO) displayed the Large T antigen with a high frequency: CP3-TO: 78.30%, CP4-TO: 69.29%, CP5-TO: 95.73%, and 14p-TO: 64.96% (FIGURE 21C). The absence of leaking of SV40LT in our mammary cells could be related to the fact that they have not undergone a selection process where p16INK4a is epigenetically inactivated. Although hTERT was not verified at late PDs, cells displayed exponential growth for a minimum of 60 PDs (FIGURE 21D).

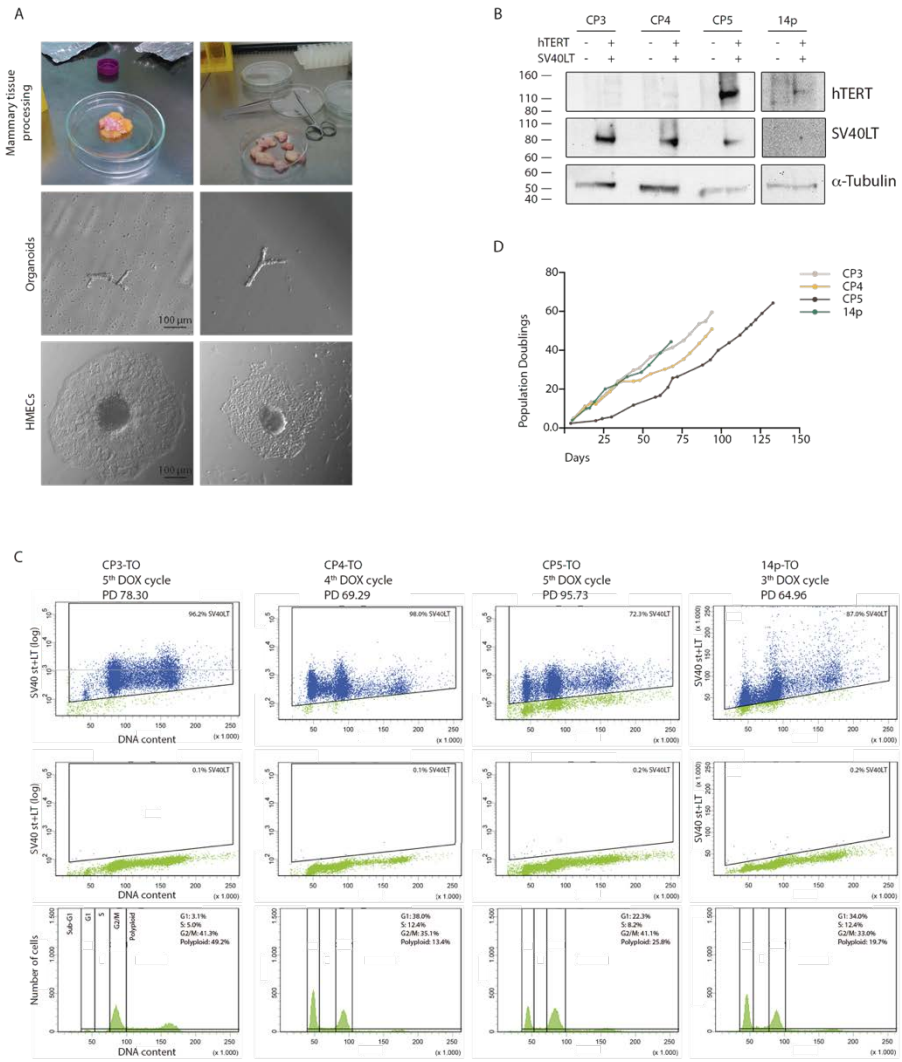

FIGURE 21. HMECs harvesting and immortalisation. **A.** Representative images of tissue processing, organoid isolation and primary HMECs growth. **B.** hTERT and SV40LT immunoblot detection. **C.** Cytometric plots of SV40 st+LT expression of HMEC-hTERT-SV40LT-TO cells at late PDs and their representative cell cycle plots. **D.** Cell growth curves of the CP3; CP4; CP5 and 14p cell lines for the initial 50 PDs.

Immortalisation of cells expressing different lineage markers

The mammary gland presents a ductal structure where luminal epithelial cells face the lumen of the duct and are surrounded by myoepithelial cells (Inman *et al*, 2015). During lactation, luminal alveolar cells synthesise and secrete milk proteins into the ducts, and the contraction of myoepithelial cells facilitates the milk transport to the nipple [Reviewed by (Inman *et al*, 2015)]. The mammary cell population remodels during the female's lifetime, mainly due to hormonal changes and age. And while the myoepithelial lineage is predominant in younger females, luminal cells expand during pregnancy and lactation, and in elder females luminal cells with basal-like features, and progenitor cells are more abundant (Garbe *et al*, 2012).

The *in vitro* culture of epithelial cells is a challenge, as culture conditions enrich for myoepithelial lineage against the luminal lineage over population doublings (PD). The maintenance of myoepithelial and luminal

lineages over cell passages is important as it has been suggested that both lineages could develop different tumour subtypes. Cells of myoepithelial origin could originate squamous cell carcinomas, while the tumours from luminal lineage are suggested to be more similar to human breast adenocarcinomas (Ince *et al*, 2007). To prevent this cell bias, organoids and epithelial cells were fed with the M87AX medium, which is a low stress medium and allows the growth of multiple mammary epithelial lineages for up to 60 population doublings before stasis, a senescence entry due to cell culture conditions (Garbe *et al*, 2009).

To test the abundance of mammary cell lineage, the presence of myoepithelial CD10 and luminal lineage CD227 (also called MUC) markers at the plasma membrane was monitored in the different cell lines between PDs 42 and 62. The four cell lines expressed both markers to a greater or lesser extent (FIGURE 22). Specifically, CP4-TO and CP5-TO cell lines mainly expressed exclusively the CD10 marker in the membrane, 49.5% and 66.4% respectively, thus suggesting that myoepithelial lineage was enriched in both cell lines. In contrast, the CP3-TO cell line mainly co-expressed both markers in the membrane (40.5%). Finally, the cells present in the 14p-TO cell line were mainly double negative from both markers (73.8%), followed by a myoepithelial lineage (17.2%), luminal lineage (5.0%) and the progenitor population (4.0%). The presence of both markers has been related to progenitor mammary cells, which increase with age *in vivo* (Garbe *et al*, 2012).

A

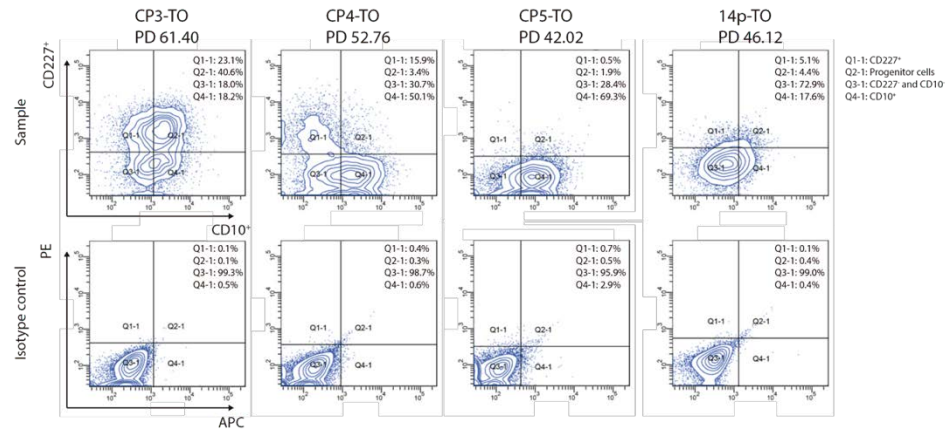

B

	CD10+ Myoepithelial lineage	CD227+ Luminal lineage	CD10+/CD227+ Progenitor cells	CD10-/CD227-
CP3-TO	17.7%	23.0%	40.5%	18.8%
CP4-TO	49.5%	15.5%	3.1%	31.9%
CP5-TO	66.4%	0.0%	1.4%	32.2%
14p-TO	17.2%	5.0%	4.0%	73.8%

FIGURE 22. Immunodetection of mammary cell lineages. A. Immunodetection of CD-10 and CD-227 for each cell line by flow cytometry. B. Summary table of mammary cell lineage proportions. The absolute percentage of CD10 and/or CD227 positive cells is shown, as the positive population of the isotype control has been subtracted.

TRF2$^{\Delta B\Delta M}$ INDUCTION, ANAPHASE BRIDGES AND END-TO-END FUSIONS

To develop CIN through shelterin deficiency-dependent CIN model in immortalised human mammary epithelial cells, HMEC-hTERT-SV cells were transduced with lentiviral particles coding for the rtTA3 and TRF2$^{\Delta B\Delta M}$ genes (HMEC-hTERT-SV-TO), hereafter HMEC-TO. Importantly, the TRF2$^{\Delta B\Delta M}$ was under a conditional promoter based on tetracycline resistance to prevent the deleterious effect of TRF2$^{\Delta B\Delta M}$ expression over cell growth, and was only expressed when doxycycline (DOX) was added to the cell medium.

To validate the efficacy of TRF2$^{\Delta B\Delta M}$ expression, DOX was added to the cell culture during 72 h. The expression of TRF2$^{\Delta B\Delta M}$ truncated protein was detected by immunoblotting and compared with uninduced protein extracts from the four cell lines (FIGURE 23A). The expression of TRF2$^{\Delta B\Delta M}$ leads to t-loop disassembly, end-to-end fusions formation and an increase in anaphase bridges (Bernal *et al*, 2018b). The anaphase bridge analysis was performed between PD 30 and PD 55. At that point, the anaphase bridge rate significantly increased after 72 h of DOX exposure in all cell lines (Fisher's exact test p-value 0.0002 for CP4-TO and p-value <0.0001 for CP3-TO, CP5-TO and 14p-TO) (FIGURE 23B) (SUPPLEMENTARY TABLE 1).

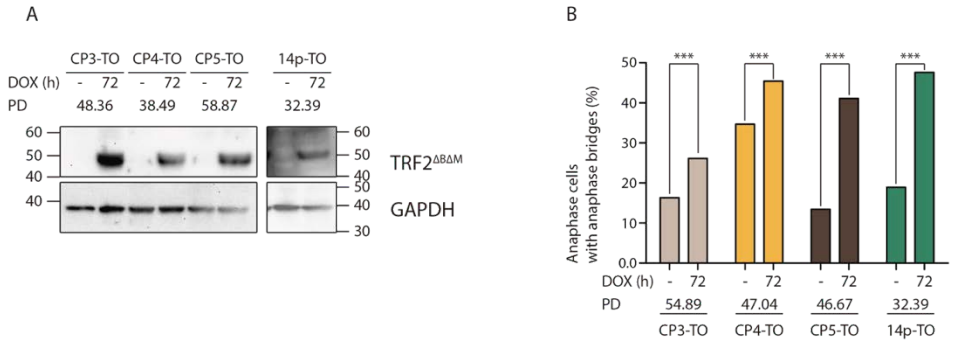

FIGURE 23. TRF2$^{\Delta B\Delta M}$ induction and anaphase bridge formation. **A.** Immunodetection of TRF2$^{\Delta B\Delta M}$ after 72 h of DOX exposure, GAPDH immunodetection was used as a loading control. **B.** TRF2$^{\Delta B\Delta M}$ expression for 72 h increased the anaphase bridges rate.

Moreover, the cell lines were tested again for TRF2 expression after long term culture in order to determine whether the inducible system was still expressed by the cells. For that purpose, a control population never exposed to DOX at PD of around 95 of CP3-TO, CP5-TO and 14p-TO was exposed to 24 h DOX and the induction of TRF2$^{\Delta B\Delta M}$ and the presence of end-to-end fusions with telomeric DNA at the junction point were recorded. The induction of TRF2$^{\Delta B\Delta M}$ expression during 24 h showed some differences at late PD with respect to the expression displayed at mid PD. While 24h of DOX in CP3-TO barely induced TRF2$^{\Delta B\Delta M}$ protein expression, the levels observed in CP5-TO and 14p-TO were extremely high (FIGURE 24A). However, basal levels of TRF2$^{\Delta B\Delta M}$ expression at uninduced CP5-TO were prominent, thus reflecting the leaking of the inducible protein. Those expression discrepancies at late PD could be due to the growth of some clones with a different expression of TRF2$^{\Delta B\Delta M}$ during cell passages.

The analysis of end-to-end fusions after 72 h DOX exposure in long term unexposed cells revealed that there was only a significant increase in the rate of metaphases showing chromosome fusions only in the 14p-TO cell line (Fisher's exact test p-value 0.0106) (FIGURE 24B) (SUPPLEMENTARY TABLE 2), as well as in the number of fusions per cell (0.042 fusions/cell in 14p-TO non-treated cells vs 0.64 fusions/cell in the 72 h TRF2$^{\Delta B\Delta M}$ induced samples; Mann-Whitney test p-value 0.0062) (FIGURE 24C), but strikingly, no telomeric signal was displayed in this cell line at the fusion point of dicentric chromosomes when compared with CP3-TO and CP5-TO (FIGURE 24D). These contradictory results could be caused by the low number of metaphase plates analysed as only 20 cells per condition and cell lines were evaluated.

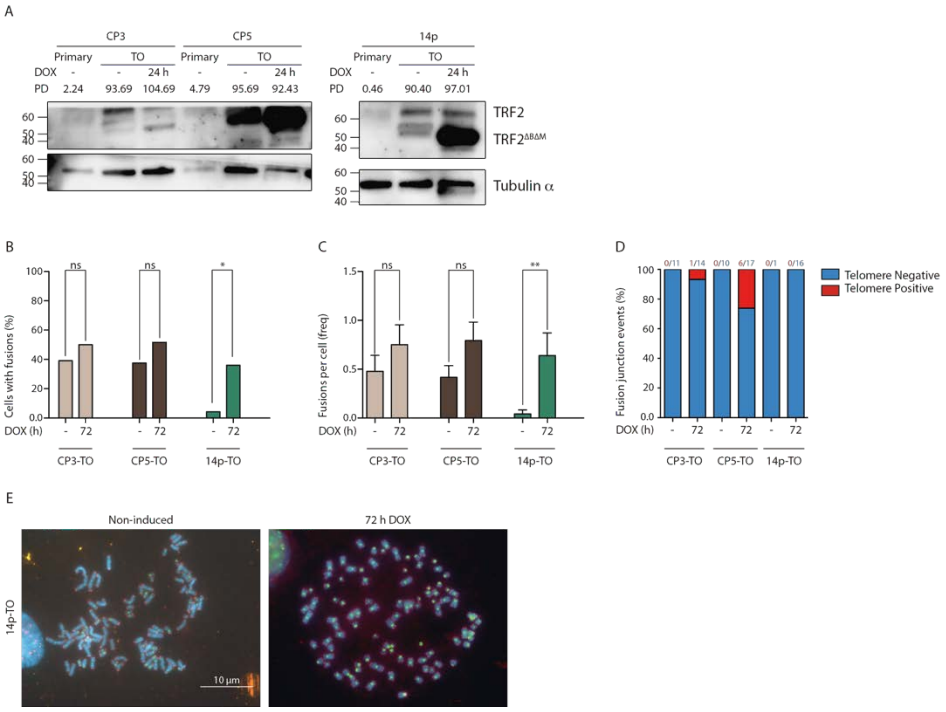

FIGURE 24. Telomere dysfunction phenotype after 72 h of TRF2$^{\Delta B\Delta M}$ induction in long term cell cultures. **A.** TRF2$^{\Delta B\Delta M}$ Immunodetection in long term unexposed cells. **B.** The presence of chromosome fusions was validated in long term cell cultures after DOX exposure for 72 h. Only 14p-TO exhibited an increase in chromosome fusions. **C.** Number of fusions per cell increased in the 14p-TO cell line at late PDs. Data were presented as mean + SEM. **D.** Surprisingly, 14p-TO did not increased end-to-end fusions displaying TTAGGG repeats at the fusion point, thus suggesting that TRF2$^{\Delta B\Delta M}$ was not behind chromosome fusions in this cell line. In contrast, telomeric fusions displaying TTAGGG repeats increased in long term cell cultures CP3-TO and CP5-TO. **E.** Representative images of 14p cell line karyotype, in uninduced and 72 h DOX treated samples. The karyotype analysis of the CP3-TO cell line was performed at PD 95.69 and 106.22 for long term unexposed and long term 72 h DOX cell cultures, respectively. The karyotype analysis of the CP5-TO cell line was performed at PD 94.08 and 97.12 for long term unexposed and long term 72 h DOX cell cultures, respectively. The karyotype analysis of the 14p-TO cell line was performed at PD 91.16 and 95.68 for long term unexposed and long term 72 h DOX cell cultures, respectively.

Telomere protection-deprotection cycles and CIN

With the aim of inducing telomere-dependent CIN, we exposed the CP3-TO, CP4-TO, CP5-TO and 14p-TO cell lines to DOX cycles and washout where cells were allowed to recover for the following 6 days. To decide the extension of the protection-deprotection cycles in HMEC-TO, we used of the results previously obtained in the MCF-10A expressing the TRF2$^{\Delta B\Delta M}$ cell line. Different DOX exposure times were tested in MCF-10A cells (24 h, 48 h, 72 h and 96 h followed by a washout) (data not shown). Whereas end-to-end fusions, anaphase bridges and a slight tetraploid increase were observed when cells were exposed to 96 h of DOX (Bernal *et al*, 2018a), this exposure time was deleterious for the proliferation of unstable cell (Bernal *et al*, 2018a). In contrast, 24 h of DOX exposure was demonstrated to be sufficient for telomere deprotection (Bernal *et al*, 2018a) and thus it could be permissive for cell proliferation. In fact, the analysis of the cell cycle profile of HMEC-TO cells suffering increased cycles of 24 h DOX demonstrated a polyploid population that increased over time (FIGURE 25).

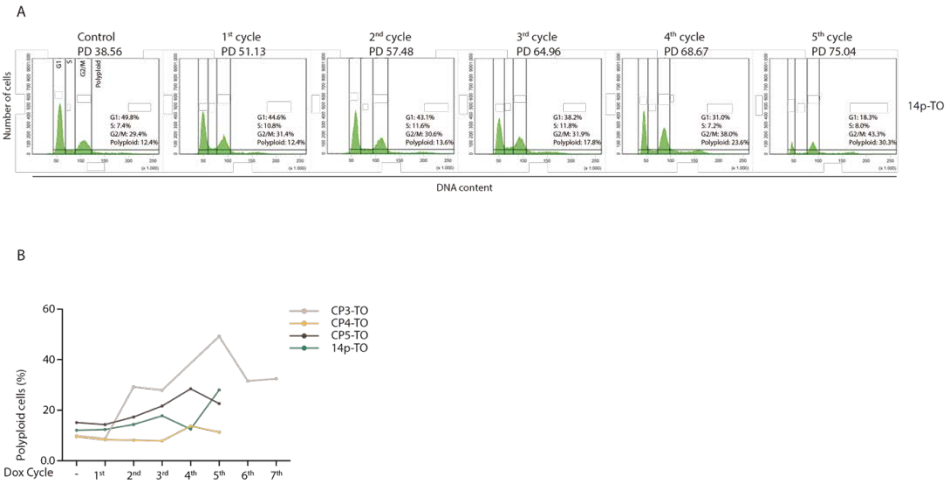

FIGURE 25. Polyploid population increased after TRF2$^{\Delta B\Delta M}$ expression cycles. **A.** Cell cycle profiles of 14p-TO cell line during the progression of protection-deprotection cycles. Note that in the last cell cycle profile only 3774 cells were analysed. **B.** Graph displaying polyploid evolution during the progression of protection-deprotection cycles.

After DOX-cycles, the CP3-TO cell line showed two polyploid subpopulations one containing 85 chromosomes (4N) (55%) and another with 160 chromosomes (8N) (10%), (SUPPLEMENTARY TABLE 2). Two subpopulations were also observed in CP5-TO but in this case, there was a near diploid population of 45 chromosomes (5%) and a tetraploid population of about 80 chromosomes (50%). Finally, the 14p-TO cell line had a modal karyotype of 86 chromosomes (37.5%). As mentioned earlier, only 24 metaphases has been analysed and the exact modal karyotype could be misinterpreted. In fact, flow cytometry cell cycle analysis exhibited a mixture of diploid and G1-tetraploid cells. Overall, these data suggested that the telomere protection and deprotection cycles were able to engender polyploid cells that persisted over time. And this fits well with some reports describing that tetraploid cells can originate through telomere dysfunction (Davoli & de Lange, 2012; Pampalona *et al*, 2012). To assure the implication of telomere dysfunction in the origin of polyploid HMEC-TO, we analysed the karyotype of unexposed cell lines at an equivalent PD. This analysis demonstrated that the unexposed CP3-TO and CP5-TO cell lines included a mixture of a near-diploid/diploid population (45 (69.57%) and 46 (34.48%) chromosomes, for CP3-TO and CP5-TO respectively) and a near tetraploid one (88 (13.04%) and 79 (37.5%) chromosomes, for CP3-TO and CP5-TO, respectively), whereas the 14p-TO cell line exhibited a single near tetraploid subpopulation of 88 chromosomes (54.17%). These results suggested that telomere dysfunction is not the cause of polyploidisation events in HMEC-TO exposed to DOX cycles. In addition, the karyotype analysis of the induced cell lines revealed, when compared with TRF2$^{\Delta B\Delta M}$ uninduced samples at a similar PDs, that chromosome fusions increased (Fisher's exact test p-value 0.0102 for the 14p-TO cell line vs 5th DOX cycle) (FIGURE 26A), and the number of fusions per cell (Mann-Whitney test p-value 0.0049 for the 14p-TO cell line vs 5th DOX cycle) (FIGURE 26B) in 14p-TO cell line. Despite the increase in chromosome fusions in the 14p-TO, only one of them was observed to display telomeric signals at the fusion point (FIGURE 26C). In addition, roughly all chromosomes contained a bright and intact telomeric signal at each end. These results suggest that telomeric fusions or chromosomal reorganisations derived from BFB cycles are rare after telomeric protection-deprotection cycles.

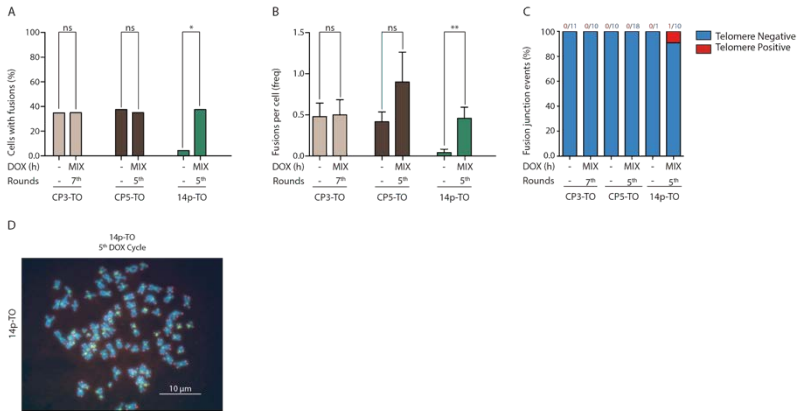

FIGURE 26. Telomere dysfunction phenotype after long term culture unexposed and exposed to successive DOX cycles. **A.** Chromosome fusions increased in the 14p-TO cell line in the 5th DOX cycle when compared to the unexposed counterpart. **B.** The number of fusions per cell increased in the 14p-TO cell line. Data were presented as mean + SEM. **C.** One telomeric fusion was observed in the 14p-TO cell line in the 5th DOX cycle. **D.** Representative image of the 14p cell line karyotype exposed to successive DOX cycles The karyotype analysis of the CP3-TO cell line was performed at PD 95.69 and 95.47 for the long term unexposed and 7th DOX cycle, respectively. The karyotype analysis of the CP5-TO cell line was performed at PD 94.08 and 98.83 for the long term unexposed and 5th DOX cycle, respectively. The karyotype analysis of the 14p-TO cell line was performed at PD 91.16 and 75.12 for the long term unexposed and 5th DOX cycle, respectively.

Given that TRF2$^{\Delta B\Delta M}$ barely produces end-to-end chromosome fusions, the increased polyploid population should be caused by the SV40LT immortalisation process. SV40LT transduction has been reported to induce genetic variability by increasing both numerical and structural chromosome aberrations (Ray *et al*, 1992; Cotsiki *et al*, 2004; Hein *et al*, 2009). As SV40LT inactivates p53 and pRb allowing a lifespan extension, the presence of karyotype abnormalities could be perpetuated and enhanced over population doublings (Shay & Wright, 1989). On the whole, the results in induced HMEC-TO are in line with the detrimental effect of TRF2$^{\Delta B\Delta M}$ overexpression, which prevents cell cycle progression of cells when a deep telomeric insult has been impinged (Bernal *et al*, 2018a).

Transformation assay of telomere-compromised cell lines in 3D cultures and in mice

The tumorigenic potential of unstable cells due to shelterin dysfunction has been proved in the mouse *in vitro* (Davoli & de Lange, 2012) and *in vivo* (Davoli & de Lange, 2012; Begus-Nahrmann *et al*, 2012) conditions. So, we were interested in knowing whether human cells suffering telomere dysfunction were also prone to transformation.

Firstly, we tested the behaviour of unexposed cells and TRF2$^{\Delta B\Delta M}$-induced cells in three dimensional cultures. Unlike monolayer, 3D cultures allow cells to adopt a conformation morphology that resemble the mammary gland, as the cells adopt the form of apicobasal polarised acini-like spheroids (Debnath & Brugge, 2005) and allow the expression of some genes that would be silenced in 2D. The 3D culture experiments were performed in collaboration with the Tumour Heterogeneity group from ECSCRI led by Dr. Matthew J. Smalley. A combined diploid and tetraploid population (Table 1) was cultured on top of the extracellular Matrigel, an extracellular matrix derived from Engelbreth-Holm-Swarm mouse sarcoma cells, and on top of the collagen:Matrigel (1:1) mixture. Both matrices allow the formation of acinar

structures that resemble bilayer acini from the mammary gland, consisting of an external myoepithelial cellular layer and an internal luminal cellular layer surrounding a hollow lumen (Debnath *et al*, 2003; Debnath & Brugge, 2005). It has been suggested that the lack of polarisation or the aberrant growth and invasion of the lumen mimics the biological events associated with epithelial cancers (Debnath & Brugge, 2005).

Table 1. Tetraploid percentage in cell lines at the beginning of 3D culture experiments

		CP3-TO	CP4-TO	CP5-TO	14p-TO
Unexposed cells	PD	72.64	60.53	77.14	63.34
	Polyploid cells (%)	20.3	8.3	0.8	1.1
TRF2$^{\Delta B\Delta M}$ -induced cells	PD	89.80	77.31	88.36	80.92
	DOX cycle	5th	4th	4th	5th
	Polyploid cells (%)	49.2	10.7	26.9	24.5

Acinar size, bud and branch formation and acini polarity

The difference between Matrigel and collagen:Matrigel extracellular matrices varies in terms of their in their stiffness. While Matrigel exerts more resistance to acini growth and tubular or branches formation due to its greater stiffness, the collagen:Matrigel mixture allows a more relaxed matrix that is permissive with acini growth and invasive structures. So it is not surprising that the acini formed in Matrigel were smaller than those formed in the collagen:Matrigel matrix (FIGURE 27) (SUPPLEMENTARY TABLE 3-4) (SUPPLEMENTARY FIGURE 1); or that the collagen:Matrigel *acini* were more prone to bud and branch formation (FIGURE 28) (SUPPLEMENTARY TABLE 5-6).

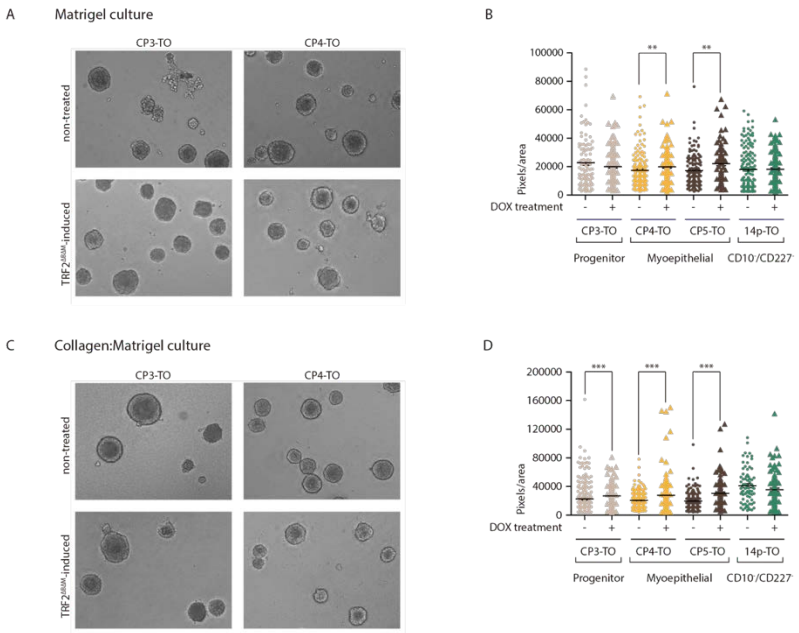

FIGURE 27. Acini size analysis. **A.** Representative images of formed *acini* on top of Matrigel in non-exposed cells and TRF2$^{\Delta B\Delta M}$-induced cells of CP3 and CP4 cell lines. **B.** TRF2$^{\Delta B\Delta M}$-induced acini of CP4 and CP5. Solid lines represent mean ± SEM.

After the repeated cycles of telomere protection-deprotection cycles only CP4-TO and CP5-TO acini, with higher levels of myoepithelial markers were larger than the non-treated controls in both matrices used (FIGURE 27) (SUPPLEMENTARY TABLE 3) (SUPPLEMENTARY FIGURE 1). Moreover, in the collagen:Matrigel, also the treated CP3-TO showed an increase in acinar growth (

SUPPLEMENTARY TABLE 4). In contrast, the ability to form buds and branches (BB) was reduced in the cell lines with myoepithelial markers (CP4-TO and CP5-TO), but enriched in those containing progenitor cells and in a double negative population of CD10 and CD227 (CP3-TO and 14p-TO cell lines, respectively) (FIGURE 28B). Nonetheless, the incidence of BB was reduced in CP3-TO and 14p-TO cells that suffered telomere protection-deprotection cycles compared to their control counterparts (SUPPLEMENTARY TABLE 6).

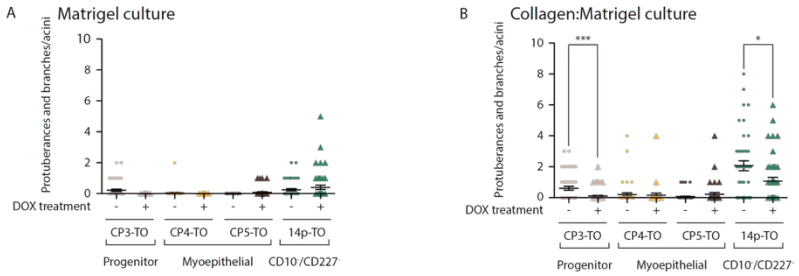

FIGURE 28. Bud and branch structures were mainly observed in unexposed CP3-TO and 14p-TO cell lines when cultured in collagen:Matrigel. **A.** Presence of buds and branches in Matrigel cultured acini. **B.** Presence of buds and branches in collagen:Matrigel cultured acini. Solid lines represent mean ± SEM.

Functional differentiation in the mammary *acinus* requires an architectural reorganisation to conform a polarised structure that could enable milk secretion (Mroue & Bissell, 2013). The lack of *acini* polarity is a hallmark of aberrant acini formation and could be related to a transformation predisposition (Debnath *et al*, 2003). Immunodetection of integrin α-6 was performed to assess *acini* polarity. Polarity analysis indicated that CP4-TO and CP5-TO, which were mainly myoepithelial cells, contained a high percentage of polarised *acini* and no differences were observed between unexposed and exposed DOX *acini* (FIGURE 29). Strikingly, CP3-TO and 14p-TO behave in the opposite way. In the case of the CP3-TO cell line, telomere protection-deprotection cycles may have a detrimental effect on the *acini* formation that lacks integrin α-6 expression in the basal membrane (FIGURE 29) (SUPPLEMENTARY TABLE 7). In contrast, telomere protection-deprotection cycles in the 14p-TO cell line may enhance the acini formation that lacks integrin α-6 (FIGURE 29) (SUPPLEMENTARY TABLE 7). The implication of TRF2 during 14p and CP3 acini polarisation remains elusive.

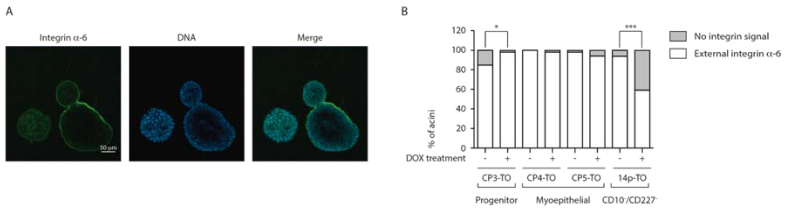

FIGURE 29. Polarity acini analysis. **A.** Representative images of polarised acinus (right) and unpolarised acinus (left). **B.** Percentage of polarised and unpolarised acini in unexposed and DOX exposed acini.

Four types of *acini* have been described depending on their cell organisation, the robustness of cell-cell adhesion and the *acini* shape (Kenny *et al*, 2007). Regarding this acini classification, CP4-TO and CP5-TO were considered mass class type acini, as they were characterised by round colony outlines, but the cells in the *acini* were disorganised and the *acini* are not fully empty at the fourth day. The CP3-TO cell line mostly adopted a grape-like class acini which form colonies with poor cell-cell contacts, although mass

class acini were also found in the CP3-TO 3D culture. In contrast, it was considered that 14p-TO formed Stellate class *acini*, as it displayed a highly ramified growth rather than a globular one. These results suggests that genetic differences between donors exists that could conditionate the acini morphology and behaviour.

Apoptosis and proliferation index in acini

After the apicobasal polarisation, lumen formation takes place. Selective apoptosis is essential for a hollow lumen formation during acinar development and this became evident by day 10 in MCF-10A cells (Debnath *et al*, 2002). However, no hollow lumen was observed, due to the possibility that fixing the cells at day 10 was too early, as in MCF-10A the complete lumen formation has been observed at day 20 (Debnath *et al*, 2003). Apoptosis index was determined by the immunodetection of cleavage-CASP3, an active marker of apoptosis. Positive stained cells were mainly observed in non-treated myoepithelial cell lines (CP4-TO and CP5-TO). In contrast, apoptosis levels sharply decreased in TRF2$^{\Delta B\Delta M}$ induced acini (FIGURE 30) (SUPPLEMENTARY TABLE 8). An in-depth analysis of the location of the apoptotic cells did not reveal any clear evidence that apoptosis had taken place in the luminal area (data not shown), which is indicative of lumen formation.

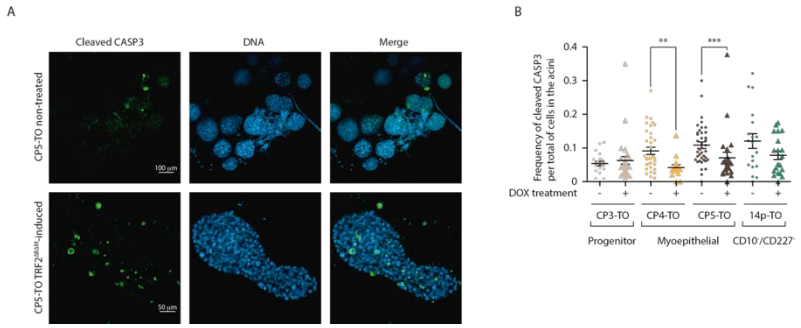

FIGURE 30. Apoptosis decrease in myoepithelial DOX exposed acini. **A.** Representative images of cleaved-CASP3 in unexposed and DOX exposed acini. **B.** Frequency of cleaved CASP3 positive cells per total of cells in the acini. Solid lines represent mean ± SEM.

Given that the analysed *acini* did not display a marked apoptosis into the lumen or even a hollow lumen, the presence of cells into the lumen could also be explained by a higher proliferation index. To address the proliferation ratio in the *acini's* lumen, the mitosis marker H3-Ser10 was detected. The proliferation index contains some inconsistencies regarding a lineage effect or TRF2$^{\Delta B\Delta M}$ expression. Statistical differences were observed in the CP3-TO and CP5-TO cell lines, in which the proliferation index in each TRF2$^{\Delta B\Delta M}$-induced *acini* were lower than the non-induced counterparts (FIGURE 31) (

SUPPLEMENTARY TABLE 9).

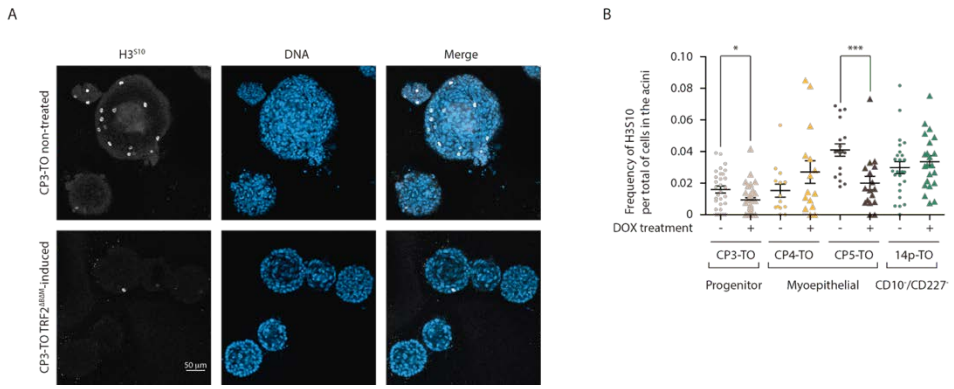

FIGURE 31. Proliferation ratio in acini. **A.** Representative images of H3-Ser10 in unexposed and DOX exposed acini. **B.** Frequency of H3-Ser10 positive cells per total of cells in the acini. Solid lines represent mean ± SEM.

Overall, the absence of a hollow lumen and a low apoptosis level in all HMEC-TO, both treated and untreated, could be explained by SV40LT overexpression. It has been reported that SV40LT expression promotes ErbB2 overexpression, which is necessary for cell growth (Li *et al*, 2008), and prevents the formation of a hollow lumen (Muthuswamy *et al*, 2001). In addition, it might be possible that experiment time was not adjusted to see the complete lumen formation. Regarding proliferation rate in *acini*, the results were inconclusive, as the different cell types followed different trends with no obvious rule, thus suggesting that other factors could be influence the proliferation index in the *acini*.

On the whole, the 3D results did not suggest that telomere dysfunction could influence *acini* growth and development. On the contrary, the differences observed could rather be related to the lineage markers and probably to their genetic background.

Cell sorting and the effects of polyploid population in mice xenografts

In addition to testing the tumorigenic potential of HMEC-TO in 3D, the capacity of the cells to form tumours was checked in immunocompromised mice. Moreover, given that according to different studies, the capacity of malignant transformation of tetraploid cells is higher than that of diploids, we sorted DOX-exposed HMEC-TO according to their ploidy. The cell sorting was only performed in the cell lines with a high number of polyploid cells, which were CP3-TO, CP5-TO and 14p-TO (FIGURE 32A). After sorting, the different fractions were expanded and a minimum of 2.2 millions of cells per condition were grafted in nude female mice. More specifically, non-induced cells (Group 1-MIX) containing a mixture of diploid and polyploid fractions, a diploid population of DOX treated cells (Group 2-2N) and a polyploid population of DOX treated cells (Group 3-4N) were ectopically grafted in the mammary gland of a minimum of three Balb/c strain females. These animal experiments were performed by Growth Factor Research Group in the Animal Facilities of the Vall d'Hebron Institute of Oncology (VHIO) according to the protocols approved by the VHIO Ethics Committee on Animal Research and Generalitat de Catalunya.

The mice were kept in the Animal Facility for a minimum of 300 days. During this time, some mice deaths were observed. However, these were related to mice sickness and no evidence of tumour growth was found after necropsy. Moreover, mice life expectancy did not displayed any relevant changes between the three mice groups in any of the three cell lines (FIGURE 32B). This suggested that non-induced cells, diploid-DOX treated cells and tetraploid-DOX treated cells did not impair mice survival due to a tumour formation or an tumour aggressive phenotype. During the time of the experiment, mice weight was monitored to detect a drop in body weight that could be indicative of tumour development. No mice from any group showed a dramatic fall in body weight (FIGURE 32C), thus suggesting normal development during mice growth. In fact, no evidence of tumour growth was found in any group of the CP3-TO, CP5-TO and 14p-TO xenografted mice groups (FIGURE 32D). Overall, these results suggest that cells that had been flowed by telomere protection-deprotection cycles were unable to initiate a carcinogenesis process into the mice mammary gland. Similarly, the polyploid cells originating from SV40LT expression had no tumorigenic potential. Regarding the tumorigenic potential of the polyploid cells originating due to SV40LT expression, some discrepancies exits. Several authors described a mild tumorigenic potential of SV40LT immortalised human cells, as small subcutaneous tumours were found, although those tumours could not metastasise (Toouli *et al*, 2002). In contrast, other authors rule out the tumorigenic potential of SV40LT-hTERT immortalised human cells grafted in mice (Elenbaas *et al*, 2001). Our results are in line with these last authors, thus suggesting that SV40LT-derived human cells have no tumorigenic potential.

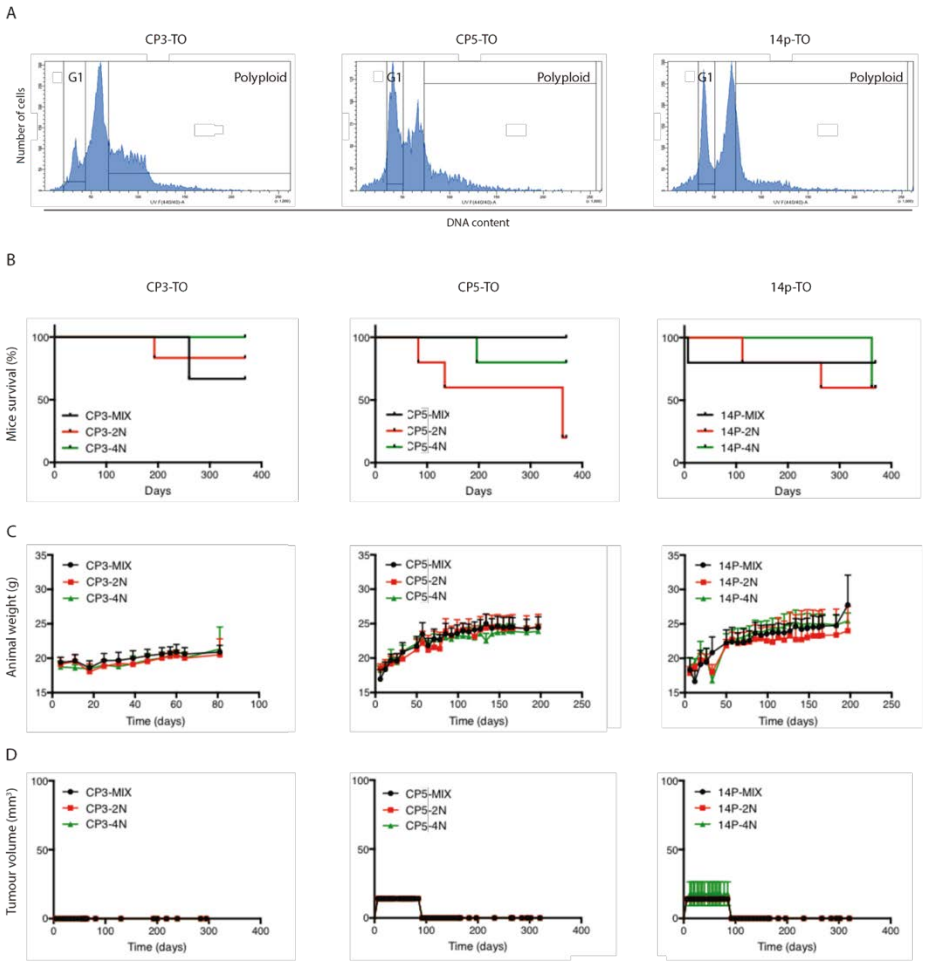

FIGURE 32. SV40LT-derived polyploid human cells do not exhibit a tumorigenic potential in xenografted mice. **A.** Diploid and polyploid population of CP3-TO, CP5-TO and 14p-TO were selected by FACS. **B.** Kaplan-Meier survival curves of long term unexposed cells, 2N DOX-exposed cells and 4N DOX-exposed cells showed no differences in any of the analysed cell lines. **C.** Animal weight in all three groups was indistinguishabled for a minimum of 2 months in all cell lines. **D.** Tumour volume was measured to evaluate a putative tumour growth. No group in any cell line showed a sharp growth increase that could give rise to the suspicion of tumour development.

Conclusions

Overall, these results obtained with HMEC-TO cells confirmed that telomere dysfunction due to the TRF2$^{\Delta B\Delta M}$ expression does not result in telomere-dependent karyotype reorganisations in human cells. Human cells unexposed and exposed to successive DOX cycles conform disorganised acini that resemble the acini growth of some tumour cell lines. However, the acini morphologies have no relation with the previous fluctuations in telomere protection. Instead, they might be biased depending on cell lineage and their genetic background, as some non-tumour cells could adopt non-organised morphologies. Human hTERT and SV40LT immortalised cells unexposed and 2N- and 4N-exposed to successive DOX cycles have no tumorigenic potential in nude mice. Our results support the model in which the simultaneous deprotection of many telomeres could exert an excessive DNA damage that prevents the progression of unstable cells, thus maintaining genomic integrity.

Methodology

Isolation of human mammary epithelial cells and culture conditions

Mammary gland tissue was obtained by surgical procedures and placed in sterile containers containing TMM medium supplemented with 10% foetal bovine serum (FBS). Prior to surgery, all patients signed a written consent form allowing their tissue to be used for biological research. All work with human tissue was reviewed and approved by the Human Subjects Protection Committee of Universitat Autònoma de Barcelona.

For the tissue digestion and organoid isolation of the CP3, CP4 and CP5 cell lines, the LaBarge and collaborators manual was followed (Table 2-4) (LaBarge *et al*, 2013). In contrast, for the 14p cell line, the organoids were obtained according to the conditions described by Ince and colleagues (Ince *et al*, 2007). After the digestion process, the digested material was seeded in a Petri dish coated with collagen type I from rat tail (Gibco), and the cells were cultured with M87AX (Garbe *et al*, 2009) and supplemented with the ROCK1 inhibitor Y27632 (Abcam) (10 μM) for the first three months. Once attached, the cells from the organoids started to grow and the HMECs were harvested and cultured separately in collagen coated flasks and fed with M87AX plus Y27632.

Table 2. Tissue Mix Medium (TMM) composition

Component	Concentration
DMEM:F12	
Penicillin Streptomycin	100 U/ml 100 mg/ml
Polymyxin B	50 U/ml
Amphotericin B	5 μg/ml
FBS	5%

Table 3. Tissue Digestion Medium (TDM) composition

Component	Concentration
DMEM:F12	
Penicillin Streptomycin	100 U/ml 100 mg/ml
Polymyxin B	50 U/ml
Amphotericin B	5 μg/ml
Hyaluronidase Collagenase A	100 U/ml 200 U/ml
Insulin	10 μg/ml
FBS	10%

Table 4. M87AX medium composition

Component	Concentration
(DMEM:F12):MCDB170	1:1
Albumax I	10%
Apotransferrin	2.5 μg/ml
BPE	35 μg/ml
Cholera Toxin	0.5 ng/ml
FBS	0.25%
hEGF	5 ng/ml
Hydrocortisone	0.3 μg/ml
Insulin	7.5 μg/ml
Isoproterenol	$5{\cdot}10^{-6}$ M
Oxytocin	0.1 nM

Fibroblast cells also were present in organoid culture. For fibroblast removal, differential trypsinisation was performed, as the fibroblasts easily become detached.

All the cultured cells were maintained at 37°C and 5% of CO_2. Accumulated cellular growth was determined by the formula: $PD=PD_{initial}+\log_2 (N_{final}/N_{initial})$, where $N_{initial}$ is the number of viable cells plated, and N_{final} is the number of viable cells harvested.

Inducible expression of TRF2$^{\Delta B\Delta M}$

TRF2$^{\Delta B\Delta M}$ expression was induced by adding doxycycline (DOX) (Sigma) (1 μg/ml) to the culture medium. TRF2$^{\Delta B\Delta M}$ expression was sustained for 24 h or 72 h, and DOX was replaced every 48 h. For the TRF2$^{\Delta B\Delta M}$ expression block, the cell medium were removed, the culture was washed twice with PBS and fresh medium was added. The cells were allowed to recover for 6 days after DOX removal.

Lentiviral particles: production and immortalisation

A tetracycline inducible lentiviral vector was generated as described in (Bernal *et al*, 2018a). In addition, lentiviral particles were generated as described in (Bernal *et al*, 2018a).

For cellular immortalisation, the HMECs were transduced at passage 1 with lentiviral particles coding for the hTERT gene product under the promoter from CMV (Addgene: 12245). After cells recovery (between PD 3 and PD 7), the HMECs were transduced with lentiviral particles coding for SV40LT under chicken ß-actin promoter, and mCherry fluorescence protein, which is under the control of an IRES, (Addgene 58993). The transduction of TRF2$^{\Delta B\Delta M}$ and rtTA3 lentiviral particles was performed at around PDs 10-18 and PDs 18-31, respectively. The TRF2$^{\Delta B\Delta M}$ gene was under the control of the CMV inducible promoter (a kindly gift from Dr Rudolph) and the rtTA3 gene was under the control of the UbC promoter (a kindly gift from Dr Fraser).

The cells transduced with TRF2$^{\Delta B\Delta M}$ and rtTA3 were selected by G418 (300 μg/ml) and hygromycin (300 μg/ml) antibiotics, respectively.

Protein expression: western blot

Proteins were extracted with 2% SDS, 67mM Tris HCl (pH 6.8) containing protease and phosphatase inhibitors. Protein extracts were sonicated twice at 25% amplitude for 15 s, centrifuged at 10,000 g for 10 min and boiled at 95°C for 10 min. The proteins were quantified using the BCA method (Life Technologies) and absorbance was measured at 540 nm with a Victor3 spectrophotometer (PerkinElmer). A total of 30 μg were separated using 3-8% Tris acetate or 10% Bis-Tris gels at 35 mAmp and transferred onto nitrocellulose or PVDF membranes at 30 V (Life Technologies). The membranes were blocked with 5% BSA or non-fat milk. The primary antibodies were: rabbit anti-hTERT (Rockland, 600-401-252S), mouse anti-SV40 st+LT (Santa Cruz Biotechnology, sc-148), mouse anti-TRF2 (Novus Biologicals, 4A794.15) mouse anti-α-Tubulin (Sigma, B-5-1-2). The secondary antibodies used were: anti-mouse or anti-rabbit horseradish peroxidase (HRP) conjugated antibodies. The primary antibodies were incubated overnight at 4°C, while the secondary antibodies were incubated at room temperature 1 h. Chemiluminiscent detection was performed using HRP solution and luminol (Millipore). Western blot images were acquired with Chemidoc and were processed with Quantity One (BioRad).

Flow cytometry and live cell sorting

Cell lineage analysis: The cells were trypsinised and resuspended in PBS-2% FBS. Between $5{\cdot}10^5$ and 10^6 cells were incubated with Anti-CD10 (Clone HI10A, Biolegend), conjugated with APC, and/or Anti-CD227 (Clone 16A, Biolegend), conjugated with PE, for 25 min at room temperature and left in dark conditions. Incubations with the isotype controls (Clone MOPC-21, Biolegend) were performed simultaneously. The samples were analysed using a FACs Canto flow cytometer (Beckton Dickinson), and excited with 488 nm for forward scatter and side scatter. For APC, excitation was done with 635 nm laser and measured on an APC detector (620/20 nm Band pass filter). For PE, excitation was done with 488 nm laser and measured on an FITC detector (530/30 nm Band pass filter). Single cells were gated first by forward scatter (FSC 488/10 nm) and side scatter (SSC 488/10 nm). CD10 and CD227 positive populations were gated in relation to their respective isotype controls. The data were analysed with BD FACSDiva software v7.0.

SV40LT detection: SV40LT protein detection was performed as described in (Bernal *et al*, 2018a).

Cell cycle: Cell cycle analysis was performed as described in (Bernal *et al*, 2018a).

FACS sorting 2N-4N: The cells were trypsinised and a total of $3{\cdot}10^6$ cells were incubated with Hoescht (5 μg/ml) for 30 min in dark conditions at 37°C. Sorting of diploid and polyploid cell populations was carried out using a FACSAria I SORP cell sorter (Beckton Dickinson). Excitation of the sample was done using a blue (488 nm) laser for FSC, a green-orange laser (561 nm) for the SSC signal, and a UV laser (350 nm) for Hoechst 33342 excitation, which was measured on a 440/40 nm detector. The cells were gated first by forward scatter and side scatter parameters and doublets were discriminated using their increased FSC-width signal. Single cells were plotted on a histogram to identify and sort G0 and polyploid cells.

2D Cell imaging

Metaphase spread, telomere and centromere detection and karyotype analysis:

Exponentially growing cell lines, control and non-induced cell lines were exposed to colcemid (Gibco) (0.2 μg/ml) for 1 h. Afterwards, the cells were trypsinised, swollen in 0.075 M KCl and fixed in methanol:acetic

acid (3:1). The cell suspension was dropped onto clean slides and stored at -20°C until use. Pepsin treatment was performed for cytoplasm removal. 10 mM of HCl solution were heated at 37°C and pepsin (Sigma) (50 mg/ml) was added and heated for 10 min. The slides were incubated in the HCl-pepsin solution at 37°C, for at least 3 min. The aggressiveness of the pepsin treatment depended on the cytoplasm present and the treatment time ranged from 3 min to 10 min. The slides were rinsed with PBS and fixed with 4% paraformaldehyde. Subsequently, telomere and centrosome PNA-FISH was performed as described in (Bernal *et al*, 2018a).

The modal karyotype was calculated over a minimum of 20 metaphases. The metaphase spreads were examined under an Olympus BX61 epifluorescence microscope. The fluorochromes were viewed through simple filters and the images were captured and analysed using Cytovision software (Applied Imaging) and/or ImageJ software (Version 2.0.0-rc-67/1.52d).

Anaphase bridges: Non-treated and 72 h DOX treated cells were cultured on coverslips. The coverslips were rinsed with PBS, fixed with 4% of paraformaldehyde at 37°C, and permeabilised with 1% Triton X-100 at room temperature. Finally, the cells were counterstained with DAPI. The cells were examined under an Olympus BX60 epifluorescence microscope. Two independent treatments were applied and a minimum of 250 of anaphase cells were recorded. The data were included in a contingency table and statistical differences were tested using Fisher's exact test, in which p-values lower than 0.05 were considered significant.

3D CULTURES

Acini growth: 5000 cells were seeded in an 8-wells chamber slide on top of a Matrigel (lot number: 6004754, Corning) surface or Matrigel:collagen bovine type I (Corning) (1:1) surface. The assay medium for acini growth was composed of M87AX medium supplemented with 2.5% of Matrigel or the Collagen:Matrigel mixture and was replaced every two days.

Cell growth analysis and 3D immunofluorescence: At day ten, acini growth was monitored with an inverted microscope (Leica) and the *acini* size was analysed with Extended-depth of field plugin from ImageJ. Afterwards, the *acini* were rinsed with PBS and fixed with 4% of formalin for 30 min at room temperature. Formalin was removed, and acini were triple-rinsed with PBS:Glycine for 10 min. Permeabilisation step was performed with 0.5% of Triton X-100 for 5 min with gentle agitation, and three washes were performed with IF-wash solution (PBS; 0,5 mg/ml sodium azide; 1 mg/ml BSA; 0,2% Triton X-100; 0,05% Tween 20, pH: 7.4) for 10 min with gentle agitation. The blocking step was performed with IF-wash solution supplemented with 10% goat serum overnight at room temperature. The primary antibodies were incubated 2 h at room temperature with gentle agitation (TABLE 5). The *acini* were triple-rinsed with IF-wash solution for 20 min before the secondary antibodies, which were incubated for 1 h. One 20 min wash with IF-wash solution was followed by a DAPI counterstaining (0,5 ng/ml) for 5 min with gentle agitation. Then two washes were performed after that, each lasting 5 and 20 min.

Table 5. Antibodies used for immunofluorescence

Primary antibodies	Host	Clone; Source
Anti-Integrin α-6	Rat	GoH3; BD
Anti-Cleaved Casp3	Rabbit	Polyclonal 9661; Cell Signaling
Anti-H3-Ser10	Rabbit	Polyclonal 9701; Cell Signaling

Secondary antibodies	Conjugated
Anti-Rat	Alexa Fluor A488
Anti-Rabbit	Alexa Fluor 647
Anti-Rabbit	Alexa Fluor A488

3D cell imaging: Acini immunofluorescence was examined under an inverted confocal microscope (Zeiss and Leica) and captured in Z-stack. The cells from the acini and positive stain were evaluated manually with ImageJ.

Mice xenografts

Mice experiments were performed by Growth Factors group from Vall d'Hebron Institute of Oncology. Mice care and procedures were conducted according to the protocols approved by the Ethics Committee on Animal Research of Vall d'Hebron Institute of Oncology and by the Departament d'Agricultura, Ramaderia, Pesca i Alimentació of Generalitat de Catalunya.

Three groups of cells from CP3, CP5 and 14p were prepared for the mice xenograft model. More specifically, group 1 included non-DOX treated cells, group 2 included DOX-treated and sorted diploid cells and lastly group 3 included DOX-treated and sorted polyploid cells. $15{\cdot}10^6$ cells were resuspended in a PBS:Matrigel solution (1:1). For each group and cell line, the cellular solution ($5{\cdot}10^6$ cells/100 μl) was injected into the mammary gland of 5 mice Balb/c nude females (Table 6). Groups 1 and 2 in the CP3 cell line consisted of 6 mice and for group 3 consisted of 4 mice. Mice care was provided by the VHIO Animal Facility until the mice were sacrificed at day 369. Tumour volume and animal weight were monitored during the time of the experiment. Tumour volume was given by the equation: $\frac{Length \times Width^2}{\pi/6}$

Table 6. Number of cells injected in mice and their population doubling

	CP3-TO	CP5-TO	14p-TO
Group 1: Non-treated cells (PD)	102.03	96.86	92.48
Injected cells per mouse	$3{\cdot}10^6$	$3{\cdot}10^6$	$2.2{\cdot}10^6$
Group 2: 2N DOX treated cells (PD)	99.34	106.20	93.99
Injected cells per mouse	$3{\cdot}10^6$	$3{\cdot}10^6$	$3{\cdot}10^6$
Group 3: 4N DOX treated cells (PD)	98.17	105.60	93.72
Injected cells per mouse	$3{\cdot}10^6$	$3{\cdot}10^6$	$3{\cdot}10^6$

Statistical analysis

Data analysis was carried out with GraphPad Prism version 5 software (GraphPad Software). Normality distribution was tested with the Saphiro-Wilk normality test. The data sets were compared using Fisher's exact test and Mann-Whitney test, and are indicated in the main test. P-values less than 0.05 were considered significant.

Bibliography

Begus-Nahrmann Y, Hartmann D, Kraus J, Eshraghi P, Scheffold A, Grieb M, Rasche V, Schirmacher P, Lee HW, Kestler HA, Lechel A & Rudolph KL (2012) **Transient telomere dysfunction induces chromosomal instability and promotes carcinogenesis - Supplemental methods**. *J. Clin. Invest.* 122: 2283–2288

Bernal A, Moltó-Abad M, Domínguez D & Tusell L (2018a) **Acute telomere deprotection prevents ongoing BFB cycles and rampant instability in p16 INK4a -deficient epithelial cells**. *Oncotarget* 9: 27151–27170

Bernal A, Zafon E, Domínguez D, Bertran E & Tusell L (2018b) **Generation of Immortalised But Unstable Cells after hTERT Introduction in Telomere-Compromised and p53-Deficient vHMECs**. *Int. J. Mol. Sci.* 19: 2078

Buscemi G, Zannini L, Fontanella E, Lecis D, Lisanti S & Delia D (2009) **The shelterin protein TRF2 inhibits Chk2 activity at telomeres in the absence of DNA damage**. *Curr. Biol.* 19: 874–879

Celli GB & de Lange T (2005) **DNA processing is not required for ATM-mediated telomere damage response after TRF2 deletion.** *Nat. Cell Biol.* 7: 712–8

Cesare AJ, Hayashi MT, Crabbe L & Karlseder J (2013) **The telomere deprotection response is functionally distinct from the genomic DNA damage response**. *Mol. Cell* 51: 141–155

Chin K, de Solorzano CO, Knowles D, Jones A, Chou W, Rodriguez EG, Kuo W-L, Ljung B-M, Chew K, Myambo K, Miranda M, Krig S, Garbe J, Stampfer M, Yaswen P, Gray JW & Lockett SJ (2004) **In situ analyses of genome instability in breast cancer**. *Nat. Genet.* 36: 984–8

Cotsiki M, Lock RL, Cheng Y, Williams GL, Zhao J, Perera D, Freire R, Entwistle A, Golemis EA, Roberts TM, Jat PS & Gjoerup OV (2004) **Simian virus 40 large T antigen targets the spindle assembly checkpoint protein Bub1**. *Natl. Acad. Sci. USA* 101: 947–952

Davoli T & de Lange T (2012) **Telomere-driven tetraploidization occurs in human cells undergoing crisis and promotes transformation of mouse cells**. *Cancer Cell* 21: 765–776

Debnath J & Brugge JS (2005) **Modelling glandular epithelial cancers in three-dimensional cultures.** *Nat. Rev. Cancer* 5: 675–688

Debnath J, Mills KR, Collins NL, Reginato MJ, Muthuswamy SK & Brugge JS (2002) **The role of apoptosis in creating and maintaining luminal space within normal and oncogene-expressing mammary acini**. *Cell* 111: 29–40

Debnath J, Muthuswamy SK & Brugge JS (2003) **Morphogenesis and oncogenesis of MCF-10A mammary epithelial acini grown in three-dimensional basement membrane cultures**. *Methods* 30: 256–268

Denchi EL & de Lange T (2007) **Protection of telomeres through independent control of ATM and ATR by TRF2 and POT1.** *Nature* 448: 1068–1071

Elenbaas B, Spirio L, Koerner F, Fleming MD, Zimonjic DB, Donaher JL, Popescu NC, Hahn WC & Weinberg R a (2001) **Human breast cancer cells generated by oncogenic transformation of primary mammary epithelial cells.** *Genes Dev.* 15: 50–65

Garbe JC, Bhattacharya S, Merchant B, Bassett E, Swisshelm K, Feiler HS, Wyrobek AJ & Stampfer MR (2009) **Molecular distinctions between stasis and telomere attrition senescence barriers shown by long-term culture of normal human mammary epithelial cells**. *Cancer Res.* 69: 7557–7568

Garbe JC, Pepin F, Pelissier FA, Sputova K, Fridriksdottir AJ, Guo DE, Villadsen R, Park M, Petersen OW, Borowsky AD, Stampfer MR & LaBarge MA (2012) **Accumulation of multipotent progenitors with a basal differentiation bias during aging of human mammary epithelia**. *Cancer Res.* 72: 3687–3701

Genescà A, Pampalona J, Frías C, Domínguez D & Tusell L (2011) **Role of telomere dysfunction in genetic intratumor diversity.**

Hein J, Boichuk S, Wu J, Cheng Y, Freire R, Jat PS, Roberts TM & Gjoerup O V. (2009) **Simian Virus 40 Large T Antigen Disrupts Genome Integrity and Activates a DNA Damage Response via Bub1 Binding**. *J. Virol.* 83: 117–127

Huschtscha LI, Neumann AA, Noble JR & Reddel RR (2001) **Effects of Simian virus 40 T-antigens on normal human mammary epithelial cells reveal evidence for spontaneous alterations in addition to loss of p16INK4a expression**. *Exp. Cell Res.* 265: 125–134

Ince TA, Richardson AL, Bell GW, Saitoh M, Godar S, Karnoub AE, Iglehart JD & Weinberg RA (2007) **Transformation of different human breast epithelial cell types leads to distinct tumor phenotypes**. *Cancer Cell* 12: 160–170

Inman JL, Robertson C, Mott JD & Bissell MJ (2015) **Mammary gland development: cell fate specification, stem cells and the microenvironment**. *Development* 142: 1028–1042

Karlseder J, Broccoli D, Dai Y, Hardy S & de Lange T (1999) **p53- and ATM-dependent apoptosis induced by telomeres lacking TRF2**. *Science* 283: 1321–1325

Kenny PA, Lee GY, Myers CA, Neve RM, Semeiks JR, Spellman PT, Lorenz K, Lee EH, Barcellos-Hoff MH, Petersen OW, Gray JW & Bissell MJ (2007) **The morphologies of breast cancer cell lines in three-dimensional assays correlate with their profiles of gene expression**. *Mol. Oncol.* 1: 84–96

LaBarge MA, Garbe JC & Stampfer MR (2013) **Processing of human reduction mammoplasty and mastectomy tissues for cell culture**. *J. Vis. Exp.*: e50011

Li A, Willimsky G, Seitz S, Xu Y, Li Y, Schwarz LE, Schlag PM & Blankenstein T (2008) **SV40 large T antigen-transformed human primary normal and cancerous mammary epithelial cells are phenotypically similar but can be distinguished in 3D culture with selection medium**. *Int. J. Cancer* 123: 1516–1525

Meeker AK, Hicks JL, Gabrielson E, Strauss WM, De Marzo AM & Argani P (2004) **Telomere shortening occurs in subsets of normal breast epithelium as well as in situ and invasive carcinoma**. *Am. J. Pathol.* 164: 925–935

Mroue R & Bissell MJ (2013) **Three-dimensional cultures of mouse mammary epithelial cells**. *Methods Mol. Biol.* 945: 221–250

Muthuswamy SK, Li D, Lelievre S, Bissell MJ & Brugge JS (2001) **ErbB2, but not ErbB1, reinitiates proliferation and induces luminal repopulation in epithelial acini**. *Nat. Cell Biol.* 3: 785–792

Okamoto K, Bartocci C, Ouzounov I, Diedrich JK, Yates III JR & Denchi EL (2013) **A two-step mechanism for TRF2-mediated chromosome-end protection**. *Nature* 494: 502–505

Pampalona J, Frías C, Genescà A & Tusell L (2012) **Progressive telomere dysfunction causes cytokinesis failure and leads to the accumulation of polyploid cells.** *PLoS Genet.* 8: e1002679

Pampalona J, Soler D, Genescà A & Tusell L (2010a) **Telomere dysfunction and chromosome structure modulate the contribution of individual chromosomes in abnormal nuclear morphologies**. *Mutat. Res. - Fundam. Mol. Mech. Mutagen.* 683: 16–22

Pampalona J, Soler D, Genescà A & Tusell L (2010b) **Whole chromosome loss is promoted by telomere dysfunction in primary cells**. *Genes. Chromosomes Cancer* 49: 368–378

Ray FA, Meyne J & Kraemer PM (1992) **SV40 T antigen induced chromosomal changes reflect a process that is both clastogenic and aneuploidogenic and is ongoing throughout neoplastic progression of human fibroblasts**. *Mutat. Res.* 284: 265–73

Raynaud CM, Hernandez J, Llorca FP, Nuciforo P, Mathieu MC, Commo F, Delaloge S, Sabatier L, André F & Soria JC (2010) **DNA damage repair and telomere length in normal breast, preneoplastic lesions, and invasive cancer**. *Am. J. Clin. Oncol. Cancer Clin. Trials* 33: 341–5

Shay JW & Wright WE (1989) **Quantitation of the frequency human diploid fibroblasts of immortalization of normal by SV40 Large T-Antigen**. *Exp. Cell Res.* 184: 109–118

Smogorzewska A & de Lange T (2002) **Different telomere damage signaling pathways in human and mouse cells**. *EMBO J.* 21: 4338–4348

Soler D, Genescà A, Arnedo G, Egozcue J & Tusell L (2005) **Telomere dysfunction drives chromosomal instability in human mammary epithelial cells.** *Genes. Chromosomes Cancer* 44: 339–50

Steensel B Van, Smogorzewska A & de Lange T (1998) **TRF2 protects human telomeres from end-to-end fusions**. *Cell* 92: 401–413

Tanaka H, Abe S, Huda N, Tu L, Beam MJ, Grimes B & Gilley D (2012) **Telomere fusions in early human breast carcinoma**. *Proc. Natl. Acad. Sci. U. S. A.* 109: 14098–14103

Toouli C, Huschtscha L & Neumann A (2002) **Comparison of human mammary epithelial cells immortalized by simian virus 40 T-Antigen or by the telomerase catalytic subunit.** *Oncogene* 21: 128–139

Tusell L, Pampalona J, Soler D, Frías C & Genescà A (2010) **Different outcomes of telomere-dependent anaphase bridges.** *Biochem. Soc. Trans.* 38**:** 1698–703

Tusell L, Soler D, Agostini M, Pampalona J & Genescà A (2008) **The number of dysfunctional telomeres in a cell: One amplifies; more than one translocate**. *Cytogenet. Genome Res.* 122**:** 315–325

SUPPLEMENTARY TABLES

Supplementary table 1. Presence of anaphase bridges and statistics

	CP3-TO		CP4-TO		CP5-TO		14p-TO	
DOX treatment	-	72 h	-	72 h	-	72 h	-	72 h
Total anaphases (n)	583	623	574	561	298	460	412	416
Anaphase with chromatin bridges (n); (%)	95 16.30%	163 26.16%	199 34.67%	255 45.45%	40 13.42%	189 41.09%	78 18.93%	198 47.60%
Fisher's exact test p-value	<0.0001		0.0002		<0.0001		<0.0001	

Supplementary table 2. Karyotype analyses after persistent or transient telomere deprotection

Cell line	DOX treatment	Cells analysed (n)	Modal karyotype	Cells with fusions (n); (%)	Fusions per cell
CP3-TO	-	23	45 88	8 39.13%	0.48
CP3-TO	72 h	20	46	10 50.00%	0.75
CP3-TO	7x24 h	20	85 160	7 35.00%	0.50
CP5-TO	-	24	46 79	9 37.50%	0.42
CP5-TO	72 h	29	46 77	15 51.72%	0.79
CP5-TO	5x24 h	20	> 80 <45	7 35.00%	0.90
14p-TO	-	24	88	1 4.167%	0.04
14p-TO	72 h	25	86	9 36.00%	0.64
14p-TO	5x24 h	24	86	9 37.50%	0.46

Supplementary table 3. Acinar size in Matrigel culture and statistics

	CP3-TO		CP4-TO		CP5-TO		14p-TO	
DOX treatment	Unexposed	Exposed 5th cycle	Unexposed	Exposed 4th cycle	Unexposed	Exposed 4th cycle	Unexposed	Exposed 5th cycle
Mean (pixels/area)	22231	19464	16869	19252	16714	21551	17546	17643
SEM	1780	993.6	929.1	858.4	936.4	1429	1192	967.2
Mann-Whitney test p-value	0.9501		0.0019		0.0050		0.2181	

Supplementary table 4. Acinar size in collagen:Matrigel culture and statistics

	CP3-TO		CP4-TO		CP5-TO		14p-TO	
DOX treatment	Unexposed	Exposed 5th cycle	Unexposed	Exposed 4th cycle	Unexposed	Exposed 4th cycle	Unexposed	Exposed 5th cycle
Mean (pixels/area)	20674	25138	18821	25893	17783	28521	39343	33694
SEM	1591	1188	809.8	1746	732.0	1839	2821	2396
Mann-Whitney test p-value	<0.0001		0.0005		<0.0001		0.0884	

Supplementary table 5. Presence of buds and branches in acini cultured in Matrigel and statistics

	CP3-TO		CP4-TO		CP5-TO		14p-TO	
DOX treatment	Unexposed	Exposed 5th cycle	Unexposed	Exposed 4th cycle	Unexposed	Exposed 4th cycle	Unexposed	Exposed 5th cycle
Mean (Buds and branches per acini)	0.217	0.000	0.040	0.000	0.000	0.080	0.245	0.408
SEM	0.076	0.000	0.040	0.000	0.000	0.039	0.075	0.137
Mann-Whitney test p-value	NA		NA		NA		0.691	

Supplementary table 6. Presence of buds and branches in acini cultured in collagen:Matrigel and statistics

	CP3-TO		CP4-TO		CP5-TO		14p-TO	
DOX treatment	Unexposed	Exposed 5th cycle	Unexposed	Exposed 4th cycle	Unexposed	Exposed 4th cycle	Unexposed	Exposed 5th cycle
Mean (Buds and branches per acini)	0.608	0.116	0.204	0.161	0.070	0.225	2.070	1.071
SEM	0.126	0.044	0.105	0.132	0.034	0.116	0.320	0.242
Mann-Whitney test p-value	0.0002		0.5863		0.3362		0.0125	

Supplementary table 7. Acini polarisation and statistics

	CP3-TO		CP4-TO		CP5-TO		14p-TO	
DOX treatment	Unexposed	Exposed 5th cycle	Unexposed	Exposed 4th cycle	Unexposed	Exposed 4th cycle	Unexposed	Exposed 5th cycle
Total acini analysed (n)	46	50	50	50	50	50	49	49
External signal (n); (%)	39 88.48%	49 98.00%	50 100.00%	49 98.00%	49 98.00%	47 94.00%	46 93.88%	29 59.18%
Lack signal (n); (%)	7 15.22%	1 2.00%	0 0.00%	1 2.00%	1 2.00%	3 6.00%	3 6.12%	20 40.82%
Fisher's exact test p-value	0.0262		1.000		0.6173		<0.0001	

Supplementary table 8. Apoptosis ratio in acini and statistics

	CP3-TO		CP4-TO		CP5-TO		14p-TO	
DOX treatment	Unexposed	Exposed 5th cycle	Unexposed	Exposed 4th cycle	Unexposed	Exposed 4th cycle	Unexposed	Exposed 5th cycle
Mean (cleaved CASP3 per total cells)	0.054	0.063	0.092	0.042	0.108	0.070	0.121	0.079
SEM	0.007	0.011	0.011	0.008	0.010	0.016	0.022	0.013
Mann-Whitney test p-value	0.9554		0.0042		0.0005		0.1001	

Supplementary table 9. Proliferation ration in acini and statistics

	CP3-TO		CP4-TO		CP5-TO		14p-TO	
DOX treatment	Unexposed	Exposed 5th cycle	Unexposed	Exposed 4th cycle	Unexposed	Exposed 4th cycle	Unexposed	Exposed 5th cycle
Mean (cleaved H3-Ser10 per total cells)	0.016	0.009	0.015	0.027	0.041	0.020	0.030	0.034
SEM	0.002	0.001	0.004	0.007	0.004	0.004	0.004	0.004
Mann-Whitney test p-value	0.0207		0.3045		0.0006		0.4949	

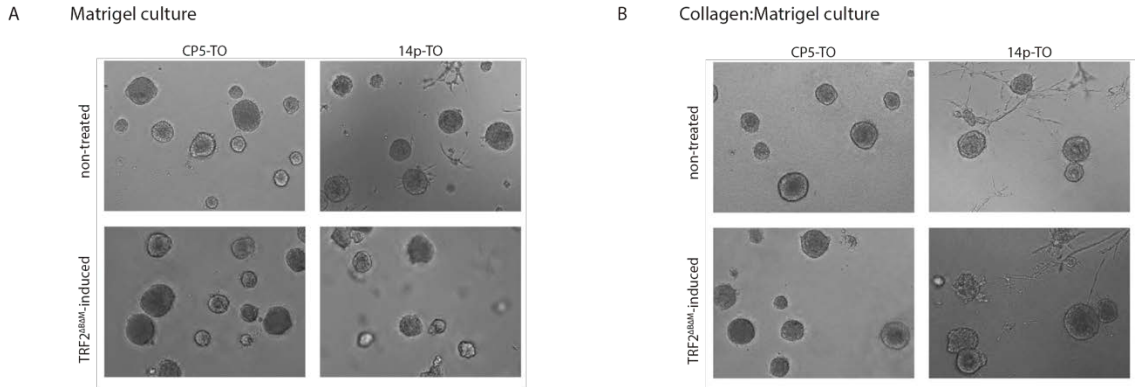

Supplementary figure 1. Acini growth of CP5-TO and 14p-TO cell lines in Matrigel (**A.**) or collagen:Matrigel (**B.**)

Appendix

International Journal of
Molecular Sciences

MDPI

Review

Telomeres: Implications for Cancer Development

Aina Bernal and Laura Tusell *

Unitat de Biologia Cel·lular, Facultat de Biociències, Universitat Autònoma de Barcelona,
08193 Cerdanyola del Vallès, Spain; aina.bernal@uab.cat
* Correspondence: laura.tusell@uab.cat; Tel.: +34-93-5811498

Received: 12 December 2017; Accepted: 16 January 2018; Published: 19 January 2018

Abstract: Telomeres facilitate the protection of natural ends of chromosomes from constitutive exposure to the DNA damage response (DDR). This is most likely achieved by a lariat structure that hides the linear telomeric DNA through protein-protein and protein-DNA interactions. The telomere shortening associated with DNA replication in the absence of a compensatory mechanism culminates in unmasked telomeres. Then, the subsequent activation of the DDR will define the fate of cells according to the functionality of cell cycle checkpoints. Dysfunctional telomeres can suppress cancer development by engaging replicative senescence or apoptotic pathways, but they can also promote tumour initiation. Studies in telomere dynamics and karyotype analysis underpin telomere crisis as a key event driving genomic instability. Significant attainment of telomerase or alternative lengthening of telomeres (ALT)-pathway to maintain telomere length may be permissive and required for clonal evolution of genomically-unstable cells during progression to malignancy. We summarise current knowledge of the role of telomeres in the maintenance of chromosomal stability and carcinogenesis.

Keywords: telomere-dysfunction; chromosome instability; cancer

1. Telomere Structure

The first evidence of telomeres, specialised nucleoprotein structures that protect the end of chromosomes, was observed in flies and maize [1,2]. After irradiation, broken chromosomes were easily fused to each other, driving genomic reorganizations, whereas the chromosome ends were protected from such events [1,2]. These experiments thus argued for specific characteristics of chromosome termini. In line with this, telomeres are composed by a guanosine rich conserved DNA that varies in length, sequence, and number of repeats between organisms. Mammalian telomeres are organised as repetitive TTAGGG sequences [3,4] that terminate in a single-stranded G-rich 3′ overhang [5,6]. In humans, the length of the double-stranded (ds) telomere track is around 9–15 kb, and the single-stranded (ss) DNA protrudes a few hundred nucleotides [7,8]. Telomeric DNA is coated by a six-protein complex known as the telosome, or shelterin (Figure 1A) [9]. This group of proteins specifically bind to telomeres throughout the cell cycle and function as a platform that recruits players from diverse pathways to the telomeres for maintenance and protection. Three shelterins bind directly to telomeric DNA through sequence recognition. TRF1 (Telomeric Repeat-binding Factor 1) and TRF2 (Telomeric Repeat-binding Factor 2) bind to ds-DNA [10–12], while POT1 (Protection Of Telomeres 1) binds to ss-DNA [13,14]. The other three proteins interact with telomeres through protein-protein interactions. TIN2 (TRF-Interacting Nuclear protein 2) links TRF1 and TRF2 proteins [15], and also interacts with TPP1 (Tripeptidyl-peptidase 1), which at the same time, binds to POT1 [16]. Therefore, TIN2 consolidates TRF1-TRF2 and POT1-TPP1 interactions at telomeric DNA [15,16]. Finally, RAP1 interacts exclusively with TRF2 [17–19] and DNA through structure recognition, but not through sequence preference [20].

Int. J. Mol. Sci. **2018**, *19*, 294

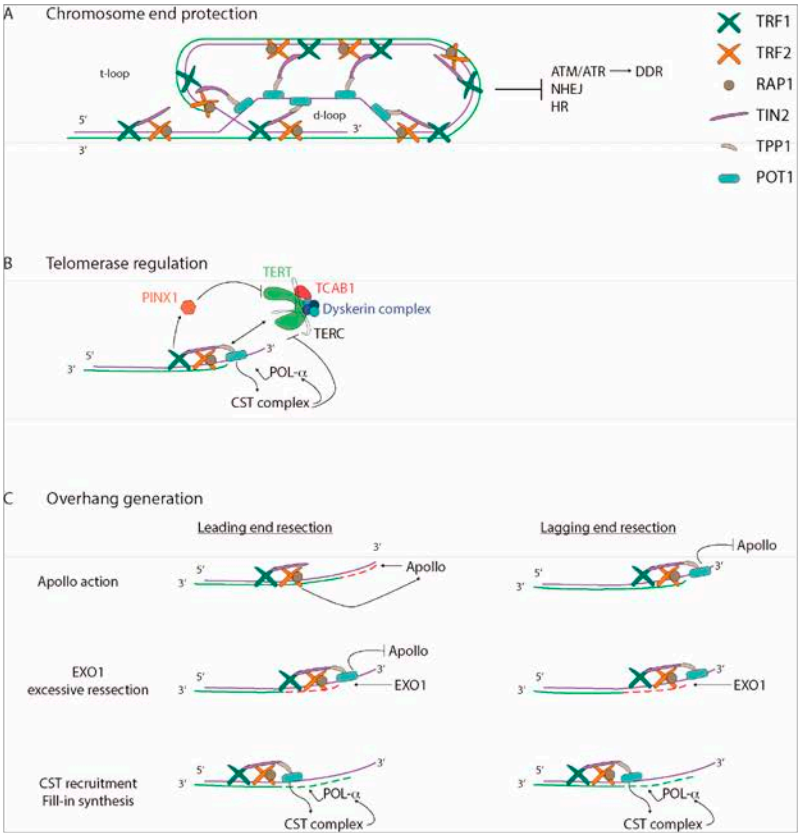

Figure 1. Telomere structure and maintenance. Human telomeres are specialised nucleoprotein structures that cap the end of chromosomes. Telomeric DNA is coated by shelterin proteins that regulate (**A**) chromosome end protection; (**B**) telomerase regulation; and (**C**) overhang generation. (**A**) Telomeres adopt a t-loop structure that prevents DNA damage response (DDR), by blocking ATM and ATR activation, and DNA repair activities via NHEJ and HR; (**B**) telomerase action is tightly regulated and only acts at telomeres during S-phase. Telomerase preferentially acts in short telomeres, maybe by indirect inhibition through TRF1 and PINX1 and/or other unknown mechanisms. TPP1 physically interacts with telomerase, and is essential for telomerase recruitment together with TIN2. It has been suggested that POT1-TPP1 is implicated in telomerase-telomere engagement. Besides that, POT1-TPP1 stimulates telomerase action until a certain threshold of telomeric repeats is reached. Once telomerase is blocked by CTC1-STN1-TEN1 (CST) and/or POT1, CST facilitates fill-in synthesis of the C-strand by polymerase-α (POL-α) recruitment; (**C**) Mammalian chromosomes terminate in a 3′ G-rich overhang that is essential for t-loop formation. DNA replication originates blunt ends in the leading strands, and non-blunt ends in the lagging strands. TRF2 recruits Apollo that resects 5′ strand from leading ends (dashed red line) to generate a 3′ overhang. Then, EXO1 excessively resects the leading and lagging strands (dashed red lines) to generate longer overhangs. In addition, finally, POT1 facilitates the 5′-strand fill-in (dashed green lines) by the recruitment of POL-α, through the CST complex.

One of the main functions of shelterins is to remodel the linear telomeric DNA to form a lariat structure that differentiates the chromosome end from a double-strand break (DSB). This arrangement is achieved through the invasion and pairing of the G-rich 3′ overhang into the preceding C-strand of the ds-telomeric tract while the telomeric G-strand is displaced. As a result, a displacement loop (d-loop) and a telomeric loop (t-loop) are formed (Figure 1A) [21]. Several studies point out the involvement of TRF2 with the generation of DNA loops in vitro [21–23], as lariat structures are not observed when TRF2 is absent [23]. The ability of TRF2 to generate t-loops lies in its capacity in modifying DNA topology by inducing positive supercoiled structures [24,25], as well as its ability to stimulate telomeric invasion [24,26] in a non-DNA-sequence specific manner [27]. Moreover, molecular dynamic simulation studies suggest that TRF2 proteins possess the ability of folding chromatin into a globular structure where DNA is compacted [28]. In agreement with this observation, super-resolution microscopy analysis has shown that human telomeres, in vivo, form hyper-compact globular chromatin structures through specific protein-protein and protein-DNA interactions between shelterin subunits and telomeric DNA that is essential for end protection. Indeed, depletion of shelterin components leads to telomeric chromatin decompaction that triggers access of DNA damage response (DDR) signals at telomere ends [29]. These data underscore a more complex picture for telomere structure organisation and end protection.

2. Maintenance of Telomere Length

Telomeres are highly dynamic structures [30] that remain in a closed-state during most cell cycle phases to protect chromosome ends. However, during S-G2 phases, telomeres become open to allow complete DNA replication and to provide a substrate for the addition of telomere repeats. Telomere elongation relies mainly on telomerase [31,32], a large ribonucleoprotein composed of an RNA template (TERC: telomerase RNA component) [33], a catalytic domain (TERT: telomerase reverse transcriptase) [34,35], the dyskerin complex composed of dyskerin-NOP10-NHP2-GAR1 [36], and TCAB1 [37]. It has been determined that telomerase assembly and maturation occurs at Cajal bodies [38,39]. However, coilin-deficient or TCAB1-deficient human cells do not present telomerase biogenesis and/or activity defects [40,41]. During cell cycle, telomerase can be located at Cajal bodies, or elsewhere in the nucleoplasm [42,43], except during S-phase when assembled telomerase is transported to telomeres [44]. Then, telomere elongation takes place shortly after duplex DNA replication is completed, and after the G-rich overhang has been processed [45]. Several mechanisms are involved in telomerase recruitment, engagement, action and disassembly.

Telomerase recruitment to the chromosome end is mainly orchestrated by the shelterin complex, and depends specifically on telomere length. Several observations note an increasing preference by telomerase for shorter telomeres [46,47]. Therefore, the classical conception of telomere length regulation is that the number of shelterin proteins inversely regulates telomerase recruitment and action by physically blocking the access of telomerase and hiding the 3′ end. However, recent studies propose a more complex regulation than a simple record of shelterin subunits. Indeed, a recent study described PINX1 as a physical interactor between TRF1 and TERT [48]. PINX1 is a telomerase inhibitor and is recruited by TRF1 at telomeres. The longer the telomere is, more TRF1 is present and more PINX1 is recruited, thus resulting in a stronger telomerase inhibition (Figure 1B). Moreover, TPP1 has been described to physically interact with telomerase, and to be essential for telomerase recruitment (Figure 1B) [49,50]. However, other studies suggest that this physical interaction is not enough for telomerase recruitment, and the cooperation of TIN2 with TPP1 is needed [51,52]. It remains unknown how the active site of telomerase captures the 3′ end, although several evidences point out POT1 into this telomere-telomerase engagement [44,53]. As a whole, further studies are needed to understand how shelterin regulates telomerase recruitment.

Once telomerase-telomere engagement has taken place, telomeric DNA aligns with TERC [33]. Then, telomerase adds de novo one telomere repeat at the 3′ DNA end [31,32,34,35] and, without dissociating from the telomere, repositions its RNA template to the new 3′ telomeric end. In human

cells undergoing homeostatic telomere length maintenance, roughly 60 nucleotides are added in a processive manner to each telomere by a single binding and extension event [54,55]. This ability to add multiple telomeric repeats, known as repeat-addition processivity (RAP) [56], obliges dissociation of the product-template duplex without product dissociation from the enzyme [57]. Due to the structural flexible nature of telomerase, the newly synthetised telomeric DNA can be looped out [56]. Then, the RNA template is fully translocated and freed for the next round of telomeric repeat synthesis [56]. Other hypothesis suggests that the DNA strand remains bound to the telomerase active site, while the RNA template slips [58]. Then, the relocation of the 3′ RNA template would allow further DNA-RNA pairing [58].

Telomere elongation is promoted by POT1-TPP1 proteins, which function as a telomerase-stimulator [59], and proceeds until telomerase is released from telomeres. It seems likely that the distance between the 5′ end from the lagging strand and the 3′ end from the leading strand may itself lead to the inhibition or termination of telomerase processivity [60]. Indeed, the presence of a G-rich overhang can encourage structural conformations that displace telomerase [60]. In this sense, it has been described that the tight binding of the CST (CTC1-STN1-TEN1) complex to the G-strand telomeric substrate of telomerase, inhibits telomerase activity through primer sequestration (Figure 1B) [61,62]. Furthermore, the CST complex also represses telomerase by physically interacting with and inhibiting the POT1-TPP1 stimulator [61,62]. Depletion of POT-TPP1 increases human CST telomere association, suggesting that the two complexes compete for telomere overhang binding [61]. Once telomerase has been blocked, the CST complex may promote fill-in synthesis of the complementary C-strand by lagging strand polymerases (POL), as human CST subunits associate with and stimulate DNA polymerase-α RNA primase complex (POL-α) (Figure 1B) [61–64].

Although the great majority of cells rely on telomerase to add de novo telomere repeats, other mechanisms exist to regulate telomere length. Alternative lengthening of telomeres (ALT) is a recombination-based mechanism that elongates telomeres in around 15% of immortalised cell lines and human cancer cells [65–67]. The ALT-pathway uses telomeric sequences from another chromosome as a copy template to lengthen telomeres [66,68]. Direct demonstrations for inter-telomeric recombination events were obtained by the progressive increase in the number of tagged telomeres with population doublings (PDs) after targeting a DNA tag into a specific telomere [69]. In addition, ALT-cells are also recognised by their telomere length heterogeneity, with some chromosomes displaying very long telomeres and a subset lacking any discernible telomere signal at their end [70], as well as by the presence of extra-chromosomal linear [71,72] or circular [73,74] telomeric repeats. Yet another way to regulate telomere length is through telomere Trimming, an additional mechanism that also seems likely to contribute to normal telomere biology. Nevertheless, in contrast to telomerase or the ALT-pathway, telomere Trimming negatively regulates telomere length through the deletion of large segments of telomeric DNA in a single resolution event [75,76]. Although the underlying mechanism most likely involves HR-mediated removal of telomere loops in the form of t-circles, telomeres are not completely deleted, as telomere Trimming does not usually initiate a DNA damage response or result in telomere signal-free ends and chromosomal fusions [75]. The observation that extra-chromosomal t-circles were found to accumulate in telomerase-positive cancer cell lines following progressive telomere lengthening by exogenous telomerase activity [75] leads to suggesting that the prominent t-circles observed in ALT cells are, in fact, the product of telomere trimming counteracting extensive recombination-mediated telomere lengthening [77].

Telomeres Shorten in Each Cell Division Cycle

As previously mentioned, telomerase is the main mechanism responsible for telomere elongation, however its expression is tightly regulated [78]. Whereas hTERC and the dyskerin complex are constitutively expressed in human tissues, hTERT is only expressed in the embryonic stem cells and in most adult stem cell compartments [33,34]. However, this is not sufficient to maintain telomere

length [33,34]. Such circumstances pose a problem for most human cells, as the absent or reduced telomerase expression, leads telomeres to shorten every cell division cycle [79].

This "end replication problem" stems from the inherent asymmetry of how linear duplex DNA is copied during each cell division [80,81]. As the replisome, a complex DNA replication machine composed of multiple polymerases, moves along the chromosome, each strand is copied by one or more polymerases dedicated to that strand. Three polymerases, POL-α, POL-ε and POL-δ, are mainly responsible for DNA synthesis in eukaryotic cells [82]. Once the ds-DNA is opened by helicases, the POL-α-RNA primase complex synthesises small complementary RNA primers and a few DNA nucleotides, which are then elongated by the other polymerases. Although it is widely accepted that the asymmetric strand replication involves two different DNA polymerases, POL-ε and POL-δ, a recent paper suggest that POL-δ is the major DNA replicase [83]. Regardless of which polymerase/s acts, both strands grow at different rates due to the anti-parallel nature of DNA and the functional needs of the polymerase. The leading strand, synthesised in 5′-3′ direction, grows in a continuous manner from the RNA primer and becomes a blunt DNA end. This is not the case for the opposite strand, the lagging strand, which grows in a discontinuous manner from multiple Okazaki fragments that are finally connected by DNA ligase1. However, at the lagging-end telomere, removal of the terminal RNA primer results in non-blunt extremities and to the loss of a very small portion of chromosomal DNA. In human cells, the average rate of telomere shortening is 50–100 bp per population doubling [84].

In addition to the replication-associated shortening, telomeres are also reduced through enzyme processing in order to generate functional 3′ overhangs [64]. In mice, the resection of the C-rich strand depends on the Apollo nuclease [85–87] and exonuclease 1 (EXO1) (Figure 1C) [64]. Given that EXO1 preferentially degrades non-blunt ds-DNA in the 5′-3′ direction [88], the leading strand is initially resected by Apollo, which is recruited to the chromosome termini by TRF2 [64,85,87]. The emergence of ss-DNA in the leading strand induces TPP1-POT1a/b recruitment to the generated overhang that, in addition to protecting the ss-DNA blocks, blocks further Apollo processing [86]. Afterwards, EXO1 generates extended overhangs at both the lagging and the leading stands during late S/G2 phases [64] until its activity is probably inhibited by RIF1 via TPP1 [89]. Once overhang resection is blocked, POT1-TPP1 recruits the CST complex to promote filling in of the C rich strand, thus reducing the length of extended 3′ overhangs (Figure 1C) [64]. As a whole, telomere shortening occurs as consequence of incomplete DNA replication of the lagging-strand and C-strand processing at both the leading-end and the lagging-end telomeres in order to generate a G-overhang.

3. Telomere Protection and Cell Proliferative Boundaries

3.1. Excessive Telomere Erosion in Normal Cells Impairs Proliferation: Shortened Telomeres Elicit DDR

In most tissues, excessive telomere shortening has been associated with a reduced cell proliferative capacity (Figure 2) [84]. The first evidence of this proliferative barrier was described by Hayflick and Moorhead in primary fibroblasts in vitro [79]. These authors observed that cultured fibroblasts possess a limited number of cell divisions, as after many cell doublings the cells lose their capacity to divide [79]. This maximum replicative potential, which occurs in different somatic cells and among different species, was called senescence [90]. The cells in this state, although metabolically active, enter a permanent cell growth arrest in G1 [79,91]. Senescence was then attributed to excessive telomere shortening, as the reactivation of telomerase compensated for telomere loss and extended cellular lifespan [92]. At present, other factors, besides telomere length, such as DNA damage, oxidative stress, modifications in chromatin, or activation of tumour suppressor proteins, are able to induce cellular senescence [91].

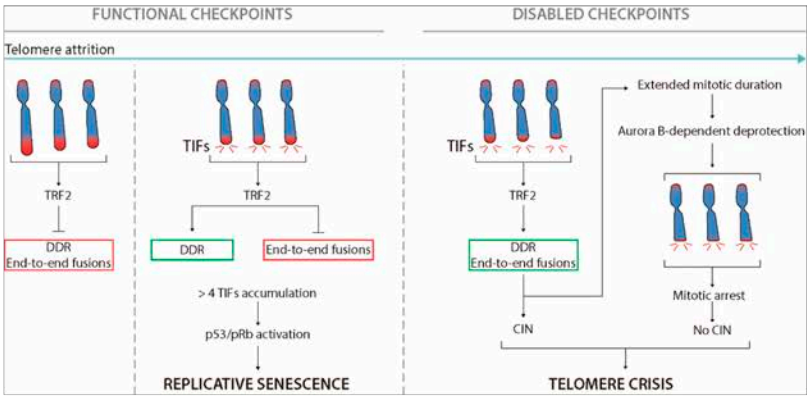

Figure 2. Telomere hypothesis of senescence and cancer. Telomere attrition occurs in cycling cells lacking telomerase activity or with reduced levels (green arrow). Long enough telomeres protect chromosome ends from DDR activation and end-to-end fusions (red box). After numerous PDs, few telomeres become too short and a local DDR signalling is activated at chromosome ends. At this stage, telomeres are not fully unprotected, as end-to-end fusions are prevented (red box) although the activation of the DDR (green box). Proliferation continues until a threshold of 4–5 TIFs directs cells to replicative arrest and senescence or apoptosis. In cells with functional checkpoints, excessive telomere shortening limits the proliferation of incipient cancer cells. Nevertheless, loss of the Rb and p53 tumour suppressors pathways allows cells to bypass cell cycle arrest in the presence of more than five telomere-induced foci (TIFs) per cell. During this lifespan extension period, further shortening leads to insufficient TRF2 retention at telomeres. These fully deprotected chromosome ends, in addition to activate the DDR, they promote the formation of end-to-end fusions (green box). It has been long speculated that the huge reorganisation of the genome associated to persistent telomere-dependent chromosomal instability (CIN) could allow the generation of pre-neoplastic cells if ultimately telomere length is stabilised. Otherwise, cells are directed to telomere crisis owing to massive genome remodelling, due to breakage-fusion-bridge (BFB) cycles, or/and to prolonged mitotic arrest and Aurora B-dependent TRF2 eviction from telomeres. Figure adapted from Arnoult and Karlseder 2015 [93].

It is currently known that replicative senescence arises when progressive reduction of telomere length ends up with t-loop collapse and dysfunctional telomeres [94]. When shelterin levels are excessively reduced, the generation of the t-loop is compromised, as there is not enough TRF2 to remodel linear telomeric DNA. Consequently, telomeres shift towards an open deprotected state that activates a local DNA damage response (DDR), a signalling pathway associated with DSBs recognition and repair. The phosphorylated form of histone H2AX protein (γH2AX), which targets DSBs, also localises at dysfunctional telomeres in conjunction with other repair proteins, such as ATM, MDC1, 53BP1, or RAD17 [95,96]. The accumulation of these repair factors at telomeres are known as telomere dysfunction foci (TIFs) (Figure 2) [95].

Kaul et al. (2012) described that human fibroblasts accumulate spontaneous TIFs during cellular lifespan [97]. Cells keep dividing until they reach 4–5 TIFs, and above this threshold persistent telomere damage enforces cells to engage replicative senescence through p53-dependent signalling [97–99]. At this point, dysfunctional telomeres can recruit DDR factors, however they remain protected as at replicative senescence end-to-end fusions are not observed [97]. This ability to activate the DDR but to prevent telomeric fusions is thought to be mediated by the retention of some TRF2 molecules at chromosome ends [100,101]. In 2009, Karlseder's Laboratory proposed that telomeres fluctuate

through different protective states that rely on the abundance of TRF2 protein at chromosome ends, rather than to telomere length itself [100]. When telomeres are long enough to accommodate sufficient TRF2 to form a functional t-loop structure they remain in a full protected state. In senescence, telomeres are not fully unprotected, but remain in an intermediate-protection state in which the absence of t-loop generation leads to DDR activation, although telomeres retain enough TRF2 to prevent end-to-end chromosome fusions [97,100–102]. This DDR modulation relies on two independent domains of TRF2 [102]. Whereas the TRFH domain represses ATM activation at chromosome termini, preventing DDR and TIFs formation, the iDDR motif within TRF2 blocks non-homologous end-joining (NHEJ) obstructing 53BP1 accumulation and propagation of the DDR signals by inhibiting ubiquitin ligase RNF168 activity [102]. Therefore, the retention of some TRF2 at telomeres allows DDR signalling and the presence of TIFs in the absence of telomeric fusions. These TIFs, which remain in a fusion-resistant state, do not activate CHK2 kinase [99]. Consequently, cells do not succumb to the activation of the G2/M checkpoint, and progress through the cell cycle [99]. The resulting daughter cells containing the inherited TIFs will continue cycling until they reach the threshold of 4–5 TIFs that will direct cells to replicative senescence (Figure 2) [97].

3.2. Extended Lifespan by Tumour Suppressors Loss-of-Function

Studies with human cells have shown that the abrogation of p53 is not enough to circumvent replicative senescence, and pRb inactivation is also needed [103]. Therefore, both pathways act together to force and maintain cell cycle arrest and induce cellular senescence. Fully deprotected telomeres are only observed when inactivation or mutation of p53 and pRb pathways allows cells to escape from replicative senescence and to continue dividing until crisis, a state where most cells die [104]. During this second proliferative phase, telomeres become even shorter, reaching a length that cannot retain enough TRF2 to inhibit NHEJ [100] and subsequent end-to-end chromosome fusions (Figure 2) [105].

It is known that uncapped telomeres can initiate endless breakage-fusion-bridge (BFB) cycles and generate elevated levels of genome remodelling [106]. A common assumption is that the huge karyotype reorganisation of cells could trigger the massive cell death associated with crisis. Recently, Hayashi et al. (2015) suggested that the underlying molecular signal that triggers cell death at crisis is not a long-term process related to ongoing BFB cycles, but to exaggerated telomere deprotection upon mitotic arrest [107]. This model proposes that the presence of chromosome end-to-end fusions extends mitotic duration and activates an Aurora kinase B mediated dissociation of TRF2 from telomeres [107]. The cellular impact of Aurora dependent TRF2 eviction from telomeres is the amplification of the telomere damage, which ensures the correct DDR activation and leads to cell death immediately during mitotic arrest or in the subsequent G1 cell cycle phase [108]. This Aurora-dependent TRF2 dissociation was first observed in primary human fibroblasts following prolonged mitotic arrest, and was dependent on the time spent in mitosis (Figure 2) [108]. More recently, Hain and colleagues investigated the molecular mechanisms involved in the telomeric DDR induced by mitotic arrest [109]. They observed a reduction of γH2AX foci and increased levels of TRF2 at telomeres when cells were treated with caspase inhibitors, or when MCL-1 was over-expressed [109]. It is known that prolonged mitotic arrest promotes a time-dependent degradation of MCL-1, an anti-apoptotic member of BCL-2 family proteins, subsequent mitochondrial outer membrane permeabilisation, and the activation of the classical caspase-9/3/7 pathway that ends-up in endonuclease CAD/DFF40 switch on [110–112]. The additional observation that TRF2 depletion was inhibited by CAD endonuclease and DNA-PK inhibitors lends support to a model where the classical caspase pathway causes DNA damage at telomeres by producing DSBs and selectively activates DNA-PK. This promotes TRF2 loss, resulting in telomere deprotection and the formation of telomeric γH2AX foci, most likely by direct phosphorylation of H2AX by DNA-PK [109]. Thus, it appears that there is a response that selects against cells that fail to undergo chromosome segregation on schedule, and which are likely to produce daughter cells that carry aberrant chromosomes. However, an unresolved question is how exactly TRF2 is removed from telomeres, and whether the caspase-pathway and subsequent

DNA-PK activation modulates Aurora B-dependent TRF2 depletion. However, specifically, in the case of telomere dysfunction, it remains to be established how the few fusions observed in crisis cells can trigger a prolonged mitosis arrest.

4. Dysfunctional Telomeres as a Source of Genome Instability and Cancer

4.1. Telomere Uncapping and Chromosome Instability

The ability of dysfunctional telomeres to promote genome instability originates in part, from their terminal chromosome location as activation of DDR at telomeres and subsequent repair activities results, primarily, in telomere fusion between distinct chromosomes or sister chromatids. Different studies in mouse and human cells suffering replicative telomere attrition have demonstrated that the chromosomes with the shorter telomeres are the first ones to become dysfunctional and to be involved in end-to-end fusions [113–117]. Similarly, telomere dysfunction, driven by shelterin modification, also results in end-to-end chromosome fusions [26]. Nevertheless, in this latter case, the dicentric chromosomes, or chromatids, do present telomere FISH signals at the fusion point when hybridised with a TTAGGG probe, as dysfunction is due to t-loop collapse and not to the shortening of the telomeric track [26].

In proliferating cells, chromosome end-to-end fusions due to telomere attrition can set BFB cycles in motion, a self-perpetuating mechanism that produces massive scrambling of the genome. When dicentric chromosomes or chromatids are pulled to opposite poles, they may lag at the cell equator, forming chromatin bridges between the two bulk chromatin-segregating complements. These anaphase bridges usually break during mitosis [118–121], and generate structural chromosome aberrations when the newly formed DSBs are repaired with either a broken end or an eroded telomere in the next generation [113]. In contrast, cells lacking TRF2 function did not show evidence for repeated BFB cycles, although end-to-end fusions are also formed [122]. Besides the limited anaphase bridge breakage, recent studies have determined that persistent chromatin bridges can also suffer extensive fragmentation, leading to chromothripsis, a mutational process in which multiple broken regions are haphazardly re-joined [123], as well as associated kataegis mutational hotspots [124]. This connection between chromothripsis and dysfunctional telomeres was observed in cells suffering induced telomere crisis through TRF2$^{\Delta B \Delta M}$ expression [124], and also highlighted by siRNA of TRF2 on p53 deficient RPE-1 cells [125]. Altogether diverse structural chromosome aberrations can originate from anaphase bridge breakage, including non-reciprocal translocations (NTRs), deletions, amplifications, new dicentric chromosomes [113,126,127], or hundreds of clustered genome rearrangements [128], which may result in loss of heterozygosity and cause oncogene amplification, amplification of oncogene containing regions and the loss of tumour suppressors.

However, breakage is not the only fate of anaphase bridges. It has been described that chromosomes with deprotected telomeres are more prone to missegregation than those with a non-critical telomere length, thus engendering aneuploid progeny [118]. The potential mechanism underlying chromosome bridge-induced aneuploidy is still unclear, although it may depend on the forces exerted by k-fibers [129]. The observation that k-fibers bound to bridge kinetochores shorten only slightly, and may even lengthen during anaphase, supports the notion that differential k-fiber dynamics may cause the bridged chromosomes to be segregated into the same daughter cell [129]. Alternatively, numerical chromosome aberrations appear when persistent chromatin bridges between segregating complements induce furrow regression and cytokinesis failure [130]. Likewise, whole genome duplication due to telomere uncapping has been described to arise in a chromatin bridge-independent manner [131]. Depletion of the shelterin proteins POT1a/b, or TRF2, in p53 defective mice, produced persistent telomeric DNA damage signalling that leads to the progressive accumulation of polyploid cells containing duplo- and quadruplo-chromosomes [103,131]. These cells experienced a prolonged G2 arrest owing to excessive damage and ATM- or ATR-pathways activation, but eventually skipped mitosis and re-entered the cell cycle in a polyploid state.

Collectively, it has been generally assumed that the autocatalytic nature of BFB cycles during telomere attrition induced crisis, massively scrambles the genome, yielding a wide range of lesions that threatens cell viability. Of note, cancer is an evolutionary disease in which the clonal nature has long been appreciated [132]. For Darwinian selection to occur, tumour cells may preserve the aptitude to maintain phenotypic heterogeneity through genomic instability [133]. Therefore, the karyotypic heterogeneity engendered through BFB-cycles may allow for the appearance of some rare advantageous mutations that would be selected and ultimately favour neoplastic progression. It has recently been proposed that telomere-driven crisis in human cells is not a long-term process that reorganises the genome, rather it is caused by generalised telomere deprotection during spontaneous mitotic arrest. Although the complete karyotype of the crisis cells was not established, telomere and centromere FISH showed only a few fusions events [107]. Therefore, it remains to be established how this observation reconciles with the generation of chromosomal instability (CIN) and the prevalent view of telomere-dependent CIN role in cancer onset and evolution.

4.2. Tumour-Promoting Effects of Telomere Dysfunction in the Mouse Not Yet Demonstrated in Humans

Studies to determine the in vivo effect of telomere dysfunction were first performed in mice that lacked the telomerase RNA component (*mTerc*$^{-/-}$) [134,135]. Cytogenetic analysis of telomerase deficient cells after successive intercrossing of *mTerc*$^{-/-}$ animals showed an increase in end-to-end chromosome fusions, NTRs, and aneuploidy [134,136]. Moreover, 6th generation *mTerc*$^{-/-}$ mice showed shortened lifespan, ageing-associated pathologies, and multiorgan degeneration. These phenotypes were linked to the impaired proliferation of progenitor cells of highly proliferative tissues, due to the loss of cell viability and an increase in apoptosis [135,137,138]. The presence of extremely short telomeres activates the p53 pathway, which induces increased levels of $p21^{CIP1/WAF1}$ and the inappropriate proliferation of damaged cells [139,140]. Consistent with these observations, *mTerc*$^{-/-}$ animals were resistant to cancer development [134,135]. Moreover, the induction of telomere dysfunction in mouse models relevant for cancer also did not denote a tumour-prone effect [141–144]. Strikingly, the abrogation of p53 function in *mTerc*$^{-/-}$ mice with dysfunctional telomeres enabled survival in the face of telomere dysfunction, and rescued many of the associated premature aging phenotypes, but at the expense of facilitating cellular transformation with MYC oncoprotein and GTPase Ras (RAS) [139]. Therefore, even although telomere-dysfunction was envisioned as a potent tumour suppressor mechanism, in the absence of functional checkpoints, it promoted genomic instability and initiated tumorigenesis. Similarly, animal studies where telomeres were rendered dysfunctional following conditional removal or hypomorphic mutations of shelterin proteins in combination with p53 mutations also lead to tumorigenesis [145–148]. However, most importantly, p53 mutations in late generation telomerase null mice produced a shift in the tumour spectrum towards epithelial cancers, the tumour type most frequent in aged humans, reinforcing a connection between telomeres and carcinomas [149]. In all, these findings demonstrate that telomere uncapping, either through loss of the G-rich overhang itself or by critically shortening the $(TTAGGG)_n$ tract of DNA, can trigger, in the setting of p53 deficiency, the genome instability that promotes the development of epithelial cancers.

Telomere dysfunction activates and sustains the CIN needed to scramble the genome and promote incipient cancer cells, nevertheless these highly reorganised cells are inevitably directed to death, unless stabilisation of the chromosome ends takes place through the activation of telomerase or recombination mechanisms. Indeed, the formation and development of a small fraction of tumours in *mTerc*$^{-/-}$ mice, despite the complete absence of telomerase, was caused by ALT-recombination pathway activation [150]. The dual role of telomere dysfunction in murine carcinogenesis has been elegantly depicted using an inducible TERT expression system [151]. The conditional expression of telomerase after a lagging time period of telomere dysfunction, in a *p53/Pten*-null mice prostate cancer model, enabled the progression of aggressive metastatic tumours. Importantly, comparative oncogenomic analysis revealed numerous recurrent amplifications and deletions of relevance to human

prostate cancer. Similarly, telomerase reactivation in T-cell lymphomas arising in $Atm^{-/-}$ mice, in the setting of telomere dysfunction led to full malignant progression, whereas telomerase extinction provoked slowdown of tumour growth [152]. Intriguingly, two tumour lines were able to resume growth, in the absence of telomerase function. Coincident with previous studies [150], these cell lines showed ALT-associated promyelocytic leukaemia bodies and extra-chromosomal telomere fragments, depicting the acquisition of alternative lengthening of telomeres.

In addition to the murine studies, mounting evidence supports a role for telomere dysfunction in human carcinogenesis. In human aging populations, cancer death is primarily due to carcinomas of the lung, liver, colorectal, stomach and breast [153]. These epithelial compartments undergo continual renewal through life, by suffering numerous cycles of proliferation and replacement. Although stem cells show active telomerase, their levels of expression are not sufficient to sustain telomere length in such compartments [154,155]. Therefore, the telomere attrition that should occur in these compartments, together with the fact that p53 mutations are observed in 20–30% of breast, 30–40% of lung, and over 40% of colorectal neoplasia [156,157], supports a permissive environment of telomere-induced genomic instability. Indeed, telomeres in human carcinoma are significantly shorter than their normal tissue counterparts [158], and telomere-to-telomere fusions have been detected in early stage breast tumours [159]. Collectively, all these data support the notion that in epithelial compartments, the combination of telomere shortening with checkpoint deficiencies could engender pre-neoplastic cells.

Besides the end-replication problem due to absent or reduced telomerase expression, recent studies have determined that mutations in the proteins belonging to the shelterin complex may lead to various malfunctions and ultimately also play a role in human tumorigenesis. Patients with early-stage chronic lymphocytic leukaemia (CLL) have an increased frequency of dysfunctional telomeres and telomere-to-telomere fusions are observed in advanced stages of the disease [160,161]. In agreement with a role of telomere-dysfunction in CLL, reduced expression levels of TRF1, RAP1 and POT1 [162], as well as TIN2 and TPP1 [161] have been detected. Furthermore, somatic mutations in POT1 account for 5% of CLL cases [163]. Of note, in addition to leukaemia, shelterin gene mutations have been described in melanoma [164,165], glioma [166] and sarcoma [167], thus indicating a broad potential relevance in non-epithelial oncogenesis.

Finally, numerous interactions between viral proteins and host telomere regulatory factors have been reported. Specifically, the Epstein–Barr virus (EBV) protein EBNA1 significantly increases the number of chromosomes with abnormal telomeres and decreases the amount of telomere-associated TRF2 through oxidative stress, but does not reduce the average telomere length or TRF2 levels in total cell lysates [168]. This is in line with the observed reduced levels of the shelterin components TRF1 and TRF2 at telomeres after the generation of reactive oxygen species [169]. Moreover, it was observed that the permanent expression of LMP1, another EBV oncoprotein, induces very short telomeres and telomere aggregates, as well as a significant downregulation of TRF1, TRF2 and POT1 at the transcriptional and translational level together with a disappearance of telomere-associated TRF2 spots, and the formation of abundant small TRF2 free telomeres [170]. Thus, the alteration of the normal host telomere structure and the generation of chromosome instability could be one of the mechanisms driving a variety of virus-induced lymphoid malignancies [171].

As a whole, although different mechanisms can modulate telomere homeostasis and drive aberrant telomeres, owing to the limiting lifespan factor of dysfunctional telomeres, the development of human neoplasia may be aborted by telomere-induced crisis long before lesions become macroscopic. Only those unstable cells able to reduce their CIN levels by stabilising their chromosome ends might further evolve and ultimately acquire a tumour phenotype. This supports the notion that approximately 80–90% of human cancers express telomerase and the remainder activate ALT-recombination-based mechanisms to cap chromosome ends [67,172].

5. Targeting Telomeres and Telomerase for Cancer Treatment

Given that telomerase expression is upregulated in the majority of carcinomas and soft tissue cancers, and that low levels of telomerase are observed in most normal tissues [173], several therapeutic strategies targeting telomerase have been developed to treat or fight cancer. The most prominent therapeutic strategy to block telomerase action is the use of antisense oligonucleotides. Imetelstat, also known as GRN163L, is an antisense oligonucleotide complementary to the template region of TERC [174], and is by far the most promising telomerase inhibitor. Several studies in vitro with human cancer cell lines have shown a strong inhibition of telomerase activity after GRN163L treatment [174,175]. Telomerase inhibition resulted in impaired cell growth and increased apoptosis, and of relevance, cell lines with critically short telomeres were the ones that were severely affected [174–176]. Moreover, persistent antisense oligonucleotide treatment also resulted in a decreased tumour take rate after engraftment of cancer cells pre-treated with Imetelstat [177]. Despite the great in vitro and in vivo potential of antisense oligonucleotides, clinical trials showed limited efficacy and nonspecific toxicity [174,178]. In addition, in addition, these therapies based on telomerase inhibitors required a long period of treatment to induce cell death. Another strategy to inhibit telomerase is the use of G-quadruplex (G4) stabilisers. G4 are secondary DNA structures rich in guanines which associate through hydrogen bonds to form planar structures that can stack and physically interfere with biological processes. Telomeres are G-rich sequences, therefore, it is not surprising to find G4 at telomeres, although they may form anywhere in the genome. Stabilisation of G4 at telomeres prevents DNA unfolding and inhibits telomerase access and subsequent elongation. However, short term G4 stabilisers treatment has very little effect on telomere length [179]. A second effect of G4 stabilisers is their capacity to displace shelterin proteins, resulting in telomere uncapping and DDR activation [180,181]. Indeed, after G4 ligand treatments, multinucleated cells and end-to-end fusions were observed to increase [179,180,182]. Although G4 stabilisers results in cell growth arrest in melanoma and brain tumour cells in vitro and in vivo [179,180,182,183], given that G4 structures are not exclusively found at telomeres, its stabilisation can induce off-target effects.

In addition to length regulation, shelterin proteins play essential roles in suppression of DNA damage signalling and inappropriate repair by homologous recombination (HR) and NHEJ at telomeres. Disruption of these protective functions occurs in ageing normal cells and can be achieved by genetic approaches. Telomere uncapping through shelterin modification precipitates telomere dysfunction and fast cell growth inhibition. One way to disrupt telomere protection is by the expression of mutant hTERC (Mt-hTERC) templates, which generates erroneous newly synthesised telomeric-strands that prevent shelterin binding and protection. After Mt-hTERC expression there were no changes on telomere length [184] and reduced TRF2 levels resulted in an increased number of γH2AX or 53BP1 foci at chromosome ends [185]. Mt-hTERC expression in immortalised hTERT fibroblast and in human cancer cell lines resulted in cell growth arrest, reduced viability and increased apoptosis [184–187]. Similarly, in vivo studies with human cells engrafted in mice resulted in the inhibition of tumour growth, increased apoptosis and minimal tumour angiogenesis [184,186]. Overall, Mt-hTERC therapies induced a cell response independent of telomere length but dependent on shelterin loss. Recently, targeted therapies to render telomeres dysfunctional through direct manipulation of shelterin proteins have been conducted. Targeting TRF2 through lentiviral vectors and RNA interference technologies inhibited the in vitro growth of primary human glioblastoma stem cells in addition to sensitising cells to temozolomide treatment [188]. Moreover, mice engrafted with the glioblastoma cells containing the TRF2 inhibiting lentivirus showed a significant extension of survival compared to those mice injected with unmodified glioblastoma cells [188]. These observances thus encouraged the use of modified shelterin for treating cancer patients. However, the toxicity of viral vectors is a major issue of concern when applying in vivo therapies in humans. Therefore, efforts have been made to design and synthesise chemical compounds that target specific shelterins. In this sense, a TRF2 permeable peptide that blocks its dimerisation domain has been developed and tested in vitro in HeLa cells [189]. Treatment with the compound for 24 h resulted in an increased number of TIFs

and DDR activation at chromosome ends that was compatible with intermediate-state telomeres, as there was an almost complete lack of 53BP1 recruitment as well as undetectable end-to-end fusions [189]. Besides TRF2 studies, therapeutic inhibition of TRF1 impaired the growth of *p53*-deficient *K-Ras*^{G12V}-induced lung cancer in the mouse independently of telomere length [190]. This decrease in proliferation was accompanied by the presence of telomeric DNA damage, apoptosis and G2 arrest already in the first mouse generation [190]. Recently, brain-specific *Trf1* genetic deletion in glioblastoma multiforme (GBM) mouse models, inhibited cancer initiation and progression by increasing telomeric DNA damage [191]. Moreover, TRF1 chemical inhibitors mimicked these effects in human GBM cells and also blocked tumour sphere formation and tumour growth in xenografts from patient-derived primary glioma stem cells [191]. As a whole, targeting telomeres throughout shelterin inhibition has been demonstrated to be an effective therapeutic strategy for glioblastoma and should probably be a valuable therapy for many other cancer types.

6. Conclusions

In recent years, much has been learned about the role of telomeres in cancer. Cancer cells require multiple mutations to become malignant, and it is clearly accepted that chromosome instability (CIN) should be a driver for this mutator phenotype. Telomere-dysfunction has proved to be an inducer of CIN when impaired checkpoints allow for cell-cycle progression of cells carrying short telomeres. However, telomere-dependent CIN must be transient to avoid the detrimental effect of telomere dysfunction. Indeed, mouse studies have evidenced the need for a period of telomere instability to remodel the genome but afterwards, telomerase or recombination mechanisms must be upregulated to lessen the excessive genome scrambling that would direct cells to crisis. Giving rise to the recent observation suggesting that cell death during telomere crisis is not due to rampant genome instability, but to the presence of excessively deprotected telomeres. The next exciting field will be to understand whether the degree of telomere dysfunction also modulates distinct cellular responses. Moreover, continued investigation on how telomere-dysfunction can promote tumour initiation in human cells will provide a greater understanding and clues to telomere biology in cancer development and treatment.

Acknowledgments: Laura Tusell laboratory is funded by MINECO (SAF2013-43801-P) and Generalitat de Catalunya (2014SGR-524). A.B. is supported by a Universitat Autònoma de Barcelona fellowship (456-01-1/2012).

Author Contributions: Aina Bernal and Laura Tusell conceived and wrote the paper.

Conflicts of Interest: The authors declare no conflict of interest.

References

1. McClintock, B. The stability of broken ends of chromosomes in Zea mays. *Genetics* **1941**, *26*, 234–282. [PubMed]
2. Müller, H.J. The remaking of chromosomes. *Collect. Net-Woods Hole* **1938**, *13*, 181–198.
3. Moyzis, R.K.; Buckingham, J.M.; Cram, L.S.; Dani, M.; Deaven, L.L.; Jones, M.D.; Meyne, J.; Ratliff, R.L.; Wu, J.-R. A highly conserved repetitive DNA sequence, (TTAGGG)n, present at the telomeres of human chromosomes. *Proc. Natl. Acad. Sci. USA* **1988**, *85*, 6622–6626. [CrossRef] [PubMed]
4. Meyne, J.; Ratliff, R.L.; Moyzis, R.K. Conservation of the human telomere sequence (TTAGGG)n among vertebrates. *Proc. Natl. Acad. Sci. USA* **1989**, *86*, 7049–7053. [CrossRef] [PubMed]
5. Makarov, V.L.; Hirose, Y.; Langmore, J.P. Long G tails at both ends of human chromosomes suggest a C strand degradation mechanism for telomere shortening. *Cell* **1997**, *88*, 657–666. [CrossRef]
6. Wright, W.E.; Tesmer, V.M.; Huffman, K.E.; Levene, S.D.; Shay, J.W. Normal human chromosomes have long G-rich telomeric overhangs at one end. *Genes Dev.* **1997**, *11*, 2801–2809. [CrossRef] [PubMed]
7. Allsopp, R.C.; Vaziri, H.; Patterson, C.; Goldstein, S.; Younglai, E.V.; Futcher, A.B.; Greider, C.W.; Harley, C.B. Telomere length predicts replicative capacity of human fibroblasts. *Proc. Natl. Acad. Sci. USA* **1992**, *89*, 10114–10118. [CrossRef] [PubMed]

8. Vaziri, H.; Dragowska, W.; Allsopp, R.C.; Thomas, T.E.; Harley, C.B.; Lansdorp, P.M. Evidence for a mitotic clock in human hematopoietic stem cells: Loss of telomeric DNA with age. *Proc. Natl. Acad. Sci. USA* **1994**, *91*, 9857–9860. [CrossRef] [PubMed]
9. De Lange, T. Shelterin: The protein complex that shapes and safeguards human telomeres. *Genes Dev.* **2005**, *19*, 2100–2110. [CrossRef] [PubMed]
10. Zhong, Z.; Shiue, L.; Kaplan, S. A mammalian factor that binds telomeric TTAGGG repeats in vitro. *Mol. Cell. Biol.* **1992**, *12*, 4834–4843. [CrossRef] [PubMed]
11. Chong, L.; van Steensel, B.; Broccoli, D.; Erdjument-Bromage, H.; Hanish, J.; Tempst, P.; de Lange, T. A Human Telomeric Protein. *Science* **1995**, *270*, 1663–1667. [CrossRef] [PubMed]
12. Broccoli, D.; Smogorzewska, A.; Chong, L.; de Lange, T. Human telomeres contain two distinct Myb-related proteins, TRF1 and TRF2. *Nat. Genet.* **1997**, *17*, 231–235. [CrossRef] [PubMed]
13. Baumann, P.; Cech, T.R. Pot1, the putative telomere end-binding protein in fission yeast and humans. *Science* **2001**, *292*, 1171–1175. [CrossRef] [PubMed]
14. Baumann, P.; Podell, E.; Cech, T.R. Human POT1 (Protection of Telomeres) Protein: Cytolocalization, gene structure, and alternative splicing. *Mol. Cell. Biol.* **2002**, *22*, 8079–8087. [CrossRef] [PubMed]
15. Ye, J.Z.S.; Donigian, J.R.; Van Overbeek, M.; Loayza, D.; Luo, Y.; Krutchinsky, A.N.; Chait, B.T.; De Lange, T. TIN2 binds TRF1 and TRF2 simultaneously and stabilizes the TRF2 complex on telomeres. *J. Biol. Chem.* **2004**, *279*, 47264–47271. [CrossRef] [PubMed]
16. Takai, K.K.; Kibe, T.; Donigian, J.R.; Frescas, D.; de Lange, T. Telomere protection by TPP1/POT1 requires tethering to TIN2. *Mol. Cell* **2011**, *44*, 647–659. [CrossRef] [PubMed]
17. Hardy, C.F.J.; Sussel, L.; Shore, D. A RAP1-interacting protein involved in transcriptional silencing and telomere length regulation. *Genes Dev.* **1992**, *6*, 801–814. [CrossRef] [PubMed]
18. Bae, N.S.; Baumann, P. A RAP1/TRF2 complex inhibits Nonhomologous End-Joining at human telomeric DNA ends. *Mol. Cell* **2007**, *26*, 323–334. [CrossRef] [PubMed]
19. Sarthy, J.; Bae, N.S.; Scrafford, J.; Baumann, P. Human RAP1 inhibits non-homologous end joining at telomeres. *EMBO J.* **2009**, *28*, 3390–3399. [CrossRef] [PubMed]
20. Arat, N.Ö.; Griffith, J.D. Human Rap1 interacts directly with telomeric DNA and regulates TRF2 localization at the telomere. *J. Biol. Chem.* **2012**, *287*, 41583–41594. [CrossRef] [PubMed]
21. Griffith, J.D.; Comeau, L.; Rosenfield, S.; Stansel, R.M.; Bianchi, A.; Moss, H.; De Lange, T. Mammalian telomeres end in a large duplex loop. *Cell* **1999**, *97*, 503–514. [CrossRef]
22. Stansel, R.M.; De Lange, T.; Griffith, J.D. T-loop assembly in vitro involves binding of TRF2 near the 3′ telomeric overhang. *EMBO J.* **2001**, *20*, 5532–5540. [CrossRef] [PubMed]
23. Doksani, Y.; Wu, J.Y.; De Lange, T.; Zhuang, X. XSuper-resolution fluorescence imaging of telomeres reveals TRF2-dependent T-loop formation. *Cell* **2013**, *155*, 345–356. [CrossRef] [PubMed]
24. Amiard, S.; Doudeau, M.; Pinte, S.; Poulet, A.; Lenain, C.; Faivre-Moskalenko, C.; Angelov, D.; Hug, N.; Vindigni, A.; Bouvet, P.; et al. A topological mechanism for TRF2-enhanced strand invasion. *Nat. Struct. Mol. Biol.* **2007**, *14*, 147–154. [CrossRef] [PubMed]
25. Benarroch-Popivker, D.; Pisano, S.; Mendez-Bermudez, A.; Lototska, L.; Kaur, P.; Bauwens, S.; Djerbi, N.; Latrick, C.M.; Fraisier, V.; Pei, B.; et al. TRF2-mediated control of telomere DNA topology as a mechanism for chromosome-end protection. *Mol. Cell* **2016**, *61*, 274–286. [CrossRef] [PubMed]
26. Van Steensel, B.; Smogorzewska, A.; de Lange, T. TRF2 protects human telomeres from end-to-end fusions. *Cell* **1998**, *92*, 401–413. [CrossRef]
27. Poulet, A.; Pisano, S.; Faivre-Moskalenko, C.; Pei, B.; Tauran, Y.; Haftek-Terreau, Z.; Brunet, F.; Le Bihan, Y.V.; Ledu, M.H.; Montel, F.; et al. The N-terminal domains of TRF1 and TRF2 regulate their ability to condense telomeric DNA. *Nucleic Acids Res.* **2012**, *40*, 2566–2576. [CrossRef] [PubMed]
28. Kaur, P.; Wu, D.; Lin, J.; Countryman, P.; Bradford, K.C.; Erie, D.A.; Riehn, R.; Opresko, P.L.; Wang, H. Enhanced electrostatic force microscopy reveals higher-order DNA looping mediated by the telomeric protein TRF2. *Sci. Rep.* **2016**, *6*, 20513. [CrossRef] [PubMed]
29. Bandaria, J.N.; Qin, P.; Berk, V.; Chu, S.; Yildiz, A. Shelterin protects chromosome ends by compacting telomeric chromatin. *Cell* **2016**, *164*, 735–746. [CrossRef] [PubMed]
30. Blackburn, E.H. Switching and signaling at the telomere. *Cell* **2001**, *106*, 661–673. [CrossRef]
31. Greider, C.W.; Blackburn, E.H. Identification of a specific telomere terminal transferase activity in tetrahymena extracts. *Cell* **1985**, *43*, 405–413. [CrossRef]

32. Greider, C.W.; Blackburn, E.H. The telomere terminal transferase of tetrahymena is a ribonucleoprotein enzyme with two kinds of primer specificity. *Cell* **1987**, *51*, 887–898. [CrossRef]
33. Feng, J.; Funk, W.D.; Wang, S.S.; Weinrich, S.L.; Avilion, A.A.; Chiu, C.P.; Adams, R.R.; Chang, E.; Allsopp, R.C.; Yu, J.; et al. The RNA component of human telomerase. *Science* **1995**, *269*, 1236–1241. [CrossRef] [PubMed]
34. Nakamura, T.M.; Morin, G.B.; Chapman, K.B.; Weinrich, S.L.; Andrews, W.H.; Lingner, J.; Harley, C.B.; Cech, T.R. Telomerase catalytic subunit homologs from fission yeast and human telomerase catalytic subunit homologs from fission yeast and human. *Science* **1997**, *277*, 955–959. [CrossRef] [PubMed]
35. Lingner, J.; Hughes, T.R.; Shevchenko, A.; Mann, M.; Lundblad, V.; Cech, T.R. Reverse transcriptase motifs in the catalytic subunit of telomerase. *Science* **1997**, *276*, 561–567. [CrossRef] [PubMed]
36. Egan, E.D.; Collins, K. Specificity and stoichiometry of subunit interactions in the human telomerase holoenzyme assembled in vivo. *Mol. Cell. Biol.* **2010**, *30*, 2775–2786. [CrossRef] [PubMed]
37. Venteicher, A.S.; Abreu, E.B.; Meng, Z.; McCann, K.E.; Terns, R.M.; Veenstra, T.D.; Terns, M.P.; Artandi, S.E. A human telomerase holoenzyme protein required for Cajal body localization and telomere synthesis. *Science* **2009**, *323*, 644–648. [CrossRef] [PubMed]
38. Egan, E.D.; Collins, K. Biogenesis of telomerase ribonucleoproteins. *RNA* **2012**, *18*, 1747–1759. [CrossRef] [PubMed]
39. Schmidt, J.C.; Cech, T.R. Human telomerase: Biogenesis, trafficking, recruitment, and activation. *Genes Dev.* **2015**, *29*, 1095–1105. [CrossRef] [PubMed]
40. Chen, Y.; Deng, Z.; Jiang, S.; Hu, Q.; Liu, H.; Songyang, Z.; Ma, W.; Chen, S.; Zhao, Y. Human cells lacking coilin and Cajal bodies are proficient in telomerase assembly, trafficking and telomere maintenance. *Nucleic Acids Res.* **2015**, *43*, 385–395. [CrossRef] [PubMed]
41. Vogan, J.M.; Zhang, X.; Youmans, D.T.; Regalado, S.G.; Johnson, J.Z.; Hockemeyer, D.; Collins, K. Minimized human telomerase maintains telomeres and resolves endogenous roles of H/ACA proteins, TCAB1, and Cajal bodies. *Elife* **2016**, *5*, e18221. [CrossRef] [PubMed]
42. Jády, B.E.; Bertrand, E.; Kiss, T. Human telomerase RNA and box H/ACA scaRNAs share a common Cajal body-specific localization signal. *J. Cell Biol.* **2004**, *164*, 647–652. [CrossRef] [PubMed]
43. Tomlinson, R.L.; Ziegler, T.D.; Supakorndej, T.; Terns, R.M.; Terns, M.P. Cell cycle-regulated trafficking of human telomerase to telomeres. *Mol. Biol. Cell* **2006**, *17*, 955–965. [CrossRef] [PubMed]
44. Hockemeyer, D.; Collins, K. Control of telomerase action at human telomeres. *Nat. Struct. Mol. Biol.* **2015**, *22*, 848–852. [CrossRef] [PubMed]
45. Dionne, I.; Wellinger, R.J. Cell cycle-regulated generation of single-stranded G-rich DNA in the absence of telomerase. *Proc. Natl. Acad. Sci. USA* **1996**, *93*, 13902–13907. [CrossRef] [PubMed]
46. Teixeira, M.T.; Arneric, M.; Sperisen, P.; Lingner, J. Telomere length homeostasis is achieved via a switch between telomerase- extendible and -nonextendible states. *Cell* **2004**, *117*, 323–335. [CrossRef]
47. Bianchi, A.; Shore, D. Increased association of telomerase with short telomeres in yeast. *Genes Dev.* **2007**, *21*, 1726–1730. [CrossRef] [PubMed]
48. Soohoo, C.Y.; Shi, R.; Lee, T.H.; Huang, P.; Lu, K.P.; Zhou, X.Z. Telomerase inhibitor PinX1 provides a link between TRF1 and telomerase to prevent telomere elongation. *J. Biol. Chem.* **2011**, *286*, 3894–3906. [CrossRef] [PubMed]
49. Zaug, A.J.; Podell, E.R.; Nandakumar, J.; Cech, T.R. Functional interaction between telomere protein TPP1 and telomerase. *Genes Dev.* **2010**, *24*, 613–622. [CrossRef] [PubMed]
50. Nandakumar, J.; Bell, C.F.; Weidenfeld, I.; Zaug, A.J.; Leinwand, L.A.; Cech, T.R. The TEL patch of telomere protein TPP1 mediates telomerase recruitment and processivity. *Nature* **2012**, *492*, 285–289. [CrossRef] [PubMed]
51. Frank, A.K.; Tran, D.C.; Qu, R.W.; Stohr, B.A.; Segal, D.J.; Xu, L. The Shelterin TIN2 Subunit Mediates Recruitment of Telomerase to Telomeres. *PLoS Genet.* **2015**, *11*, 31005410. [CrossRef] [PubMed]
52. Abreu, E.; Aritonovska, E.; Reichenbach, P.; Cristofari, G.; Culp, B.; Terns, R.M.; Lingner, J.; Terns, M.P. TIN2-tethered TPP1 recruits human telomerase to telomeres in vivo. *Mol. Cell. Biol.* **2010**, *30*, 2971–2982. [CrossRef] [PubMed]
53. Hwang, H.; Buncher, N.; Opresko, P.L.; Myong, S. POT1-TPP1 regulates telomeric overhang structural dynamics. *Structure* **2012**, *20*, 1872–1880. [CrossRef] [PubMed]

54. Zhao, Y.; Abreu, E.; Kim, J.; Stadler, G.; Eskiocak, U.; Terns, M.P.; Terns, R.M.; Shay, J.W.; Wright, W.E. Processive and Distributive Extension of Human Telomeres by Telomerase under Homeostatic and Nonequilibrium Conditions. *Mol. Cell* **2011**, *42*, 297–307. [CrossRef] [PubMed]
55. Zhao, Y.; Sfeir, A.J.; Zou, Y.; Buseman, C.M.; Chow, T.T.; Shay, J.W.; Wright, W.E. Telomere Extension Occurs at Most Chromosome Ends and Is Uncoupled from Fill-In in Human Cancer Cells. *Cell* **2009**, *138*, 463–475. [CrossRef] [PubMed]
56. Yang, W.; Lee, Y.S. A DNA-hairpin model for repeat-addition processivity in telomere synthesis. *Nat. Struct. Mol. Biol.* **2015**, *22*, 844–847. [CrossRef] [PubMed]
57. Wu, R.A.; Upton, H.E.; Vogan, J.M.; Collins, K. Telomerase mechanism of telomere synthesis. *Annu. Rev. Biochem.* **2017**, *86*, 439–460. [CrossRef] [PubMed]
58. Wu, R.A.; Tam, J.; Collins, K. DNA-binding determinants and cellular thresholds for human telomerase repeat addition processivity. *EMBO J.* **2017**, *36*, 1908–1927. [CrossRef] [PubMed]
59. Wang, F.; Podell, E.R.; Zaug, A.J.; Yang, Y.; Baciu, P.; Cech, T.R.; Lei, M. The POT1–TPP1 telomere complex is a telomerase processivity factor. *Nature* **2007**, *445*, 506–510. [CrossRef] [PubMed]
60. Armstrong, C.A.; Tomita, K. Fundamental mechanisms of telomerase action in yeasts and mammals: Understanding telomeres and telomerase in cancer cells. *Open Biol.* **2017**, *7*, 160338. [CrossRef] [PubMed]
61. Chen, L.Y.; Redon, S.; Lingner, J. The human CST complex is a terminator of telomerase activity. *Nature* **2012**, *488*, 540–544. [CrossRef] [PubMed]
62. Feng, X.; Hsu, S.J.; Kasbek, C.; Chaiken, M.; Price, C.M. CTC1-mediated C-strand fill-in is an essential step in telomere length maintenance. *Nucleic Acids Res.* **2017**, *45*, 4281–4293. [CrossRef] [PubMed]
63. Casteel, D.E.; Zhuang, S.; Zeng, Y.; Perrino, F.W.; Boss, G.R.; Goulian, M.; Pilz, R.B. A DNA polymerase-a-primase cofactor with homology to replication protein A-32 regulates DNA replication in mammalian cells. *J. Biol. Chem.* **2009**, *284*, 5807–5818. [CrossRef] [PubMed]
64. Wu, P.; Takai, H.; De Lange, T. Telomeric 3′ overhangs derive from resection by Exo1 and Apollo and fill-in by POT1b-associated CST. *Cell* **2012**, *150*, 39–52. [CrossRef] [PubMed]
65. Shay, J.W.; Bacchetti, S. A survey of telomerase activity in human cancer. *Eur. J. Cancer* **1997**, *33*, 787–791. [CrossRef]
66. Bryan, T.M.; Englezou, A.; Gupta, J.; Bacchetti, S.; Reddel, R.R. Telomere elongation in immortal human cells without detectable telomerase activity. *Embo J* **1995**, *14*, 4240–4248. [PubMed]
67. Bryan, T.M.; Englezou, A.; Dalla-Pozza, L.; Dunham, M.A.; Reddel, R.R. Evidence for an alternative mechanism for maintaining telomere length in human tumors and tumor-derived cell lines. *Nat. Med.* **1997**, *3*, 1271–1274. [CrossRef] [PubMed]
68. Lundblad, V.; Blackburn, E.H. An alternative pathway for yeast telomere maintenance rescues est1-senescence. *Cell* **1993**, *73*, 347–360. [CrossRef]
69. Dunham, M.A.; Neumann, A.A.; Fasching, C.L.; Reddel, R.R. Telomere maintenance by recombination in human cells. *Nat. Genet.* **2000**, *26*, 447–450. [CrossRef] [PubMed]
70. Henson, J.D.; Neumann, A.A.; Yeager, T.R.; Reddel, R.R. Alternative lengthening of telomeres in mammalian cells. *Oncogene* **2002**, *21*, 598–610. [CrossRef] [PubMed]
71. Tokutake, Y.; Matsumoto, T.; Watanabe, T.; Maeda, S.; Tahara, H.; Sakamoto, S.; Niida, H.; Sugimoto, M.; Ide, T.; Furuichi, Y. Extra-chromosomal telomere repeat DNA in telomerase-negative immortalized cell lines. *Biochem. Biophys. Res. Commun.* **1998**, *247*, 765–772. [CrossRef] [PubMed]
72. Ogino, H.; Nakabayashi, K.; Suzuki, M.; Takahashi, E.; Fujii, M.; Suzuki, T.; Ayusawa, D. Release of telomeric DNA from chromosomes in immortal human cells lacking telomerase activity. *Biochem Biophys Res Commun* **1998**, *248*, 223–227. [CrossRef] [PubMed]
73. Wang, R.C.; Smogorzewska, A.; De Lange, T. Homologous recombination generates t-loop-sized deletions at human telomeres. *Cell* **2004**, *119*, 355–368. [CrossRef] [PubMed]
74. Cesare, A.J.; Griffith, J.D. Telomeric DNA in ALT cells is characterized by free telomeric circles and heterogeneous t-loops. *Mol. Cell. Biol* **2004**, *24*, 9948–9957. [CrossRef] [PubMed]
75. Pickett, H.A.; Cesare, A.J.; Johnston, R.L.; Neumann, A.A.; Reddel, R.R. Control of telomere length by a trimming mechanism that involves generation of t-circles. *EMBO J.* **2009**, *28*, 799–809. [CrossRef] [PubMed]
76. Li, B.; Lustig, A.J. A novel mechanism for telomere size control in Saccharomyces cerevisiae. *Genes Dev.* **1996**, *10*, 1310–1326. [CrossRef] [PubMed]

77. Pickett, H.A.; Reddel, R.R. The role of telomere trimming in normal telomere length dynamics. *Cell Cycle* **2012**, *11*, 1309–1315. [CrossRef] [PubMed]
78. Lewis, K.A.; Tollefsbol, T.O. Regulation of the telomerase reverse transcriptase subunit through epigenetic mechanisms. *Front. Genet.* **2016**, *7*, 1–12. [CrossRef] [PubMed]
79. Hayflick, L.; Moorhead, P.S. The serial cultivation of human diploid cell strains. *Exp. Cell Res.* **1961**, *25*, 585–621. [CrossRef]
80. Okazaki, R.; Okazaki, T.; Sakabe, K.; Sugimoto, K.; Sugino, A. Mechanism of DNA chain growth. I. Possible discontinuity and unusual secondary structure of newly synthesized chains. *Proc. Natl. Acad. Sci. USA* **1968**, *59*, 598–605. [CrossRef] [PubMed]
81. Sugimoto, K.; Okazaki, T.; Okazaki, R. Mechanism of DNA chain growth, II. Accumulation of newly synthesized short chains in E. coli infected with ligase-defective T4 phages. *Proc. Natl. Acad. Sci. USA* **1968**, *60*, 1356–1362. [CrossRef] [PubMed]
82. Burgers, P.M.J.; Kunkel, T.A. Eukaryotic DNA replication fork. *Annu. Rev. Biochem* **2017**, *86*, 1–922. [CrossRef] [PubMed]
83. Johnson, R.E.; Klassen, R.; Prakash, L.; Prakash, S. A major role of DNA polymerase d in replication of both the leading and lagging DNA strands. *Mol. Cell* **2015**, *59*, 163–175. [CrossRef] [PubMed]
84. Harley, C.B.; Futcher, A.B.; Greider, C.W. Telomeres shorten during ageing of human fibroblasts. *Nature* **1990**, *345*, 458–460. [CrossRef] [PubMed]
85. Wu, P.; van Overbeek, M.; Rooney, S.; De Lange, T. Apollo contributes to G-overhang maintenance and protects leading-end telomeres. *Mol. Cell* **2010**, *39*, 606–617. [CrossRef] [PubMed]
86. Lam, Y.C.; Akhter, S.; Gu, P.; Ye, J.; Poulet, A.; Giraud-Panis, M.-J.; Bailey, S.M.; Gilson, E.; Legerski, R.J.; Chang, S. SNMIB/Apollo protects leading-strand telomeres against NHEJ-mediated repair. *EMBO J.* **2010**, *29*, 2230–2241. [CrossRef] [PubMed]
87. Van Overbeek, M.; de Lange, T. Apollo, an Artemis-related nuclease, interacts with TRF2 and protects human telomeres in S phase. *Curr. Biol.* **2006**, *16*, 1295–1302. [CrossRef] [PubMed]
88. Cannavo, E.; Cejka, P.; Kowalczykowski, S.C. Relationship of DNA degradation by Saccharomyces cerevisiae Exonuclease 1 and its stimulation by RPA and Mre11-Rad50-Xrs2 to DNA end resection. *Proc. Natl. Acad. Sci. USA* **2013**, *110*, E1661–E1668. [CrossRef] [PubMed]
89. Kibe, T.; Zimmermann, M.; de Lange, T. TPP1 blocks an ATR-mediated resection mechanism at telomeres. *Mol. Cell* **2016**, *61*, 236–246. [CrossRef] [PubMed]
90. Harley, C.B. Telomere loss: Mitotic clock or genetic time bomb? *Mutat. Res.* **1991**, *256*, 271–282. [CrossRef]
91. Campisi, J.; d'Adda di Fagagna, F. Cellular senescence: When bad things happen to good cells. *Nat. Rev. Mol. Cell Biol.* **2007**, *8*, 729–740. [CrossRef] [PubMed]
92. Bodnar, A.G.; Quellette, M.; Frolkis, M.; Holt, S.E.; Chiu, C.-P.; Morin, G.B.; Harley, C.B.; Shay, J.W.; Lichtsteiner, S.; Wright, W.E. Extension of life-span by introduction of telomerase into normal human cells. *Science* **1998**, *279*, 349–352. [CrossRef] [PubMed]
93. Arnoult, N.; Karlseder, J. Complex interactions between the DNA-damage response and mammalian telomeres. *Nat. Struct. Mol. Biol.* **2015**, *22*, 859–866. [CrossRef] [PubMed]
94. Karlseder, J.; Smogorzewska, A.; de Lange, T. Senescence induced by altered telomere state, not telomere loss. *Science* **2002**, *295*, 2446–2449. [CrossRef] [PubMed]
95. Takai, H.; Smogorzewska, A.; de Lange, T. DNA damage foci at dysfunctional telomeres. *Curr. Biol.* **2003**, *13*, 1549–1556. [CrossRef]
96. Dimitrova, N.; De Lange, T. MDC1 accelerates nonhomologous end-joining of dysfunctional telomeres. *Genes Dev.* **2006**, *20*, 3238–3243. [CrossRef] [PubMed]
97. Kaul, Z.; Cesare, A.J.; Huschtscha, L.I.; Neumann, A.A.; Reddel, R.R. Five dysfunctional telomeres predict onset of senescence in human cells. *EMBO Rep.* **2012**, *13*, 52–59. [CrossRef] [PubMed]
98. Di Fagagna d'Adda, F.; Reaper, P.M.; Clay-Farrace, L.; Fiegler, H.; Carr, P.; von Zglinicki, T.; Saretzki, G.; Carter, N.P.; Jackson, S.P. A DNA damage checkpoint response in telomere-initiated senescence. *Nature* **2003**, *426*, 194–198. [CrossRef]
99. Cesare, A.J.; Hayashi, M.T.; Crabbe, L.; Karlseder, J. The telomere deprotection response is functionally distinct from the genomic DNA damage response. *Mol. Cell* **2013**, *51*, 141–155. [CrossRef] [PubMed]

100. Cesare, A.J.; Kaul, Z.; Cohen, S.B.; Napier, C.E.; Pickett, H.A.; Neumann, A.A.; Reddel, R.R. Spontaneous occurrence of telomeric DNA damage response in the absence of chromosome fusions. *Nat. Struct. Mol. Biol.* **2009**, *16*, 1244–1251. [CrossRef] [PubMed]
101. Cesare, A.J.; Karlseder, J. A three-state model of telomere control over human proliferative boundaries. *Curr. Opin. Cell Biol.* **2013**, *24*, 731–738. [CrossRef] [PubMed]
102. Okamoto, K.; Bartocci, C.; Ouzounov, I.; Diedrich, J.K.; Yates, J.R., III; Denchi, E.L. A two-step mechanism for TRF2-mediated chromosome-end protection. *Nature* **2013**, *494*, 502–505. [CrossRef] [PubMed]
103. Smogorzewska, A.; de Lange, T. Different telomere damage signaling pathways in human and mouse cells. *EMBO J.* **2002**, *21*, 4338–4348. [CrossRef] [PubMed]
104. Wright, W.E.; Shay, J.W. The two-stage mechanism controlling cellular senescence and immortalization. *Exp. Gerontol.* **1992**, *27*, 383–389. [CrossRef]
105. Counter, C.M.; Avilion, A.A.; Lefeuvrel, C.E.; Stewart, N.G.; Greider, C.W.; Harley, C.B.; Bacchettil, S. Telomere shortening associated with chromosome instability is arrested in immortal cells which express telomerase activity. *EMBO J.* **1992**, *1*, 1921–1929.
106. Feijoo, P.; Dominguez, D.; Tusell, L.; Genesca, A. Telomere-dependent genomic integrity: Evolution of the fusion-bridge-breakage cycle concept. *Curr. Pharm. Des.* **2014**, *20*, 6375–6385. [CrossRef] [PubMed]
107. Hayashi, M.T.; Cesare, A.J.; Rivera, T.; Karlseder, J. Cell death during crisis is mediated by mitotic telomere deprotection. *Nature* **2015**, *522*, 492–496. [CrossRef] [PubMed]
108. Hayashi, M.T.; Cesare, A.J.; Fitzpatrick, J.A.J.; Denchi, E.L.; Karlseder, J. A telomere-dependent DNA damage checkpoint induced by prolonged mitotic arrest. *Nat. Struct. Mol. Biol.* **2012**, *19*, 387–395. [CrossRef] [PubMed]
109. Hain, K.O.; Colin, D.J.; Rastogi, S.; Allan, L.A.; Clarke, P.R. Prolonged mitotic arrest induces a caspase-dependent DNA damage response at telomeres that determines cell survival. *Sci. Rep.* **2016**, *6*, 26766. [CrossRef] [PubMed]
110. Craig, R.W. MCL1 provides a window on the role of the BCL2 family in cell proliferation, differentiation and tumorigenesis. *Leukemia* **2002**, *16*, 444–454. [CrossRef] [PubMed]
111. Ertel, F.; Nguyen, M.; Roulston, A.; Shore, G.C. Programming cancer cells for high expression levels of Mcl1. *EMBO Rep.* **2013**, *14*, 328–336. [CrossRef] [PubMed]
112. Woo, E.J.; Kim, Y.G.; Kim, M.S.; Han, W.D.; Shin, S.; Robinson, H.; Park, S.Y.; Oh, B.H. Structural mechanism for inactivation and activation of CAD/DFF40 in the apoptotic pathway. *Mol. Cell* **2004**, *14*, 531–539. [CrossRef]
113. Soler, D.; Genescà, A.; Arnedo, G.; Egozcue, J.; Tusell, L. Telomere dysfunction drives chromosomal instability in human mammary epithelial cells. *Genes. Chromosomes Cancer* **2005**, *44*, 339–350. [CrossRef] [PubMed]
114. Deng, W.; Tsao, S.W.; Guan, X.Y.; Lucas, J.N.; Cheung, A.L.M. Role of short telomeres in inducing preferential chromosomal aberrations in human ovarian surface epithelial cells: A combined telomere quantitative fluorescence in situ hybridization and whole-chromosome painting study. *Genes Chromosom. Cancer* **2003**, *37*, 92–97. [CrossRef] [PubMed]
115. Deng, W.; Tsao, S.W.; Guan, X.Y.; Lucas, J.N.; Si, H.X.; Leung, C.S.; Mak, P.; Wang, L.D.; Cheung, A.L.M. Distinct profiles of critically short telomeres are a key determinant of different chromosome aberrations in immortalized human cells: Whole-genome evidence from multiple cell lines. *Oncogene* **2004**, *23*, 9090–9101. [CrossRef] [PubMed]
116. Der-Sarkissian, H.; Bacchetti, S.; Cazes, L.; Londoño-Vallejo, J.A. The shortest telomeres drive karyotype evolution in transformed cells. *Oncogene* **2004**, *23*, 1221–1228. [CrossRef] [PubMed]
117. Plug-DeMaggio, A.W.; Sundsvold, T.; Wurscher, M.A.; Koop, J.I.; Klingelhutz, A.J.; McDougall, J.K. Telomere erosion and chromosomal instability in cells expressing the HPV oncogene 16E6. *Oncogene* **2004**, *23*, 3561–3571. [CrossRef] [PubMed]
118. Pampalona, J.; Soler, D.; Genescà, A.; Tusell, L. Whole chromosome loss is promoted by telomere dysfunction in primary cells. *Genes. Chromosomes Cancer* **2010**, *49*, 368–378. [CrossRef] [PubMed]
119. Hoffelder, D.; Luo, L.; Burke, N.; Watkins, S.; Gollin, S.; Saunders, W. Resolution of anaphase bridges in cancer cells. *Chromosoma* **2004**, *112*, 389–397. [CrossRef] [PubMed]
120. Shimizu, N.; Shingaki, K.; Kaneko-Sasaguri, Y.; Hashizume, T.; Kanda, T. When, where and how the bridge breaks: Anaphase bridge breakage plays a crucial role in gene amplification and HSR generation. *Exp. Cell Res.* **2005**, *302*, 233–243. [CrossRef] [PubMed]

121. Titen, S.W.A.; Golic, K.G. Telomere loss provokes multiple pathways to apoptosis and produces genomic instability in Drosophila melanogaster. *Genetics* **2008**, *180*, 1821–1832. [CrossRef] [PubMed]
122. Smogorzewska, A.; Karlseder, J.; Holtgreve-Grez, H.; Jauch, A.; De Lange, T. DNA ligase IV-dependent NHEJ of deprotected mammalian telomeres in G1 and G2. *Curr. Biol.* **2002**, *12*, 1635–1644. [CrossRef]
123. Stephens, P.J.; Greenman, C.D.; Fu, B.; Yang, F.; Bignell, G.R.; Mudie, L.J.; Pleasance, E.D.; Lau, K.W.; Beare, D.; Stebbings, L.A.; et al. Massive genomic rearrangement acquired in a single catastrophic event during cancer development. *Cell* **2011**, *144*, 27–40. [CrossRef] [PubMed]
124. Maciejowski, J.; Li, Y.; Bosco, N.; Campbell, P.J.; De Lange, T. Chromothripsis and kataegis induced by telomere crisis. *Cell* **2015**, *163*, 1641–1654. [CrossRef] [PubMed]
125. Mardin, B.R.; Drainas, A.P.; Waszak, S.M.; Weischenfeldt, J.; Isokane, M.; Stütz, A.M.; Raeder, B.; Efthymiopoulos, T.; Buccitelli, C.; Segura-Wang, M.; et al. A cell-based model system links chromothripsis with hyperploidy. *Mol. Syst. Biol.* **2015**, *11*, 828. [CrossRef] [PubMed]
126. Lo, A.W.I.; Sabatier, L.; Fouladi, B.; Pottiert, G.; Ricoul, M.; Murnane, J.P. DNA amplification by breakage/fusion/bridge cycles initiated by spontaneous telomere loss in a human cancer cell line. *Neoplasia* **2002**, *4*, 531–538. [CrossRef] [PubMed]
127. Tusell, L.; Soler, D.; Agostini, M.; Pampalona, J.; Genescà, A. The number of dysfunctional telomeres in a cell: One amplifies; more than one translocate. *Cytogenet. Genome Res.* **2008**, *122*, 315–325. [CrossRef] [PubMed]
128. Forment, J.V.; Kaidi, A.; Jackson, S.P. Chromothripsis and cancer: Causes and consequences of chromosome shattering. *Nat. Rev. Cancer* **2012**, *12*, 663–670. [CrossRef] [PubMed]
129. Pampalona, J.; Roscioli, E.; Silkworth, W.T.; Bowden, B.; Genescà, A.; Tusell, L.; Cimini, D. Chromosome bridges maintain kinetochore-microtubule attachment throughout mitosis and rarely break during anaphase. *PLoS ONE* **2016**, *11*, e0147420. [CrossRef] [PubMed]
130. Pampalona, J.; Frías, C.; Genescà, A.; Tusell, L. Progressive telomere dysfunction causes cytokinesis failure and leads to the accumulation of polyploid cells. *PLoS Genet.* **2012**, *8*, e1002679. [CrossRef] [PubMed]
131. Davoli, T.; de Lange, T. The causes and consequences of polyploidy in normal cevelopment and Cancer. *Annu. Rev. Cell Dev. Biol.* **2010**, 585–610. [CrossRef]
132. Nowell Peter, C. The clonal evolution of tumor cell populations. *Science* **1976**, *194*, 23–28. [CrossRef]
133. Yates, L.R.; Campbell, P.J. Evolution of the cancer genome. *Nat. Rev. Genet.* **2012**, *13*, 795–806. [CrossRef] [PubMed]
134. Blasco, M.A.; Lee, H.-W.; Hande, M.P.; Samper, E.; Lansdorp, P.M.; DePinho, R.A.; Greider, C.W. Telomere shortening and tumor formation by mouse cells lacking telomerase RNA. *Cell* **1997**, *91*, 25–34. [CrossRef]
135. Lee, H.; Blasco, M.A.; Gottlieb, G.J.; Il, J.W.H.; Greider, C.W.; DePinho, R.A. Essential role of mouse telomerase in highly proliferative organs. *Nature* **1998**, *392*, 569–574. [CrossRef] [PubMed]
136. Hande, M.P.; Samper, E.; Lansdorp, P.; Blasco, M.A. Telomere length dynamics and chromosome instability in cells derived from telomerase null mice. *J. Cell Biol.* **1999**, *144*, 589–601. [CrossRef] [PubMed]
137. Herrera, E.; Samper, E.; Blasco, M.A. Telomere shortening in mTR$^{-/-}$ embryos is associated with failure to close the neural tube. *EMBO J.* **1999**, *18*, 1172–1181. [CrossRef] [PubMed]
138. Feldser, D.M.; Greider, C.W. Short Telomeres Limit Tumor Progression In Vivo by Inducing Senescence. *Cancer Cell* **2007**, *11*, 461–469. [CrossRef] [PubMed]
139. Chin, L.; Artandi, S.E.; Shen, Q.; Tam, A.; Lee, S.-L.; Gottlieb, G.J.; Greider, C.W.; Depinho, R.A. p53 deficiency rescues the adverse effects of telomere loss and cooperates with telomere dysfunction to accelerate carcinogenesis. *Cell* **1999**, *97*, 527–538. [CrossRef]
140. Cosme-Blanco, W.; Shen, M.F.; Lazar, A.J.F.; Pathak, S.; Lozano, G.; Multani, A.S.; Chang, S. Telomere dysfunction suppresses spontaneous tumorigenesis in vivo by initiating p53-dependent cellular senescence. *EMBO Rep.* **2007**, *8*, 497–503. [CrossRef] [PubMed]
141. Greenberg, R.A.; Chin, L.; Femino, A.; Kee-Ho, L.; Gottlieb, G.J.; Singer, R.H.; Greider, C.W.; DePinho, R.A. Short dysfunctional telomeres impair tumorigenesis in the INK4a(Δ2/3) cancer-prone mouse. *Cell* **1999**, *97*, 515–525. [CrossRef]
142. Rudolph, K.L.; Millard, M.; Bosenberg, M.W.; DePinho, R.A. Telomere dysfunction and evolution of intestinal carcinoma in mice and humans. *Nat. Genet.* **2001**, *28*, 155–159. [CrossRef] [PubMed]
143. Qi, L.; Strong, M.A.; Karim, B.O.; Armanios, M.; Huso, D.L.; Greider, C.W. Short telomeres and ataxia-telangiectasia mutated deficiency cooperatively increase telomere dysfunction and suppress tumorigenesis. *Cancer Res.* **2003**, *63*, 8188–8196. [PubMed]

144. Farazi, P.A.; Glickman, J.; Jiang, S.; Yu, A.; Rudolph, K.L.; DePinho, R.A. Differential impact of telomere dysfunction on initiation and progression of hepatocellular carcinoma. *Cancer Res.* **2003**, *63*, 5021–5027. [PubMed]
145. Martínez, P.; Thanasoula, M.; Muñoz, P.; Liao, C.; Tejera, A.; McNees, C.; Flores, J.M.; Fernández-Capetillo, O.; Tarsounas, M.; Blasco, M.A. Increased telomere fragility and fusions resulting from TRF1 deficiency lead to degenerative pathologies and increased cancer in mice. *Genes Dev.* **2009**, *23*, 2060–2075. [CrossRef] [PubMed]
146. Pinzaru, A.M.; Hom, R.A.; Beal, A.; Phillips, A.F.; Ni, E.; Cardozo, T.; Nair, N.; Choi, J.; Wuttke, D.S.; Sfeir, A.; et al. Telomere replication stress induced by POT1 inactivation accelerates tumorigenesis. *Cell Rep.* **2016**, *15*, 2170–2184. [CrossRef] [PubMed]
147. Akbay, E.A.; Peña, C.G.; Ruder, D.; Michel, J.A.; Nakada, Y.; Pathak, S.; Multani, A.S.; Chang, S.; Castrillon, D.H. Cooperation between p53 and the telomere-protecting shelterin component Pot1a in endometrial carcinogenesis. *Oncogene* **2013**, *32*, 2211–2219. [CrossRef] [PubMed]
148. Else, T.; Trovato, A.; Kim, A.C.; Wu, Y.; Ferguson, D.O.; Kuick, R.D.; Lucas, P.C.; Hammer, G.D. Genetic p53 deficiency partially rescues the adrenocortical dysplasia phenotype at the expense of increased tumorigenesis. *Cancer Cell* **2009**, *15*, 465–476. [CrossRef] [PubMed]
149. Artandi, S.E.; Chang, S.; Lee, S.L.; Alson, S.; Gottlieb, G.J.; Chin, L.; DePinho, R.A. Telomere dysfunction promotes non-reciprocal translocations and epithelial cancers in mice. *Nature* **2000**, *406*, 641–645. [CrossRef] [PubMed]
150. Morrish, T.A.; Greider, C.W. Short telomeres initiate telomere recombination in primary and tumor cells. *PLoS Genet.* **2009**, *5*. [CrossRef] [PubMed]
151. Ding, Z.; Wu, C.J.; Jaskelioff, M.; Ivanova, E.; Kost-Alimova, M.; Protopopov, A.; Chu, G.C.; Wang, G.; Lu, X.; Labrot, E.S.; et al. Telomerase reactivation following telomere dysfunction yields murine prostate tumors with bone metastases. *Cell* **2012**, *148*, 896–907. [CrossRef] [PubMed]
152. Hu, J.; Hwang, S.S.; Liesa, M.; Gan, B.; Sahin, E.; Jaskelioff, M.; Ding, Z.; Ying, H.; Boutin, A.T.; Zhang, H.; et al. Antitelomerase therapy provokes ALT and mitochondrial adaptive mechanisms in cancer. *Cell* **2012**, *148*, 651–663. [CrossRef] [PubMed]
153. Cancer Fact Sheet. (February 2017). Available online: http://www.who.int/mediacentre/factsheets/fs297/en/ (accessed on 8 December 2017).
154. Takubo, K.; Aida, J.; Izumiyama-Shimomura, N.; Ishikawa, N.; Sawabe, M.; Kurabayashi, R.; Shiraishi, H.; Arai, T.; Nakamura, K.I. Changes of telomere length with aging. *Geriatr. Gerontol. Int.* **2010**, *10*, S197–S206. [CrossRef] [PubMed]
155. Martinez, P.; Blasco, M.A. Role of shelterin in cancer and aging. *Aging Cell* **2010**, *9*, 653–666. [CrossRef] [PubMed]
156. Somatic Mutations, TP53 Mutation Prevalence by Tumor Site. IARC TP53 Database, R18 (April 2016). Available online: http://p53.iarc.fr/SelectedStatistics.aspx (accessed on 8 December 2017).
157. Olivier, M.; Hollstein, M.; Hainaut, P. TP53 mutations in human cancers: Origins, consequences, and clinical use. *Cold Spring Harb. Perspect. Biol.* **2010**, *2*, 1–17. [CrossRef] [PubMed]
158. Meeker, A.K.; Hicks, J.L.; Iacobuzio-Donahue, C.A.; Montgomery, E.A.; Westra, W.H.; Chan, T.Y.; Ronnett, B.M.; De Marzo, A.M. Telomere length abnormalities occur early in the initiation of epithelial carcinogenesis telomere length abnormalities occur early in the initiation of epithelial carcinogenesis. *Clin. Cancer Res.* **2004**, *10*, 3317–3326. [CrossRef] [PubMed]
159. Tanaka, H.; Abe, S.; Huda, N.; Tu, L.; Beam, M.J.; Grimes, B.; Gilley, D. Telomere fusions in early human breast carcinoma. *Proc. Natl. Acad. Sci. USA* **2012**, *109*, 14098–14103. [CrossRef] [PubMed]
160. Lin, T.T.; Letsolo, B.T.; Jones, R.E.; Rowson, J.; Pratt, G.; Fegan, C.; Pepper, C.; Baird, D.M. Telomere dysfunction and fusion during the progression of a human malignancy. *Blood* **2010**, *44*, 1899–1908. [CrossRef] [PubMed]
161. Augereau, A.; t'knit de Roodenbeke, C.; Simonet, T.; Bauwens, S.; Horard, B.; Callanan, M.; Leroux, D.; Jallades, L.; Salles, G.; Gilson, E.; et al. Telomeric damage in early stage of chronic lymphocytic leukemia correlates with shelterin dysregulation. *Blood* **2011**, *118*, 1316–1322. [CrossRef] [PubMed]
162. Poncet, D.; Belleville, A.; t'knit de Roodenbeke, C.; Roborel de Climens, A.; Ben Simon, E.; Merle-Beral, H.; Callet-Bauchu, E.; Salles, G.; Sabatier, L.; Delic, J.; et al. Changes in the expression of telomere maintenance genes suggest global telomere dysfunction in B-chronic lymphocytic leukemia. *Blood* **2008**, *111*, 2388–2391. [CrossRef] [PubMed]

163. Ramsay, A.J.; Quesada, V.; Foronda, M.; Conde, L.; Martínez-Trillos, A.; Villamor, N.; Rodríguez, D.; Kwarciak, A.; Garabaya, C.; Gallardo, M.; et al. POT1 mutations cause telomere dysfunction in chronic lymphocytic leukemia. *Nat. Genet.* **2013**, *45*, 526–530. [CrossRef] [PubMed]
164. Aoude, L.G.; Pritchard, A.L.; Robles-Espinoza, C.D.; Wadt, K.; Harland, M.; Choi, J.; Gartside, M.; Quesada, V.; Johansson, P.; Palmer, J.M.; et al. Nonsense mutations in the shelterin complex genes ACD and TERF2IP in familial melanoma. *J. Natl. Cancer Inst.* **2015**, *107*, 1–7. [CrossRef] [PubMed]
165. Robles-Espinoza, C.D.; Harland, M.; Ramsay, A.J.; Aoude, L.G.; Quesada, V.; Ding, Z.; Pooley, K.A.; Pritchard, A.L.; Tiffen, J.C.; Petljak, M.; et al. POT1 loss-of-function variants predispose to familial melanoma. *Nat. Genet.* **2014**, *46*, 478–481. [CrossRef] [PubMed]
166. Bainbridge, M.N.; Armstrong, G.N.; Gramatges, M.M.; Bertuch, A.A.; Jhangiani, S.N.; Doddapaneni, H.; Lewis, L.; Tombrello, J.; Tsavachidis, S.; Liu, Y.; et al. Germline mutations in shelterin complex genes are associated with familial glioma. *J. Natl. Cancer Inst.* **2015**, *107*, 1–4. [CrossRef] [PubMed]
167. Calvete, O.; Martinez, P.; Garcia-Pavia, P.; Benitez-Buelga, C.; Paumard-Hernández, B.; Fernandez, V.; Dominguez, F.; Salas, C.; Romero-Laorden, N.; Garcia-Donas, J.; et al. A mutation in the POT1 gene is responsible for cardiac angiosarcoma in TP53-negative Li-Fraumeni-like families. *Nat. Commun.* **2015**, *6*, 8383. [CrossRef] [PubMed]
168. Kamranvar, S.A.; Masucci, M.G. The Epstein-Barr virus nuclear antigen-1 promotes telomere dysfunction via induction of oxidative stress. *Leukemia* **2011**, *25*, 1017–1025. [CrossRef] [PubMed]
169. Opresko, P.L.; Fan, J.; Danzy, S.; Wilson, D.M.; Bohr, V.A. Oxidative damage in telomeric DNA disrupts recognition by TRF1 and TRF2. *Nucleic Acids Res.* **2005**, *33*, 1230–1239. [CrossRef] [PubMed]
170. Lajoie, V.; Lemieux, B.; Sawan, B.; Lichtensztejn, D.; Lichtensztejn, Z.; Wellinger, R.; Mai, S.; Knecht, H. LMP1 mediates multinuclearity through downregulation of shelterin proteins and formation of telomeric aggregates. *Blood* **2015**, *125*, 2101–2110. [CrossRef] [PubMed]
171. Deng, Z.; Wang, Z.; Lieberman, P.M. Telomeres and viruses: Common themes of genome maintenance. *Front. Oncol.* **2012**, *2*, 201. [CrossRef] [PubMed]
172. Kim, N.W.; Piatyszek, M.A.; Prowse, K.R.; Harley, C.B.; West, D.; Ho, P.L.C.; Coviello, G.M.; Wright, W.E.; Weinrich, S.L.; Shay, W.; et al. Specific association of human telomerase activity with immortal cells and cancer. *Science* **1994**, *266*, 2011–2015. [CrossRef] [PubMed]
173. Forsyth, N.R.; Wright, W.E.; Shay, J.W. Telomerase and differentiation in multicellular organisms: Turn it off, turn it on, and turn it off again. *Differentiation* **2002**, *69*, 188–197. [CrossRef] [PubMed]
174. Asai, A.; Oshima, Y.; Yamamoto, Y.; Uochi, T.; Kusaka, H.; Akinaga, S.; Yamashita, Y.; Pongracz, K.; Pruzan, R.; Wunder, E.; et al. A novel telomerase template antagonist (GRN163) as a potential anticancer agent. *Cancer Res.* **2003**, *63*, 3931–3939. [PubMed]
175. Burchett, K.M.; Yan, Y.; Ouellette, M.M. Telomerase inhibitor Imetelstat (GRN163L) limits the lifespan of human pancreatic cancer cells. *PLoS ONE* **2014**, *9*, e85155. [CrossRef] [PubMed]
176. Gómez-Millan, J.; Goldblatt, E.M.; Gryaznov, S.M.; Mendonca, M.S.; Herbert, B.-S. Specific telomere dysfunction induced by GRN163L increases radiation sensitivity in breast cancer cells. *Int. J. Radiat. Oncol.* **2007**, *67*, 897–905. [CrossRef] [PubMed]
177. Joseph, I.; Tressler, R.; Bassett, E.; Harley, C.; Buseman, C.M.; Pattamatta, P.; Wright, W.E.; Shay, J.W.; Go, N.F. The telomerase inhibitor Imetelstat depletes cancer stem cells in breast and pancreatic cancer cell lines. *Cancer Res.* **2010**, *70*, 9494–9505. [CrossRef] [PubMed]
178. Chiappori, A.A.; Kolevska, T.; Spigel, D.R.; Hager, S.; Rarick, M.; Gadgeel, S.; Blais, N.; Von Pawel, J.; Hart, L.; Reck, M.; et al. A randomized phase II study of the telomerase inhibitor imetelstat as maintenance therapy for advanced non-small-cell lung cancer. *Ann. Oncol.* **2015**, *26*, 354–362. [CrossRef] [PubMed]
179. Merle, P.; Evrard, B.; Petitjean, A.; Lehn, J.-M.; Teulade-Fichou, M.-P.; Chautard, E.; De Cian, A.; Guittat, L.; Tran, P.L.T.; Mergny, J.-L.; et al. Telomere Targeting with a New G4 Ligand Enhances Radiation-Induced Killing of Human Glioblastoma Cells. *Mol. Cancer Ther.* **2011**, *10*, 1784–1795. [CrossRef] [PubMed]
180. Leonetti, C.; Amodei, S.; D'Angelo, C.; Rizzo, A.; Benassi, B.; Antonelli, A.; Elli, R.; Stevens, M.F.G.; D'Incalci, M.; Zupi, G.; et al. Biological activity of the G-quadruplex ligand RHPS4 (3,11-methosulfate) is associated with telomere capping alteration. *Mol. Pharmacol.* **2004**, *66*, 1138–1146. [CrossRef] [PubMed]

181. Phatak, P.; Cookson, J.C.; Dai, F.; Smith, V.; Gartenhaus, R.B.; Stevens, M.F.G.; Burger, A.M. Telomere uncapping by the G-quadruplex ligand RHPS4 inhibits clonogenic tumour cell growth in vitro and in vivo consistent with a cancer stem cell targeting mechanism. *Br. J. Cancer* **2007**, *96*, 1223–1233. [CrossRef] [PubMed]
182. Zhou, G.; Liu, X.; Li, Y.; Xu, S.; Ma, C.; Wu, X.; Cheng, Y.; Yu, Z.; Zhao, G.; Chen, Y. Telomere targeting with a novel G-quadruplex-interactive ligand BRACO-19 induces T-loop disassembly and telomerase displacement in human glioblastoma cells. *Oncotarget* **2016**, *7*, 14925–14939. [CrossRef] [PubMed]
183. Lagah, S.; Tan, I.L.; Radhakrishnan, P.; Hirst, R.A.; Ward, J.H.; O'Callaghan, C.; Smith, S.J.; Stevens, M.F.G.; Grundy, R.G.; Rahman, R. RHPS4 G-quadruplex ligand induces anti-proliferative effects in brain tumor cells. *PLoS ONE* **2014**, *9*, e86187. [CrossRef] [PubMed]
184. Li, S.; Rosenberg, J.E.; Donjacour, A.A.; Botchkina, I.L.; Hom, Y.K.; Cunha, G.R.; Blackburn, E.H. Rapid inhibition of cancer cell growth induced by lentiviral delivery and expression of mutant-template telomerase RNA and anti-telomerase short-interfering RNA. *Cancer Res.* **2004**, *64*, 4833–4840. [CrossRef] [PubMed]
185. Mahalingam, D.; Tay, L.L.; Tan, W.H.; Chai, J.H.; Wang, X. Mutant telomerase RNAs induce DNA damage and apoptosis via the TRF2-ATM pathway in telomerase-overexpressing primary fibroblasts. *FEBS J.* **2011**, *278*, 3724–3738. [CrossRef] [PubMed]
186. Kim, M.M.; Rivera, M.A.; Botchkina, I.L.; Shalaby, R.; Thor, A.D.; Blackburn, E.H. A low threshold level of expression of mutant-template telomerase RNA inhibits human tumor cell proliferation. *Pnas* **2001**, *98*, 7982–7987. [CrossRef] [PubMed]
187. Goldkorn, A.; Blackburn, E.H. Assembly of mutant-template telomerase RNA into catalytically active telomerase ribonucleoprotein that can act on telomeres is required for apoptosis and cell cycle arrest in human cancer cells. *Cancer Res.* **2006**, *66*, 5763–5772. [CrossRef] [PubMed]
188. Bai, Y.; Lathia, J.D.; Zhang, P.; Flavahan, W.; Rich, J.N.; Mattson, M.P. Molecular targeting of TRF2 suppresses the growth and tumorigenesis of glioblastoma stem cells. *Glia* **2014**, *62*, 1687–1698. [CrossRef] [PubMed]
189. Di Maro, S.; Zizza, P.; Salvati, E.; De Luca, V.; Capasso, C.; Fotticchia, I.; Pagano, B.; Marinelli, L.; Gilson, E.; Novellino, E.; et al. Shading the TRF2 recruiting function: A new horizon in drug development. *J. Am. Chem. Soc.* **2014**, *136*, 16708–16711. [CrossRef] [PubMed]
190. García-Beccaria, M.; Martínez, P.; Méndez-Pertuz, M.; Martínez, S.; Blanco-Aparicio, C.; Cañamero, M.; Mulero, F.; Ambrogio, C.; Flores, J.M.; Megias, D.; et al. Therapeutic inhibition of TRF1 impairs the growth of p53-deficient K-RasG12V-induced lung cancer by induction of telomeric DNA damage. *EMBO Mol. Med.* **2015**, *7*, 930–949. [CrossRef] [PubMed]
191. Bejarano, L.; Schuhmacher, A.J.; Méndez, M.; Megías, D.; Blanco-Aparicio, C.; Martínez, S.; Pastor, J.; Squatrito, M.; Blasco, M.A. Inhibition of TRF1 Telomere Protein Impairs Tumor Initiation and Progression in Glioblastoma Mouse Models and Patient-Derived Xenografts. *Cancer Cell* **2017**, *32*, 590–607.e4. [CrossRef] [PubMed]

Discussion

Versió en Català

La pèrdua contínua de repeticions telomèriques i/o el mal funcionament o mutacions de les proteïnes shelterin condueixen a la disfunció telomèrica per l'inhabilitat de mantenir l'estructura de *t-loop* (Cesare & Karlseder, 2013). Estudis murins han establert que la disfunció telomèrica juntament amb la inactivació de p53 (Artandi *et al*, 2000; Chin *et al*, 1999) i la reactivació de la telomerasa (Hu *et al*, 2012; Ding *et al*, 2012), potencia la transformació cel·lular i la tumorigènesis. En humans, tot i que no està formalment demostrat, a mesura que els individus envelleixen es produeix un escurçament telomèric en la major part dels teixits (Harley *et al*, 1990). Aquesta podria estar relacionada amb l'increment en la incidència del càncer amb l'edat dels individus, conjuntament amb l'acumulació de mutacions al llarg de la vida, els canvis epigenètics i els canvis el microambient de estroma (DePinho, 2000). Per altra banda, certa controvèrsia existeix en la implicació de les proteïnes shelterin en l'establiment d'una població potencialment tumoral. En humans, mutacions en les proteïnes shelterin no són freqüents en els tumors (Sanger Institute, 2018). Fins l'actualitat, s'han descrit mutacions no sinònimes de sentit erroni (mutations *missense*) en les proteïnes POT1 (Ramsay *et al*, 2013; Shi *et al*, 2014; Robles-Espinoza *et al*, 2014; Calvete *et al*, 2015; Bainbridge *et al*, 2015), TPP1 (Aoude *et al*, 2015; Spinella *et al*, 2015) i RAP1 (Aoude *et al*, 2015) que podrien estar directament relacionades amb la incidència de càncer familiars. Aquesta baixa incidència de mutacions en les proteïnes shelterin podria estar associada amb l'efecte deleteri que tenen sobre la viabilitat cel·lular. De fet, els models murins *knockouts* de proteïnes shelterin demostren que la seva deficiència, excepte per RAP1 (Sfeir *et al*, 2010), és letal pel desenvolupament embrionari dels ratolins (Celli & de Lange, 2005; Karlseder *et al*, 2003; Hockemeyer *et al*, 2006; Wu *et al*, 2006; Martínez *et al*, 2009; Okamoto *et al*, 2008). Per contra, la disfunció transitòria de les proteïnes shelterin TRF2 (Begus-Nahrmann *et al*, 2012) i POT1A (Davoli & de Lange, 2012) en cèl·lules de ratolí indueix la formació de tumors.

Amb l'objectiu de determinar la capacitat de la disfunció telomèrica d'originar cèl·lules humanes altament reorganitzades i amb potencial tumorigènic s'han establert línies cel·lulars epitelials mamàries que han experimentat disfunció telomèrica, tant per escurçament de la longitud telomèrica com per deficiències en la proteïna shelterin TRF2 ($TRF2^{\Delta B\Delta M}$). Els resultats obtinguts reforcen un model en el qual la cèl·lula és capaç de tolerar el dany gradual derivat del escurçament telomèric progressiu i seguir proliferant. El restabliment de la funcionalitat telomèrica i la immortalització cel·lular podria afavorir una població susceptible a la transformació cel·lular. Per contra, la deficiència de TRF2, una proteïna clau en la protecció del telòmer, indueix un dany extensiu i global en la cèl·lula, el que provoca una forta activació de la DDR, un arrest cel·lular que seria incompatible amb la proliferació de les cèl·lules susceptibles d'esdevenir altament reorganitzades.

1. La disfunció telomèrica, el dany progressiu vs el dany agut

Els efectes de l'escurçament telomèric progressiu en la integritat genòmica es van estudiar en les cèl·lules vHMECs amb $p16^{INK4a}$ inactivat (**Treball I**). La inactivació del promotor del gen *CDKN2A* permet a les cèl·lules superar la senescència i continuar proliferant en un ambient sense activitat telomerasa (Brenner *et al*, 1998; Romanov *et al*, 2001). En les HMECs, els mecanismes que controlen la proliferació cel·lular

en altres teixits o tipus cel·lulars semblen ser més restrictius. En fibroblasts humans, l'escurçament telomèric progressiu condueix a la senescència replicativa (Bodnar *et al*, 1998). Aquest arrest és produeix principalment per l'activació de p53 i $p16^{INK4a}$ i, per tant la seva inactivació evita l'arrest cel·lular i afavoreix la proliferació cel·lular (Beauséjour *et al*, 2003; Shay & Wright, 1989). S'ha demostrat que la senescència es produeix per l'acumulació de telòmers excessivament curts i disfuncionals en les cèl·lules (Kaul *et al*, 2012). Més concretament, el dany acumulatiu de 4-5 telòmers disfuncionals (*telomere induced foci*, TIFs) és suficient per activar p53 i l'entrada en senescència. Aquests TIFs són resistents a processos de fusió i per aquest motiu les cèl·lules senescents no presenten cromosomes dicèntrics en el seu cariotip (Kaul *et al*, 2012). Diferents estudis han demostrat que la resistència a les fusions telomèriques està modulada per la permamència de la proteïna shelterin TRF2 als telòmers. A mesura que el telòmer es va escurçant, la conformació el *t-loop* i la modulació de l'activació de la DDR resten limitades. No obstant, tot i que l'estructura de llaç no es pugui formar, el telòmer conté suficient quantitat de TRF2 per evitar l'activació dels mecanismes de reparació (Cesare *et al*, 2009, 2013).

Malgrat que la inactivació de $p16^{INK4a}$ permet prolongar la proliferació de les vHMECs més enllà de la senescència (Huschtscha *et al*, 1998), aquestes cèl·lules no proliferen indefinidament sinó que finalment moren (**Treball I**) (Romanov *et al*, 2001; Garbe *et al*, 2007; Feijoo *et al*, 2016), en un procés denominat agonescència (Romanov *et al*, 2001) que es troba regulat per p53 (Garbe *et al*, 2007). Es creu que l'activació de p53 ve determinada per l'increment del dany causat per telòmers disfuncionals juntament amb els DSBs originats a través dels trencaments cromosòmics associats a cicles BFB (Huschtscha *et al*, 2009). De fet a mesura que s'agreuja la disfunció telomèrica hi ha un increment de reorganitzacions cromosòmiques que va acompanyada per un increment de p53-Ser15, Chk2-Thr68, γ-H2AX i 53BP1 (**Treball I**) (Zhang *et al*, 2006b; Garbe *et al*, 2009; Domínguez *et al*, 2015). Aquestes reorganitzacions cromosòmiques no responen únicament a la fusió de dos extrems amb telòmers desprotegits, sinó també a la fusió DSBs resultants de cicles BFB (McClintock, 1941) amb altres extrems trencats o telòmers disfuncionals (Latre *et al*, 2003; Soler *et al*, 2005; Tusell *et al*, 2008). El **Treball I** mostra, d'acord amb altres estudis (Soler *et al*, 2005; Tusell *et al*, 2008) com a mesura que s'incrementen el nombre de PDs, hi ha un increment tant en el nombre de *end-to-end* fusions com de fragments cèntrics i acèntrics que podrien ser derivats dels successius cicles BFB. Alhora, l'increment de cèl·lules aneuploides i poliploides associada a la disfunció telomèrica progressiva detectada en el **Treball I** i prèviament descrita per altres autors (Pampalona *et al*, 2012; Davoli & de Lange, 2012) podria contribuir també a incrementar la DDR en les cèl·lules amb disfunció telomèrica agreujada. Així doncs, en les vHMECs amb p53 funcional l'escurçament telomèric progressiu conduiria al desenvolupament de CIN gràcies a la generació de cicles BFB i el nombre creixent de dany cromosòmic associat induiria l'activació de p53 i l'agonescència.

De forma rellevant però, la inactivació de p53 en les vHMEC no evita la seva mort (**Treball I**) (Wright & Shay, 1992). En aquest cas, les cèl·lules moren per crisi, un procés de mort massiva relacionada amb mecanismes independents de p53 (Romanov *et al*, 2001) i la reorganització massiva del genoma. Per tant,

la funcionalitat de p53 determina si les cèl·lules moren per agonescència o per crisi. En les vHMECs analitzades, la crisi cel·lular després d'haver inactivat p53 mitjançant un *short hairpin* de RNA ocorre a un PD no gaire més elevat al que es produeix l'agonescència en les vHMECs amb p53 funcional, suggerint que la inactivació de p53 no permet allargar gaire més la vida del cultiu (Treball I). La inactivació de p53 produeix un increment en quant a la freqüència d'anomalies estructurals i numèriques respecte el cultiu amb p53 funcional (Treball I), tal i com ha estat descrit a la literatura (Chin *et al*, 1999; Artandi *et al*, 2000; Roake & Artandi, 2017). I afavoreix la viabilitat de les cèl·lules tetraploides, tal i com es descriu a l'apartat 4.3. Però, per molt que l'absència de p53 funcional permet que les cèl·lules siguin més tolerants al dany genòmic (Cesare et al, 2009; Kaul et al, 2012), el desenvolupament d'un genoma massa inestable pot concloure en la mort cel·lular (Kops *et al*, 2004; Weaver *et al*, 2007; Ganem *et al*, 2009; Janssen *et al*, 2009; Bakhoum & Landau, 2017). Per tant, independentment de la funcionalitat dels *checkpoints* de cicle cel·lular, la presència de telòmers excessivament curts i l'elevada reorganització del genoma conduiria irremeiablement a la mort cel·lular.

En ratolins, la reactivació de la telomerasa després d'un període de disfunció telomèrica alleugereix el dany telomèric i permet la progressió tumoral (Ding *et al*, 2012; Hu *et al*, 2012). Més concretament, mentre la disfunció telomèrica pot incrementar la variabilitat genòmica, conferint noves característiques a les cèl·lules, la reactivació de la telomerasa seleccionaria aquelles amb una avantatge proliferativa i/o metastàtica (Ding *et al*, 2012). Tanmateix, la immortalització de les vHMECs-shp53 amb la subunitat catalítica de la telomerasa redueix de manera dràstica la CIN, tot suggerint que l'expressió de hTERT restableix la funcionalitat telomèrica i permet la proliferació cel·lular de les cèl·lules menys reorganitzades (Treball I). La disminució de la inestabilitat cromosòmica podria estar relacionada amb el llindar de dany que una cèl·lula pot tolerar. Mentre una presència baixa d'anomalies seria permissiva amb la viabilitat cel·lular, una elevada reorganització cariotípica podria ser letal per les cèl·lules.

La disfunció telomèrica a més de produir-se per escurçament telomèric, pot generar-se artificialment mitjançant la modificació de les proteïnes shelterin (Karlseder *et al*, 2002; Cesare & Karlseder, 2013) i específicament manipulant TRF2. L'expressió de TRF2$^{\Delta B \Delta M}$, una proteïna truncada deficient en el domini Myb i Bàsic, permet la dimerització de TRF2 però evita la seva unió al DNA telomèric i, per tant compromet la formació del t-loop. Cal destacar que en aquest cas, es produeix una desprotecció aguda del telòmers (Takai *et al*, 2003) que indueix un fort arrest cel·lular depenent de p53 i pRb en fibroblasts humans (Steensel *et al*, 1998; Smogorzewska & de Lange, 2002; Jacobs & de Lange, 2004) o apoptosi en cas de cèl·lules epitelials (Karlseder *et al*, 1999). Per evitar l'aturada del creixement cel·lular i controlar l'expressió del TRF2$^{\Delta B \Delta M}$ es va desenvolupar un model d'expressió condicional de TRF2$^{\Delta B \Delta M}$ regulat per doxiciclina. Primerament es va establir en la línia cel·lular mamària immortalitzada MCF-10A no tumorigència (Treball II) (Soule *et al*, 1990) i posteriorment en cèl·lules epitelials primàries derivades de glàndula mamària (Treball III). Mitjançant aquest sistema es van desprotegir els telòmers de forma controlada i s'observaren les conseqüències sobre les cèl·lules a curt i a llarg termini, demostrant-se els

efectes antagònics en el desenvolupament de la CIN quan s'indueix disfunció telomèrica al expressar la proteïna truncada TRF2$^{\Delta B\Delta M}$ respecte a quan es produeix escurçament telomèric progressiu (**Treball I**).

L'expressió de TRF2$^{\Delta B\Delta M}$ i la desprotecció telomèrica va verificar-se mitjançant western blot i la presència de TIFs després de 24 h d'inducció (**Treball II**) en 3 línies cel·lulars derivades de la línia cel·lular MCF-10A, que presentaven diferents funcionalitats dels *checkpoints* de cicle cel·lular (TO amb inactivació de p16^{INK4a}; SH-TO amb inactivació de p16^{INK4a} i p53; SV-TO amb inactivació de p53 i pRb). A més, l'expressió continuada del dominant negatiu de TRF2 al llarg de 96 h, resultà en un increment de fusions cromosòmiques amb DNA telomèric intersticial i un increment de ponts anafàsics, tal i com havia estat descrit anteriorment (Steensel *et al*, 1998; Karlseder *et al*, 1999; Smogorzewska & de Lange, 2002; Jacobs & de Lange, 2004), en les tres línies testades derivades de les MCF-10A (**Treball II**). A més, la freqüència d'anomalies es veia incrementada en funció de la funcionalitat de les vies de p53/pRb (**Treball II**), demostrant altra vegada que la inactivació dels *checkpoints* permet la proliferació de cèl·lules que presenten un nombre elevat d'anomalies cromosòmiques. En un ambient amb escurçament telomèric progressiu com ara les vHMECs, la presència de ponts anafàsics s'ha relacionat amb l'entrada de les fusions cromosòmiques en cicles BFB i subseqüent reorganització del genoma a nivell estructural (Soler *et al*, 2005; Pampalona *et al*, 2010; **Treball I**) i numèric (Pampalona *et al*, 2010, 2012). No obstant, en el cas de l'expressió del TRF2$^{\Delta B\Delta M}$ no va observar-se un increment de cèl·lules amb reorganitzacions estructurals ni aneuploïdes compatibles amb la generació de cicles BFB en cap de les línies testades, tot i l'increment en el nombre de fusions i formació de ponts anafàsics (**Treball II**). Es podria especular que 96 h d'inducció del TRF2$^{\Delta B\Delta M}$ no són suficients per tal de visualitzar els efectes dels cicles BFB. Tanmateix, després d'induir durant 5 setmanes cicles de protecció i desprotecció telomèrica tampoc es va observar un increment en reorganitzacions cromosòmiques secundaries derivades de cicles BFB o un augment en la incidència de cèl·lules tetraploides (**Treball II**). A més, aquesta absència en la generació de CIN no era deguda a una pèrdua de l'eficiència d'expressió de TRF2$^{\Delta B\Delta M}$ (**Treball II**), a diferència del que s'ha observat en fibroblasts de ratolí amb p16^{INK4a} inactivat (Zhang *et al*, 2012). Els efectes de l'expressió de TRF2$^{\Delta B\Delta M}$ a llarg termini també van ser avaluats en línies cel·lulars induïbles després de modificar genèticament cèl·lules epitelials primàries procedents de reduccions mamàries de 4 pacients sanes (**Treball III**). La funcionalitat del casset induïble va ser confirmada mitjançant western blot i la inducció de ponts cromatínics després d'exposar les 3 línies a 72 h de DOX a PDs inicials (**Treball III**). Tanmateix, i coincidint amb els resultats en les línies modificades de les MCF10A (**Treball II**), tampoc s'observaren un nombre creixent de fusions cromosòmiques amb telòmers intersticials o reorganitzacions cariotípiques característiques de l'entrada en cicles BFB després de diversos cicles de protecció i desprotecció telomèrica (**Treball III**). En resum, els nostres estudis indiquen que l'expressió transitòria de TRF2$^{\Delta B\Delta M}$ produeix un un dany telomèricque és deleteri per a les cèl·lules, evitant que aquestes proliferin i s'iniciïn cicles BFB i CIN.

Aquest efecte nociu s'havia descrit anteriorment en fibroblasts de ratolí i d'humà quan l'expressió del TRF2$^{\Delta B\Delta M}$ fou constitutiva o es va induir la deleció de TRF2 de les cèl·lules. A conseqüència, les cèl·lules en funció de la línia cel·lular entraven en senescència o bé induïen l'apoptosi (Steensel *et al*, 1998; Karlseder *et al*, 1999; Smogorzewska & de Lange, 2002; Jacobs & de Lange, 2004). En les MCF10A, no

s'han observat cèl·lules amb cossos apoptòtics o l'acumulació de debris al medi de cultiu compatible amb fenòmens d'apoptosi, ni tampoc un increment de cèl·lules amb marcatge de β-galactosidasa signe de senescència cel·lular després d'expressar TRF2$^{\Delta B\Delta M}$ durant 24 h o 96 h (**Treball II**). Tot plegat i conjuntament a L'absència de defectes en el perfil de cicle cel·lular de les cèl·lules tractades *versus* les no tractades, indicaria que la desprotecció massiva dels telòmers en una cèl·lula suposaria un senyal d'estrès massiu que conduiria a l'arrest cel·lular i posterior mort. Cal destacar que existeix una variabilitat en quant a l'expressió de TRF2$^{\Delta B\Delta M}$ en les línies cel·lulars generades. Aquesta variabilitat pot condicionar el nivell de desprotecció telomèrica que presenten les cèl·lules i la seva resposta al dany infligit. La clonació homogeneïtzaria l'expressió de TRF2$^{\Delta B\Delta M}$, i en conseqüència la desprotecció telomèrica, i permetria així una visió més acurada de la resposta cel·lular al dany telomèric ocasionat.

Estudis recents en fibroblasts humans han suggerit que una desprotecció telomèrica exagerada és la causa de la crisi cel·lular (Hayashi *et al*, 2015). Més concretament, la presència de fusions cromosòmiques provocaria un atur perllongat durant la mitosi cel·lular, durant el qual es promouria l'eliminació de proteïnes TRF2 del telòmer via Aurora B (Hayashi *et al*, 2012, 2015). Aquesta eliminació provocaria una desprotecció telomèrica massiva agreujant encara més el dany cel·lular, activant la DDR per sobre d'un llindar que conduiria a la mort cel·lular per mecanismes dependents (Hayashi *et al*, 2012) o independents de p53 (Hayashi *et al*, 2015). En el seu conjunt, els resultats obtinguts tant al **Treball II** com al **Treball III** anirien en concordança amb els resultats descrits pel laboratori del Dr. Karlseder (Hayashi *et al*, 2012, 2015), però amb certs matisos. En les MCF10A, l'exposició a 24 h sostingudes de TRF2$^{\Delta B\Delta M}$, produeix un nombre aproximat de 17 TIFs en les TO i les SH-TO (**Treball II**) mentre que en les línies cel·lulars epitelials amb p53 funcional presentarien menys de 5 TIFs (Kaul *et al*, 2012). Donat aquest model d'agreujament de la desprotecció telomèrica, podríem especular que el baix nombre de telòmers desprotegits de manera simultània en les vHMECs activaria la DDR localment, permetent a la cèl·lula reparar els extrems desprotegits via NHEJ i iniciar cicles BFB i CIN. Tanmateix, la progressiva erosió telomèrica conjuntament amb els DSBs derivats dels cicles BFB, conduiria a la coexistència d'un nombre més elevat d'extrems desprotegits i s'incrementaria el nivell de dany. La conjunció del dany genòmic i la desprotecció telomèrica mediada per Aurora B durant l'arrest mitòtic agreujaria el dany genòmic assegurant la correcta activació de la DDR i la mort cel·lular (Hayashi *et al*, 2012, 2015). Per altra banda, la desprotecció simultània d'un nombre elevat de telòmers mitjançant l'expressió del TRF2$^{\Delta B\Delta M}$ conduiria directament a les cèl·lules a un nivell d'activació de la DDR per sobre d'un llindar compatible amb la viabilitat cel·lular. A conseqüència, les cèl·lules restarien aturades o s'induiria l'apoptosi evitant així que les cèl·lules amb un elevat dany cel·lular i amb un potencial risc d'esdevenir inestables puguin continuar proliferant.

2. Immortalització de cèl·lules telomèricament estables o inestables

En el transcurs d'aquesta tesi s'ha treballat amb dues estratègies d'immortalització cel·lular. Per una banda s'ha reactivat la telomerasa mitjançant la transducció del seu domini catalític (hTERT) en cèl·lules vHMECs proficients i deficients per la proteïna p53 (**Treball I**). Per altra banda s'ha combinat la utilització d'hTERT amb la transducció de l'antigen Large T del virus SV40 (SV40LT) (**Treball III**). La utilització d'una o altra estratègia d'immortalització ha estat determinada per la necessitat d'inactivar conjuntament els *checkpoints* de cicle cel·lular.

Les vHMECs són cèl·lules finites i, tal com s'ha esmentat a l'apartat 4.1, sucumbeixen a l'agonescència (Romanov *et al*, 2001) o crisi (Garbe *et al*, 2007) en funció de la funcionalitat de p53. A finals dels anys 1990 va determinar-se que l'expressió ectòpica d'hTERT en fibroblasts humans permet allargar la longitud telomèrica tot evitant la senescència replicativa (Bodnar *et al*, 1998). De forma rellevant, en el procés d'immortalització de fibroblasts humans mitjançant la sobreexpressió d'hTERT poden diferenciar-se dues etapes de comportament. En una primera etapa, les cèl·lules presenten una dinàmica de creixement amb característiques pròpies de cèl·lules normals tals com: un cariotip diploide (Bodnar *et al*, 1998), la capacitat de diferenciació cel·lular, la inhibició per contacte (Milyavsky *et al*, 2003) o el creixement dependent d'ancoratge (Lee *et al*, 2004). En el cas concret de les cèl·lules epitelials mamàries, la introducció d'hTERT a PDs inicials després de la selecció permet mantenir un cariotip gairebé estable al llarg de com a mínim uns 130 PDs en cultiu (**Treball I**). Malgrat això, les cèl·lules que sobreexpressen hTERT acumulen diferents anomalies clonals, com és el cas de la trisomia del cromosoma 20 (Coursen *et al*, 1997; Toouli *et al*, 2002; Rao *et al*, 2003; Garbe *et al*, 2014) i que sembla estar relacionada amb el procés d'immortalització en si (Jin *et al*, 2004; Zhang *et al*, 2006a; Coursen *et al*, 1997; Savelieva *et al*, 1997; Liu *et al*, 2010). En una segona etapa i després de més de 150 PDs en cultiu, els fibroblasts humans immortalitzats es caracteritzen per presentar una taxa de proliferació cel·lular incrementada que no està limitada pel contacte entre cèl·lules (Milyavsky *et al*, 2003) i que fomenta una proliferació cel·lular descontrolada. Aquest canvi en la dinàmica de les cèl·lules s'ha relacionat amb una baixa expressió o la inactivació de $p16^{INK4a}$ (Milyavsky *et al*, 2003). D'acord amb aquests resultats, la inactivació de $p16^{INK4a}$ (característica que presenten les cèl·lules epitelials mamàries humanes *in vitro* (Brenner *et al*, 1998)) podria facilitar la seva immortalització i posterior deriva genètica. De fet, la inactivació de $p16^{INK4a}$ succeeix *in vivo* en la glàndula mamària de dones sanes (Holst *et al*, 2003), a més s'ha observat la presencia de fusions telomèriques a l'inici de la tumorigènesis mamària (Tanaka *et al*, 2012) el que voldria dir que la inactivació de p16 i la disfunció telomèrica afavoririen la inestabilitat cromosòmica. Els estudis realitzats amb les vHMECs que sobreexpressen hTERT (vHMEC-hTERT) se situen a un PD 130 i, tot i que presenta dos cromosomes marcadors, podríem considerar que aquestes cèl·lules no han patit una forta deriva genètica (**Treball I**). Així doncs, seria interessant determinar si les vHMECs-hTERT més enllà del PD 150 són susceptibles d'adquirir noves mutacions que li podrien atorgar una avantatge proliferativa que podria afavorir la transformació cel·lular.

Mentre que la immortalització de vHMECs a PDs inicials no produeix a mig termini una elevada CIN, l'expressió d'hTERT en cèl·lules telomèricament compromeses que presenten CIN, podria generar cèl·lules immortals cromosòmicament aberrants. De fet, es creu que la contínua reorganització del cariotip en cèl·lules immortals podria conduir a la generació d'un procés tumoral gràcies a l'estabilització de la longitud telomèrica. Però, en el cas concret de les vHMECs, la immortalització de les cèl·lules p53 proficients (vHMECs-p53$^{+/+}$) a PDs més avançats i que presentaven telòmers disfuncionals no es va aconseguir (**Treball I**). S'ha descrit que les vHMECs-p53$^{+/+}$ requereixen un temps de conversió durant el qual es produeixen canvis epigenètics i d'adaptació necessaris per adquirir finalment la immortalització completa (Stampfer *et al*, 1997, 2001, 2003). El temps de conversió oscil·la entre 10 i 30 passatges, i s'inicia per una fase d'immortalització condicional caracteritzada per la presència de telòmers excessivament curts (TRF ≤3 kb), creixement cel·lular lent i l'expressió de p57 (Stampfer *et al*, 1997) un regulador negatiu de la proliferació cel·lular (Guo *et al*, 2010). La immortalització completa, s'assoleix quan les cèl·lules no expressen p57, són capaces de créixer independentment del factor TGF-β, i la longitud telomèrica es situa entre els 3 i 7 kb (Stampfer *et al*, 1997). TGF-β és un regulador negatiu de la proliferació i possible inhibidor de l'expressió de la telomerasa (Li *et al*, 2006), per tant s'ha suggerit que l'expressió de hTERT requeriria un canvi epigenètic i induiria la resistència a l'acció del TGF-β (Stampfer *et al*, 2001). Així doncs, durant el temps de conversió en les nostres cèl·lules, l'activitat de la telomerasa era possiblement baixa i, aquest fet conjuntament amb l'absència de marcador de selecció en el constructe que permetés forçar la seva expressió (**Treball I**), probablement conduí a un escurçament de la longitud telomèrica i a l'acumulació d'un excessiu nombre de telòmers disfuncionals abans d'aconseguir la immortalització completa. Tot això suggereix que, per tal d'immortalitzar les vHMECs-p53$^{+/+}$ s'ha d'establir un equilibri entre la longitud telomèrica, la ratio de creixement i el temps de conversió. En altres paraules, les cèl·lules vHMEC-p53$^{+/+}$ immortalitzades seran aquelles que hauran assolit el procés de conversió abans de presentar un llindar de dany suficient capaç de desencadenar l'agonescència cel·lular.

S'ha descrit que aquest procés de conversió no ocorre en les vHMECs deficients per la proteïna p53 (vHMEC-p53$^{-/-}$) (Stampfer *et al*, 2003). Aquestes cèl·lules no expressen p57 i després de la transducció d'hTERT presenten un creixement cel·lular independent de TGF-β, assolint la immortalització cel·lular pocs PDs després de la transfecció/transducció de hTERT (Stampfer *et al*, 2003). Tot plegat suggeriria que la proteïna p53 estaria implicada en els canvis que ocorren entre la transducció d'hTERT i la completa immortalització cel·lular. Com s'ha esmentat, la immortalització de vHMECs en un ambient de disfunció telomèrica estaria regida per un llindar en el nombre de telòmers disfuncionals que evita una activació completa de la DDR. La inactivació de p53 permet una major tolerància al dany genòmic, visualitzat per l'acumulació de més reorganitzacions cromosòmiques en les cèl·lules vHMECs-shp53 (**Treball I i Treball II**) o en el nombre de TIFs basals en diferents tipus cel·lulars (Cesare *et al*, 2009; Kaul *et al*, 2012). Així doncs, aquestes dades suggeririen que les vHMECs-shp53 s'immortalitzarien ràpidament a un PD més avançat que les vHMECs-p53$^{+/+}$, la qual cosa queda demostrada al **Treball I** en la línia vHMEC estudiada. Tal i com s'ha comentat anteriorment, la presència d'inestabilitat cromosòmica en les vHMEC-shp53 s'incrementa amb els PDs, però el restabliment de la funcionalitat telomèrica mitjançant la sobreexpressió d'hTERT, immortalitza les cèl·lules (vHMECs-shp53-hTERT) i redueix dràsticament la inestabilitat cromosòmica present en aquestes. Tot i així, la reducció no és absoluta i les vHMEC-shp53-hTERT

segueixen presentant alguns cromosomes dicèntrics i fragments cromosòmics, i signes de cicles BFB com ara ponts anafàsics i cromatina retardada en la migració als pols durant la mitosi (**Treball I**). El manteniment d'un nivell baix d'inestabilitat permetria a les cèl·lules seguir proliferant i derivant genèticament. De fet, la CIN requereix un temps llarg de latència que, condicionada per l'atzar i l'evolució Darwiniana, podria originar una població altament reorganitzada o amb signes de transformació cel·lular (Weaver *et al*, 2007). Els tumors humans d'origen epitelial presenten una elevada heterogeneïtat cariotípica presentant translocacions recíproques, delecions, amplificacions, cromosomes dicèntrics, guanys i pèrdues de cromosomes i/o un cariotip quasi tetraploide(Mitelman *et al*, 2018). S'ha estimat que les cèl·lules cancerígenes presenten almenys 1 mutació en un oncogen, 3 mutacions en gens supressors de tumors, 3 amplificacions, 5 delecions, 2 guanys de cromosomes sencers, 2 pèrdues de cromosomes sencers, 12 delecions focals i 11 amplificacions focals (Zack *et al*, 2013; Davoli *et al*, 2013). L'elevada quantitat d'anomalies en cèl·lules tumorals contrasta amb el nombre d'anomalies obtingudes al immortalitzar amb hTERT cèl·lules vHMECs-shp53 telomèricament inestables (**Treball I**), indicant que per generar el cariotip altament reorganitzat de les cèl·lules tumorals és possiblement necessària la combinació de diferents mecanismes generadors de CIN. Entre aquests, es situen a més de la disfunció telomèrica (Maciejowski & de Lange, 2017; Bernal & Tusell, 2018), l'estrès replicatiu (Burrell *et al*, 2013), defectes en l'ancoratge i la segregació dels cromosomes (Ganem *et al*, 2009; Silkworth & Cimini, 2012) i mutacions/deficiències en proteïnes involucrades en la reparació del DNA (Sishc & Davis, 2017). Aquests mecanismes no són exclusius i podrien coexistir, provocant un efecte sinèrgic sobre la CIN el que afavoriria la transformació cel·lular.

Una altra estratègia emprada per immortalitzar cèl·lules en aquesta tesi va ser mitjançant la combinació d'hTERT amb l'antigen SV40LT (**Treball III**). Aquesta tàctica d'immortalització incloïa doncs la reactivació de la telomerasa i la inactivació de les vies de senyalització regulades per p53 i pRb. L'antigen SV40LT interfereix en la interacció de les proteïnes pRb-*pocket proteins* (pRb; p107; p130) amb els factors de transcripció E2F (E2F1-8) i, a més s'ha descrit que també interacciona amb p53, estabilitzant-la i bloquejant la seva interacció amb altres proteïnes [revisat per (Ahuja *et al*, 2005)]. Tal i com s'ha explicat en l'apartat 1.4 d'aquesta tesi, l'eliminació de TRF2 del telòmer desprotegeix el telòmer, activa la DDR i condueix la cèl·lula a la senescència cel·lular o l'apoptosi mediades per les proteïnes p53 i pRb (Karlseder *et al*, 1999). Per poder estudiar la resposta de cèl·lules primàries derivades de glàndula mamària a disfunció telomèrica induïda per TRF2$^{\Delta B\Delta M}$ i evitar l'efecte deleteri de l'expressió d'aquest, es van inactivar els *checkpoints* de cicle cel·lular mitjançant l'expressió de l'antigen SV40LT (**Treball III**). A més d'en les HMEC, l'antigen SV40LT també va utilitzar-se per inactivar els *checkpoints* de cicle cel·lular en les MCF10A, MCF-10A-SV-TO (**Treball II**). Curiosament, encara que va utilitzar-se el mateix constructe en les transduccions d'ambdós tipus de cèl·lules, l'expressió del SV40LT en les MCF10A s'acaba perdent (**Treball II**). Aquest fet s'ha descrit en cèl·lules epitelials mamàries humanes que presenten p16^{INK4a} inactivat (Huschtscha *et al*, 2001; Toouli *et al*, 2002). I s'ha suggerit que les vHMECs, apart de presentar la inactivació de p16^{INK4a}, presenten altres canvis epigenètics que impedirien la immortalització mitjançant l'antigen SV40LT (Huschtscha *et al*, 2001; Toouli *et al*, 2002). A partir d'aquí, podria suggerir-se que l'expressió del SV40LT podria inactivar-se o bé ser deleteri per les cèl·lules epitelials mamàries variants. A conseqüència de la pèrdua de l'antigen SV40LT en les MCF-10A, els efectes citogenètics de l'SV40LT

no són comparables a llarg termini en les dues línies cel·lulars. L'antigen SV40LT interacciona amb proteïnes relacionades amb la formació i l'estabilització dels microtúbuls, com TACC2 (Tei *et al*, 2009), i amb les proteïnes BUB1 i BUB3 relacionades amb el punt de control de la mitosi(Cotsiki *et al*, 2004). Aquestes interaccions provoquen la desestabilització dels microtúbuls (Tei *et al*, 2009) i defectes en la formació del fus (Tei *et al*, 2009) però eviten l'activació del punt de control de la mitosi (Cotsiki *et al*, 2004). Això comporta la generació d'errors en la segregació cromosòmica i es fomenta l'aneuploidïa i la tetrapoidització cel·lular al llarg de les divisions (Ray *et al*, 1992; Cotsiki *et al*, 2004; Hein *et al*, 2009). Coincidint amb aquestes observacions la pèrdua de l'SV40LT en les MCF10A-SV-TO evita l'acumulació d'anomalies numèriques amb els PDs (Treball II). Mentre que en les HMEC-hTERT-SV-TO, on l'antigen SV40LT no desapareix amb el temps, la població aneuploide i poliploide incrementa a mesura que passen els PDs (Treball III). Aquests resultats demostren els efectes colaterals de la inactivació de p53 i pRb mitjançant l'expressió de l'antigen SV40LT, ja que aquest interfereix en la funcionalitat de múltiples proteïnes. Per evitar aquests efectes i inactivar específicament p53 i pRb, altres estratègies podrien ser més idònies. Per exemple, les vHMECs podrien immortalitzar-se mitjançant les proteïnes E6 E7 del virus HPV-16, (Band *et al*, 1991; Wazer *et al*, 1995), les quals degraden p53 (Scheffner *et al*, 1993) i pRb (Boyer *et al*, 1996), no obstant aquesta immortalització també estaria lligada a l'increment de la inestabilitat cromosòmica (Coursen *et al*, 1997; Savelieva *et al*, 1997). També es podrien utilitzar altres procediments a l'ús de proteïnes víriques com és l'expressió de *short-hairpins* específics o la modificació gènica mitjançant la tecnologia CRISPR.

3. Telòmers disfuncionals, tetraploidització i carcinogènesis

Les cèl·lules procedents dels tumors epitelials presenten un genoma altament reorganitzant que es caracteritza per cariotips quasi tetraploides que presenten un gran ventall d'anomalies estructurals com numèriques (Mitelman *et al*, 2018). Diferents simulacions computacionals suggereixen que les tetraploides inestables són les responsables de l'elevada reorganització cromosòmica i heterogeneïtat cariotípica (Shackney *et al*, 1989; Laughney *et al*, 2015). La presència de múltiples centrosomes durant la divisió cel·lular de les cèl·lules tetraploides afavoreix la segregació anòmala dels cromosomes i una elevada taxa en la pèrdua d'aquests. Aquesta elevada l'heterogeneïtat genòmica facilitaria el ressorgiment d'una població altament reorganitzada i amb capacitat proliferativa a un menor cost a diferència de les cèl·lules diploides que no serien tan tolerables a la pèrdua de cromosomes i una elevada reorganització genòmica (Laughney *et al*, 2015). El potencial tumorigènic de les cèl·lules tetraploides inestables fou demostrat tant *in vitro* com *in vivo* en cèl·lules de ratolí (Fujiwara *et al*, 2005). Més concretament, les cèl·lules tetraploides inestables foren capaces de créixer de forma independent d'ancoratge i formar tumors quan foren injectades en ratolins immunodeprimits (Fujiwara *et al*, 2005).

La disfunció telomèrica origina cèl·lules tetraploides telomèricament inestables mitjançant endoreduplicació (Davoli *et al*, 2010; Davoli & de Lange, 2012) o regressió de la citocinesi, (Pampalona *et al*, 2012). Mentre que els fenòmens d'endoreduplicació són freqüents en fibroblasts humans, la regressió de la citocinesi és més pròpia de les cèl·lules epitelials mamàries humanes (Davoli & de Lange,

2012). De fet, l'estudi de diferents línies de vHMECs han demostrat que en totes elles es produeix un increment de la tetraploidització cel·lular a mesura que les cèl·lules van envellint, però el percentatge d'inducció és variable (Pampalona *et al*, 2012; Domínguez *et al*, 2015) (**Treball I**). Malgrat la creixent inducció de cèl·lules tetraploides en vHMECs-p53$^{+/+}$ a mesura que envelleixen en cultiu, quan aquestes s'immortalitzen mitjançant d'hTERT, la fracció tetraploide acaba desapareixent del cultiu (Pampalona *et al*, 2012) fent palès la seva incapacitat proliferativa. De fet, en les vHMECs-p53$^{+/+}$ no apareix un pic creixent de cèl·lules 8C en el citòmetre (Pampalona *et al*, 2012) (**Treball I**) demostrant que l'acumulació de cèl·lules tetraploides es produeix bàsicament per la continua regressió de l'anell contràctil en cèl·lules telomèricament inestables. De fet, la presència de p53 funcional en les cèl·lules tetraploides atura el cicle cel·lular a G1 evitant la proliferació de les cèl·lules tetraploides (Margolis *et al*, 2003). Recentment s'ha descrit que la via de senyalització supressora de tumors Hippo estaria implicada en l'arrest cel·lular de les cèl·lules tetraploides però no de les aneuploides (Ganem *et al*, 2014). La presència de centrosomes extres seria l'estímul per activar la via de senyalització Hippo que a través de la proteïna LATS2 estabilitzaria p53 i inhibiria els reguladors transcripcionals YAP1 i WWTR1 (Ganem *et al*, 2014). Aquests reguladors transcripcionals tenen un paper important en el control de la mida cel·lular, limiten la proliferació cel·lular i indueixen l'apoptosi (Gumbiner & Kim, 2014). Tot plegat aquesta via de senyalització arrestaria les cèl·lules tetraploides a G1 i evitaria la seva proliferació. Conseqüentment, la inactivació de p53 afavoriria la proliferació de cèl·lules tetraploides tal i com s'ha descrit a la literatura (Andreassen *et al*, 2001) i observat al **Treball I** i al **Treball II**. I no sols això, sinó que aquestes cèl·lules 4N presenten una taxa d'anomalies cromosòmiques més elevada que les cèl·lules p53 competents. La inactivació de p53 també permet l'acumulació d'anomalies, tals com cèl·lules quasi diploides i quasi tetraploides o la presència de centrosomes supernumeraris (Pantic *et al*, 2006). La presència de centrosomes supernumeraris durant la divisió cel·lular afavoreix les unions merotèliques entre els cinetocors i els microtúbuls i indueix la formació de divisions pseudobipolars o multipolars (Cimini *et al*, 2002; Ganem *et al*, 2009). Aquesta elevada reorganització cel·lular i la seva permissivitat conferiria noves característiques com el creixement independent d'ancoratge (Ho *et al*, 2010).

De forma rellevant, la reactivació de la telomerasa després d'un període de disfunció telomèrica alleugereix el dany telomèric i permet la progressió tumoral en models murins de càncer de pròstata i limfomes de les cèl·lules T (Ding *et al*, 2012; Hu *et al*, 2012). Tanmateix la transducció d'hTERT en cèl·lules vHMEC-p53$^{-/-}$ telomèricament inestables va disminuir dràsticament la població tetraploide i la taxa d'anomalies inestables com ara cromosomes dicèntrics (**Treball I**). Tot i aquesta reducció, les cèl·lules tetraploides persisteixen al cultiu, amb un nivell similar al que presenten les cèl·lules epitelials mamàries a un PD baix però a diferència, presenten una taxa d'anomalies cromosòmiques inestables més elevada que podrien anar reorganitzant el cariotip al llarg del temps (**Treball I**). S'ha descrit que l'estrès replicatiu és inherent en les cèl·lules tetraploides i afavoriria una elevada taxa d'errors de segregació que seria compatible amb la viabilitat cel·lular (Wangsa *et al*, 2018). Per tant, la confluència d'almenys quatre factors que són la inactivació de p53 (Ganem *et al*, 2014), la sobreexpressió d'hTERT (Ding *et al*, 2012), les divisions pseudobipolars o multipolars degudes a centrosomes supernumeraris (Ganem *et al*, 2009) i l'estrès replicatiu (Wangsa *et al*, 2018), podrien donar lloc amb el temps a una població tetraploide o quasi

tetraploide immortalitzada que evolucionés cariotípicament i adquirís característiques pròpies de la transformació cel·lular.

Fenòmens de tetraploidització cel·lular també s'observen quan es modifiquen les proteïnes shelterin (Davoli *et al*, 2010; Davoli & de Lange, 2012), indicant que aquest és un efecte intrínsec a la disfunció telomèrica. A més, la disfunció condicional de POT1A en fibroblasts de ratolí que expressaven SV40LT va induir la formació de cèl·lules tetraploides inestables les quals van ser capaces de créixer de forma independent d'ancoratge i de generar tumors en ratolins immunodeprimits (Davoli & de Lange, 2012). Els tumors originats a partir d'aquestes cèl·lules 4N presentaven un cariotip quasi tetraploide, que suggereix que les cèl·lules tetraploides inestables presenten una evolució cariotípica que afavoreix la pèrdua de cromosomes (Davoli & de Lange, 2012). De fet, les divisions multipolars i les divisions pseudobipolars són responsables de l'elevada plasticitat de les cèl·lules tetraploides [revisat per (Vitale et al, 2011)]. Aquests resultats ens van animar a determinar si la disfunció telomèrica mitjançant l'expressió intermitent de TRF2$^{\Delta B\Delta M}$ en cèl·lules epitelials mamàries humanes també era capaç d'originar cèl·lules tetraploides potencialment tumorigèniques (**Treball II** i **Treball III**).

Després de derivar HMECs directament de teixit glandular, es van generar diferents línies cel·lular immortals que expressaven TRF2$^{\Delta B\Delta M}$ de forma condicional i regulada per doxiciclina (**Treball III**). Es van realitzar un mínim de 5 cicles intermitents de disfunció telomèrica i es va valorar el potencial tumorigènic de les cèl·lules resultants. Una estratègia per testar *in vitro* el potencial transformador de les cèl·lules és mitjançant el seu cultiu en matrius tridimensionals. En Matrigel, les cèl·lules epitelials mamàries no tumorals tendeixen a originar *acini* organitzats i lúmens buits, mentre que les tumorals tendeixen a formar estructures no polaritzades (Petersen *et al*, 1992) i desorganitzades i que podrien evitar la formació del lumen del *acini* (Debnath *et al*, 2002) o inclús envair-lo. L'anàlisi de quatre línies cel·lulars que havien patit diversos cicles de doxiciclina i que presentaven una taxa de tetraploidització d'entre 11% i 49% no mostraren diferencies substancials entre elles que indicaren algun efecte diferencial (**Treball III**). Les diferències observades entre els grups control i els grups que van patir cicles de protecció-desprotecció telomèrica semblen estar lligades al llinatge majoritari que presentava cadascuna de les línies cel·lulars generades (**Treball III**). S'ha descrit que el perfil genètic pot condicionar la morfologia que presenten els *acini* formats (Kenny *et al*, 2007). Els *acini* del tipus estrellat presenten un fenotip més invasiu i estan formats per cèl·lules basals del subtipus B, les quals expressen vimentina i un perfil d'expressió propi de les cèl·lules mare i podrien estar relacionats amb els tumors triple-negatius (Neve *et al*, 2006). Les línies cel·lulars emprades en aquesta tesi presenten algunes similituds amb els *acini* derivats de cèl·lules tumorals, com l'absència de lumen buit, una estructura acinar desorganitzada, i en alguns casos una estructura més invasiva. Però no ens demostren el potencial tumorigènic que podrien tenir aquestes cèl·lules, tant les cèl·lules que no havien patit cicles de disfunció telomèrica com les que si.

El potencial tumorigènic va ser testat en ratolins immunodeprimits després de separar les cèl·lules diploides i poliploides originades després de diversos cicles de protecció-desprotecció telomèrica. Però, a diferència de l'estudi de Davoli & de Lange, 2012 en cèl·lules murines, les cèl·lules humanes tetraploides no van ser capaces de generar tumors (**Treball III**). Cal destacar que l'anàlisi del cariotip de les cèl·lules

HMECs-hTERT-SV-TO a PD avançats que no havien rebut doxiciclina va demostrar en totes elles uns alts nivells de poliploidització cel·lular (Treball III). Aquests resultats, conjuntament amb la baixa incidència de fusions telomèriques i reorganitzacions cromosòmiques secundaries derivades dels cicles BFB en les HMECs-hTERT-SV-TO induïdes, demostrarien que l'expressió de l'antigen SV40LT és el responsable de l'increment en la ploïdia cel·lular observada, tal i com ha estat prèviament descrit (Ray *et al*, 1992; Cotsiki *et al*, 2004; Tei *et al*, 2009; Hein *et al*, 2009). De fet, aquest increment de la poliploïdia estaria associat al procés d'immortalització de les cèl·lules HMEC mitjançant l'antigen SV40LT, el qual hauria interferit en l'anàlisi dels efectes de la disfunció de la proteïna TRF2 en les cèl·lules epitelials mamàries humanes emprades en el Treball III. Tant mateix, la CIN associada a la presencia de SV40LT no és suficient per induir la formació de tumors en ratolins immunodeprimits (Treball III), i per tant, es requeriria d'altres estímuls com una elevada expressió de H-RAS per transformar les cèl·lules (Elenbaas *et al*, 2001). Aquesta manca de desenvolupament tumoral descrita al Treball III contrasta amb els estudis murins en els quals es desenvolupen carcinomes hepatocel·lulars desrpés d'inocular cèl·lules telomèricament inestables que havien expressat intermitentment TRF2$^{\Delta B\Delta M}$ (Begus-Nahrmann *et al*, 2012). L'expressió de la telomerasa en cèl·lules que presentaven CIN depenent de disfunció telomèrica afavoriria la viabilitat de les cèl·lules inestables i promouria el desenvolupament tumoral (Begus-Nahrmann *et al*, 2012). L'absència d'evidències tant *in vivo* com *in vitro* que impliquin la disfunció telomèrica transitòria deguda a l'expressió del TRF2$^{\Delta B\Delta M}$ en cèl·lules epitelials humanes amb el desenvolupament tumoral suggereix que les cèl·lules murines i les cèl·lules epitelials mamàries humanes no es comporten igual. En el seu conjunt, suggeriria que el control exercit sobre la proliferació cel·lular en cèl·lules humanes és possiblement més rigorós que en les cèl·lules de ratolí.

Les cèl·lules de ratolí expressen constitutivament la telomerasa i la seva proliferació no està condicionada per l'escurçament telomèric. No obstant, l'escurçament telomèric degut a l'absència de la telomerasa en cèl·lules TERC$^{-/-}$ murines (Lee *et al*, 1998), i la inactivació de p53 (Chin *et al*, 1999) afavoreixen la formació de carcinomes amb una elevada inestabilitat cromosòmica (Artandi *et al*, 2000). Aquests tumors tindrien un límit proliferatiu degut a l'escurçament exagerat de la longitud telomèrica i posterior crisi cel·lular (Ding *et al*, 2012). La reactivació de la telomerasa estabilitzaria aquest dany i obriria un nou horitzó en el desenvolupament tumoral (Hu *et al*, 2012; Ding *et al*, 2012). Per contra, les cèl·lules humanes requeririen de múltiples mutacions que afectarien a les proteïnes supressores de tumors com p53, pRb, proteïnes implicades en la proliferació cel·lular com les pertanyents a la família RAS i l'estabilització telomèrica (Elenbaas *et al*, 2001; Rao *et al*, 2003; Ince *et al*, 2007), entre d'altres (Hanahan & Weinberg, 2011).

4. Consideracions finals

Les cèl·lules tumorals poden presentar una elevada heterogeneïtat genòmica associada a la CIN. Diferents estudis suggereixen que els nivells de CIN han de mantenir-se en un rang òptim, ni molt alta ni molt baixa, per tal d'originar i perpetuar una població cromosòmicament inestable (Bakhoum & Landau, 2017). Si els nivell de CIN són baixos, la penetrància de les reorganitzacions cromosòmiques serà baixa. Per contra, elevats nivells de CIN podrien ser letals per la cèl·lula o originar cèl·lules filles no viables (Kops *et al*, 2004; Weaver *et al*, 2007; Ganem *et al*, 2009; Janssen *et al*, 2009). Per tant, per iniciar el procés tumoral i

promoure la seva evolució caldria una CIN capaç de generar una elevada plasticitat cariotípica que fos permissiva amb la viabilitat cel·lular (Bakhoum & Landau, 2017).

La disfunció telomèrica podria ser descrita com un mecanisme dual en el manteniment de la integritat genòmica, que evita la proliferació d'aquelles cèl·lules amb telòmers curts o bé promou la CIN que afavoriria la generació d'una població susceptible a la transformació cel·lular. Aquesta dualitat dependria principalment de la funcionalitat dels *checkpoints* cel·lulars i la estabilització de la funcionalitat telomèrica. El **Treball I** mostra com l'escurçament telomèric pot ser inductor de CIN i possiblement promotor de la transformació cel·lular. Per contra, el **Treball II** i l'**Treball III** mostren que la disfunció telomèrica deguda a disfunció de TRF2 evita la proliferació de cèl·lules amb una agreujada disfunció telomèrica. Aquesta doble acció és possiblement deguda al nivell de dany ocorregut al telòmer. En el cas de la disfunció telomèrica deguda a escurçament telomèric progressiu (**Treball II**), quan un o varis telòmers queden desprotegits alhora el dany és reparat immediatament en forma de fusió cromosòmica. Un cop reparat, la cèl·lula pot seguir proliferant, tot i que la presència de fusions cromosòmiques poden iniciar cicles BFB, derivant llavors en CIN i l'evolució contínua del cariotip. Per altra banda, la disfunció de les proteïnes shelterin provoca un dany telomèric global que seria letal per la viabilitat cel·lular. Específicament, l'absència de proteïna TRF2 causa l'obertura del llaç telomèric i exposa els extrems cromosòmics a les proteïnes implicades en la senyalització i reparació del dany genòmic. L'excessiva desprotecció telomèrica derivada de l'expressió del mutant TRF2$^{\Delta B\Delta M}$ provoca un elevat dany cel·lular, indueix una forta aturada del cicle cel·lular i promouria la mort cel·lular. El dany telomèric infligit, inclús quan l'expressió del TRF2$^{\Delta B\Delta M}$ ocorre en breus cicles de desprotecció, impedeix el ressorgiment d'una població inestable deguda a l'expressió del TRF2$^{\Delta B\Delta M}$. De fet, el **Treball II** i l'**Treball III** demostren que la desprotecció massiva i de forma simultània dels telòmers indueix un dany tal que evita la proliferació cel·lular. Aquests **Treballs II** i **III** reforcen l'existència d'un mecanisme addicional per tal de mantenir la integritat genòmica de les cèl·lules humanes.

Recentment, diferents estudis *in vitro* proposen la utilització de les proteïnes shelterin TRF1 (Bejarano *et al*, 2017; García-Beccaria *et al*, 2015) i TRF2 (Bai *et al*, 2014; Di Maro *et al*, 2014) com a dianes terapèutiques per lluitar contra el càncer. Aquesta proposta es basaria en la forta activació de la DDR i la disminució del creixement cel·lular quan aquestes s'eliminen del telòmer. Més concretament, la deleció de *Trf1* en un model murí de glioblastoma i de càncer de pulmó redueix la mida dels tumors i incrementa la supervivència dels ratolins independentment de la longitud telomèrica (Bejarano *et al*, 2017; García-Beccaria *et al*, 2015). Per altra banda, la inhibició de TRF2 mitjançant *short-hairpin* en cèl·lules de glioblastoma inhibeix la proliferació de cèl·lules mare i promou la diferenciació cel·lular, l'arrest cel·lular i l'apoptosi (Bai *et al*, 2014). Aquests efectes afavoreixen la supervivència dels ratolins xenotransplantats amb cèl·lules humanes de glioblastoma modificades genèticament (Bai *et al*, 2014). Tanmateix, la inhibició de les proteïnes shelterin mitjançant adenovirus (García-Beccaria *et al*, 2015) i lentivirus (**Treball II; Treball III**) (Bai *et al*, 2014; Bejarano *et al*, 2017) per tal d'introduir els gens d'interès en humans *in vivo* pot suposar problemes de bioseguretat, tècnics i ètics, degut a la introducció al cos de partícules virals. Per aquest motiu és important desenvolupar diferents inhibidors sintètics (García-Beccaria *et al*, 2015; Di Maro *et al*, 2014) podrien obrir noves estratègies de tractament anti-tumoral.

Conclusions

1. Progressive telomere shortening results in a telomere insult that is permissive with cell viability and allows the reorganisation of the genome through telomere-dependent CIN. But, once telomere damage exceeds a certain threshold, cells succumb to agonescence or crisis. The immortalisation of telomere unstable cells results in a dramatic reduction of CIN levels, as telomerase reactivation relieves telomere damage. Albeit this reduction the p53-deficient, immortalised cells still display some degree of instability that, with continuous proliferation, could probably evolve to originate a highly reorganised unstable cell line.

2. Brief periods of massive telomere deprotection due to shelterin dysfunction prevents the emergence of CIN in immortalised human cell lines. After TRF2 depletion, signs of telomere deprotection such as TIFs and end-to-end fusions are evident. But once telomere protection is restored, scars of ongoing BFB-cycles and the emergence of unstable cells are unnoticed, thus evincing a withdrawal of damaged cells. Therefore, the deprotection of many telomeres simultaneously might exceed a damage threshold that prevents proliferation of cells that could be at risk of transformation.

3. Successive periods of shelterin dysfunction in hTERT- and SV40LT-immortalised human primary mammary epithelial cells also impeded the generation of telomere-compromised unstable cells, though cells developed reorganised karyotypes due to SV40-LT transformation side-effects. Nonetheless, none of the reorganised cells displayed tumourigenic features in three dimensional cultures nor formed tumours in immunocompromised mice, thus suggesting that a reorganised karyotype showing diploid- and tetraploid-unstable cells is not enough for the onset of human mammary carcinogenesis.

4. The level of telomere damage controls the proliferative limits of the cell. Progressive telomere shortening results in a minor telomere damage that promotes DNA repair and is compatible with cell viability. This proliferative extension is at the expense of CIN emergence, through the initiation of BFB-cycles. In contrast, the simultaneous confluence of a high number of unprotected telomeres, due to the TRF2 displacement, exceeds a damage threshold that prevents cell cycle progression of those cells suffering severe telomere uncapping. Overall, severe telomere deprotection emerges as an universal strategy to quickly impair the growth of dividing cells and, specifically, cancer cells under the new concept of “too much telomeric damage is lethal”.

Bibliography

Abreu E, Aritonovska E, Reichenbach P, Cristofari G, Culp B, Terns RM, Lingner J & Terns MP (2010) TIN2-tethered TPP1 recruits human telomerase to telomeres in vivo. *Mol. Cell. Biol.* 30: 2971–82

Ahuja D, Sáenz-Robles MT & Pipas JM (2005) SV40 large T antigen targets multiple cellular pathways to elicit cellular transformation. *Oncogene* 24: 7729–7745

Akbay EA, Peña CG, Ruder D, Michel JA, Nakada Y, Pathak S, Multani AS, Chang S & Castrillon DH (2013) Cooperation between p53 and the telomere-protecting shelterin component Pot1a in endometrial carcinogenesis. *Oncogene* 32: 2211–2219

Allsopp RC, Vaziri H, Patterson C, Goldstein S, Younglai E V, Futcher AB, Greider CW & Harley CB (1992) Telomere length predicts replicative capacity of human fibroblasts. *Proc.Natl.Acad.Sci.U.S.A* 89: 10114–10118

Amiard S, Doudeau M, Pinte S, Poulet A, Lenain C, Faivre-Moskalenko C, Angelov D, Hug N, Vindigni A, Bouvet P, Paoletti J, Gilson E & Giraud-Panis M-J (2007) A topological mechanism for TRF2-enhanced strand invasion. *Nat. Struct. Mol. Biol.* 14: 147–54

Andreassen PR, Lohez OD, Lacroix FB & Margolis RL (2001) Tetraploid state induces p53-dependent arrest of nontransformed mammalian cells in G1. *Mol. Biol. Cell* 12: 1315–28

Aoude LG, Pritchard AL, Robles-Espinoza CD, Wadt K, Harland M, Choi J, Gartside M, Quesada V, Johansson P, Palmer JM, Ramsay AJ, Zhang X, Jones K, Symmons J, Holland EA, Schmid H, Bonazzi V, Woods S, Dutton-Regester K, Stark MS, et al (2015) Nonsense mutations in the shelterin complex genes ACD and TERF2IP in familial melanoma. *J. Natl. Cancer Inst.* 107: 1–7

Arat NÖ & Griffith JD (2012) Human Rap1 interacts directly with telomeric DNA and regulates TRF2 localization at the telomere. *J. Biol. Chem.* 287: 41583–41594

Armstrong CA & Tomita K (2017) Fundamental mechanisms of telomerase action in yeasts and mammals: understanding telomeres and telomerase in cancer cells. *Open Biol.* 7: 160338

Arnoult N & Karlseder J (2015) Complex interactions between the DNA-damage response and mammalian telomeres. *Nat Struct Mol Biol* 22: 859–866

Artandi SE, Chang S, Lee SL, Alson S, Gottlieb GJ, Chin L & DePinho RA (2000) Telomere dysfunction promotes non-reciprocal translocations and epithelial cancers in mice. *Nature* 406: 641–645

Artandi SE & DePinho RA (2010) Telomeres and telomerase in cancer. *Carcinogenesis* 31: 9–18

Audebert M, Salles B & Calsou P (2004) Involvement of poly(ADP-ribose) polymerase-1 and XRCC1/DNA ligase III in an alternative route for DNA double-strand breaks rejoining. *J. Biol. Chem.* 279: 55117–55126

Bae NS & Baumann P (2007) A RAP1/TRF2 complex inhibits Nonhomologous End-Joining at human telomeric DNA ends. *Mol. Cell* 26: 323–334

Bai Y, Lathia JD, Zhang P, Flavahan W, Rich JN & Mattson MP (2014) Molecular targeting of TRF2 suppresses the growth and tumorigenesis of glioblastoma stem cells. *Glia* 62: 1687–1698

Bailey SM, Cornforth MN, Kurimasa A, Chen DJ & Goodwin EH (2001) Strand-specific postreplicative processing of mammalian telomeres. *Science* 293: 2462–2465

Bainbridge MN, Armstrong GN, Gramatges MM, Bertuch AA, Jhangiani SN, Doddapaneni H, Lewis L, Tombrello J, Tsavachidis S, Liu Y, Jalali A, Plon SE, Lau CC, Parsons DW, Claus EB, Barnholtz-Sloan J, Il'yasova D, Schildkraut J, Ali-Osman F, Sadetzki S, et al (2015) Germline mutations in shelterin complex genes are associated with familial glioma. *J. Natl. Cancer Inst.* 107: 4–7

Bakhoum SF & Landau DA (2017) Chromosomal instability as a driver of tumor heterogeneity and evolution. *Cold Spring Harb. Perspect. Med.* 7: a029611

Band V, Caprio JA De, Delmolino L, Kulesa V & Sager R (1991) Loss of p53 protein in human papillomavirus type 16 E6-immortalized human mammary epithelial cells. *J. Virol.* 65: 6671–6

Bartkova J, Horejsi Z, Koed K, Krämer A, Tort F, Zieger K, Guldberg P, Sehested M, Nesland JM, Lukas C, Orntoft T, Lukas J & Bartek J (2005) DNA damage response as a candidate anti-cancer barrier in early human tumorigenesis. *Nature* 434: 864–70

Baumann P & Cech TR (2001) Pot1, the putative telomere end-binding protein in fission yeast and humans. *Science* 292: 1171–5

Baumann P, Podell E & Cech TR (2002) Human POT1 (Protection of Telomeres) Protein:

cytolocalization, gene structure, and alternative splicing. *Mol. Cell. Biol.* 22: 8079–8087

Beauséjour CM, Krtolica A, Galimi F, Narita M, Lowe SW, Yaswen P & Campisi J (2003) Reversal of human cellular senescence: Roles of the p53 and p16 pathways. *EMBO J.* 22: 4212–4222

Begus-Nahrmann Y, Hartmann D, Kraus J, Eshraghi P, Scheffold A, Grieb M, Rasche V, Schirmacher P, Lee HW, Kestler HA, Lechel A & Rudolph KL (2012) Transient telomere dysfunction induces chromosomal instability and promotes carcinogenesis - Supplemental methods. *J. Clin. Invest.* 122: 2283–2288

Bejarano L, Schuhmacher AJ, Méndez M, Megías D, Blanco-Aparicio C, Martínez S, Pastor J, Squatrito M & Blasco MA (2017) Inhibition of TRF1 telomere protein impairs tumor initiation and progression in glioblastoma mouse models and patient-derived xenografts. *Cancer Cell* 32: 590–607.e4

Bernal A & Tusell L (2018) Telomeres: Implications for Cancer Development. *Int. J. Mol. Sci.* 19: 294

Bianchi A & Shore D (2007) Increased association of telomerase with short telomeres in yeast. *Genes Dev.* 21: 1726–1730

Blackburn E & Gall J (1978) A tandemly repeated sequence at the termini of the extrachromosomal ribosomal RNA genes in Tetrahymena. *J. Mol. Biol.* 120: 33–53

Blasco MA, Lee H-W, Hande MP, Samper E, Lansdorp PM, DePinho RA & Greider CW (1997) Telomere shortening and tumor formation by mouse cells lacking telomerase RNA. *Cell* 91: 25–34

Bodnar AG, Quellette M, Frolkis M, Holt SE, Chiu C-P, Morin GB, Harley CB, Shay JW, Lichtsteiner S & Wright WE (1998) Extension of life-span by introduction of telomerase into normal human cells. *Science* 279: 349–352

Bosco N & de Lange T (2012) A TRF1-controlled common fragile site containing interstitial telomeric sequences. *Chromosoma* 121: 465–474

Boyer SN, Wazer DE & Band V (1996) E7 protein of human papilloma virus-16 induces degradation of retinoblastoma protein through the ubiquitin-proteasome pathway. *Cancer Res.* 56: 4620–4624

Brenner AJ, Stampfer MR & Aldaz CM (1998) Increased p16 expression with first senescence arrest in human mammary epithelial cells and extended growth capacity with p16 inactivation. *Oncogene* 17: 199–205

Brinkley BR (2001) Managing the centrosome numbers game: From chaos to stability in cancer cell division. *Trends Cell Biol.* 11: 18–21

Broccoli D, Smogorzewska A, Chong L & de Lange T (1997) Human telomeres contain two distinct Myb-related proteins, TRF1 and TRF2. *Nat. Genet.* 17: 231–5

Bryan TM, Englezou A, Gupta J, Bacchetti S & Reddel RR (1995) Telomere elongation in immortal human cells without detectable telomerase activity. *Embo J* 14: 4240–4248

Bryan TM & Reddel RR (1997) Telomere dynamics and telomerase activity in in vitro immortalised human cells. *Eur. J. Cancer* 33: 767–773

Bunting SF, Callén E, Wong N, Chen HT, Polato F, Gunn A, Bothmer A, Feldhahn N, Fernandez-Capetillo O, Cao L, Xu X, Deng CX, Finkel T, Nussenzweig M, Stark JM & Nussenzweig A (2010) 53BP1 inhibits homologous recombination in Brca1-deficient cells by blocking resection of DNA breaks. *Cell* 141: 243–254

Burrell R a, McClelland SE, Endesfelder D, Groth P, Weller M-C, Shaikh N, Domingo E, Kanu N, Dewhurst SM, Gronroos E, Chew SK, Rowan AJ, Schenk A, Sheffer M, Howell M, Kschischo M, Behrens A, Helleday T, Bartek J, Tomlinson IP, et al (2013) Replication stress links structural and numerical cancer chromosomal instability. *Nature* 494: 492–6

Buscemi G, Zannini L, Fontanella E, Lecis D, Lisanti S & Delia D (2009) The shelterin protein TRF2 inhibits Chk2 activity at telomeres in the absence of DNA damage. *Curr. Biol.* 19: 874–879

Calsou P, Delteil C, Frit P, Drouet J & Salles B (2003) Coordinated assembly of Ku and p460 subunits of the DNA-dependent protein kinase on DNA ends is necessary for XRCC4-ligase IV recruitment. *J. Mol. Biol.* 326: 93–103

Calvete O, Martinez P, Garcia-Pavia P, Benitez-Buelga C, Paumard-Hernández B, Fernandez V,

Dominguez F, Salas C, Romero-Laorden N, Garcia-Donas J, Carrillo J, Perona R, Trivinõ JC, Andrés R, Cano JM, Rivera B, Alonso-Pulpon L, Setien F, Esteller M, Rodriguez-Perales S, et al (2015) A mutation in the POT1 gene is responsible for cardiac angiosarcoma in TP53-negative Li-Fraumeni-like families. *Nat. Commun.* 6: 8383

Campisi J & d'Adda di Fagagna F (2007) Cellular senescence: when bad things happen to good cells. *Nat. Rev. Mol. Cell Biol.* 8: 729–740

Cannavo E, Cejka P & Kowalczykowski SC (2013) Relationship of DNA degradation by Saccharomyces cerevisiae Exonuclease 1 and its stimulation by RPA and Mre11-Rad50-Xrs2 to DNA end resection. *Proc. Natl. Acad. Sci.* 110: E1661–E1668

Carter SL, Eklund AC, Kohane IS, Harris LN & Szallasi Z (2006) A signature of chromosomal instability inferred from gene expression profiles predicts clinical outcome in multiple human cancers. *Nat. Genet.* 38: 1043–1048

Ceccaldi R, Rondinelli B & Andrea ADD (2016) Repair pathway choices and consequences at the DSB. *Trends* 26: 52–64

Celli GB, Denchi EL & de Lange T (2006) Ku70 stimulates fusion of dysfunctional telomeres yet protects chromosome ends from homologous recombination. *Nat. Cell Biol.* 8: 885–90

Celli GB & de Lange T (2005) DNA processing is not required for ATM-mediated telomere damage response after TRF2 deletion. *Nat. Cell Biol.* 7: 712–8

Cesare AJ & Griffith JD (2004) Telomeric DNA in ALT cells is characterized by free telomeric circles and heterogeneous t-loops. *Mol Cell Biol* 24: 9948–9957

Cesare AJ, Hayashi MT, Crabbe L & Karlseder J (2013) The telomere deprotection response is functionally distinct from the genomic DNA damage response. *Mol. Cell* 51: 141–155

Cesare AJ & Karlseder J (2013) A three-state model of telomere control over human proliferative boundaries. *Curr. Opin. Cell Biol.* 24: 731–738

Cesare AJ, Kaul Z, Cohen SB, Napier CE, Pickett HA, Neumann AA & Reddel RR (2009) Spontaneous occurrence of telomeric DNA damage response in the absence of chromosome fusions. *Nat Struct Mol Biol* 16: 1244–1251

Cesare AJ, Quinney N, Willcox S, Subramanian D & Griffith JD (2003) Telomere looping in P. sativum (common garden pea). *Plant J.* 36: 271–279

Cesare AJ & Reddel RR (2010) Alternative lengthening of telomeres: models, mechanisms and implications. *Nat. Rev. Genet.* 11: 319–330

Chen LY, Redon S & Lingner J (2012) The human CST complex is a terminator of telomerase activity. *Nature* 488: 540–544

Chen Y, Rai R, Zhou ZR, Kanoh J, Ribeyre C, Yang Y, Zheng H, Damay P, Wang F, Tsujii H, Hiraoka Y, Shore D, Hu HY, Chang S & Lei M (2011) A conserved motif within RAP1 has diversified roles in telomere protection and regulation in different organisms. *Nat. Struct. Mol. Biol.* 18: 213–223

Chen Y, Yang Y, Overbeek M van, Donigian JR, Baciu P, de Lange T & Lei M (2008) A shared docking motif in TRF1 and TRF2 used for differential recruitment of telomeric proteins. *Science* 319: 1092–1096

Cheng Q, Barboule N, Frit P, Gomez D, Bombarde O, Couderc B, Ren GS, Salles B & Calsou P (2011) Ku counteracts mobilization of PARP1 and MRN in chromatin damaged with DNA double-strand breaks. *Nucleic Acids Res.* 39: 9605–9619

Chiang YJ, Kim S-H, Tessarollo L, Campisi J & Hodes RJ (2004) Telomere-associated protein TIN2 is essential for early embryonic development through a telomerase-independent pathway. *Mol. Cell. Biol.* 24: 6631–6634

Chin K, de Solorzano CO, Knowles D, Jones A, Chou W, Rodriguez EG, Kuo W-L, Ljung B-M, Chew K, Myambo K, Miranda M, Krig S, Garbe J, Stampfer M, Yaswen P, Gray JW & Lockett SJ (2004) In situ analyses of genome instability in breast cancer. *Nat. Genet.* 36: 984–8

Chin L, Artandi SE, Shen Q, Tam A, Lee S-L, Gottlieb GJ, Greider CW & DePinho RA (1999) p53 deficiency rescues the adverse effects of telomere loss and cooperates with telomere dysfunction to accelerate carcinogenesis. *Cell* 97: 527–538

Chong L, van Steensel B, Broccoli D, Erdjument-Bromage H, Hanish J, Tempst P & de Lange T (1995) Human Telomeric Protein. *Science* 270: 1663–7

Cimini D, Fioravanti D, Salmon ED & Degrassi F (2002) Merotelic kinetochore orientation versus chromosome mono-orientation in the origin of lagging chromosomes in human primary cells. *J. Cell Sci.* 115: 507–15

Cotsiki M, Lock RL, Cheng Y, Williams GL, Zhao J, Perera D, Freire R, Entwistle A, Golemis EA, Roberts TM, Jat PS & Gjoerup OV (2004) Simian virus 40 large T antigen targets the spindle assembly checkpoint protein Bub1. *Natl. Acad. Sci. USA* 101: 947–952

Coursen JD, Bennett WP, Gollahon L, Shay JW & Harris CC (1997) Genomic instability and telomerase activity in human bronchial epithelial cells during immortalization by human papillomavirus-16 E6 and E7 genes. *Exp. Cell Res.* 235: 245–253

D'Alcontres MS, Palacios JA, Mejias D & Blasco MA (2014) TopoIIα prevents telomere fragility and formation of ultra thin DNA bridges during mitosis through TRF1-dependent binding to telomeres. *Cell Cycle* 13: 1463–1481

Davoli T, Denchi EL & de Lange T (2010) Persistent telomere damage induces bypass of mitosis and tetraploidy. *Cell* 141: 81–93

Davoli T & de Lange T (2012) Telomere-driven tetraploidization occurs in human cells undergoing crisis and promotes transformation of mouse cells. *Cancer Cell* 21: 765–776

Davoli T, Xu AW, Mengwasser KE, Sack LM, Yoon JC, Park PJ & Elledge SJ (2013) Cumulative haploinsufficiency and triplosensitivity drive aneuploidy patterns and shape the cancer genome. *Cell* 155: 948–962

Debnath J, Mills KR, Collins NL, Reginato MJ, Muthuswamy SK & Brugge JS (2002) The role of apoptosis in creating and maintaining luminal space within normal and oncogene-expressing mammary acini. *Cell* 111: 29–40

Denchi EL & de Lange T (2007) Protection of telomeres through independent control of ATM and ATR by TRF2 and POT1. *Nature* 448: 1068–1071

DePinho RA (2000) The age of cancer. *Nature* 408: 248–254

Dimitrova N, Chen Y-CM, Spector DL & de Lange T (2008) 53BP1 promotes non-homologous end joining of telomeres by increasing chromatin mobility. *Nature* 456: 524–528

Ding Z, Wu CJ, Jaskelioff M, Ivanova E, Kost-Alimova M, Protopopov A, Chu GC, Wang G, Lu X, Labrot ES, Hu J, Wang W, Xiao Y, Zhang H, Zhang J, Zhang J, Gan B, Perry SR, Jiang S, Li L, et al (2012) Telomerase reactivation following telomere dysfunction yields murine prostate tumors with bone metastases. *Cell* 148: 896–907

Dionne I & Wellinger RJ (1996) Cell cycle-regulated generation of single-stranded G-rich DNA in the absence of telomerase. *Proc Natl Acad Sci U S A* 93: 13902–13907

Doksani Y, Wu JY, de Lange T & Zhuang X (2013) Super-resolution fluorescence imaging of telomeres reveals TRF2-dependent t-loop formation. *Cell* 155: 345–356

Domínguez D, Feijoo P, Bernal A, Ercilla A, Agell N, Genescà A & Tusell L (2015) Centrosome aberrations in human mammary epithelial cells driven by cooperative interactions between p16 INK4a deficiency and telomere-dependent genotoxic stress. *Oncotarget* 6: 28238–28256

Dunham M a, Neumann A a, Fasching CL & Reddel RR (2000) Telomere maintenance by recombination in human cells. *Nat. Genet.* 26: 447–450

Egan ED & Collins K (2010) Specificity and stoichiometry of subunit interactions in the human telomerase holoenzyme assembled in vivo. *Mol. Cell. Biol.* 30: 2775–2786

Elenbaas B, Spirio L, Koerner F, Fleming MD, Zimonjic DB, Donaher JL, Popescu NC, Hahn WC & Weinberg R a (2001) Human breast cancer cells generated by oncogenic transformation of primary mammary epithelial cells. *Genes Dev.* 15: 50–65

Else T, Trovato A, Kim AC, Wu Y, Ferguson DO, Kuick RD, Lucas PC & Hammer GD (2009) Genetic p53 deficiency partially rescues the adrenocortical dysplasia phenotype at the expense of increased tumorigenesis. *Cancer Cell* 15: 465–476

di Fagagna F d'Adda, Reaper PM, Clay-Farrace L, Fiegler H, Carr P, von Zglinicki T, Saretzki G, Carter NP & Jackson SP (2003) A DNA damage checkpoint response in telomere-initiated senescence. *Nature* 426: 194–198

Feijoo P, Terradas M, Soler D, Domínguez D, Tusell L & Genescà A (2016) Breast primary epithelial cells that escape p16-dependent stasis enter a telomere-driven crisis state. *Breast Cancer Res.* 18: 7

Feng J, Funk WD, Wang SS, Weinrich SL, Avilion AA, Chiu CP, Adams RR, Chang E, Allsopp RC, Yu J, Le S, West MD, Harley CB, Andrews WH, Greider CW & Villeponteau B (1995) The RNA component of human telomerase. *Science* 269: 1236–41

Feng X, Hsu SJ, Kasbek C, Chaiken M & Price CM (2017) CTC1-mediated C-strand fill-in is an essential step in telomere length maintenance. *Nucleic Acids Res.* 45: 4281–4293

Flynn RL, Centore RC, O'Sullivan RJ, Rai R, Tse A, Songyang Z, Chang S, Karlseder J & Zou L (2011) TERRA and hnRNPA1 orchestrate an RPA-to-POT1 switch on telomeric single-stranded DNA. *Nature* 471: 532–538

Fouché N, Cesare AJ, Willcox S, Özgür S, Compton SA & Griffith JD (2006a) The basic domain of TRF2 directs binding to DNA junctions irrespective of the presence of TTAGGG repeats. *J. Biol. Chem.* 281: 37486–37495

Fouché N, Özgür S, Roy D & Griffith JD (2006b) Replication fork regression in repetitive DNAs. *Nucleic Acids Res.* 34: 6044–6050

Franco S, Segura I, Riese HH & Blasco MA (2002) Decreased B16F10 melanoma growth and impaired vascularization in telomerase-deficient mice with critically short telomeres. *Cancer Res.* 62: 552–559

Frank AK, Tran DC, Qu RW, Stohr BA, Segal DJ & Xu L (2015) The shelterin TIN2 subunit mediates recruitment of telomerase to telomeres. *PLoS Genet.* 11: 31005410

Frescas D & de Lange T (2014) TRF2-tethered TIN2 can mediate telomere protection by TPP1/POT1. *Mol. Cell. Biol.* 34: 1349–1362

Fujiwara T, Bandi M, Nitta M, Ivanova E V, Bronson RT & Pellman D (2005) Cytokinesis failure generating tetraploids promotes tumorigenesis in p53-null cells. *Nature* 437: 1043–7

Ganem NJ, Cornils H, Chiu SY, O'Rourke KP, Arnaud J, Yimlamai D, Théry M, Camargo FD & Pellman D (2014) Cytokinesis failure triggers hippo tumor suppressor pathway activation. *Cell* 158: 833–848

Ganem NJ, Godinho S a & Pellman D (2009) A mechanism linking extra centrosomes to chromosomal instability. *Nature* 460: 278–82

Ganem NJ, Storchova Z & Pellman D (2007) Tetraploidy, aneuploidy and cancer. *Curr. Opin. Genet. Dev.* 17: 157–162

Garbe JC, Bhattacharya S, Merchant B, Bassett E, Swisshelm K, Feiler HS, Wyrobek AJ & Stampfer MR (2009) Molecular distinctions between stasis and telomere attrition senescence barriers shown by long-term culture of normal human mammary epithelial cells. *Cancer Res.* 69: 7557–7568

Garbe JC, Holst CR, Bassett E, Tlsty T & Stampfer MR (2007) Inactivation of p53 function in cultured human mammary epithelial cells turns the telomere-length dependent senescence barrier from agonescence into crisis. *Cell Cycle* 6: 1927–1936

Garbe JC, Vrba L, Sputova K, Fuchs L, Novak P, Brothman AR, Jackson M, Chin K, La Barge MA, Watts G, Futscher BW & Stampfer MR (2014) Immortalization of normal human mammary epithelial cells in two steps by direct targeting of senescence barriers does not require gross genomic alterations. *Cell Cycle* 13: 3423–3435

García-Beccaria M, Martínez P, Méndez-Pertuz M, Martínez S, Blanco-Aparicio C, Cañamero M, Mulero F, Ambrogio C, Flores JM, Megias D, Barbacid M, Pastor J & Blasco M a (2015) Therapeutic inhibition of TRF1 impairs the growth of p53-deficient K-RasG12V-induced lung cancer by induction of telomeric DNA damage. *EMBO Mol. Med.* 7: 930–49

Genescà A, Pampalona J, Frías C, Domínguez D & Tusell L (2011) Role of telomere dysfunction in genetic intratumor diversity.

Gocha ARS, Harris J & Groden J (2013) Alternative mechanisms of telomere lengthening: Permissive

mutations, DNA repair proteins and tumorigenic progression. *Mutat. Res.* 743–733: 142–150
Gong Y & de Lange T (2010) A Shld1-Controlled POT1a provides support for repression of ATR signaling at telomeres through RPA exclusion. *Mol. Cell* 40: 377–387
González-Suárez E, Samper E, Flores JM & Blasco MA (2000) Telomerase-deficient mice with short telomeres are resistant to skin tumorigenesis. *Nat. Genet.* 26: 114–117
Gorgoulis VG, Vassiliou LVF, Karakaidos P, Zacharatos P, Kotsinas A, Liloglou T, Venere M, DiTullio RA, Kastrinakis NG, Levy B, Kletsas D, Yoneta A, Herlyn M, Kittas C & Halazonetis TD (2005) Activation of the DNA damage checkpoint and genomic instability in human precancerous lesions. *Nature* 434: 907–913
Gottlieb TM & Jackson SP (1993) The DNA-dependent protein kinase: Requirement for DNA ends and association with Ku antigen. *Cell* 72: 131–142
Greenberg RA, Chin L, Femino A, Kee-Ho L, Gottlieb GJ, Singer RH, Greider CW & DePinho RA (1999) Short dysfunctional telomeres impair tumorigenesis in the INK4a(Δ2/3) cancer-prone mouse. *Cell* 97: 515–525
Greider CW (1991) Telomerase is processive. *Mol. Cell. Biol.* 11: 4572–80
Greider CW & Blackburn EH (1985) Identification of a specific telomere terminal transferase activity in tetrahymena extracts. *Cell* 43: 405–413
Greider CW & Blackburn EH (1987) The telomere terminal transferase of tetrahymena is a ribonucleoprotein enzyme with two kinds of primer specificity. *Cell* 51: 887–898
Griffith JD, Comeau L, Rosenfield S, Stansel RM, Bianchi A, Moss H & de Lange T (1999) Mammalian telomeres end in a large duplex loop. *Cell* 97: 503–514
Gumbiner BM & Kim N-G (2014) The Hippo-YAP signaling pathway and contact inhibition of growth. *J Cell Sci* 127: 709–717
Guo H, Tian T, Nan K & Wang W (2010) p57: A multifunctional protein in cancer. *Int. J. Oncol.* 36: 1321–1329
Guo X, Deng Y, Lin Y, Cosme-Blanco W, Chan S, He H, Yuan G, Brown EJ & Chang S (2007) Dysfunctional telomeres activate an ATM-ATR-dependent DNA damage response to suppress tumorigenesis. *EMBO J.* 26: 4709–4719
Hanahan D & Weinberg R a (2011) Hallmarks of cancer: the next generation. *Cell* 144: 646–74
Hänsel-Hertsch R, Di Antonio M & Balasubramanian S (2017) DNA G-quadruplexes in the human genome: detection, functions and therapeutic potential. *Nat. Rev. Mol. Cell Biol.* 18: 279–284
Hara E, Tsurui H, Shinozaki A, Nakada S & Oda K (1991) Cooperative effect of antisense-Rb and antisense-p53 oligomers on the extension of life span in human diploid fibroblasts, TIG-1. *Biochem. Biophys. Res. Commun.* 179: 528–534
Hardy CFJ, Sussel L & Shore D (1992) A RAP1-interacting protein involved in transcriptional silencing and telomere length regulation. *Genes Dev.* 6: 801–814
Harley CB, Futcher AB & Greider CW (1990) Telomeres shorten during ageing of human fibroblasts. *Nature* 345: 458–60
Hayashi MT, Cesare AJ, Fitzpatrick JAJ, Denchi EL & Karlseder J (2012) A telomere-dependent DNA damage checkpoint induced by prolonged mitotic arrest. *Nat. Struct. Mol. Biol.* 19: 387–395
Hayashi MT, Cesare AJ, Rivera T & Karlseder J (2015) Cell death during crisis is mediated by mitotic telomere deprotection. *Nature* 522: 492–6
Hayflick L & Moorhead PS (1961) The serial cultivation of human diploid cell strains. *Exp. Cell Res.* 25: 585–621
Van Heek NT, Meeker AK, Kern SE, Yeo CJ, Lillemoe KD, Cameron JL, Offerhaus GJA, Hicks JL, Wilentz RE, Goggins MG, De Marzo AM, Hruban RH & Maitra A (2002) Telomere shortening is nearly universal in pancreatic intraepithelial neoplasia. *Am. J. Pathol.* 161: 1541–1547
Hein J, Boichuk S, Wu J, Cheng Y, Freire R, Jat PS, Roberts TM & Gjoerup O V. (2009) Simian Virus 40 Large T Antigen Disrupts Genome Integrity and Activates a DNA Damage Response via Bub1 Binding. *J. Virol.* 83: 117–127

Henson JD, Neumann AA, Yeager TR & Reddel RR (2002) Alternative lengthening of telomeres in mammalian cells. *Oncogene* 21: 598–610

Herrera E, Martínez-A C & Blasco MA (2000) Impaired germinal center reaction in mice with short telomeres. *EMBO J.* 19: 472–481

Herrera E, Samper E & Blasco MA (1999a) Telomere shortening in mTR−/− embryos is associated with failure to close the neural tube. *EMBO J.* 18: 1172–1181

Herrera E, Samper E, Martín-Caballero J, Flores JM, Lee HW & Blasco MA (1999b) Disease states associated with telomerase deficiency appear earlier in mice with short telomeres. *EMBO J.* 18: 2950–2960

Ho CC, Hau PM, Marxer M & Poon RYC (2010) The requirement of p53 for maintaining chromosomal stability during tetraploidization. *Oncotarget* 1: 583–595

Hockemeyer D & Collins K (2015) Control of telomerase action at human telomeres. *Nat. Struct. Mol. Biol.* 22: 848–852

Hockemeyer D, Daniels JP, Takai H & de Lange T (2006) Recent expansion of the telomeric complex in rodents: two distinct POT1 proteins protect mouse telomeres. *Cell* 126: 63–77

Hockemeyer D, Palm W, Else T, Daniels JP, Takai KK, Ye JZS, Keegan CE, de Lange T & Hammer GD (2007) Telomere protection by mammalian Pot1 requires interaction with Tpp1. *Nat. Struct. Mol. Biol.* 14: 754–761

Hoffelder D, Luo L, Burke N, Watkins S, Gollin S & Saunders W (2004) Resolution of anaphase bridges in cancer cells. *Chromosoma* 112: 389–397

Holst CR, Nuovo GJ, Esteller M, Chew K, Baylin SB, Herman JG & Tlsty TD (2003) Methylation of p16INK4a promoters occurs in vivo in histologically normal human mammary epithelia. *Cancer Res.* 63: 1596–1601

Hu J, Hwang SS, Liesa M, Gan B, Sahin E, Jaskelioff M, Ding Z, Ying H, Boutin AT, Zhang H, Johnson S, Ivanova E, Kost-Alimova M, Protopopov A, Wang YA, Shirihai OS, Chin L & Depinho RA (2012) Antitelomerase therapy provokes ALT and mitochondrial adaptive mechanisms in cancer. *Cell* 148: 651–663

Huschtscha LI, Moore JD, Noble JR, Campbell HG, Royds JA, Braithwaite AW & Reddel RR (2009) Normal human mammary epithelial cells proliferate rapidly in the presence of elevated levels of the tumor suppressors p53 and p21(WAF1/CIP1). *J Cell Sci* 122: 2989–2995

Huschtscha LI, Neumann AA, Noble JR & Reddel RR (2001) Effects of Simian virus 40 T-antigens on normal human mammary epithelial cells reveal evidence for spontaneous alterations in addition to loss of p16INK4a expression. *Exp. Cell Res.* 265: 125–134

Huschtscha LI, Noble JR, Neumann AA, Moy EL, Barry P, Melki JR, Clark SJ & Reddel RR (1998) Loss of p16(INK4) expression by methylation is associated with lifespan extension of human mammary epithelial cells. *Cancer Res.* 58: 3508–12

Hwang H, Buncher N, Opresko PL & Myong S (2012) POT1-TPP1 regulates telomeric overhang structural dynamics. *Structure* 20: 1872–1880

Ince TA, Richardson AL, Bell GW, Saitoh M, Godar S, Karnoub AE, Iglehart JD & Weinberg RA (2007) Transformation of different human breast epithelial cell types leads to distinct tumor phenotypes. *Cancer Cell* 12: 160–170

Jaco I, Muñoz P, Goytisolo F, Wesoly J, Bailey S, Taccioli G & Blasco MA (2003) Role of mammalian Rad54 in telomere length maintenance. *Mol. Cell. Biol.* 23: 5572–80

Jacobs JJ. L & de Lange T (2004) Significant role for p16INK4a in p53-independent telomere-directed senescence. *Curr. Biol.* 14: 2302–2308

Janoušková E, Nečasová I, Pavloušková J, Zimmermann M, Hluchý M, Marini V, Nováková M & Hofr C (2015) Human Rap1 modulates TRF2 attraction to telomeric DNA. *Nucleic Acids Res.* 43: 2691–2700

Janssen A, Kops GJPL & Medema RH (2009) Elevating the frequency of chromosome mis-segregation as a strategy to kill tumor cells. *Proc Natl Acad Sci U S A* 106: 19108–19113

Jin Y, Zhang H, Tsao SW, Jin C, Lv M, Strömbeck B, Wiegant J, Wan TSK, Yuen PW & Kwong YL (2004)

Cytogenetic and molecular genetic characterization of immortalized human ovarian surface epithelial cell lines: Consistent loss of chromosome 13 and amplification of chromosome 20. *Gynecol. Oncol.* 92: 183–191

Kabir S, Sfeir A & de Lange T (2010) Taking apart Rap1: An adaptor protein with telomeric and non-telomeric functions. *Cell Cycle* 9: 4061–4067

Karlseder J, Broccoli D, Dai Y, Hardy S & de Lange T (1999) p53- and ATM-dependent apoptosis induced by telomeres lacking TRF2. *Science* 283: 1321–1325

Karlseder J, Hoke K, Mirzoeva OK, Bakkenist C, Kastan MB, Petrini JHJ & de Lange T (2004) The telomeric protein TRF2 binds the ATM kinase and can inhibit the ATM-dependent DNA damage response. *PLoS Biol.* 2: 1150–1156

Karlseder J, Kachatrian L, Takai H, Mercer K, Hingorani S, Jacks T & de Lange T (2003) Targeted deletion reveals an essential function for the telomere length regulator Trf1. *Mol. Cell. Biol.* 23: 6533–41

Karlseder J, Smogorzewska A & de Lange T (2002) Senescence induced by altered telomere state, not telomere loss. *Science* 295: 2446–9

Kaul Z, Cesare AJ, Huschtscha LI, Neumann AA & Reddel RR (2012) Five dysfunctional telomeres predict onset of senescence in human cells. *EMBO Rep.* 13: 52–59

Kelleher C, Kurth I & Lingner J (2005) Human Protection of Telomeres 1 (POT1) is a negative regulator of telomerase activity in vitro. *Mol. Cell. Biol.* 25: 808–818

Kenny PA, Lee GY, Myers CA, Neve RM, Semeiks JR, Spellman PT, Lorenz K, Lee EH, Barcellos-Hoff MH, Petersen OW, Gray JW & Bissell MJ (2007) The morphologies of breast cancer cell lines in three-dimensional assays correlate with their profiles of gene expression. *Mol. Oncol.* 1: 84–96

Kibe T, Osawa GA, Keegan CE & de Lange T (2010) Telomere protection by TPP1 is mediated by POT1a and POT1b. *Mol. Cell. Biol.* 30: 1059–1066

Kibe T, Zimmermann M & de Lange T (2016) TPP1 blocks an ATR-mediated resection mechanism at telomeres. *Mol. Cell* 61: 236–246

Kim H, Lee O-H, Xin H, Chen L-Y, Qin J, Chae HK, Lin S-Y, Safari A, Liu D & Songyang Z (2009) TRF2 functions as a protein hub and regulates telomere maintenance by recognizing specific peptide motifs. *Nat. Struct. Mol. Biol.* 16: 372–9

Kim NW, Piatyszek M a, Prowse KR, Harley CB, West D, Ho PLC, Coviello GM, Wright WE, Weinrich SL, Shay W, West MD & Shay JW (1994) Specific association of human telomerase activity with immortal cells and cancer. *Science (80-.).* 266: 2011–2015

Kitada T, Seki S, Kawakita N, Kuroki T & Monna T (1995) Telomere shortening in chronic liver diseases. *Biochem. Biophys. Res. Commun.* 211: 33–39

Klobutcher LA, Swanton MT, Donini P & Prescott DM (1981) All gene-sized DNA molecules in four species of hypotrichs have the same terminal sequence and an unusual 3' terminus. *Proc. Natl. Acad. Sci.* 78: 3015–3019

Kops GJPL, Foltz DR & Cleveland DW (2004) Lethality to human cancer cells through massive chromosome loss by inhibition of the mitotic checkpoint. *Proc. Natl. Acad. Sci.* 101: 8699–8704

Lam YC, Akhter S, Gu P, Ye J, Poulet A, Giraud-Panis M-J, Bailey SM, Gilson E, Legerski RJ & Chang S (2010) SNMIB/Apollo protects leading-strand telomeres against NHEJ-mediated repair. *EMBO J.* 29: 2230–2241

Latre L, Tusell L, Martin M, Miró R, Egozcue J, Blasco MA & Genescà A (2003) Shortened telomeres join to DNA breaks interfering with their correct repair. *Exp. Cell Res.* 287: 282–288

Laughney AM, Elizalde S, Genovese G & Bakhoum SF (2015) Dynamics of tumor heterogeneity derived from clonal karyotypic evolution. *Cell Rep.* 12: 809–820

Lazzerini-Denchi E & Sfeir A (2016) Stop pulling my strings — what telomeres taught us about the DNA damage response. *Nat. Rev. Mol. Cell Biol.* 17: 364–378

Lee-Theilen M, Matthews AJ, Kelly D, Zheng S & Chaudhuri J (2011) CtIP promotes microhomology-mediated alternative end joining during class-switch recombination. *Nat. Struct. Mol. Biol.* 18: 75–

80
Lee H, Blasco MA, Gottlieb GJ, Il JWH, Greider CW & DePinho RA (1998) **Essential role of mouse telomerase in highly proliferative organs**. *Nature* 392: 569–574
Lee KM, Choi KH & Ouellette MM (2004) **Use of exogenous hTERT to immortalize primary human cells**. *Cytotechnology* 45: 33–38
Lee YW, Arora R, Wischnewski H & Azzalin CM (2018) **TRF1 participates in chromosome end protection by averting TRF2-dependent telomeric R loops**. *Nat. Struct. Mol. Biol.* 25: 147–153
Leman AR, Dheekollu J, Deng Z, Lee SW, Das MM, Lieberman PM & Noguchi E (2012) **Timeless preserves telomere length by promoting efficient DNA replication through human telomeres**. *Cell Cycle* 11: 2337–2347
Lengauer C, Kinzler KW & Vogelstein B (1997) **Genetic instability in colorectal cancers**. *Nature* 386: 623–627
Lengauer C, Kinzler KW & Vogelstein B (1998) **Genetic instabilities in human cancers.** *Nature* 396: 643–649
Leri A, Franco S, Zacheo A, Barlucchi L, Chimenti S, Limana F, Nadal-Ginard B, Kajstura J, Anversa P & Blasco MA (2003) **Ablation of telomerase and telomere loss leads to cardiac dilatation and heart failure associated with p53 upregulation**. *EMBO J.* 22: 131–139
Lewis KA & Tollefsbol TO (2016) **Regulation of the telomerase reverse transcriptase subunit through epigenetic mechanisms**. *Front. Genet.* 7: 1–12
Li B, Oestreich S & de Lange T (2000) **Identification of human Rap1: Implications for telomere evolution**. *Cell* 101: 471–483
Li H, Xu D, Toh BH & Liu JP (2006) **TGF-β and cancer: Is Smad3 a repressor of hTERT gene?** *Cell Res.* 16: 169–173
Lieber MR (2010) **The mechanism of double-strand DNA break repair by the nonhomologous DNA end-joining pathway**. *Annu. Rev. Biochem.* 79: 181–211
Lim CJ, Zaug AJ, Kim HJ & Cech TR (2017) **Reconstitution of human shelterin complexes reveals unexpected stoichiometry and dual pathways to enhance telomerase processivity**. *Nat. Commun.* 8:
Lingner J, Hughes TR, Shevchenko A, Mann M, Lundblad V & Cech TR (1997) **Reverse transcriptase motifs in the catalytic subunit of telomerase.** *Science* 276: 561–7
Liu D, O'Connor MS, Qin J & Songyang Z (2004a) **Telosome, a mammalian telomere-associated complex formed by multiple telomeric proteins**. *J. Biol. Chem.* 279: 51338–51342
Liu D, Safari A, O'Connor MS, Chan DW, Laegeler A, Qin J & Songyang Z (2004b) **PTOP interacts with POT1 and regulates its localization to telomeres**. *Nat. Cell Biol.* 6: 673–680
Liu S, Hatton MP, Khandelwal P & Sullivan DA (2010) **Culture, immortalization, and characterization of human Meibomian gland epithelial cells**. *Investig. Ophthalmol. Vis. Sci.* 51: 3993–4005
Loayza D & de Lange T (2003) **POT1 as a terminal transducer of TRF1 telomere length control**. *Nature* 423: 1013–1018
Loayza D, Parsons H, Donigian J, Hoke K & de Lange T (2004) **DNA binding features of human POT1: A nonamer 5′-TAGGGTTAG-3′ minimal binding site, sequence specificity, and internal binding to multimeric sites**. *J. Biol. Chem.* 279: 13241–13248
Lukusa T & Fryns JP (2008) **Human chromosome fragility**. *Biochim. Biophys. Acta - Gene Regul. Mech.* 1779: 3–16
Lundblad V & Blackburn EH (1993) **An alternative pathway for yeast telomere maintenance rescues est1- senescence**. *Cell* 73: 347–360
Lundblad V & Szostak JW (1989) **A mutant with a defect in telomere elongation leads to senescence in yeast**. *Cell* 57: 633–643
Van Ly D, Low RRJ, Frölich S, Bartolec TK, Kafer GR, Pickett HA, Gaus K & Cesare AJ (2018) **Telomere Loop Dynamics in Chromosome End Protection**. *Mol. Cell*: 1–16
Maciejowski J & de Lange T (2017) **Telomeres in cancer: tumour suppression and genome instability**. *Nat. Rev. Mol. Cell Biol.* 18: 175–186

Maciejowski J, Li Y, Bosco N, Campbell PJ & de Lange T (2015) **Chromothripsis and kataegis induced by telomere crisis**. *Cell* 163: 1641–1654

Makarov VL, Hirose Y & Langmore JP (1997) **Long G tails at both ends of human chromosomes suggest a C strand degradation mechanism for telomere shortening**. *Cell* 88: 657–666

Margolis RL, Lohez OD & Andreassen PR (2003) **G1 tetraploidy checkpoint and the suppression of tumorigenesis**. *J. Cell. Biochem.* 88: 673–683

Di Maro S, Zizza P, Salvati E, De Luca V, Capasso C, Fotticchia I, Pagano B, Marinelli L, Gilson E, Novellino E, Cosconati S & Biroccio A (2014) **Shading the TRF2 recruiting function: A new horizon in drug development**. *J. Am. Chem. Soc.* 136: 16708–16711

Martínez P, Thanasoula M, Muñoz P, Liao C, Tejera A, McNees C, Flores JM, Fernández-Capetillo O, Tarsounas M & Blasco MA (2009) **Increased telomere fragility and fusions resulting from TRF1 deficiency lead to degenerative pathologies and increased cancer in mice**. *Genes Dev.* 23: 2060–2075

Mateos-Gomez PA, Gong F, Nair N, Miller KM, Lazzerini-Denchi E & Sfeir A (2015) **Mammalian polymerase θ promotes alternative NHEJ and suppresses recombination**. *Nature* 518: 254–257

McClintock B (1941) **The stability of broken ends of chromosomes in Zea mays**. *Genetics* 26: 234–282

Meeker AK, Hicks JL, Gabrielson E, Strauss WM, De Marzo AM & Argani P (2004a) **Telomere shortening occurs in subsets of normal breast epithelium as well as in situ and invasive carcinoma**. *Am. J. Pathol.* 164: 925–935

Meeker AK, Hicks JL, Iacobuzio-Donahue CA, Montgomery EA, Westra WH, Chan TY, Ronnett BM & De Marzo AM (2004b) **Telomere length abnormalities occur early in the initiation of epithelial carcinogenesis**. *Clin. Cancer Res.* 10: 3317–3326

Meyne J, Ratliff RL & Moyzis RK (1989) **Conservation of the human telomere sequence (TTAGGG)n among vertebrates**. *Proc Natl Acad Sci U S A* 86: 7049–7053

Milyavsky M, Shats I, Erez N, Tang X, Senderovich S, Meerson A, Tabach Y, Goldfinger N, Ginsberg D, Harris CC & Rotter V (2003) **Prolonged culture of telomerase-immortalized human fibroblasts leads to a premalignant phenotype**. *Cancer Res.* 63: 7147–7157

Mitelman F, Johansson B & Mertens F (2018) **Mitelman database of chromosome aberrations and gene fusions in cancer**.

Mitton-Fry RM, Anderson EM, Hughes TR, Lundblad V & Wuttke DS (2002) **Conserved structure for single-stranded telomeric DNA recognition**. *Science (80-.).* 296: 145–147

Moyzis RK, Buckingham JM, Cram LS, Dani M, Deaven LL, Jones MD, Meyne J, Ratliff RL & Wu J-R (1988) **A highly conserved repetitive DNA sequence, (TTAGGG)n, present at the telomeres of human chromosomes**. *Proc Natl Acad Sci U S A* 85: 6622–6626

Muller HJ (1938) **The remaking of chromosomes**. *Collect. Net-Woods Hole* 13: 181–198

Muñoz-Jordán JL, Cross GAM, de Lange T & Griffith JD (2001) **T-Loops at trypanosome telomeres**. *EMBO J.* 20: 579–588

Muñoz P, Blanco R, de Carcer G, Schoeftner S, Benetti R, Flores JM, Malumbres M & Blasco MA (2009) **TRF1 controls telomere length and mitotic fidelity in epithelial homeostasis**. *Mol. Cell. Biol.* 29: 1608–1625

Murnane JP, Sabatier L, Marder BA & Morgan WF (1994) **Telomere dynamics in an immortal human cell line.** *EMBO J.* 13: 4953–62

Murti KG & Prescott DM (1999) **Telomeres of polytene chromosomes in a ciliated protozoan terminate in duplex DNA loops**. *PNAS* 96: 14436–14439

Nabetani A & Ishikawa F (2009) **Unusual telomeric DNAs in human telomerase-negative immortalized cells**. *Mol. Cell. Biol.* 29: 703–713

Nakamura M, Zhou XZ, Kishi S, Kosugi I, Tsutsui Y & Lu KP (2001) **A specific interaction between the telomeric protein Pin2/TRF1 and the mitotic spindle**. *Curr. Biol.* 11: 1512–1516

Nakamura TM, Morin GB, Chapman KB, Weinrich SL, Andrews WH, Lingner J, Harley CB & Cech TR (1997) **Telomerase catalytic subunit homologs from fission yeast and human**. *Science* 277: 955–

959
Nandakumar J, Bell CF, Weidenfeld I, Zaug AJ, Leinwand LA & Cech TR (2012) The TEL patch of telomere protein TPP1 mediates telomerase recruitment and processivity. *Nature* 492: 285–289
Nečasová I, Janoušková E, Klumpler T & Hofr C (2017) Basic domain of telomere guardian TRF2 reduces D-loop unwinding whereas Rap1 restores it. *Nucleic Acids Res.* 45: 12170–12180
Negrini S, Gorgoulis VG & Halazonetis TD (2010) Genomic instability - an evolving hallmark of cancer. *Nat. Rev. Mol. Cell Biol.* 11: 220–8
Neve RM, Chin K, Fridlyand J, Yeh J, Baehner FL, Fevr T, Clark L, Bayani N, Coppe JP, Tong F, Speed T, Spellman PT, DeVries S, Lapuk A, Wang NJ, Kuo WL, Stilwell JL, Pinkel D, Albertson DG, Waldman FM, et al (2006) A collection of breast cancer cell lines for the study of functionally distinct cancer subtypes. *Cancer Cell* 10: 515–527
Nik-Zainal S, Alexandrov LB, Wedge DC, Van Loo P, Greenman CD, Raine K, Jones D, Hinton J, Marshall J, Stebbings LA, Menzies A, Martin S, Leung K, Chen L, Leroy C, Ramakrishna M, Rance R, Lau KW, Mudie LJ, Varela I, et al (2012) Mutational processes molding the genomes of 21 breast cancers. *Cell* 149: 979–993
Nora GJ, Buncher NA & Opresko PL (2010) Telomeric protein TRF2 protects Holliday junctions with telomeric arms from displacement by the Werner syndrome helicase. *Nucleic Acids Res.* 38: 3984–3998
Nowell Peter C. (1976) The clonal evolution of tumor cell populations. *Science (80-.).* 194: 23–28
Nussenzweig A & Nussenzweig MC (2007) A backup DNA repair pathway moves to the forefront. *Cell* 131: 223–225
O'Connor MS, Safari A, Liu D, Qin J & Songyang Z (2004) The human Rap1 protein complex and modulation of telomere length. *J. Biol. Chem.* 279: 28585–28591
O'Donnell M, Langston L & Stillman B (2013) Principles and concepts of DNA replication in Bacteria, Archea, and Eukarya. *Cold Spring Harb. Perspect. Biol.* 5: a010180
Ohishi T, Hirota T, Tsuruo T & Seimiya H (2010) TRF1 mediates mitotic abnormalities induced by Aurora-A overexpression. *Cancer Res.* 70: 2041–2052
Ohishi T, Muramatsu Y, Yoshida H & Seimiya H (2014) TRF1 ensures the centromeric function of Aurora-B and proper chromosome segregation. *Mol. Cell. Biol.* 34: 2464–2478
Okamoto K, Bartocci C, Ouzounov I, Diedrich JK, Yates III JR & Denchi EL (2013) A two-step mechanism for TRF2-mediated chromosome-end protection. *Nature* 494: 502–505
Okamoto K, Iwano T, Tachibana M & Shinkai Y (2008) Distinct roles of TRF1 in the regulation of telomere structure and lengthening. *J. Biol. Chem.* 283: 23981–23988
Okazaki R, Okazaki T, Sakabe K, Sugimoto K & Sugino A (1968) Mechanism of DNA chain growth. I. Possible discontinuity and unusual secondary structure of newly synthesized chains. *Proc. Natl. Acad. Sci. U. S. A.* 59: 598–605
Olovnikov AM (1973) A theory of marginotomy. The incomplete copying of template margin in enzymic synthesis of polynucleotides and biological significance of the phenomenon. *J. Theor. Biol.* 41: 181–190
OMIM. Human genetics knowledge for the world (2018)
Opresko PL (2008) Telomere ResQue and preservation - Roles for the Werner syndrome protein and other RecQ helicases. *Mech. Ageing Dev.* 129: 79–90
van Overbeek M & de Lange T (2006) Apollo, an Artemis-related nuclease, interacts with TRF2 and protects human telomeres in S phase. *Curr. Biol.* 16: 1295–1302
Palm W, Hockemeyer D, Kibe T & de Lange T (2009) Functional Dissection of Human and Mouse POT1 Proteins. *Mol. Cell. Biol.* 29: 471–482
Palm W & de Lange T (2008) How shelterin protects mammalian telomeres. *Annu. Rev. Genet.* 42: 301–334
Pampalona J, Frías C, Genescà A & Tusell L (2012) Progressive telomere dysfunction causes cytokinesis failure and leads to the accumulation of polyploid cells. *PLoS Genet.* 8: e1002679
Pampalona J, Roscioli E, Silkworth WT, Bowden B, Genescà A, Tusell L & Cimini D (2016) Chromosome

bridges maintain kinetochore-microtubule attachment throughout mitosis and rarely break during anaphase. *PLoS One* 11: 1–17

Pampalona J, Soler D, Genescà A & Tusell L (2010) Whole chromosome loss is promoted by telomere dysfunction in primary cells. *Genes. Chromosomes Cancer* 49: 368–378

Pantic M, Zimmermann S, El Daly H, Opitz OG, Popp S, Boukamp P & Martens UM (2006) Telomere dysfunction and loss of p53 cooperate in defective mitotic segregation of chromosomes in cancer cells. *Oncogene* 25: 4413–4420

Petersen OW, Ronnov-Jessen L, Howlett AR & Bissell MJ (1992) Interaction with basement membrane serves to rapidly distinguish growth and differentiation pattern of normal and malignant human breast epithelial cells. *Proc. Natl. Acad. Sci.* 89: 9064–9068

Pickett HA, Cesare AJ, Johnston RL, Neumann AA & Reddel RR (2009) Control of telomere length by a trimming mechanism that involves generation of t-circles. *EMBO J.* 28: 799–809

Pickett HA, Henson JD, Au AYM, Neumann AA & Reddel RR (2011) Normal mammalian cells negatively regulate telomere length by telomere trimming. *Hum. Mol. Genet.* 20: 4684–4692

Pickett HA & Reddel RR (2015) Molecular mechanisms of activity and derepression of Alternative Lengthening of Telomeres. *Nat Struct Mol Biol* 22: 875–880

Pinzaru AM, Hom RA, Beal A, Phillips AF, Ni E, Cardozo T, Nair N, Choi J, Wuttke DS, Sfeir A & Denchi EL (2016) Telomere replication stress induced by POT1 inactivation accelerates tumorigenesis. *Cell Rep.* 15: 2170–2184

Poulet A, Buisson R, Faivre-Moskalenko C, Koelblen M, Amiard S, Montel F, Cuesta-Lopez S, Bornet O, Guerlesquin F, Godet T, Moukhtar J, Argoul F, Déclais A-C, Lilley DMJ, Ip SCY, West SC, Gilson E & Giraud-Panis M-J (2009) TRF2 promotes, remodels and protects telomeric Holliday junctions. *EMBO J.* 28: 641–51

Poulet A, Pisano S, Faivre-Moskalenko C, Pei B, Tauran Y, Haftek-Terreau Z, Brunet F, Le Bihan YV, Ledu MH, Montel F, Hugo N, Amiard S, Argoul F, Chaboud A, Gilson E & Giraud-Panis MJ (2012) The N-terminal domains of TRF1 and TRF2 regulate their ability to condense telomeric DNA. *Nucleic Acids Res.* 40: 2566–2576

Prowse KR & Greider CW (1995) Developmental and tissue-specific regulation of mouse telomerase and telomere length. *Proc. Natl. Acad. Sci.* 92: 4818–4822

Rai R, Chen Y, Lei M & Chang S (2016) TRF2-RAP1 is required to protect telomeres from engaging in homologous recombination-mediated deletions and fusions. *Nat. Commun.* 7: 1–13

Rai R, Zheng H, He H, Luo Y, Multani A, Carpenter PB & Chang S (2010) The function of classical and alternative non-homologous end-joining pathways in the fusion of dysfunctional telomeres. *EMBO J.* 29: 2598–2610

Raices M, Verdun RE, Compton SA, Haggblom CI, Griffith JD, Dillin A & Karlseder J (2008) C. elegans telomeres contain G-strand and C-strand overhangs that are bound by distinct proteins. *Cell* 132: 745–757

Ramsay AJ, Quesada V, Foronda M, Conde L, Martínez-Trillos A, Villamor N, Rodríguez D, Kwarciak A, Garabaya C, Gallardo M, López-Guerra M, López-Guillermo A, Puente XS, Blasco MA, Campo E & López-Otín C (2013) POT1 mutations cause telomere dysfunction in chronic lymphocytic leukemia. *Nat. Genet.* 45: 526–530

Rao K, Bryant E, O'Hara Larivee S & McDougall JK (2003) Production of spindle cell carcinoma by transduction of H-Ras 61L into immortalized human mammary epithelial cells. *Cancer Lett* 201: 79–88

Rass E, Grabarz A, Plo I, Gautier J, Bertrand P & Lopez BS (2009) Role of Mre11 in chromosomal nonhomologous end joining in mammalian cells. *Nat. Struct. Mol. Biol.* 16: 819–824

Ray FA, Meyne J & Kraemer PM (1992) SV40 T antigen induced chromosomal changes reflect a process that is both clastogenic and aneuploidogenic and is ongoing throughout neoplastic progression of human fibroblasts. *Mutat. Res.* 284: 265–73

Raynaud CM, Hernandez J, Llorca FP, Nuciforo P, Mathieu MC, Commo F, Delaloge S, Sabatier L,

André F & Soria JC (2010) DNA damage repair and telomere length in normal breast, preneoplastic lesions, and invasive cancer. *Am. J. Clin. Oncol. Cancer Clin. Trials* 33: 341–5

Ribes-Zamora A, Indiviglio SM, Mihalek I, Williams CL & Bertuch AA (2013) TRF2 interaction with Ku heterotetramerization interface gives insight into c-NHEJ prevention at human telomeres. *Cell Rep.* 5: 194–206

Rivera T, Haggblom C, Cosconati S & Karlseder J (2017) A balance between elongation and trimming regulates telomere stability in stem cells. *Nat. Struct. Mol. Biol.* 24: 30–39

Roake CM & Artandi SE (2017) Control of Cellular Aging, Tissue Function, and Cancer by p53 Downstream of Telomeres. *Cold Spring Harb. Perspect. Med.* 7: a026088

Robert I, Dantzer F & Reina-San-Martin B (2009) Parp1 facilitates alternative NHEJ, whereas Parp2 suppresses IgH/c-myc translocations during immunoglobulin class switch recombination. *J. Exp. Med.* 206: 1047–1056

Roberts SA, Lawrence MS, Klimczak LJ, Grimm SA, Fargo D, Stojanov P, Kiezun A, Kryukov G V., Carter SL, Saksena G, Harris S, Shah RR, Resnick MA, Getz G & Gordenin DA (2013) An APOBEC cytidine deaminase mutagenesis pattern is widespread in human cancers. *Nat. Genet.* 45: 970–976

Robles-Espinoza CD, Harland M, Ramsay AJ, Aoude LG, Quesada V, Ding Z, Pooley KA, Pritchard AL, Tiffen JC, Petljak M, Palmer JM, Symmons J, Johansson P, Stark MS, Gartside MG, Snowden H, Montgomery GW, Martin NG, Liu JZ, Choi J, et al (2014) POT1 loss-of-function variants predispose to familial melanoma. *Nat. Genet.* 46: 478–481

Romanov SR, Kozakiewicz BK, Holst CR, Stampfer MR, Haupt LM & Tlsty TD (2001) Normal human mammary epithelial cells spontaneously escape senescence and acquire genomic changes. *Nature* 409: 633–637

Rudolph KL, Chang S, Lee HW, Blasco M, Gottlieb GJ, Greider C & DePinho RA (1999) Longevity, stress response, and cancer in aging telomerase-deficient mice. *Cell* 96: 701–12

Rybanska-Spaeder I, Ghosh R & Franco S (2014) 53BP1 mediates the fusion of mammalian telomeres rendered dysfunctional by DNA-PKcs loss or Inhibition. *PLoS One* 9:

Sanger Institute (2018) Cosmic, Catalog of somatic mutations in cancer.

Sarek G, Vannier J, Panier S, Petrini JHJ & Boulton SJ (2015) TRF2 recruits RTEL1 to telomeres in S phase to promote T-loop unwinding. *Mol. Cell* 57: 622–635

Sarthy J, Bae NS, Scrafford J & Baumann P (2009) Human RAP1 inhibits non-homologous end joining at telomeres. *EMBO J.* 28: 3390–3399

Savelieva E, Belair CD, Newton MA, DeVries S, Gray JW, Waldman F & Reznikoff CA (1997) 20q gain associates with immortalization: 20q13.2 amplification correlates with genome instability in human papillomavirus 16 E7 transformed human uroepithelial cells. *Oncogene* 14: 551–560

Scheffner M, Huibregtse JM, Vierstra RD & Howley PM (1993) The HPV-16 E6 and E6-AP complex functions as a ubiquitin-protein ligase in the ubiquitination of p53. *Cell* 75: 495–505

Schmidt JC & Cech TR (2015) Human telomerase: biogenesis, trafficking, recruitment, and activation. *Genes Dev.* 29: 1095–1105

Schvartzman JM, Sotillo R & Benezra R (2010) Mitotic chromosomal instability and cancer: Mouse modelling of the human disease. *Nat. Rev. Cancer* 10: 102–115

Sfeir A, Kabir S, van Overbeek M, Celli GB & de Lange T (2010) Loss of Rap1 induces telomere recombination in the absence of NHEJ or a DNA damage signal. *Science* 327: 1657–1661

Sfeir A, Kosiyatrakul ST, Hockemeyer D, MacRae SL, Karlseder J, Schildkraut CL & de Lange T (2009) Mammalian telomeres resemble fragile sites and require TRF1 for efficient replication. *Cell* 138: 90–103

Sfeir A & de Lange T (2012) Removal of shelterin reveals the telomere end-protection problem. *Science* 336: 593–7

Shackney SE, Smith CA, Miller BW, Burholt DR, Murtha K, Giles HRH, Ketterer DM & Pollice AA (1989) Model for the genetic evolution of human solid tumors. *Cancer Res.* 49: 3344–3354

Shampay J, Szostak JW & Blackburn EH (1984) DNA sequences of telomeres maintained in yeast.

Nature 310: 154–7
Shay JW & Bacchetti S (1997) **A survey of telomerase activity in human cancer**. *Eur. J. Cancer* 33: 787–791
Shay JW, Pereira-Smith OM & Wright WE (1991) **A role for both RB and p53 in the regulation of human cellular senescence**. *Exp. Cell Res.* 196: 33–39
Shay JW & Wright WE (1989) **Quantitation of the frequency human diploid fibroblasts of immortalization of normal by SV40 Large T-Antigen**. *Exp. Cell Res.* 184: 109–118
Shi J, Yang XR, Ballew B, Rotunno M, Calista D, Fargnoli MC, Ghiorzo P, Paillerets BB, Nagore E, Avril MF, Caporaso NE, McMaster ML, Cullen M, Wang Z, Zhang X, Group NCI DCEG Cancer Sequencing Working, Laboratory NCI DCEG Cancer Genomics Research, Group French Familial Melanoma Study, Bruno W, Pastorino L, et al (2014) **Rare missense variants in POT1 predispose to familial cutaneous malignant melanoma**. *Nat. Genet.* 46: 482–486
Silkworth WT & Cimini D (2012) **Transient defects of mitotic spindle geometry and chromosome segregation errors**. *Cell Div.* 7: 1–8
Silkworth WT, Nardi IK, Scholl LM & Cimini D (2009) **Multipolar spindle pole coalescence is a major source of kinetochore mis-attachment and chromosome mis-segregation in cancer cells.** *PLoS One* 4: e6564
Simsek D, Brunet E, Wong SYW, Katyal S, Gao Y, McKinnon PJ, Lou J, Zhang L, Li J, Rebar EJ, Gregory PD, Holmes MC & Jasin M (2011) **DNA ligase III promotes alternative nonhomologous end-joining during chromosomal translocation formation**. *PLoS Genet.* 7: 1–11
Sishc BJ & Davis AJ (2017) **The role of the core non-homologous end joining factors in carcinogenesis and cancer**. *Cancers (Basel).* 9: p81
Smith S & de Lange T (2000) **Tankyrase promotes telomere elongation in human cells**. *Curr. Biol.* 10: 1299–1302
Smogorzewska A, Karlseder J, Holtgreve-Grez H, Jauch A & de Lange T (2002) **DNA ligase IV-dependent NHEJ of deprotected mammalian telomeres in G1 and G2**. *Curr. Biol.* 12: 1635–1644
Smogorzewska A & de Lange T (2002) **Different telomere damage signaling pathways in human and mouse cells**. *EMBO J.* 21: 4338–4348
Smogorzewska A, van Steensel B, Bianchi A, Oelmann S, Schaefer MR, Schnapp G & de Lange T (2000) **Control of human telomere length by TRF1 and TRF2**. *Mol Cell Biol* 20: 1659–1668
Soler D, Genescà A, Arnedo G, Egozcue J & Tusell L (2005) **Telomere dysfunction drives chromosomal instability in human mammary epithelial cells.** *Genes. Chromosomes Cancer* 44: 339–50
Soohoo CY, Shi R, Lee TH, Huang P, Lu KP & Zhou XZ (2011) **Telomerase inhibitor PinX1 provides a link between TRF1 and telomerase to prevent telomere elongation**. *J. Biol. Chem.* 286: 3894–3906
Soule HD, Maloney TM, Wolman SR, Peterson WD, Brenz R, Mcgrath CM, Russo J, Pauley RJ, Jones RF & Brooks SC (1990) **Isolation and characterization of a spontaneously immortalized isolation and characterization of a spontaneously immortalized human breast**. *Cancer*: 6075–6086
Spinella JF, Cassart P, Garnier N, Rousseau P, Drullion C, Richer C, Ouimet M, Saillour V, Healy J, Autexier C & Sinnett D (2015) **A novel somatic mutation in ACD induces telomere lengthening and apoptosis resistance in leukemia cells**. *BMC Cancer* 15: 1–8
Stampfer MR, Bodnar A, Garbe J, Wong M, Pan A, Villeponteau B & Yaswen P (1997) **Gradual phenotypic conversion associated with immortalization of cultured human mammary epithelial cells**. *Mol. Biol. Cell* 8: 2391–2405
Stampfer MR, Garbe J, Levine G, Lichtsteiner S, Vasserot AP & Yaswen P (2001) **Expression of the telomerase catalytic subunit, hTERT, induces resistance to transforming growth factor B growth inhibition in p16**. *Pnas* 98: 4498–4503
Stampfer MR, Garbe J, Nijjar T, Wigington D, Swisshelm K & Yaswen P (2003) **Loss of p53 function accelerates acquisition of telomerase activity in indefinite lifespan human mammary epithelial cell lines**. *Oncogene* 22: 5238–5251

Stansel RM, de Lange T & Griffith JD (2001) T-loop assembly in vitro involves binding of TRF2 near the 3′ telomeric overhang. *EMBO J.* 20: 5532–5540

Van Steensel B & de Lange T (1997) Control of telomere length by the human telomeric protein TRF1. *Nature* 385: 740–743

Steensel B Van, Smogorzewska A & de Lange T (1998) TRF2 protects human telomeres from end-to-end fusions. *Cell* 92: 401–413

Stephens PJ, Greenman CD, Fu B, Yang F, Bignell GR, Mudie LJ, Pleasance ED, Lau KW, Beare D, Stebbings LA, Mclaren S, Lin M, Mcbride DJ, Varela I, Nik-Zainal S, Leroy C, Jia M, Menzies A, Butler AP, Teague JW, et al (2011) Massive genomic rearrangement acquired in a single catastrophic event during cancer development. *Cell* 144: 27–40

Stewart SA & Weinberg RA (2006) Telomeres: cancer to human aging. *Annu. Rev. Cell Dev. Biol.* 22: 531–557

Sugimoto K, Okazaki T & Okazaki R (1968) Mechanism of DNA chain growth, II. Accumulation of newly synthesized short chains in E. coli infected with ligase-defective T4 phages. *Proc. Natl. Acad. Sci.* 60: 1356–1362

Szostak JW & Blackburn EH (1982) Cloning yeast telomeres on linear plasmid vectors. *Cell* 29: 245–255

Takai H, Smogorzewska A & de Lange T (2003) DNA damage foci at dysfunctional telomeres. *Curr. Biol.* 13: 1549–1556

Takai KK, Hooper S, Blackwood S, Gandhi R & de Lange T (2010) In vivo stoichiometry of shelterin components. *J. Biol. Chem.* 285: 1457–1467

Takai KK, Kibe T, Donigian JR, Frescas D & de Lange T (2011) Telomere protection by TPP1/POT1 requires tethering to TIN2. *Mol. Cell* 44: 647–659

Tanaka H, Abe S, Huda N, Tu L, Beam MJ, Grimes B & Gilley D (2012) Telomere fusions in early human breast carcinoma. *Proc. Natl. Acad. Sci. U. S. A.* 109: 14098–14103

Tarsounas M, Muñoz P, Claas A, Smiraldo PG, Pittman DL, Blasco MA & West SC (2004) Telomere maintenance requires the RAD51D recombination/repair protein. *Cell* 117: 337–347

Tei S, Saitoh N, Funahara T, Iida S -i., Nakatsu Y, Kinoshita K, Kinoshita Y, Saya H & Nakao M (2009) Simian virus 40 large T antigen targets the microtubule-stabilizing protein TACC2. *J. Cell Sci.* 122: 3190–3198

Teixeira MT, Arneric M, Sperisen P & Lingner J (2004) Telomere length homeostasis is achieved via a switch between telomerase- extendible and -nonextendible states. *Cell* 117: 323–335

Telomerase Database (2013)

Thompson SL & Compton D a (2008) Examining the link between chromosomal instability and aneuploidy in human cells. *J. Cell Biol.* 180: 665–72

Tomlinson RL, Ziegler TD, Supakorndej T, Terns RM & Terns MP (2006) Cell cycle-regulated trafficking of human telomerase to telomeres. *Mol. Biol. Cell* 17: 955–965

Toouli C, Huschtscha L & Neumann A (2002) Comparison of human mammary epithelial cells immortalized by simian virus 40 T-Antigen or by the telomerase catalytic subunit. *Oncogene* 21: 128–139

Tusell L, Soler D, Agostini M, Pampalona J & Genescà A (2008) The number of dysfunctional telomeres in a cell: One amplifies; more than one translocate. *Cytogenet. Genome Res.* 122: 315–325

Vannier JB, Pavicic-Kaltenbrunner V, Petalcorin MIR, Ding H & Boulton SJ (2012) RTEL1 dismantles T loops and counteracts telomeric G4-DNA to maintain telomere integrity. *Cell* 149: 795–806

Venteicher AS, Abreu EB, Meng Z, McCann KE, Terns RM, Veenstra TD, Terns MP & Artandi SE (2009) A human telomerase holoenzyme protein required for Cajal body localization and telomere synthesis. *Science* 323: 644–648

Verdun RE, Crabbe L, Haggblom C & Karlseder J (2005) Functional human telomeres are recognized as DNA damage in G2 of the cell cycle. *Mol. Cell* 20: 551–561

Verdun RE & Karlseder J (2006) The DNA damage machinery and Homologous Recombination pathway act consecutively to protect human telomeres. *Cell* 127: 709–720

Vitale I, Galluzzi L, Senovilla L, Criollo A, Jemaà M, Castedo M & Kroemer G (2011) **Illicit survival of cancer cells during polyploidization and depolyploidization**. *Cell Death Differ.* 18: 1403–1413

Wang F, Podell ER, Zaug AJ, Yang Y, Baciu P, Cech TR & Lei M (2007) **The POT1–TPP1 telomere complex is a telomerase processivity factor**. *Nature* 445: 506–510

Wang H, Rosidi B, Perrault R, Wang M, Zhang L, Windhofer F & Iliakis G (2005) **DNA Ligase III as a candidate component of backup pathways of nonhomologous end joining**. *Cancer Res.* 65: 4020–4030

Wang M, Wu W, Wu W, Rosidi B, Zhang L, Wang H & Iliakis G (2006) **PARP-1 and Ku compete for repair of DNA double strand breaks by distinct NHEJ pathways**. *Nucleic Acids Res.* 34: 6170–6182

Wang RC, Smogorzewska A & de Lange T (2004) **Homologous recombination generates t-loop-sized deletions at human telomeres**. *Cell* 119: 355–368

Wangsa D, Quintanilla I, Torabi K, Vila-Casadesús M, Ercilla A, Klus G, Yuce Z, Galofré C, Cuatrecasas M, Lozano JJ, Agell N, Cimini D, Castells A, Ried T & Camps J (2018) **Near-tetraploid cancer cells show chromosome instability triggered by replication stress and exhibit enhanced invasiveness**. *FASEB J.* 32: 3502–3517

Watson JD (1972) **Origin of concatemeric T7 DNA**. *Nat. New Biol.* 239: 197–201

Wazer DE, Liu X, Chu Q, Gao Q & Band V (1995) **Immortalization of human mammary epithelial cell types by human papillomavirus 16 E6 or E7**. *Proc.Natl.Acad.Sci.U.S.A* 92: 3687–3691

Weaver BAA, Silk AD, Montagna C, Verdier-Pinard P & Cleveland DW (2007) **Aneuploidy acts both oncogenically and as a tumor suppressor**. *Cancer Cell* 11: 25–36

Williams BR, Prabhu VR, Hunter KE, Glazier CM, Whittaker C a, Housman DE & Amon A (2008) **Aneuploidy affects proliferation and spontaneous immortalization in mammalian cells**. *Science* 322: 703–710

Wood RD & Doublié S (2016) **DNA polymerase θ (POLQ), double-strand break repair, and cancer**. *DNA Repair (Amst).* 44: 22–32

Wright WE & Shay JW (1992) **The two-stage mechanism controlling cellular senescence and immortalization**. *Exp. Gerontol.* 27: 383–389

Wright WE, Tesmer VM, Huffman KE, Levene SD & Shay JW (1997) **Normal human chromosomes have long G-rich telomeric overhangs at one end**. *Genes Dev.* 11: 2801–2809

Wu L, Multani AS, He H, Cosme-Blanco W, Deng Y, Deng JM, Bachilo O, Pathak S, Tahara H, Bailey SM, Deng Y, Behringer RR & Chang S (2006) **Pot1 deficiency initiates DNA damage checkpoint activation and aberrant homologous recombination at telomeres**. *Cell* 126: 49–62

Wu P, van Overbeek M, Rooney S & de Lange T (2010) **Apollo contributes to G-overhang maintenance and protects leading-end telomeres**. *Mol Cell* 39: 606–617

Wu P, Takai H & de Lange T (2012) **Telomeric 3′ overhangs derive from resection by Exo1 and Apollo and fill-in by POT1b-associated CST**. *Cell* 150: 39–52

Wu RA, Upton HE, Vogan JM & Collins K (2017) **Telomerase mechanism of telomere synthesis**. *Annu. Rev. Biochem.* 86: 439–460

Xin H, Liu D, Wan M, Safari A, Kim H, Sun W, O'Connor MS & Songyang Z (2007) **TPP1 is a homologue of ciliate TEBP-β and interacts with POT1 to recruit telomerase**. *Nature* 445: 559–562

Yang W & Lee YS (2015) **A DNA-hairpin model for repeat-addition processivity in telomere synthesis**. *Nat. Struct. Mol. Biol.* 22: 844–847

Ye J, Lenain C, Bauwens S, Rizzo A, Saint-Léger A, Poulet A, Benarroch D, Magdinier F, Morere J, Amiard S, Verhoeyen E, Britton S, Calsou P, Salles B, Bizard A, Nadal M, Salvati E, Sabatier L, Wu Y, Biroccio A, et al (2010) **TRF2 and Apollo cooperate with topoisomerase 2α to protect human telomeres from replicative damage**. *Cell* 142: 230–242

Ye JZ-S, Donigian JR, Van Overbeek M, Loayza D, Luo Y, Krutchinsky AN, Chait BT & de Lange T (2004a) **TIN2 binds TRF1 and TRF2 simultaneously and stabilizes the TRF2 complex on telomeres**. *J. Biol. Chem.* 279: 47264–47271

Ye JZ-S, Hockemeyer D, Krutchinsky AN, Loayza D, Hooper M, Chait BT & de Lange T (2004b) **POT1-interacting protein PIP1: a telomere length regulator that recruits POT1 to the TIN2/TRF1 complex**. *Genes Dev.* 18: 1649–1654

Ye JZ-S & de Lange T (2004) **TIN2 is a tankyrase 1 PARP modulator in the TRF1 telomere length control complex**. *Nat. Genet.* 36: 618–623

Yeager TR, Neumann AA, Englezou A, Huschtscha LI, Noble JR & Reddel RR (1999) **Telomerase-negative immortalized human cells contain a novel type of Promyelocytic Leukemia (PML) body**. *cancer Res.* 59: 4175–4179

Zack TI, Schumacher SE, Carter SL, Cherniack AD, Saksena G, Tabak B, Lawrence MS, Zhang CZ, Wala J, Mermel CH, Sougnez C, Gabriel SB, Hernandez B, Shen H, Laird PW, Getz G, Meyerson M & Beroukhim R (2013) **Pan-cancer patterns of somatic copy number alteration**. *Nat. Genet.* 45: 1134–1140

Zaug AJ, Podell ER, Nandakumar J & Cech TR (2010) **Functional interaction between telomere protein TPP1 and telomerase**. *Genes Dev.* 24: 613–622

Zhang H, Jin Y, Chen X, Jin C, Law S, Tsao SW & Kwong YL (2006a) **Cytogenetic aberrations in immortalization of esophageal epithelial cells**. *Cancer Genet. Cytogenet.* 165: 25–35

Zhang J, Pickering CR, Holst CR, Gauthier ML & Tlsty TD (2006b) **p16INK4a modulates p53 in primary human mammary epithelial cells**. *Cancer Res.* 66: 10325–10331

Zhang X, Wu X, Tang W & Luo Y (2012) **Loss of p16Ink4a function rescues cellular senescence induced by telomere dysfunction**. *Int. J. Mol. Sci.* 13: 5866–5877

Zhang Y & Jasin M (2011) **An essential role for CtIP in chromosomal translocation formation through an alternative end-joining pathway**. *Nat. Struct. Mol. Biol.* 18: 80–85

Zhao Y, Abreu E, Kim J, Stadler G, Eskiocak U, Terns MP, Terns RM, Shay JW & Wright WE (2011) **Processive and distributive extension of human telomeres by telomerase under homeostatic and nonequilibrium conditions**. *Mol. Cell* 42: 297–307

Zhao Y, Sfeir AJ, Zou Y, Buseman CM, Chow TT, Shay JW & Wright WE (2009) **Telomere extension occurs at most chromosome ends and is uncoupled from fill-in in human cancer cells**. *Cell* 138: 463–475

Zhong FL, Batista LFZ, Freund A, Pech MF, Venteicher AS & Artandi SE (2012) **TPP1 OB-fold domain controls telomere maintenance by recruiting telomerase to chromosome ends**. *Cell* 150: 481–494

Zhong Z, Shiue L & Kaplan S (1992) **A mammalian factor that binds telomeric TTAGGG repeats in vitro**. *Mol. Cell. Biol.* 12: 4834–4843

Zijlmans JM, Martens UM, Poon SS, Raap AK, Tanke HJ, Ward RK & Lansdorp PM (1997) **Telomeres in the mouse have large inter-chromosomal variations in the number of T2AG3 repeats.** *Proc. Natl. Acad. Sci. U. S. A.* 94: 7423–8

Zimmermann M, Kibe T, Kabir S & de Lange T (2014) **TRF1 negotiates TTAGGG repeat-associated replication problems by recruiting the BLM helicase and the TPP1/POT1 repressor of ATR signaling**. *Genes Dev.* 28: 2477–2491

Zimmermann M, Lottersberger F, Buonomo SB, Sfeir A & de Lange T (2013) **53BP1 regulates DSB repair using Rif1 to control 5′ end resection**. *Sci. (New York, NY)* 339: 700–705